

**The Effect of Silicon, Silica and Silicates on the Osteoblast *in vitro*.**

Susan I Anderson BSc, M Med Sc.



School of Biomedical Sciences  
Medical School  
University of Nottingham  
Nottingham  
UK

Thesis submitted to the University of Nottingham for the degree  
of Doctor of Philosophy

June 2001

# CONTENTS

<b>Contents.</b>	<b>i</b>
<b>Acknowledgements.</b>	<b>vi</b>
<b>Abstract.</b>	<b>vii</b>
<b>List of Abbreviations.</b>	<b>viii</b>
<b>Chapter 1 General Introduction.</b>	<b>1</b>
1.1 Bone structure and formation.	1
1.1.1 Bone cells.	2
1.1.2 Bone matrix.	7
1.1.3 Bone development.	9
1.1.4 Mineralisation of bone.	10
1.1.5 Bone replacement and biomaterials.	13
1.2 The chemistry and uses of silicon.	15
1.2.1 The occurrence of silicon.	17
1.2.2 Silica in higher animals and man.	19
1.2.3 Silica as an essential trace element.	20
1.2.4 Silica containing biomaterials.	21
1.3 Aims.	24
<b>Chapter 2 Isolation, Culture and Mineralisation of Human Osteoblasts (HOBs).</b>	<b>26</b>
2.1 Introduction.	26
2.2 Materials and methods.	31
2.2.1 Isolation of primary human osteoblasts.	31
2.2.2 Long term cell culture.	32
2.2.2.1 Cell morphology.	32
2.2.2.2 Cell activity and cell number.	32
2.2.3 Characterisation of the osteoblast phenotype.	33
2.2.3.1 Alkaline phosphatase activity.	33

2.2.3.2	Immunofluorescence labelling of osteoblast markers.	33
2.2.4	Cell ultrastructure.	34
2.2.4.1	Scanning electron microscopy (SEM).	34
2.2.4.2	Transmission electron microscopy (TEM).	35
2.2.5	Mineralisation.	35
2.2.6	Effect of mineral supplements.	36
2.3	Results.	37
2.3.1	Isolation and culture of HOBs.	37
2.3.2	Long term culture of primary human osteoblasts.	38
2.3.2.1	Cell morphology.	38
2.3.2.2	Cell activity and cell number.	39
2.3.3	Expression of phenotypic markers.	40
2.3.3.1	Alkaline phosphatase activity.	40
2.3.3.2	Immunolocalisation of osteoblast markers.	40
2.3.4	Ultrastructure.	42
2.3.4.1	Scanning electron microscopy (SEM).	42
2.3.4.2	Transmission electron microscopy (TEM).	42
2.3.5	Mineralisation.	47
2.3.6	The effect of mineral supplements.	48
2.4	Discussion.	51
 <b>Chapter 3 The Effect of Silica Supplementation on Osteoblast Growth and Mineralisation <i>in vitro</i>.</b>		 <b>56</b>
3.1	Introduction.	56
3.2	Materials and Methods.	60
3.2.1	Preparation of silica containing medium.	60
3.2.2	Effect of silicate supplementation on initial cell attachment and growth.	60
3.2.2.1	Protein adsorption.	60
3.2.2.2	Cytoskeletal organisation and vinculin receptor staining.	61
3.2.2.3	Cell activity and cell number.	62
3.2.3	The effect of silicate supplementation on osteoblast growth and differentiation in long term cell culture.	63
3.2.4	The effect of silicate supplementation on osteoblast mineralisation <i>in vitro</i> .	63
3.3	Results.	65
3.3.1	Effect of silicate supplementation on initial cell attachment and growth.	65

3.3.1.1	Protein adsorption.	65
3.3.1.2	Cytoskeletal organisation and vinculin receptor staining.	67
3.3.1.3	Cell activity and cell number.	68
3.3.2	Effect of silicate supplementation on osteoblast growth and differentiation in long term culture.	69
3.3.3	The effect of silicate supplementation on osteoblast mineralisation <i>in vitro</i> .	71
3.4	Discussion.	75
 <b>Chapter 4 Silicate Toxicity.</b>		<b>79</b>
4.1	Introduction.	79
4.2	Materials and Methods.	82
4.2.1	Preparation of silica containing medium.	82
4.2.2	Morphology of cell death.	82
4.2.3	Cell death of attached cells in monolayer culture.	82
4.2.4	Analysis of membrane integrity.	83
4.2.5	Recovery of HOBs from toxic levels of silicate supplementation.	83
4.2.6	Effect of silicate supplementation on different cell types.	83
4.3	Results.	85
4.3.1	Morphology of cell death.	85
4.3.2	Cells in monolayer culture.	90
4.3.3	Analysis of membrane damage.	92
4.3.4	Cell recovery.	94
4.3.5	Effect of silicate supplementation on different cell types.	97
4.4	Discussion.	99
 <b>Chapter 5 The Osteoblast Response to a Silica gel <i>in vitro</i>.</b>		<b>104</b>
5.1	Introduction.	104
5.2	Materials and Methods.	108
5.2.1	Preparation of biomaterials.	108
5.2.2	Characterisation of silica gel.	108
5.2.2.1	Bioactivity.	108
5.2.2.2	Release of silicic acid.	109
5.2.3	Osteoblast response to the silica gel.	109

5.2.3.1	Cell morphology and ultrastructure.	109
5.2.3.2	Cell activity and differentiation.	109
5.2.3.3	Uptake of silicic acid by osteoblasts.	110
5.2.3.4	Mineralisation.	110
5.3	Results.	112
5.3.1	Characterisation of silica gel.	112
5.3.1.1	Surface analysis.	112
5.3.1.2	Bioactivity.	112
5.3.1.3	Silicic acid release.	112
5.3.2	Osteoblast response to silica gel coatings.	116
5.3.2.1	Morphology and ultrastructure.	116
5.3.2.2	Cell activity and differentiation.	119
5.3.2.3	Silicic acid uptake by HOBs.	119
5.3.2.4	Mineralisation.	122
5.4	Discussion.	123
 <b>Chapter 6 Comparison of the Growth of Human Osteoblasts (HOBs) on Silicon (Si), Etched Silicon (ESi) and Patterned Si/ESi Surfaces.</b>		 <b>126</b>
6.1	Introduction.	126
6.2	Materials and Methods.	129
6.2.1	Preparation of Si and ESi surfaces.	129
6.2.2	Surface analysis.	129
6.2.2.1	Calcium phosphate layer formation in SBF and silicic acid release.	129
6.2.3	Cell response to Si and ESi surfaces.	130
6.2.3.1	Cell attachment and spreading.	130
6.2.3.2	Nodule formation.	130
6.2.4	Use of patterned surfaces.	131
6.2.4.1	Chemical patterning of surfaces.	131
6.2.4.2	Characterisation of the patterned surface.	133
6.2.4.3	Cell attachment and Nodule formation.	133
6.3	Results.	134
6.3.1	Surface analysis of Si and ESi surfaces.	134
6.3.1.1	CaPi layer formation in SBF and silicic acid release.	134
6.3.2	Cell responses to Si and ESi surfaces.	138
6.3.2.1	Cell attachment and spreading.	138

6.3.2.2	Nodule formation.	141
6.3.3	Use of patterned surfaces.	142
6.3.3.1	Characterisation of the surface.	142
6.3.3.2	Cell response.	145
6.4	Discussion.	152
 <b>Chapter 7 The incorporation of silica into a PCL polymer system.</b>		<b>155</b>
7.1	Introduction.	155
7.2	Materials and Methods.	158
7.2.1	Formation of silica particles from TEOS.	158
7.2.2	Formation of silica particles from TCS.	158
7.2.3	Incorporation of silica into PCL.	158
7.2.4	EDX analysis and elemental mapping.	159
7.2.5	CaPi layer formation and silicic acid release.	159
7.2.6	Cell response to silica containing polymers.	160
7.3	Results.	161
7.3.1	Analysis of silica particle formation.	161
7.3.2	Surface analysis of silica containing polymers.	161
7.3.3	CaPi layer formation and silicic acid release in SBF.	163
7.3.4	Initial cell response.	165
7.4	Discussion.	167
 <b>Chapter 8 General Discussion.</b>		<b>170</b>
 <b>References.</b>		<b>180</b>

## ACKNOWLEDGEMENTS

I would like to thank the many people who have helped me throughout the years. Firstly I would like to thank Professors Paul O'Shea and Sandra Downes for their support, encouragement and patience during the course of this work. I would also like to thank Professors Ian Mac Donald and Chris Gregory for believing I could undertake a PhD part time and for supporting me in my career over the years.

Dr Carole Perry and Dr Ana-Maria Caballero were collaborators in the work described in Chapter 5 and I would like to thank them for their contribution to this work. The studies undertaken in Chapter 6 were as a result of a collaboration with Martin Winklemann at the ETH in Zurich and I would like to thank him for preparing the samples and his friendship, reliability and enthusiasm. Dr Paul Christian from the Department of Mechanical Engineering at the University of Nottingham prepared the polymer samples used in Chapter 7 and I would like to thank him for his contribution to this work and his enlightening chemical discussions.

I received help and guidance from many of the technical staff and postdoctoral research assistants during the course of this work and I would like to thank Bushra Sim, Dr Rachael Sawtell and Rachel Budworth for training in cell culture and biochemical assay techniques, Dr Michael Garle and Pam Flemming for help with the molybdenum blue assay and Nikki Bock and Jenny Armitage for help with ESEM.

I would also like to thank the various members of the Biomaterials group and other PhD students for their lively discussion of results and for making the last few years really enjoyable. Thanks to Michael Ball, Julie Gough, Kathleen McDougall, Debbie Heath, Harry Gidda, Dave Sokal, Maria Schumlikova and all my friends.

Finally, I would like to thank my husband Brendan, my daughter Katherine and my parents Ita and Peter for their support, love and tolerance while I carried out this work.

## ABSTRACT

Silica is an essential trace element in human nutrition and dietary deficiency leads to abnormal bone formation in experimental animal studies (Carlisle, 1972, Schwartz, 1972). Silica-containing glasses and glass ceramics, within a certain range, are bioactive, forming a strong bond with bone and soft tissue when they are used as bone replacement materials. The aim of this work was to investigate the effect of silica on the osteoblast *in vitro* with a view to its eventual incorporation into biomaterials to improve bone-bonding properties.

Two distinct approaches were used. The first involved the analysis of silica as a nutrient, by supplementing osteoblast growth medium with sodium metasilicate, and evaluating the osteoblast response in terms of cell growth, mineralisation and cytotoxicity. The second approach examined the response of osteoblasts to silica as a biomaterial. A silica gel was used to isolate the effects of silica on the osteoblast *in vitro* without the effects of the other ions present in bioactive glass. The biocompatibility of patterned silicon wafers was investigated to evaluate the potential use of these materials in the field of biomaterials. Finally, the bioactivity and osteoblast response to a novel silicon/polymer composite was assessed as a potential biomaterial.

The results of nutrition studies showed that in some cases low levels (1-100ppm) of silicate appeared to have a beneficial effect on bone formation in terms of nodule formation and mineralisation. Higher levels of silicate supplementation (>300ppm) caused rapid apoptosis in osteoblasts, fibroblasts and macrophages and affected cell spreading.

The biomaterial studies showed that the silica gel surface was bioactive and osteoblasts responded favourably demonstrating enhanced, earlier nodule formation. Bioactive surfaces formed a calcium phosphate (CaPi) layer and released silicic acid when incubated in a simulated body fluid (SBF). Bulk silicon wafers (Si) supported osteoblast growth however, the removal of the oxide layer by wet etching (ESi) imparted bioactive properties to the wafer. Patterned Si/ESi surfaces supported the formation of a CaPi layer over the entire surface and demonstrated osteoblast preferences for bioactive surfaces. The incorporation of silica particles into a bioabsorbable polymer matrix rendered the composite bioactive and supported osteoblast growth.

The results of this work demonstrate the importance of silica in bone mineralisation, osteoblast apoptosis and particularly the potential benefits of the use of silica and silicon to improve bone bonding in non-bioactive biomaterials and biosensors.

## List of Abbreviations

<b>ACP</b>	Amorphous calcium phosphate
<b>ALP</b>	Alkaline phosphatase
<b>BGP</b>	Sodium $\beta$ glycerophosphate
<b>BSA</b>	Bovine serum albumin
<b>CaPi</b>	Calcium phosphate
<b>CFC</b>	Craniofacial cells
<b>CLSM</b>	Confocal laser scanning microscopy
<b>DABCO</b>	Diazabicyclo[2.2.2]octane
<b>DAPI</b>	4,6-Diamidino-2-phenylindole
<b>DEX</b>	Dexamethasone
<b>DMEM</b>	Dulbeccos Modified eagles medium
<b>DMSO</b>	Dimethyl Sulfoxide
<b>EBSS</b>	Earles' Balanced Salt Solution
<b>ECM</b>	Extracellular Matrix
<b>EDTA</b>	Ethylenediaminetetraacetic acid
<b>EDX</b>	Energy dispersive X-ray microanalysis
<b>ER</b>	Endoplasmic reticulum
<b>ESEM</b>	Environmental scanning electron microscopy
<b>ESi</b>	Etched silicon
<b>FCS</b>	Foetal calf serum
<b>FITC</b>	Fluorescein Isothiocyanate
<b>HA</b>	Hydroxyapatite
<b>HCA</b>	Carbon containing hydroxyapatite
<b>HBSS</b>	Hanks' Balanced Salt Solution
<b>HMDS</b>	Hexamethyldisilazane
<b>HOB</b>	Human osteoblast
<b>MV</b>	Matrix vessicles
<b>OC</b>	Osteocalcin
<b>OCP</b>	Octacalcium phosphate
<b>ON</b>	Osteonectin
<b>OP</b>	Osteopontin
<b>OPC</b>	Osteoprogenitor cell
<b>PBS</b>	Phosphate buffered saline
<b>PCL</b>	Poly- $\epsilon$ -caprolactone
<b>PEG</b>	Polyethylene Glycol
<b>PESF</b>	Polyether sulfone
<b>PI</b>	Propidium Iodide
<b>PMMA</b>	Poly(methyl methacrylate)
<b>PTH</b>	Parathyroid hormone
<b>TCS</b>	Tetrachlorosilane
<b>TEM</b>	Transmission electron microscopy
<b>TEOS</b>	Tetraethoxysilane
<b>TRITC</b>	Tetra Rhodamine Isothiocyanate
<b>rER</b>	Rough endoplasmic reticulum
<b>SBF</b>	Simulated body fluid
<b>SEM</b>	Scanning electron microscopy
<b>XPS</b>	X-ray photoelectron spectroscopy

# **Chapter 1**

## **General Introduction.**

The aim of this project is to examine the effect of silica on osteoblasts *in vitro*, with a view to the eventual incorporation of silica into materials, such as polymers and ceramics, to enhance bioactivity and bone bonding. The following sections outline the normal structure of bone, the mineralization process, the incidence and effect of silica in the body and the current research concerning silica-containing biomaterials.

### 1.1 Bone Structure and Formation.

Bone is a living, dynamic tissue that provides the skeletal support for the body. Bone may be categorised as spongy (cancellous, trabecular) or compact (dense, cortical) (Figure 1.1). Spongy bone (20%) contains many spaces and is found in short, flat bones and in the epiphyses of long bones. It provides elasticity and storage space for bone marrow. Compact bone (80%) is densely packed with a structure of Haversian systems or osteons (Figure 1.2). It overlies spongy bone and gives bone its load bearing properties (Tortora and Anagnostakos, 1987). It is a dense connective tissue and as such consists of cells embedded in a mineralised extracellular matrix (Figure 1.3).

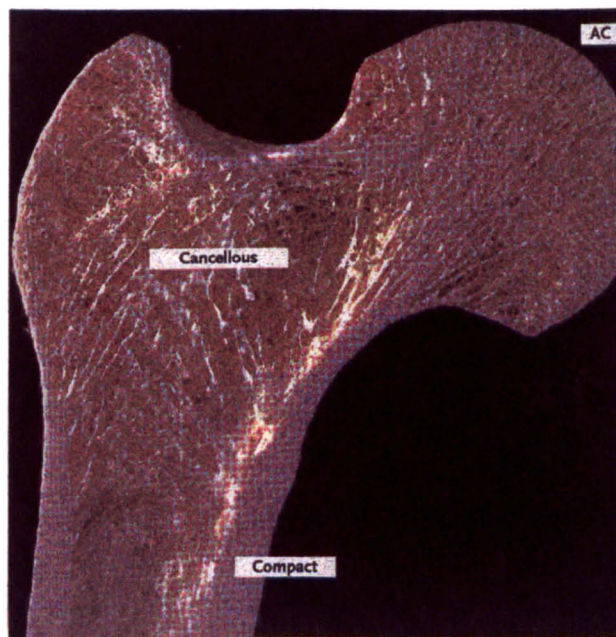


**Figure 1.1** The structure of bone (from: Kerr, 1999)

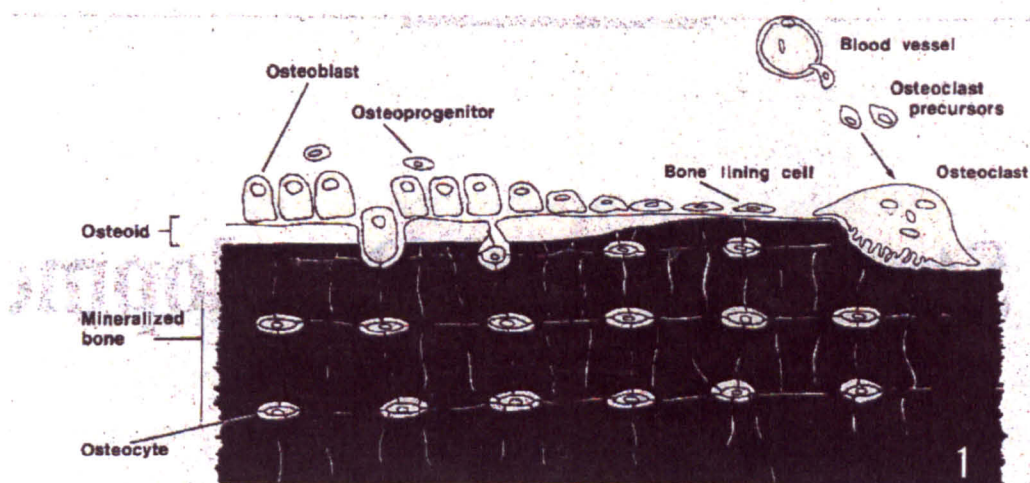


**Figure 1.2** Schematic representation of the structure of bone (From: Marks and Hermey, 1996) showing the flattened osteoprogenitor and bone lining cells and the cuboidal osteoblasts at the bone surface. Osteoblasts initially lay down an unmineralised ECM (osteoid) which later becomes mineralised enveloping some of the osteoblasts which become osteocytes. Osteoclasts resorb bone and come from a haemopoietic cell lineage.

### 1.1.1 Bone Cells.

(a) Osteoprogenitor cells. Osteoprogenitor cells are small spindle shaped mesenchymal cells. They are found in sheets on non resorbing bone surfaces such as the endosteum and the inner part of the periosteum. When stimulated to proliferate these cells differentiate into osteoblasts or chondroblasts depending on the vascularisation of the region (Cormack, 1984).

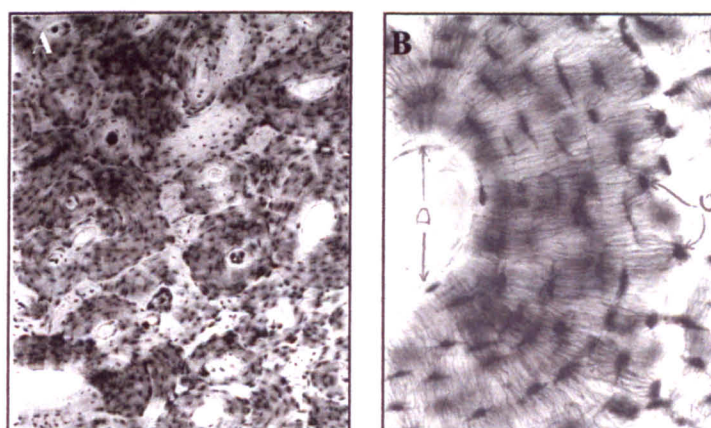


**Figure 1.3** The histological structure of bone. Discrete units or osteons are seen in (a). A higher magnification view (b) shows osteocytes (o) in lacunae with numerous cytoplasmic processes. The haversian canal is labelled (d).

The transition from osteoprogenitor cell to osteoblast is unclear and information is difficult to obtain due to the relatively undifferentiated state making immunocharacterisation difficult (Aubin and Liu, 1996). Recent studies have suggested that osteoprogenitor cells attach selectively to lamimin-1 but inhibit the attachment of other cells in rat calvarial cultures (Roche *et al*, 1999). Results are sometimes contradictory but the transition seems to involve a number of stages during which the cell is referred to as a preosteoblast. Preosteoblasts retain the capacity for cell division but this is gradually decreased as the preosteoblast matures. There is a concomitant increase in differentiation in terms of expression of bone markers such as bone sialoprotein and osteocalcin. The current research on the various stages of progression from osteogenic cell to committed osteoblast is reviewed in Aubin and Liu (1996).

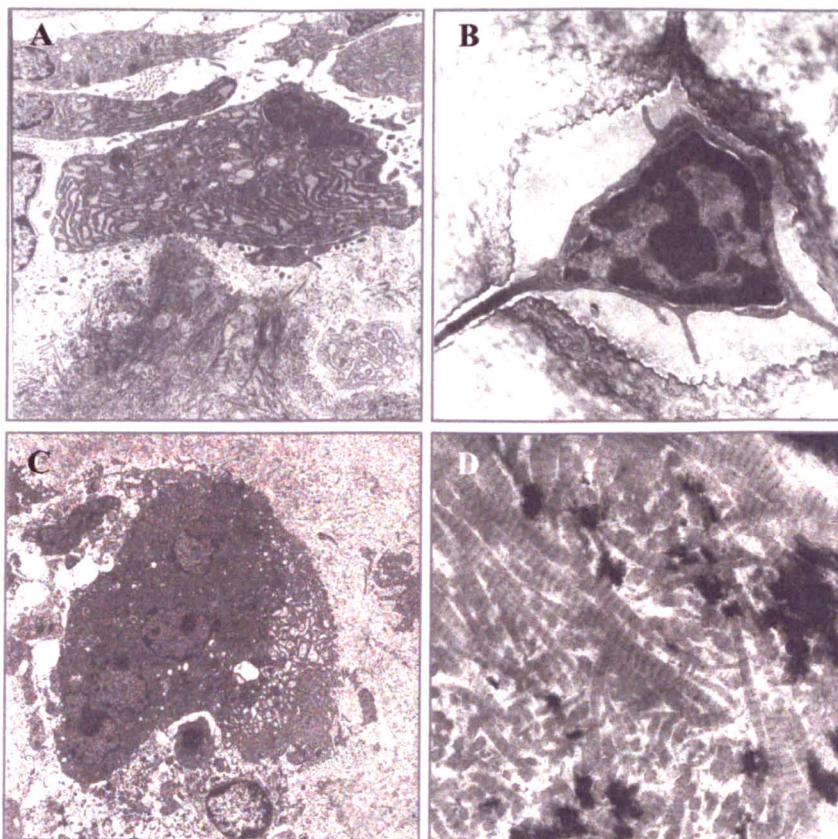


**Figure 1.4** Transmission electron micrographs of an osteoblast (a), Osteocyte (b), osteoclast (c) and the extracellular matrix of bone (d) containing collagen-1 and bone mineral.

(b) Osteoblasts. Osteoblasts are non-dividing cells that synthesise and secrete the organic components of bone matrix (osteoid) and regulate mineralisation. They are large cuboidal cells with an eccentrically placed nucleus and numerous fine processes (Figure 1.4a). Their cytoplasm is that of an actively secreting cell and contains

abundant rough endoplasmic reticulum and a prominent golgi apparatus (Cormack, 1984). They are found in layers at the growing surfaces of bone and are attached to each other by gap junctions (Cross, 1993). They deposit around 0.5mm of matrix per day in a bone forming cycle that lasts about 100 days (Billah, 1996). Osteoblasts are rich in alkaline phosphatase (ALP), an enzyme involved in calcification. They also secrete a number of proteins (i-vii below) linked to the mineralisation and maturation of bone matrix including:

- (i) Osteocalcin (OC), a 5800Da protein, is the most abundant noncollagenous protein in bone. It binds calcium and is dependant on vitamin K. Its expression and secretion are increased by PTH and vitamin D<sub>3</sub>. The level of expression increases with increasing cell differentiation and it is highly expressed by the mature osteoblast and preosteocyte. Little is known about its function however, but suggested roles include an involvement in bone resorption as it acts as a chemotactic agent for osteoclasts (Bodine and Komm, 1999) and in crystal maturation (Boskey *et al.*, 1994) as it binds to mineral crystals (Cross, 1993). Recently ablation of OC genes in mice resulted in increased bone formation (Ducy *et al.*, 1996) suggesting an inhibitory effect on osteoblast activity and a receptor has been identified in immortalised human osteoblasts (Bodine and Komm, 1999).
- (ii) Bone matrix protein, a 59kDa protein which enables osteoblasts and osteoclasts to bind to bone matrix via their  $\beta$ 3 integrin.
- (iii) Bone sialoprotein II (BSP-II), a 46-75kDa protein, which is maximally expressed during late stages of osteoblast development and early matrix mineralisation. It can nucleate HA and has calcium ion binding properties. It can bind to cells and can also mediate cell attachment via the vitronectin receptor. Its suggested role is in the initiation of mineralisation (Gehron Robey, 1996).
- (iv) Osteopontin, a 41kDa protein involved in mineralisation and resorption. It is maximally expressed just prior to mineralisation and is intensely stained at the mineralising front using immunolocalisation techniques (Butler *et al.*, 1996). High levels of osteopontin inhibit hydroxyapatite but low levels promote hydroxyapatite

formation. Osteopontin can bind equally to hydroxyapatite and collagen, suggesting it may help to initially orientate hydroxyapatite crystals on collagen fibres (Billah, 1996). It cannot nucleate HA. Osteopontin promotes cell attachment and spreading for osteoblasts, osteoclasts and fibroblasts and may facilitate the attachment of these cells to the ECM (Butler *et al.*, 1996). It can mediate osteoclast attachment and may help osteoclasts anchor to the bone surface via the  $\alpha v \beta 3$  integrin (Billah, 1996).

(v) Osteonectin, a 32kDa protein binds to collagen, calcium ions and hydroxyapatite and may be involved in extracellular matrix proteolysis and in coupling osteoblast and osteoclast action (Billah, 1996). It can nucleate hydroxyapatite and has been reported to influence the cell cycle (Gehron Robey, 1996).

(vi) Collagenase is synthesised by osteoblasts in response to resorption stimulators such as (Parathyroid hormone) PTH and vitamin D<sub>3</sub>.

(vii) Osteoblasts secrete the third component of complement (C3) and may aid osteoclast differentiation suggesting that osteoblasts may play a role in the regulation of osteoclasts (Billah, 1996).

It is possible to isolate and culture osteoblasts *in vitro* and the characteristics and uses of these will be elaborated in Chapter 2.

(c) Osteocytes. These are mature osteoblasts and do not divide. They are the most abundant cells in bone numbering more than ten times the number of osteoblasts (Nijewerde *et al.*, 1996). They are smaller and less active than osteoblasts (Cross, 1993). Their cytoplasm is less rich than the osteoblast which is consistent with their function in the maintenance and turnover of bone matrix (Cormack, 1984). Osteocytes are located in lacunae and have extensive processes which pass through bony channels, or canaliculi. The processes interact via gap junctions which provide a network for communication between osteocytes and also to osteoblasts (Figure 1.4b). Nutrients diffuse from blood vessels to osteocytes through canaliculi and through the cells themselves but diffusion distance is limited and the cells need to be within 0.2mm of a blood vessel to survive. This defines the size of spongy bone and the structural unit of

compact bone, the Haversian system (Cross, 1993). They are sensitive to parathyroid hormone and calcitonin and this suggests they may have a role in the exchange of mineral between bone and the extracellular fluid compartment (Billah, 1996).

(d) Osteoclasts. Osteoclasts are found at the resorbing surfaces of bone and can be visualised histologically by staining with acid phosphatase (Evans *et al.*, 1980). They are present as only a small fraction of the number of osteoblasts (Nijwerde *et al.*, 1996). They can be distinguished by their large size which is typically around 100µm. The cells are multinucleate and have an extensive ruffled border which has an underlying clear zone containing abundant actin microfilaments. Their cytoplasm contains abundant mitochondria and golgi apparatus (Figure 1.4c). Osteoclasts arise from the monocyte-macrophage cell lineage (Cormack, 1984). Their role is to resorb bone by attacking the inorganic amorphous content of bone and producing focal demineralisation. Osteopontin and bone matrix protein are thought to play a role in the attachment of osteoclasts to the bone surface (Billah, 1996).

The site of resorption is an extracellular pit between the osteoclast and the bone surface (Cross, 1993). Lysosomal enzymes such as cysteine proteases, cathepsin, plasminogen and collagenase are exocytosed into the pit, these degrade organic components such as collagen and proteoglycans. A proton pump in the ruffled border pumps H<sup>+</sup> (derived from the cells' rich supply of carbonic anhydrase) ions out of the cell and the resulting low pH dissolves hydroxyapatite. Osteoclasts are unique in that lysosomal enzymes operate outside the cell however, the amount of calcium released during osteoclast digestive activity would be incompatible with normal cellular function (Cross, 1993). In fact, increased calcium levels inside the osteoclast may signal the cells to stop bone resorption (Billah, 1996).

Although the mechanism of osteoclast activity is not fully understood it appears to be regulated by a variety of stimulators and inhibitors including parathyroid hormone (PTH), calcitrol (1,25(OH)<sub>2</sub>D), interleukin-1 (IL-1), and prostaglandin-E<sub>2</sub> (PGE<sub>2</sub>) (Billah 1996). Osteoclasts and osteoblasts work together to continually remodel bone and allow it to grow e.g. osteoclasts on the interior of the skull co-operate with osteoblasts on the outside to increase skull size so the developing brain is

accommodated (Cross, 1993). There is some evidence to suggest that osteoblasts are essential for both bone formation and resorption because, in culture, osteoclasts will not resorb without osteoblasts. In addition the PTH receptor, which increases bone resorption and osteoclast activity, is found only on osteoblasts (Cross, 1993). Many bone diseases result from a dysfunction of the balance between formation and remodelling. These include osteoporosis (Reviewed in Rodan *et al.*, 1996) and osteopetrosis (reviewed in Lyndon Key and Reis, 1996).

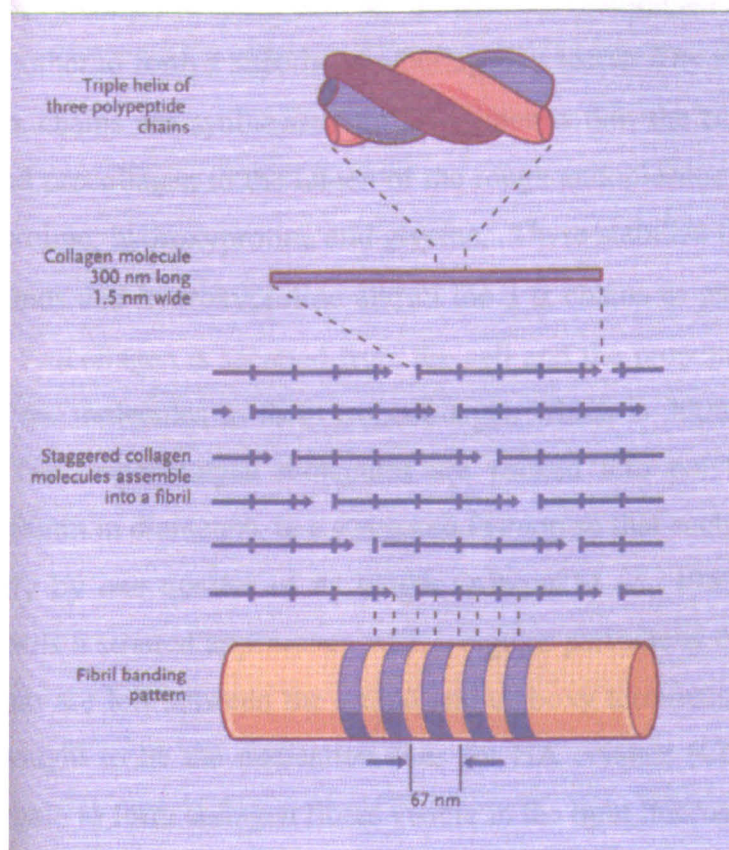


**Figure 1.5** The structure of type 1 collagen (From: Kerr, 1999)

### 1.1.2 Bone Matrix.

The extracellular matrix (ECM) of bone is composed of an inorganic mineral component deposited on a complex organic matrix (Figure 1.4d). The unmineralized matrix is called osteoid and is clearly differentiated from the mineralised matrix. Type-1 collagen is the main fibrous protein in the organic ECM (Figure 1.5), with mucopolysaccharides, glycoproteins and proteoglycans also present. The inorganic

component of bone is a poorly crystalline, carbonate-containing analogue of hydroxyapatite (HA) with the chemical formula  $\text{Ca}_{10}(\text{PO}_4)_6(\text{OH})_2$  (Boskey, 1981). Small amounts of other compounds containing calcium, phosphorous, magnesium, sodium and fluorine are also found (Billah, 1996). The ECM accounts for 90% of the weight of compact bone. Sixty percent of total bone weight is made up of the inorganic component while the organic component accounts for 30% (Cormack, 1984).

Type-1 collagen has a triple stranded helical structure which consists of three chains of polypeptides, called  $\alpha$  chains. These are around 1000 amino acids long and are wound around each other to form a superhelix. Collagen is secreted by many connective tissue cells. Pro  $\alpha$  chains are synthesised on ribosomes within the cell. These form triple helices called procollagen in the lumen of the rough endoplasmic reticulum. Collagens are rich in proline, hydroxyproline and glycine. These stabilise the helical structure by hydrogen bonds and hydroxyproline allows the 3  $\alpha$  chains to pack tightly to form the superhelix. Procollagen is secreted from the cell and the propeptides are cleaved from the ends of the molecules to form tropocollagen which is 300nm long and 1.5nm in diameter. The tropocollagen molecules are packed into polymers, called collagen fibrils (10-300nm in diameter), in a staggered fashion so that each molecule is displaced longitudinally by one quarter of its length (Alberts *et al.*, 1989). This arrangement gives the fibrils a striated appearance with a regular periodicity of 67nm (Figure 1.4d). Gaps of 35nm are left between the amino and carboxy terminals of adjacent units and these are thought to be the nucleation sites for HA crystals (Cross, 1993). Collagen fibrils aggregate to form collagen fibres visible in the light microscope.

Proteoglycans are macromolecules of regularly repeating disaccharide units consisting of an amino sugar and an acidic sugar. Glycoproteins are similar but have a small number of monosaccharide residues in each chain. Proteoglycans and glycoproteins enhance the strength of collagen fibres by attracting water and cations to form a hydrated network due to their overall negative charge (Billah, 1996).

### **1.1.3 Bone Development.**

Bone development is known as osteogenesis or ossification. Bones are derived from mesenchyme but in one of two different ways depending on the type of bones they are. Some are derived from neural crest mesenchyme i.e. the mandible, maxilla and temporal bones while others are derived from the neural crest tissue itself i.e. parts of the hyoid bone are from neural crest and the rest is from neural crest cartilage, also styloid processes of temporal bone and stapes (Gilbert, 1994) Flat bones (and other non-long bones) develop in vascularised areas by a process called intramembranous ossification. Long bones develop in a more indirect way in poorly vascularised areas using a cartilage model. This process is known as endochondral ossification. Both processes give rise to the same bone tissue.

#### (a) Intramembranous Ossification.

Mesenchymal cells differentiate into osteogenic cells in areas supplied by capillaries. This is known as a centre of ossification. The osteogenic cells differentiate into osteoblasts which lay down, and become surrounded by, matrix which becomes calcified. The small, irregularly shaped spicules of bone lengthen to become trabeculae which incorporate capillaries as they widen. The bone is now characteristic of spongy bone. Bone growth only occurs by apposition i.e. it takes place on a pre-existing surface and is laid down in layers. This is because osteoblasts do not divide and also because the matrix calcifies soon after being laid down preventing internal expansion of the tissue. Spongy bone is converted to compact bone by continued deposition of layers of bone matrix being laid down on trabeculae, each successive layer making the bone more compact (Cormack, 1994).

#### (b) Endochondral Ossification.

Mesenchymal cells differentiate into chondroblasts which secrete cartilage matrix in the shape of a long bone. In the fourth week of foetal development the cartilage model begins to be replaced by bone in the following manner. Calcium salts are deposited in the cartilage matrix in the mid region of the model (diaphysis) causing chondrocytes to

die. Capillaries then grow into the perichondrium causing it to produce osteoblasts which initiate the primary centre of ossification. Secondary centres of ossification develop in the epiphyses in the same way and the model is eventually totally replaced by bone with the exception of the epiphyseal plates. These facilitate long bone growth by a highly ordered sequence of events involving the proliferation, maturation and degeneration of the chondrocytes. The chondrocytes are resorbed by osteoclasts forming space for the ingrowth of capillaries and the accompanying osteoprogenitor cells (Cormack, 1994).

#### 1.1.4 Mineralization of Bone.

Mineralisation is defined as the deposition of inorganic chemical compounds under normal or pathologic conditions (Boskey, 1981). In addition, calcification is defined as the deposition of insoluble calcium salts in any tissue (Cormack, 1984). These terms are typically used interchangeably when referring to bone as the major inorganic minerals deposited are calcium compounds. Alternatively, ossification is the process by which bone tissue is secreted and calcified.

The inorganic component of mature bone is a poorly crystalline form of hydroxyapatite which has a Ca/P molar ratio of  $\sim 1.5$ . Crystalline HA has a Ca:Pi ratio of 1.67 (Landis and Glimcher, 1978). The nature of the initial phase of the mineral in immature bone and the sequence of events in the mineralisation process itself are difficult to study because of the heterogeneity of the inorganic particles which is due to the stage of maturation, source of tissue, age and location. The presence of water during processing for many techniques used to identify mineral, including electron microscopy, X-ray microanalysis, electron diffraction and electron microprobe microanalysis, causes artefacts which result from problems of mineral retention, crystal size, location and orientation and mineral phase transformations (Dickson, 1984; Landis and Glimcher, 1978; Landis *et al.*, 1977). For example amorphous calcium phosphate (ACP) and octacalcium phosphate (OCP) are labile and are easily transformed to poorly crystalline HA when exposed to water, dehydration methods or heat. Many theories exist regarding the process of mineralisation including physiochemical mechanisms, local ion

---

concentrating mechanisms and removal of calcification inhibitors. A review of these is given in Anderson (1980).

Many phases of calcium phosphate have been implicated as the initial mineral formed during bone mineralisation such as OCP, ACP brushite and HA itself. It has been shown *in vitro* that HA can grow on brushite crystals and that brushite is identified in the earliest stages of mineralisation in the embryos of chicks and calves by X-ray diffraction (Boskey, 1981). Small clusters of mineral particles in the osteoid did not have an X-ray diffraction pattern but larger osteoid crystals and more heavily calcified regions showed poorly crystalline HA patterns, indicating either an increase in crystallinity or size or both (Landis and Glimcher, 1978). Recent studies using infra red spectroscopy coupled with light microscopy indicate that the only mineral present in bone is a poorly crystalline apatite (Boskey, 1994). The mineral increases in size, perfection and amount, progressing from the cartilaginous growth plate to the dense cortical bone. As the mineral matures the carbonate and acid phosphate content is decreased (Boskey, 1994).

The majority of mineral in bone is associated with type-1 collagen and only 10% of ECM space is not taken up with collagen (Glimcher, 1990). Collagen has long been considered as the initial site for mineral deposition. It was thought that CaPi crystals were deposited in the hole zone of collagen in the early stages of mineralisation and that later they are also deposited in the collagen pores (Glimcher, 1990). This view is not universally accepted because collagen alone, without matrix proteins, cannot nucleate apatite. Type-1 collagen is present in relatively small amounts in calcified cartilage (Boskey, 1994). It is more likely that collagen acts as a template along which the crystals align themselves. The c axis of the mineral crystals are aligned parallel to each other and to the collagen fibre (Boskey, 1981). A scanning electron microscope (SEM) study on immature and adult bone revealed that, in adult bone, collagen mineralises first, followed by the ground substance, whereas in immature bone, both areas mineralise together (Boyde, 1980).

Matrix vesicles (MVs) have been suggested as the initial site of HA deposition. Matrix vesicles were discovered independently by Anderson and Bonnucci in growth plate

cartilage in 1967. They were observed in bone by Bernard and Pease in 1969 who called them osteoblastic buds. (Anderson, 1980; Bernard, 1969). It is still unclear whether MVs are associated with mineral deposition in bone (Boskey, 1981). Matrix vesicles are small (~2,000 angstroms), membrane bound bodies which are thought to be of cellular origin but may be products of cellular degeneration (Boskey, 1981). They are found in osteoid and vesicle distribution is closely linked with areas of calcification. They contain acidic phospholipids which attract calcium ions. MVs are rich in alkaline phosphatase, which can concentrate phosphate ions by hydrolysis of phosphate esters (Anderson, 1980). It is thought that the role of MVs is to promote calcification by transporting calcium and phosphate ions and removing inhibitors of calcification such as pyrophosphate and ATP (Boskey, 1981). Mineral crystals are thought to rupture the MVs and spread into the matrix where they orientate themselves along the collagen (Billah, 1996; Boskey, 1994).

Other research suggests that the precursors to calcification may already be present in the osteogenic cell even before the ECM is laid down (Landis and Glimcher, 1978). Brighton and Hunt, (1976) have shown by histochemical staining that calcium is accumulated in the mitochondrial and cell membranes in the growth plate and that this is gradually depleted in the degenerating zone. This is linked to a concomitant increase in the calcium concentration in the matrix vesicles. Landis and Glimcher (1978) used a combination of techniques on anhydrously processed chick bone to examine these mitochondrial granules. Electron microprobe analysis revealed that they contained a large amount of calcium and phosphorous which probably exists as calcium phosphate. This was probably non crystalline as there was no identifiable X-ray diffraction pattern. The Ca:Pi ratio of the granules was significantly lower than the extracellular calcium phosphate phases. No phosphorous or calcium was detected in the extramitochondrial cytoplasm. Inhibitors may be present in the mitochondria which prevent maturation of the particles inside the cell. It is likely that mitochondria serve to concentrate calcium and phosphorous and then release it for use by the matrix vesicles (Anderson, 1980).

The individual crystals are very small (~5nm) and they form needle or plate-like aggregates frequently contain impurities (Simkiss, 1975). Calcification will only take place if the local concentrations of calcium and phosphate ions reaches the level

required for calcium phosphate deposition (Cormack, 1984) In order for a crystal to be formed, groups of ions must come together with sufficient collision energy and the right orientation to form a critical nucleus (the smallest stable combination of ions with the structure of the crystalline material that can persist in solution). As more ions are added to the critical nucleus the crystal grows. New nuclei form on the surface of growing crystals (secondary nucleation) and this provides more sites for crystal proliferation. Mineral is probably deposited in bone by heterogeneous nucleation (Boskey, 1981; 1994; Glimcher, 1990).

The osteoblasts has a role in regulating the mineralisation process by secreting collagen, along which the crystals orientate themselves and by the matrix components and enzymes that regulate mineralisation. The matrix proteins probably control initial crystal deposition and may regulate the shape size and orientation of crystals for example, osteopontin may retard crystal growth and osteocalcin may regulate crystal size and turnover. It is a combination of matrix proteins, enzymes, collagen and cells which determine the nature of the matrix and its ability to become calcified (Boskey, 1994).

### **1.1.5 Bone Replacement and Biomaterials.**

Implantation of materials into bone is the most frequently performed surgical implant procedure (Strnad, 1992). More than 40 different parts of the body are now being repaired or replaced with more than forty different types of biomaterial (Hench, 2000). However there is much room for improvement as the long term (>10yr) survival rates of these implants is variable (Lobel *et al.*, 2000). New materials are constantly being sought for different applications (Turnya *et al.*, 1996). A biomaterial is defined as ‘a material intended to interface with biological systems to evaluate, treat, augment or replace any tissue organ or function of the body’ (de Bruijn, 1993). The failure of an implant is often caused by osteolysis, the destruction of bone tissue surrounding an implant. This is commonly caused by wear debris from implant surfaces which cause an adverse foreign body response leading to the production of proteolytic enzymes and inflammatory mediators (De Giglio *et al.*, 2001). Aseptic loosening is the destabilisation of an implant as a result of macrophage activation, which causes a

cascade of events leading to bone resorption. The onset of this condition, which is irreversible, after total joint replacement is the most common reason for long term implant failure (Santerre *et al.*, 2000)

There are four main types of biomaterial: metals, ceramics, polymers and composites (de Bruijn, 1993). More than forty different types are currently used clinically in over forty anatomic sites (Lobel *et al.*, 2000). Most biomaterials currently in use are described as bioinert, generating a minimal tissue response (Lobel *et al.*, 2000). These materials are clinically successful in the short term but achieving long term (>10yrs) stability has proved more elusive. Attempts to improve implant fixation using porous materials and porous coatings on implants (termed biological fixation) have proved less successful than standard cement fixation methods (Lobel *et al.*, 2000).

Some materials are described as bioactive allowing physicochemical bonding between the implant and bone tissue. The concept of bioactivity was introduced by Hench *et al.* in 1971 using a silicate glass in the system  $\text{SiO}_2\text{-CaO-P}_2\text{O}_5\text{-Na}_2\text{O}$ . All known bioactive glasses and glass-ceramics are silica based, however the presence of silica is not a requirement for bioactivity as both hydroxyapatite and titania gels exhibit bone bonding (Oliveira *et al.*, 1995). It has been proposed that a prerequisite to bone bonding is the formation of a biologically active carbonate containing hydroxyapatite layer on the material surface under physiological conditions (Kokubo, 1992; Hench, 1991.) and this is discussed further in section 1.2.4. Bone bonding mechanisms may be different for different biomaterials such as surface active glass ceramics, surface active ceramics and resorbable ceramics (Neo *et al.*, 1993).

The next generation of biomaterials are intended to enhance tissue regeneration rather than to replace it (Lobel *et al.*, 2000). Biodegradable scaffolds for tissue ingrowth and eventual replacement are currently being developed for use in bony sites and for organs and tissues around the body. The research into the development of these materials and their use to control and manipulate the tissue response has been termed tissue engineering. Recent research from the Shakesheff group has focussed on the immobilisation of peptide sequences on polymer scaffolds to control cell adhesion

(Quirk *et al.*, 2001) and the patterning of biomolecules onto tissue engineering scaffolds and biosensors (Patel *et al.*, 2000).

## 1.2 The Chemistry and Uses of Silicon

Silicon is situated in the fourth group of the periodic table, below carbon and between aluminium and phosphorous with which it shares similar atomic size, ionisation energy and electron negativities. These elements can be substituted for each other in many compounds (Da Silva and Williams, 1991). Silicon forms the largest number of compounds with other elements after carbon, but not for the same reasons. Carbons bond energies for C-C, C-O and C-H are about equal whereas silicon forms a much stronger bond with oxygen than either silicon or carbon resulting in much of silicon chemistry being based on the Si-O-Si chain (Leibau, 1985). The strength of the Si-O bond is such that it is considered not vulnerable to metabolic influence (Lobel *et al.*, 2000).

Silica and silicates are used extensively as raw materials and have been since the dawn of time. The flint industry dates to prehistoric times (Iler, 1955), granite and sandstone are used for building, clay and limestone mixtures are used to make Portland cement. Production of silicate glass and silicate based ceramics are long standing, world-wide industries (Leibau, 1985, Iler, 1955).

Amorphous silicas are polymers of silicic acids which are made up of interlinked  $\text{SiO}_4$  tetrahedra. The structure at the surface is highly disordered and terminates in either a siloxane (Si-O-Si) or a form of silanol group (Si-OH) of which there are many types (Vansant *et al.*, 1995a). Table 1.1 lists the chemical formulae and structures of the main forms of silica used in this thesis.

Type of Silica	Formula	Structure
Silicon	Si	-
Silica (silicon dioxide)	SiO <sub>2</sub>	O=Si=O
Silicic acid	Si(OH) <sub>4</sub>	$\begin{array}{c} \text{OH} \\   \\ \text{OH} - \text{Si} - \text{OH} \\   \\ \text{OH} \end{array}$
Sodium silicate	Na <sub>2</sub> SiO <sub>3</sub>	
Tetraethyl orthosilicate (TEOS)	Si(CH <sub>3</sub> CH <sub>2</sub> O) <sub>4</sub>	$\begin{array}{c} \text{C}_2\text{H}_5 \\   \\ \text{O} \\   \\ \text{C}_2\text{H}_5 - \text{O} - \text{Si} - \text{O} - \text{C}_2\text{H}_5 \\   \\ \text{O} \\   \\ \text{C}_2\text{H}_5 \end{array}$
Tetrachlorosilane (TCS)	SiCl <sub>4</sub>	$\begin{array}{c} \text{Cl} \\   \\ \text{Cl} - \text{Si} - \text{Cl} \\   \\ \text{Cl} \end{array}$
Silanol	SiOH	Si-OH

**Table 1.1** Chemical formula and structure of the main types of silica used in this thesis.

Silicon in biology is an amorphous product with the general formula:



and it exists in a variety of structural forms (Mann and Perry, 1986).

Much of the silica used in chemistry has a synthetic origin. Amorphous synthetic silica occurs in various forms including sols, gels, sheets and powders and is used in a variety of applications according to its properties (Table 1.2) (Vansant *et al.*, 1995b).

Property	Application
Porosity	Phase in liquid chromatography
Active surface adsorption	Flatten colour in paints and dyes Catalyst base in liquid chromatography Desiccant
Hardness	Reinforcing agent
Particle size	Flow aids
Viscosity and thixotropy	Thickens paints and pharmaceuticals.

**Table 1.2** Properties and uses of synthetic silica.

### 1.2.1 The Occurrence of Silicon.

Silicon is one of the most widely occurring elements in the universe. Silicon is a component in interstellar material, cosmic dust and meteorites and measurements of the prevalence of elements in the solar system have placed silicon below only hydrogen, helium, carbon, nitrogen and oxygen in terms of relative abundance (Leibau, 1985). Silicon is the second most abundant element on earth (25.7%), after oxygen (49.5%) in terms of number of atoms and weight (Leibau, 1985; Dobbie, 1982; Carlisle, 1982; Carlisle, 1974). Sixty percent of the earth's crust is composed of silica ( $\text{SiO}_2$ ) and silicates (including quartz and other rock forming silicates) occupy more than 95% of the volume (Leibau, 1985, Iler, 1955). Crystalline silica occurs naturally in minerals such as quartz and flint (Da Silva and Williams, 1991). Diatomaceous earth on the ocean bed is rich in amorphous silica (Lobel *et al.*, 2000) and volcanic ash is a rich source of soluble silica (Iler, 1955).

It is perhaps surprising that silicon is not commonly associated with life processes considering its abundance and proximity to carbon, the element on which all life depends, in the periodic table. Silica is more often associated with primitive organisms such as diatoms and plants of the horsetail family and may point to a possible role of more importance in the origin of life (Iler, 1955, Hench, 1989).

---

Silica is slightly soluble in water but the mechanisms by which it is dissolved and redeposited remain unclear (Iler, 1955). Silicon exists in seawater mainly as dissolved silica. (2-14,000 $\mu$ g/L; Iler, 1955) Even though the concentration of silica in water is only a few parts per million (ppm) it is utilised by unicellular marine organisms such as diatoms and assembled in an array of wonderfully intricate skeletal cell walls (frustules). The manner in which these skeletons are assembled provides clues as to how silica reacts with water. Siliceous sponges also remove silica from seawater to form skeletons. Hot springs contain more silica (around 700ppm; Iler, 1955) and silicon compounds are vital to certain bacteria that live in them, to the extent that some of them substitute silicon for phosphorous in phospholipids (Liebau, 1955).

Silica is found in large amounts in certain plants and grasses including horsetail, rice, feather grass, bamboo and reed where it has a structural role and contributes to the strength of leaves and stems. The silica content is so high that horsetail has been used for centuries as a 'scouring rush' due to its abrasive properties and bamboo secretes silica into its hollow stems so that a hydrated pure silica gel, tabashir, is formed. This was once believed to be beneficial in treating asthma and tuberculosis. Sodium silicate was prepared from tabashir as long ago as 1791 (Iler, 1955).

The mechanism by which silica is carried into plants and animals is not clear. In view of its low solubility it must be first dissolved from mineral silica and absorbed as monosilicic acid. Plant cell membranes can be penetrated by soluble silicic acid but not by colloidal silica, the same may be true for animal cells (Iler, 1955). Some soluble silica may be present in the soil due to the weathering of rocks. There is some evidence to suggest that acidic compounds such as tannins may be released from plant roots in the soil and that the acidic environment liberates silicic acid from mineral silica (Iler, 1955). It is difficult to prove a nutritional role for silica in plants, as silica free culture media is difficult to prepare. It appears to have an essential role in the growth of beets and is necessary in the normal opening and growth of ears in rice. Silica appears to have importance in the growth of barley and sunflowers. Apart from a few cases there is no evidence to suggest that silica is essential to the growth of most plants. It may have a function in stimulating plants to greater growth by liberating phosphate ions and in maintaining the equilibrium of soil nutrients (Iler, 1955). The importance of silicon in

---

plant life is due to the fact that the fertility of soil relies on the ability of clay minerals to absorb and release water and this is fundamental to plant life and consequently to animals who feed on them (Leibau, 1985).

Silicon is a major structural element in plants and unicellular organisms and forms a major building unit of many amorphous hard structures (da Silva and Williams, 1991). Despite the abundance of the element and the longstanding and widespread use of silica and silicates, many questions still exist in relation to silica in nature. The almost perfectly formed fossils are those petrified with silica but the means whereby silica replaces cellulose and lignin in petrified wood to form an exact replica of the organic matter is not understood (Iler, 1955). It is thought that the silica is initially formed from the decomposition of silicate materials and is both soluble and amorphous in nature allowing diffusion through the specimen (Iler, 1955).

### **1.2.2 Silica in Higher Animals and Man.**

There is considerable variance in the reported tissue concentrations of silica and early measurements reporting higher levels may be unreliable due to the leaching of silica from glassware (Dobbie and Smith, 1982b; Carlisle, 1982). The normal blood level of silica in humans is reported as less than 5ppm and the daily output is around 9mg (Carlisle 1974). Schwartz and Milne (1972) measured the silicon levels in blood and other organs and found the blood level to be ~1ppm. The levels of silicon in parenchymal organs such as brain and muscle varied between 2 and 10ppm. The silicon content of bone and other connective tissues was found to be much higher ranging between 12 and 100ppm (Carlisle, 1986; Schwartz and Milne, 1972). In animals silicon is found in the mucopolysaccharides of skin, muscle, tendon, hair and feathers where it has a structural role (Dobbie, 1982). Silicon has been localised in the intima of blood vessels and the content is decreased in atherosclerosis (Schwartz, 1977). Other body fluids including cerebrospinal, pleural, peritoneal and synovial fluids, measured by atomic absorption spectroscopy, have a silica concentration in the same range as human serum (Dobbie and Smith, 1982b).

Silica enters the human body by ingestion or inhalation. Silica is ingested in food, as cereals, (60%) and beverages, as water and beer (20%) and the average British person consumes 20-50mg of silica per day (Bellia *et al.*, 1994, Birchall, 1995). Ingested silica crosses the small intestinal mucosa where it enters the bloodstream and is cleared from the kidneys (Dobbie and Smith, 1982b; Carlisle, 1982). The nature of the silica absorbed in the gut and the transport mechanisms involved have not been clarified (Rucker *et al.*, 1994) but it is thought that silica is absorbed in the small intestine as silicic acid (Birchall, 1995). Considering that silica is easily excreted in urine (Iler, 1955), it is unclear why it is accumulated in the body in a selective manner.

Inhalation of siliceous dusts have been shown to cause silicosis, a progressive, fibrogenic lung disease (Bagchi, 1992). Renal damage has been associated with the intake of silica in water (Dobbie and Smith, 1992a) and as antacids (Newberne and Wilson, 1970; Dobbie, 1986). A more detailed review of toxic effects of silica is given in Chapter 4.

Silica may have a relationship with molybdenum as plasma and tissue levels of silica are reduced by intake of molybdenum (Carlisle, 1979). A relationship between silica and aluminium in the body has also been suggested (Fahal *et al.*, 1994; Edwardson *et al.*, 1993). Silicic acid seems to react with aluminium to form hydroxyaluminosilicates, thus limiting the availability of aluminium to the body (Fahal *et al.*, 1994; Edwardson *et al.*, 1993). Silica and aluminium are found in the cores of senile plaques and in the neurofibrillary tangles of patients with Alzheimer's disease (Edwardson *et al.*, 1993). The solubility of silica in body fluids is reduced in the presence of certain metal salts including iron and aluminium (Iler, 1955).

### **1.2.3 Silica as an Essential Trace Element.**

The essentiality of silicon in the chick was proposed by Carlisle (1972). Silica was administered in the form of sodium metasilicate ( $\text{Na}_2\text{SiO}_3 \cdot 9\text{H}_2\text{O}$ ) at 100ppm and resulted in enhanced bone growth. In the same year a study by Schwartz and Milne (1972) evaluated the effect of sodium metasilicate supplementation in rats and found similar results. A series of experiments followed which led to silica being accepted as

an essential trace element in animal nutrition (Carlisle, 1972; 1974; 1976a, b; 1980a; 1980b; 1982; 1986; Carlisle and Alpenfels, 1980; Carlisle and Alpenfels, 1986). These centred on the two criteria for establishing essentiality which are 1) repeated and significant responses in growth or health to dietary supplements of the element and that element alone, and 2) development of a deficiency state on a diet which is otherwise adequate (Carlisle, 1974).

Dietary silica supplementation caused increased growth rate, increased amounts of articular cartilage, increased bone water content and biochemical changes in the mineral, hexosamine and collagen content of bone (Carlisle, 1974; 1980a). A silicon deficient diet resulted in stunted bone growth, thinner cortex, altered epiphyseal cartilage morphology and reduced collagen content in chicks (Carlisle, 1980b). A fuller description of the effect of dietary silica supplementaton is given in Chapter 3.

#### 1.2.4 Silica-Containing Biomaterials.

A range of glasses in the system  $\text{SiO}_2\text{-CaO-P}_2\text{O}_5\text{-Na}_2\text{O}$  are defined as having class A bioactivity and bind to bone and soft connective tissues (Lobel and Hench, 1996; Kokubo, 1992; Hench, 1991). They have been used clinically as middle ear implants and endosseous alveolar ridge maintenance implants and show good long term survivability (Hench and Wilson, 1996). The strength of the bond in hard tissues is as strong as bone within 3-6 months and in soft tissues is as strong as the cohesive bond between collagen fibres (Hench, 1998a, b). These materials are reported to cause increased proliferation of osteoblasts and are termed osteoproduative (Wilson and Low, 1992). They are also osteoconductive, in common with class B bioactive materials (such as hydroxyapatite ceramics), meaning that bone grows in direct contact with the implant surface in the body (Hench, 1998a, b).

Silica glass ceramics exhibit bone bonding e.g.. Ceravital, Cerabone and Bioverit (Oliveira *et al.*, 1995; Neo *et al.*, 1993). Bioactive glasses and glass ceramics are used in a range of situations. Apatite- and wollastonite (A/W) containing glass ceramic  $[\text{Ca}_{10}(\text{PO}_4)_6(\text{O},\text{F}_2)]$  is widely used because of its mechanical strength. This material appears to initiate mineralisation in bone cell cultures (Sautier *et al.*, 1994). It is has

proved successful after short and long-term implantation in rat tibiae and human bone and its surface is eventually partially replaced by bone (Neo *et al.*, 1993; 1994). Kokubo (1991) has reviewed the mechanical and biological properties of an A-W glass ceramic. A/W glass ceramic has been used clinically to repair iliac crest donor site defects and to replace vertebrae successfully. Other bioactive, silica containing materials include  $\beta$  wollastonite ( $\text{CaO} \cdot \text{SiO}_2$ ) (Cho *et al.*, 1996b). Silica is the main component of these materials and their bioactivity is dependent to a large extent on the silica content of the material. They lose bone bonding ability when the silica content exceeds 60 mol% (Kokubo, 1992; Hench and Wilson, 1986, Hench, 1991).

A prerequisite to bone bonding is the formation of a biologically active carbonate containing hydroxyapatite layer on a material surface under physiological conditions (Hench, 1991; Kokubo, 1993). Hydrated silica, which is formed on bioactive silica surfaces in the body, nucleates the apatite layer on the implant surface (Hench and Wilson, 1986; Kokubo, 1991). This intermediate apatite layer has compositional and structural characteristics common to those of bone apatite allowing continuity between the implant and bone (Kitsugi *et al.*, 1995). X-ray microanalysis of the surface of some glass ceramics shows that the structure is indistinguishable from the biological apatite of bone (Boyde *et al.*, 1990).

The process by which an apatite layer is formed on a silica surface has been described by Hench (1991) and is summarised in figure 1.6. Initially, alkaline ions are exchanged with hydrogen ions from solution and soluble silica,  $\text{Si}(\text{OH})_4$ , is lost to the solution. A hydrated silica layer is formed at the surface of the material. Subsequently, calcium ions migrate to the surface through the  $\text{SiO}_2$  rich layer and an amorphous  $\text{CaO-P}_2\text{O}_5$  film is precipitated from the supersaturated solution (Hench, 1991). Finally, the film is crystallised by incorporation of hydroxyl or carbonate anions from the solution (Fresa *et al.*, 1996).

It is thought that leaching of the material exposes silanol groups which induce apatite formation at a certain level by taking calcium and phosphate from the body fluid (Oliveira *et al.*, 1995) and liberating some calcium from the implant (Li *et al.*, 1994a, b). A study by Gatti *et al.* (1994) investigated the reactions of a bioactive glass

implanted in soft and hard tissue and concluded that the release of calcium from the glass is enough to form the Ca-P layer but that the release of phosphate is not sufficient indicating that there may be a requirement for phosphate from the tissue fluid. Andersson and Karlsson (1992) noted that the phosphate concentration in the solution increases until the apatite starts to form and then decreases.

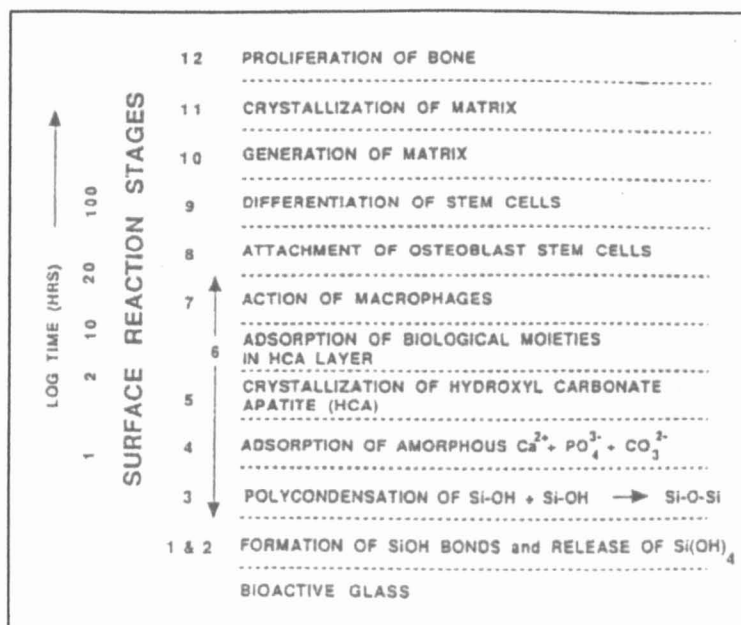


**Figure 1.6** The stages involved in the reaction of a bioactive glass in a biological environment (From: Lobel and Hench, 1996).

It is difficult to study the involvement of silica in bone bonding because apatite inducers (such as  $\text{CaO}$ ,  $\text{Na}_2\text{O}$  and  $\text{P}_2\text{O}_5$ ) dissolve from the materials. This problem has been overcome by the use of a pure silica gel prepared by hydrolysis and polycondensation of tetraethoxysilane (TEOS) in aqueous solution containing poly(ethylene glycol) to study the mechanism of apatite formation (Li *et al.*, 1992; 1995).

Sol-gel prepared silica forms an apatite layer on its surface when immersed in physiological fluid whereas silica glass and quartz do not (Li *et al.*, 1992). The surface structure of the gel is altered by dissolution, ion leaching and precipitation until the surface is stabilised and bone bonding occurs (Andersson and Karlsson, 1992). Dissolution involves the breakdown of the silica network and the release of its constituent elements. Leaching is a rapid process involving the release of other

elements, leaving a silica gel at the surface of the glass. A hydroxycarbonate apatite layer is precipitated onto the surface of the gel and it is this surface to which bone firmly adheres. The thickness of the gel layer is inversely proportional to the failure strength of an implant but only a thin layer (1-2 $\mu$ m) is required for bioactivity (Andersson and Karlsson, 1992). The recent literature concerning the biocompatibility of silica gel *in vivo* and *in vitro* is outlined in Chapter 5.

Recently silica has been incorporated into other biomaterials. A system combining silica glass and poly(methyl methacrylate) PMMA polymer was successfully used as a bioactive, controlled drug delivery system (Arcos *et al.*, 2001). The addition of bioglass to HA ceramics has been reported to increase the bioactivity and fracture toughness of the material, but the overall mechanical strength of the implant was not improved. In contrast, the addition of some phosphate based glasses to HA ceramics caused the mechanical strength to be significantly increased (Tancred *et al.*, 2001).

### 1.3 Aims.

The overall aim of this work is to gain a fuller understanding of the role of silica in the osteoblast. The eventual goal is to incorporate silica into biomaterials to increase biocompatibility should it prove useful in imparting bioactivity to the material. The specific aims are:

1. To establish an *in vitro* cell culture system suitable for investigation of the potential role of silica on osteoblast development.
2. To attempt to validate the work of Carlisle (1972) and Schwartz (1972) *in vitro* using sodium metasilicate supplementation of bone cell cultures to identify any effect on osteoblast differentiation and matrix mineralisation.
3. To assess potential toxic effects of silica resulting from its' use in biomaterials and in the drug industry.

4. To isolate the effect of silica on the osteoblast, in terms of cellular responses to biomaterial surfaces, by producing a silica gel and examining the response of the osteoblast to its surface.

5. To examine the possibilities of including bioactive silica into other biomaterials with the specific aim of improving biocompatibility.

In these ways it is hoped to come to a fuller understanding of the effect of silica on the osteoblast from both the nutritional, toxicity and tissue engineering perspectives to allow future exploitation.

## **Chapter 2**

# **Isolation, Culture and Mineralisation of Human Osteoblasts (HOBs)**

## 2.1 Introduction.

Osteoblast-like cell cultures are a useful way to study isolated cell responses to different substances (eg growth factors and hormones), cell-matrix interactions and the mineralisation process in a controlled environment (Gehron-Robey, 1995). The potential of novel biomaterials can also be evaluated by assessing osteoblast responses to their surfaces *in vitro* (Bosetti *et al.*, 2001). More recently attention has been focussed on tissue engineering applications, where 3-D scaffolds are seeded with autologous cultured bone cells prior to implantation (Anselme *et al.*, 1999) and potential applications in gene therapy (Oreffo and Triffitt, 1999).

The first bone culture system was established by Peck *et al.* (1964). Since then a wide range of culture systems have been developed. The main approaches have been isolation and short term culture after removal from the tissue (primary culture) or establishment of permanent cell lines. Primary cultures are often used as they are thought to retain similar cellular properties to those from the tissue of origin. The sources of the cells are diverse, using cells obtained from donors of different species (mouse, rat, rabbit, chick and human), ages (foetal, neonatal, adult), anatomic locations (marrow stroma, long bone, calvaria, trabecular bone) and cell populations (osteoprogenitor cells (Bellows *et al.*, 1990) preosteoblasts, committed osteoblasts and possibly, osteocytes (Gehron-Robey, 1995). The main limitations of primary cell cultures are that they may consist of mixed cell populations and have the potential to dedifferentiate in terms of phenotypic expression and osteogenic capacity with serial subculture (Majeska, 1996).

Permanent cell lines exist which have been derived from osteosarcomas from rat (ROS, UMR) and human (MG-63 and HOS TE-85) sources. These are large, stable cell populations which exhibit a consistent phenotype, but may have adapted to an *in vitro* environment in terms of growth and phenotypic expression (Majeska, 1996). In addition, cell lines from normal bone have been established. The MC3T3 E1 cell line was established by cloning an alkaline phosphatase rich subpopulation from a mouse calvarial osteoblast culture (Sudo *et al.*, 1983).

As the primary function of osteoblasts is to deposit a mineralised type-1 collagen extracellular matrix, the ability of culture systems to mineralise is of critical importance. Mineralisation *in vitro* occurs in three stages: proliferation of osteoprogenitor cells, matrix deposition and matrix mineralisation. Cell culture methods have allowed the sequence of expression of osteoblast proteins during mineralisation to be elucidated (Boskey, 1994) and helps to clarify their function. When initially plated in culture osteoblast-like cells proliferate rapidly then synthesise collagen and non-collagenous proteins, nodule formation follows and it is these areas, where the microenvironment is controlled, which eventually mineralise. Differentiation of osteoblast cultures *in vitro* follows a distinct set of events as summarised in figure 2.1.1. Components involved in matrix production eg type-1 collagen, fibronectin and osteopontin are expressed early followed by osteonectin and alkaline phosphatase and eventually by osteocalcin (Figure 2.1.1).

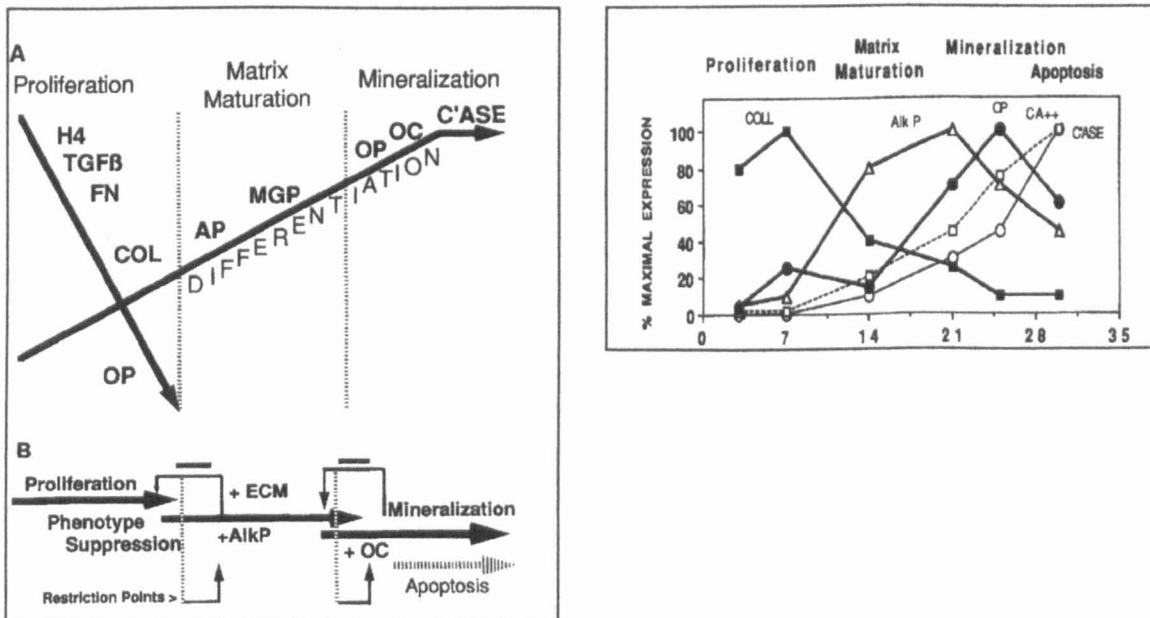


**Figure 2.1.1** Representation of the expression of markers of osteoblast differentiation during mineralisation *in vitro* (From: Stein *et al.*, 1996).

A wider understanding of osteoblast differentiation *in vitro* is seen in the recent literature. Some of the genes and transcription factors controlling bone cells have been recognised (Lechner *et al.*, 2000; Matsuo *et al.*, 1999; Karsenty *et al.*, 1999). Recently new techniques using gene arrays have identified hundreds of genes associated with osteoblast differentiation *in vitro* (Xynos *et al.*, 2001). Substances enhancing osteoblast

proliferation and differentiation include growth factors (such as IGF-1 and 2, TGF $\beta$  1,2 and 3, FGF-1 and 2, PDGF), BMPs, cytokines, fluoride and PTH (Canalis, 1996). Epinephrine stimulated DNA synthesis and ALP activity in MC3T3-E1 cells but had little effect on collagen synthesis and osteocalcin (Suzuki *et al.*, 1998). Chevalley *et al.* (1998) reported that supplementation of MC3T3-E1 cells with arginine caused increased IGF-1 production, collagen-1 synthesis, ALP activity and reduced osteocalcin production. Recently, the induction of a mineralised collagenous matrix has been described in the absence of cells using a mixture of collagen-I and a nucleating protein composed of collagen binding proteins and BSP (Hunter *et al.*, 2000).

Osteoblast-like cultures do not mineralise without the addition of certain supplements. Ascorbic acid is necessary for collagen cross-linking and is used almost universally in bone culture systems (Majeska, 1996). It has also been implicated in the stimulation of cell proliferation and alkaline phosphatase activity and in modifying the effect of vitamin D on osteoblast differentiation (Gronowicz and Raisz, 1996). Other supplements are used whose method of action remains unclear. Calcium and sodium  $\beta$  glycerophosphate (BGP) are known to promote mineral formation in cultured cells (Ralphs and Ali, 1986). This is achieved because BGP is a substrate for alkaline phosphatase and increases the amount of available phosphate to the cells (Gronowicz and Raisz, 1996). Dexamethasone (DEX) is a synthetic fluorinated glucocorticoid which is reported to induce the differentiation of osteoblasts from marrow stromal populations (Rickard *et al.*, 1994). The osteoblast phenotype is not expressed in marrow stromal cultures without its addition (Ohgushi *et al.*, 1996). The addition of DEX to foetal rat calvarial cultures causes an increase in the size and number of nodules (Bellows *et al.*, 1987). Both DEX and BGP are used in many marrow (Ohgushi *et al.*, 1996; Morais *et al.* 1998) and calvarial cultures (Bellows *et al.*, 1987; Bellows *et al.*, 1990).

Many cell lines do not appear to have osteogenic potential, that is, the ability to form a mineralised extracellular matrix, *in vitro*. Most cell lines established from osteosarcomas do not mineralise including SaOS-2, ROS, UMR and MG-63 (Ikeda *et al.*, 1992). The notable exception here is the cell line HOS TE-85 which develops a mineralised extracellular matrix with a Ca:P ratio of 1.34 when cultured with the addition of BGP (but not without). The electron diffraction patterns of the mineralised areas were

identical to those of synthetic non-oriented HA crystals. In these cultures mineral deposits were initially identified in matrix vesicles (Ikeda *et al.*, 1992). Permanent cell lines from normal bone have a mixed ability to form bone *in vitro*. The ROB-C26 multipotential cell line from rat calvaria has the ability to synthesise osteocalcin when supplemented with BMP-2, retinoic acid and vitamin D but its' osteogenic capacity remains unclear (Kirk and Kahn, 1995). The MC3T3 E1 cell line has the capacity to form mineralised nodules, via matrix vesicles, in the absence of BGP, DEX or ascorbate supplementation after extended periods of culture. The mineral formed had a Ca:Pi ratio close to that of HA and was identified as non oriented HA by electron diffraction (Sudo *et al.*, 1983). The cells express osteoblastic markers such as alkaline phosphatase and osteocalcin and the parathyroid hormone receptor (Fratzl-Zelman *et al.*, 1997).

Many primary cultures derived from animal sources have shown osteogenic potential *in vitro*. Foetal rat calvarial cells have the capacity to form a mineralised matrix when BGP is added to the growth medium (Bellows *et al.*, 1990). Newborn mouse calvarial cells produced mineral only in the presence of BGP (Ecarot-Charrier, 1983). Chick calvarial cells produced non matrix vesicle associated mineralised deposits with a Ca:Pi ratio of 1.1-1.4 when BGP was included in the growth medium. The deposits were identified as poorly crystalline HA (Gerstenfeld, 1988). Primary cultures from bone marrow stromal cells have the ability to mineralise also. The system developed by Maniopoulos *et al.* (1988) forms mineralised nodules in the presence of ascorbate, BGP and DEX. The mineral produced can be identified as poorly crystalline carbonated HA by FT-IR and XRD techniques and is similar to that of rat bone (Ohgushi *et al.*, 1996)

Human primary osteoblast culture models have been developed and these also demonstrate a mixed capacity for mineralised matrix production. One of the first primary human cultures was established by Wergedal and Baylink in 1984 using isolations from human iliac crest and femoral head which which had an alkaline phosphatase rich subpopulation but osteogenic potential was not demonstrated. Subsequently, Marie *et al.* (1990, 1995) isolated human endosteal osteoblastic cells from the trabecular bone surface of iliac crest. The characteristics of these cells included high alkaline phosphatase activity, cAMP production in response to parathyroid hormone,

---

responsiveness to vitamin D<sub>3</sub>, production of type-1 collagen, osteocalcin, osteopontin, bone sialoprotein and thrombospondin but did not produce mineral.

Mineralisation has occurred in human primary cultures however. Physiological concentrations of glucocorticoid were required for induction of osteogenic potential in adult human trabecular bone cultures (HBDC) which produced type-1 collagen, alkaline phosphatase and osteocalcin without its addition (Gundle and Beresford, 1995). Osteoblastic cells have been isolated from adult human trabecular bone fragments. These cultures form collagen rich nodules that start to mineralise using matrix vesicles but never become heavily mineralised (Gehron-Robey 1995). Primary human osteoblasts isolated from femoral heads removed during surgery have been characterised by Di Silvio (1995). These cells exhibit a typical osteoblast morphology, form multilayers and become mineralised over a period of ~4 weeks without supplementation with inducers of mineralisation. Markers of osteoblast differentiation were also expressed including alkaline phosphatase activity, osteocalcin and type-1 collagen production as well as cyclic AMP production in response to parathyroid hormone.

The overall aim of this thesis is to investigate the role of silica in the osteoblast both from nutritional and biomaterial points of view. It is desirable to first identify the characteristics and limitations of the chosen osteoblast model. The system used by Di Silvio (1995) purports to form mineral without the addition of DEX and BGP and will be used in these studies. Little is known about the cell ultrastructure during extended culture (4 weeks) and the formation of mineral. The aim of this Chapter is to describe the isolation and characterisation of a primary human osteoblast culture from femoral head trabecular bone and to characterise the system over extended periods of culture in terms of expression of osteoblastic markers and osteogenic potential. The ultrastructure of the cells as they undergo mineralisation and the effect of DEX and BGP on the process will also be investigated.

## 2.2 Materials and Methods.

### 2.2.1 Isolation of Primary Human Osteoblasts.

Human Osteoblasts (HOBs) were isolated from the trabecular bone of patients undergoing total hip arthroplasty according to the method of Di Silvio (1995). The femoral head was obtained from surgery and fragments of trabecular bone (1-2mm) were excised from the cut surface of the neck under sterile conditions. These were rinsed several times in sterile phosphate buffered saline (PBS) to remove blood cells and fat. The bone chips were then placed in petri dishes containing Dulbeccos modified eagles medium (DMEM) supplemented with 10% foetal bovine serum (batch 06F7267B; Gibco), 0.02M L glutamine, 0.01M Hepes, 1% non essential amino acids, 150µg/ml 1 ascorbic acid and 100 units/ml penicillin streptomycin solution. These were maintained at 37°C in a humidified atmosphere of 5% CO<sub>2</sub>; 95% air. The medium was changed daily. After 4-5 days crescents of long spindle shaped cells were seen on the surface of the bone chips (Figure 2.1a). After 2 weeks in culture the chips were digested to allow for the release of bone cells. The bone fragments were incubated in a mixture of trypsin (0.02%) and collagenase (100 units/ml), buffered with Hepes (0.01M), for 20 min at 37°C on a rotary mixer. The bone chips were then removed from the solution which was centrifuged at 1000rpm for 10 min to obtain a cell pellet. The cells were resuspended in fresh medium, seeded into a 25cm<sup>2</sup> sterile tissue culture flask (Falcon) and maintained in culture for several weeks. The spindle-shaped cells were eventually replaced with squat polygonal cells which assumed a cuboidal morphology once confluency was reached (Figure 2.1b-d). The osteoblast-like nature of the cells was characterised by the cuboidal morphology (Figure 2.3.1c) and activity of the alkaline phosphatase enzyme. Cells were passaged using a trypsin / Hepes (0.02% trypsin; 1% Hepes) solution in PBS and cells at various passages were frozen in 10% DMSO in FBS and stored in liquid nitrogen for future use. Cells from two separate primary cultures were used in this work. The first were cells from the primary isolation carried out by Di Silvio (1995) and had been characterised by the production of ALP, collagen-1, osteocalcin and cAMP production in response to parathyroid hormone. The second isolation was prepared during the course of this thesis and were characterised by the production of ALP, collagen-1 and nodule

formation. Cells were passaged up to 40 times without noticeable loss of phenotype in terms of ALP and nodule formation.

## **2.2.2 Long Term Cell Culture.**

### **2.2.2.1 Cell morphology.**

For long term cell culture experiments (up to 28 days) cells were trypsinised and seeded at a density of  $8 \times 10^4$  cells/ml on Thermanox coverslips (Nunc) in 24 well Falcon tissue culture plates. The cultures were re-fed every 2-3 days. At various stages during long term experiments cultures were photographed using a Nikon EM camera mounted on a Nikon Diaphot inverted phase contrast microscope.

### **2.2.2.2 Cell activity and cell number.**

The alamar Blue assay (Serotec) was used to measure cell activity in osteoblast cultures up to 28 days. This assay quantifies metabolic activity by utilising a REDOX indicator that is changed to a fluorescent product in response to the chemical reduction of the medium by growing cells. Recent research suggests the active indicator to be resazurin, which is converted to the fluorescent resorufin by reduction and that the test is a measure of the redox status of the cells (Rasmussen, 1999). The medium was removed from the cultures and they were gently rinsed in Earles' balanced salt solution (EBSS). A 1 in 20 dilution of alamar Blue dye in Hanks' balanced salt solution (HBSS) was prepared and 1ml of this solution was added to each well. The plate was incubated under normal conditions for 20 mins. Aliquots (100 $\mu$ l) from each well were placed in a 96 well plate and the fluorescence was measured at 560nm excitation wavelength and 590nm emission wavelength on a cytofluor plate reader.

The cultures were then rinsed in sterile PBS and 1ml of sterile double distilled water was added to each well. The cells were lysed by repeated freeze thaw and stored at  $-20^{\circ}\text{C}$  for analysis of cell number and alkaline phosphatase activity.

Cell number was determined using the fluorochrome bisbenzimidazole (Hoechst 33258, Sigma) as described by Rago *et al.* (1990). This fluorochrome binds cellular DNA which causes enhanced fluorescence and a specific shift in emission wavelength which results in a linear relationship between fluorescence and DNA content. DNA standards were prepared from 20µg/ml stock solutions of purified calf thymus DNA (Sigma) to give a DNA content of 10, 6, 5, 4, 3, 2, 1, 0.5 and 0.25 µg/ml per well. Aliquots from cell lysates were placed in 96 well tissue culture plates. A 1 in 50 dilution of the dye in TNE buffer (10mM Tris, 2M NaCl and 1mM EDTA; pH 7.4) was prepared from a 1mg/ml stock solution and an equal volume of this (100µl) was added to the test solutions and standards in the plate. Fluorescence was measured immediately at 350nm excitation wavelength and 460nm emission wavelength on a cytofluor. A standard curve was prepared and DNA values were calculated.

### **2.2.3 Characterisation of the Osteoblast Phenotype.**

#### **2.2.3.1 Alkaline phosphatase activity.**

Alkaline phosphatase activity of cell lysates was measured. The alkaline phosphatase assay was performed at room temperature (pH 9.8) using the Granutest kit for detection of alkaline phosphatase (ALP) activity (Merck). The assay works on the principle that 4-nitrophenylphosphate is converted to 4-nitrophenol and phosphate in the presence of alkaline phosphatase. The rate of increase in 4-nitrophenol is directly proportional to the AP activity in the sample and can be determined colorimetrically. Equal volumes (50µl) of 4-nitrophenol phosphate and test sample were added to a 96 well plate. The absorbance was read after 5 min on an Anthos plate reader using 405nm as the test wavelength and 620nm as the reference wavelength.

#### **2.2.3.2 Immunofluorescence labelling of osteoblast markers**

Osteoblast cultures were labelled at 7 days with monoclonal antibodies to osteopontin (MPIIB10), osteonectin (AON-1) and alkaline phosphatase (B4-50) The antibodies were obtained from the Developmental Studies Hybridoma Bank developed under the auspices of the NICHD and maintained by The University of Iowa, Department of

Biological Sciences, Iowa City, IA 52242. Cultures were stained at 7 and 21 days with a collagen-1 antibody (Sigma). The staining protocol was similar for all antibodies. Cultures in which the primary antibody was substituted with either PBS or normal mouse serum were used as controls. Cells were fixed in 4% paraformaldehyde for 30min. They were permeabilised in a triton X-100 mixture (0.5% Triton X-100 in 20mM Hepes, 300mM sucrose, 50mM NaCl, and 3mM MgCl<sub>2</sub>) for 5min at -20°C and incubated in several changes of 1% PBS/BSA before being incubated in the primary antibody for 1hr at 37°C. Osteopontin, osteonectin and alkaline phosphatase antibodies were used undiluted and collagen-1 was diluted 1:1000 in PBS/BSA. The cells were thoroughly rinsed in 1% PBS/BSA and incubated in an FITC (fluorescein isothiocyanate) conjugated secondary antibody (1:20 rat anti-mouse antibody, DAKO) for 1hr at 37°C. After rinsing the cells were counter-stained using 0.01mg/ml propidium iodide (PI) for 30 seconds, mounted in glycerol DABCO (2mg/ml DABCO (Diazabicyclo[2.2.2]octane)in PBS, combined with glycerol/ PBS mix, 9:1) and viewed using a Leica TCS 4D confocal laser scanning microscope (CLSM). The green fluorescence of the antibody staining was viewed using the 488nm laser line. The red fluorescence of PI was viewed simultaneously using the 568nm laser line.

## **2.2.4 Cell Ultrastructure.**

### **2.2.4.1 Scanning electron microscopy (SEM).**

Cells on Thermanox discs (2 and 28 days) were fixed in 1.5% glutaraldehyde in 0.2M hepes buffer for 30 min and post fixed in 1% osmium tetroxide in Millonigs buffer (OsO<sub>4</sub>) for 30 min. Discs were then dehydrated through a graded ethanol series, immersed in hexamethyldisilazane (HMDS) for 10 min and air-dried. Samples were mounted on aluminium stubs using sticky carbon tabs. The samples were coated with gold using an Emscope sputter coater for 2 min at 25mA. The discs were viewed using a Philips 501B SEM operated at 10kV. For some 28 day cultures the upper layer of cells were removed using sticky tape and the resulting sample was recoated and examined in a Philips XL30 Field emission environmental scanning electron microscope (FEG-ESEM). Likely areas of mineralisation were analysed using EDX microanalysis.

#### 2.2.4.2 Transmission electron microscopy (TEM).

At 7, 14, 21 and 28 days, cells were fixed and dehydrated as described above. Discs were placed in a glass petri dish containing dried acetone for 5 min and then transferred into Transmit resin (TAAB) for 3hrs. The discs were then inverted onto plastic capsules containing fresh resin and polymerised overnight at 70°C. The following day the discs were fractured off the resin using liquid nitrogen, leaving the cells embedded in the resin block. The block was then re-embedded in fresh resin and polymerised as before. The resulting block was trimmed and remounted on a pre-formed block for sectioning. This allowed the cell layer to be sectioned *in situ*, without disturbing the ultrastructure of the nodules. Sections (70-90nm) were cut using a Reichert Ultracut E microtome. These were contrasted with uranyl acetate and Reynolds lead citrate and viewed in a Philips 410 TEM operated at 80kV.

#### 2.2.5 Mineralisation.

Mature cultures (28 days) were stained with Alizarin red S according to a method adapted from Fernandes *et al.* (1997) to identify calcium deposits. Bone chips were used as positive controls and were stained using the same method. The medium was removed from the cultures and they were rinsed in tris buffered saline (TBS, 0.45% NaCl, 0.6% tris base, 2.5% 1M HCl, pH 7.4). Cultures were fixed in 4% paraformaldehyde for 5 min and stained with a 1% Alizarin red S solution in 0.028% NH<sub>4</sub>OH for 2 min after which the samples were rinsed in TBS, mounted in glycerol DABCO and photographed immediately.

Von Kossa's staining method was used to visualise calcium deposits in HOB cell cultures at 28 days. This technique substitutes silver for calcium ions in calcium phosphate. The silver salt produced is reduced to black metallic silver under UV light. The method used was modified from Fernandes *et al.*, (1997). Cultures were fixed in 1.5% glutaraldehyde in 0.1M sodium cacodylate buffer for 30 minutes. The fix was removed, cells rinsed in TBS and covered with a 5% silver nitrate (Sigma) solution for 30 min under UV light. Cells were rinsed in water and covered with 5% sodium

thiosulphate solution for 2 min. Calcium deposits stained black. Cultures were mounted in glycerol and photographed.

### **2.2.6 Effect of Mineral Supplements.**

In some cultures the tissue culture medium was supplemented with Dexamethasone ( $10^{-8}$  M; Sigma) and/or sodium  $\beta$  glycerophosphate (10mM; Sigma) to test their efficacy as promoters of calcification. Cultures were stained with alizarin red S to identify mineralised areas at 14, 21 and 28 days.

A semi-quantitative method for the detection of calcium in bone cultures (Hale and Santerre, 2000) was carried out at 21 and 28 days. The HOB cultures were incubated with medium containing  $1\mu\text{g/ml}$  calcein (Sigma) for 4hrs. The medium was then removed and the cultures overlaid with 1ml of PBS and read on a cytofluor at 485nm excitation, 530nm emission.

Immunofluorescence labelling of calcium with calcein was carried out at 21 days (Hale and Santerre, 2000). Cells were treated with culture medium containing  $5\mu\text{g/ml}$  calcein overnight, rinsed with PBS and viewed using a Leica TCS 4D CLSM. The 488nm laser line was used to view the green fluorescence of the calcein labelling. The samples were counter-stained with PI so the cell nuclei could be visualised using the 568nm laser line.

TEM was carried out, to visualise any mineral formed by HOBs in the presence of DEX and BGP. Cultures were fixed and processed at 21days as previously described. Cells grown for 21days in control medium were used as controls.

Statistical analysis of all assays in this section was carried out using a one way analysis of variance (ANOVA) with a Tukey-Kramer post test for multiple comparisons.

## 2.3 Results.

### 2.3.1 Isolation and Culture of HOBs

Figure 2.1 shows the isolation process and morphology of cultured human osteoblasts. Cells grew on the surfaces of bone chips in culture and these were released with trypsin and plated in tissue culture flasks. The cells were spindle shaped at first, but after a period of weeks became squat and polygonal in shape. Confluent cell monolayers had a cobblestone appearance.

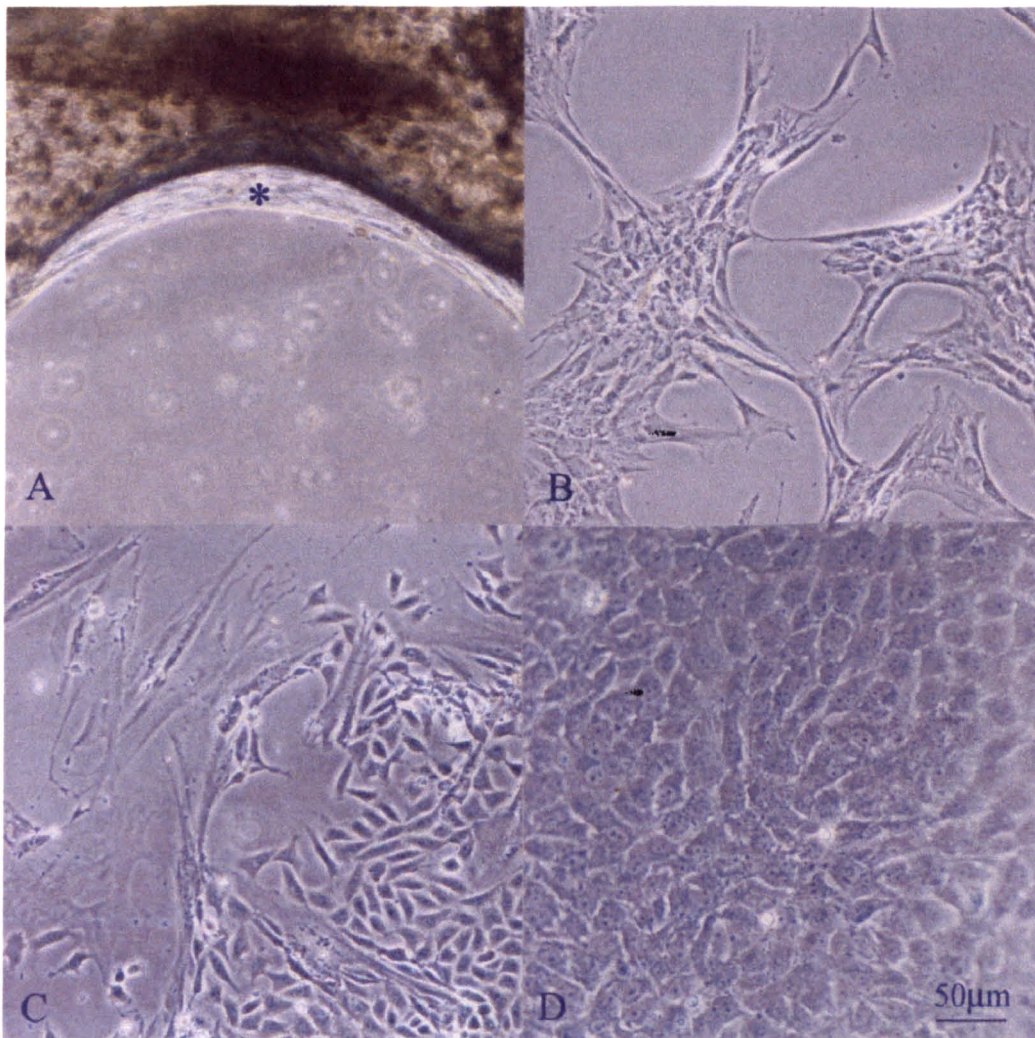


**Figure 2.1** Phase contrast images of the isolation and culture of primary human osteoblasts (HOBs). (A) A bone chip in growth medium for 5 days showing crescents of cells attached to the bone surface (\*). (B) Morphology of primary osteoblasts in culture after collagenase digestion showing spindle shaped cells. (C) Morphology of HOBs after 2-3 weeks in culture showing the changing morphology of the cells to a squat, polyhedral shape. (D) A confluent layer of HOB cells with a typical cuboidal morphology.

### 2.3.2 Long Term Culture of Primary Osteoblasts.

#### 2.3.2.1 Cell morphology.

Human osteoblasts were successfully cultured on Thermanox discs in 24 well Falcon tissue culture plates for up to 35 days. Figure 2.2 shows phase contrast images of the time course of HOB differentiation in culture. The cells were confluent by 48 hours and had started to form layers by 4 days. At 7 days multiple layers of cells were present. At some time between 10 and 20 days in culture the cells began to form clusters in some areas. These later developed into nodular structures which eventually became distinct, mature nodules. Nodules started to form at any time between 20 and 30 days cell culture. Numerous large (up to 0.5mm across) nodules formed in each well and they were visible to the naked eye.

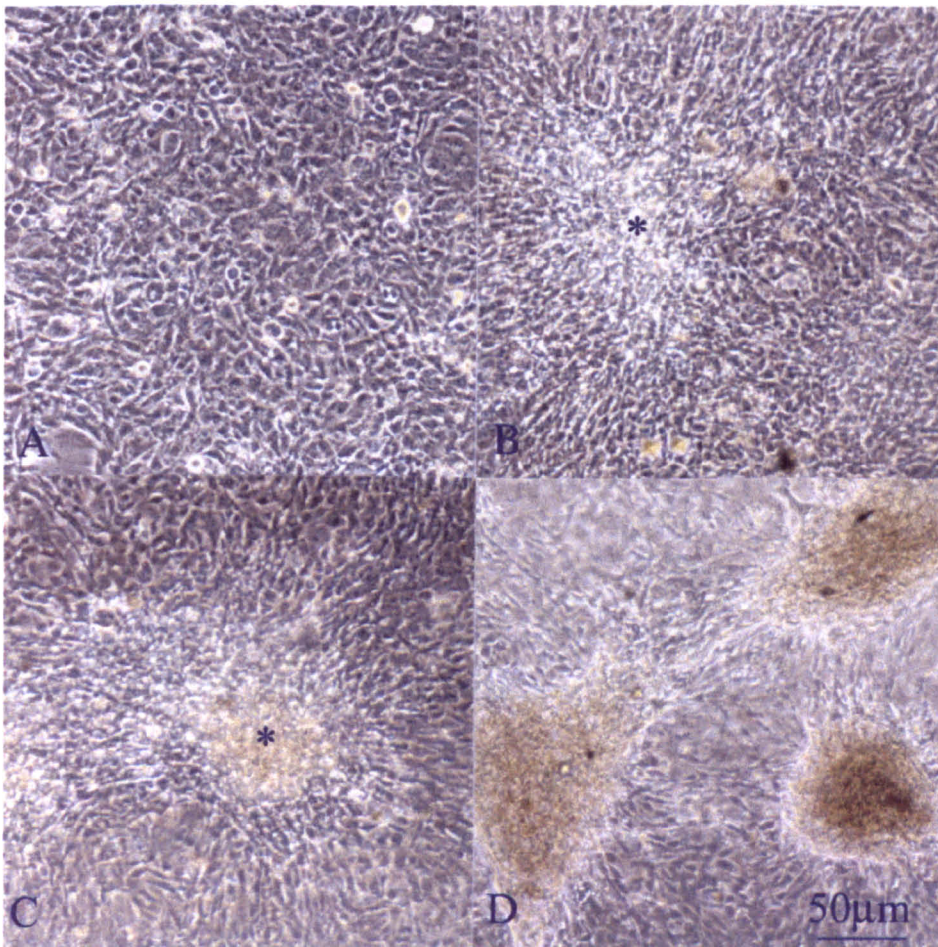


**Figure 2.2** Phase contrast images of HOBs showing the different stages of development during long term cell culture. (A) HOB cells cultured for 7 days showing a confluent multilayer. (B) HOBs cultured for 14 days showing localised cell clusters (\*). (C) At 21 days nodular structures are present (\*). (D) By 28 days nodules are large and well defined.

## 2.3.2.2 Cell activity and cell number

Figure 2.3.3 shows the mitochondrial activity, measured by alamar blue reduction (a) and number of HOBs (b) during long term culture (up to 28 days) studies. A standard calibration for the DNA assay is shown in (c).

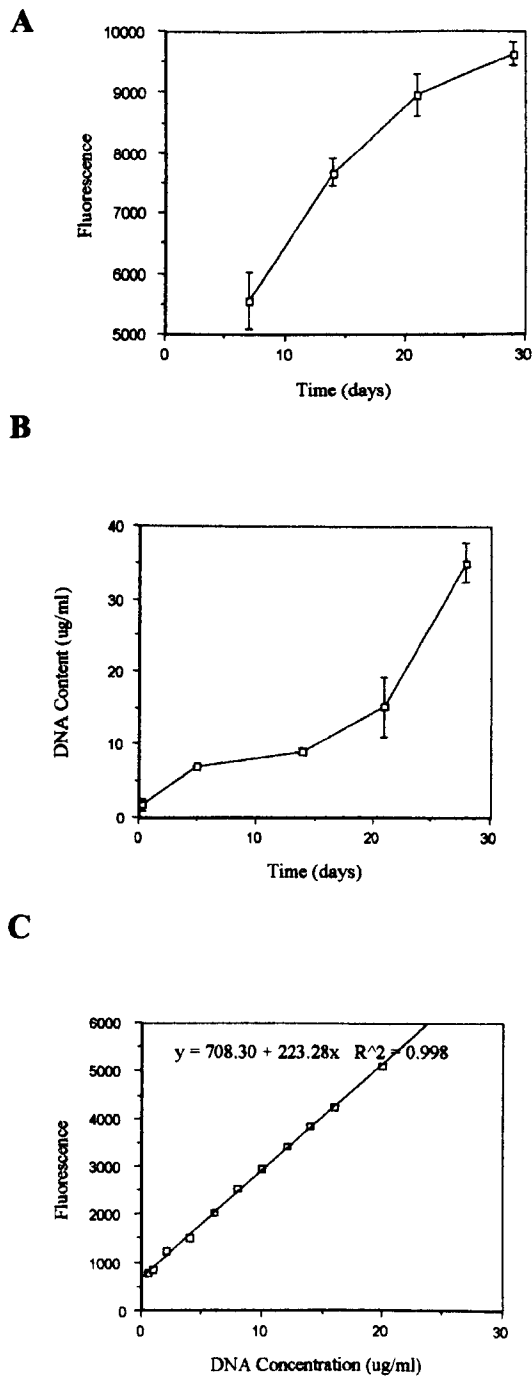


**Figure 2.3.3** Cell activity measured by alamar blue reduction (a) and DNA content (b) of HOBs cultured for 4 weeks. Bar represents standard error of the mean, n=4. (c) shows the calibration for the DNA assay.

Generally both these increased with increasing lengths of time in culture. Occasionally cell activity and number were reduced between days 25 and 28.

### 2.3.3 Expression of Phenotypic Markers.

#### 2.3.3.1 Alkaline phosphatase activity.

Human osteoblasts produced alkaline phosphatase as demonstrated by the assay for ALP activity (Figure 2.4)

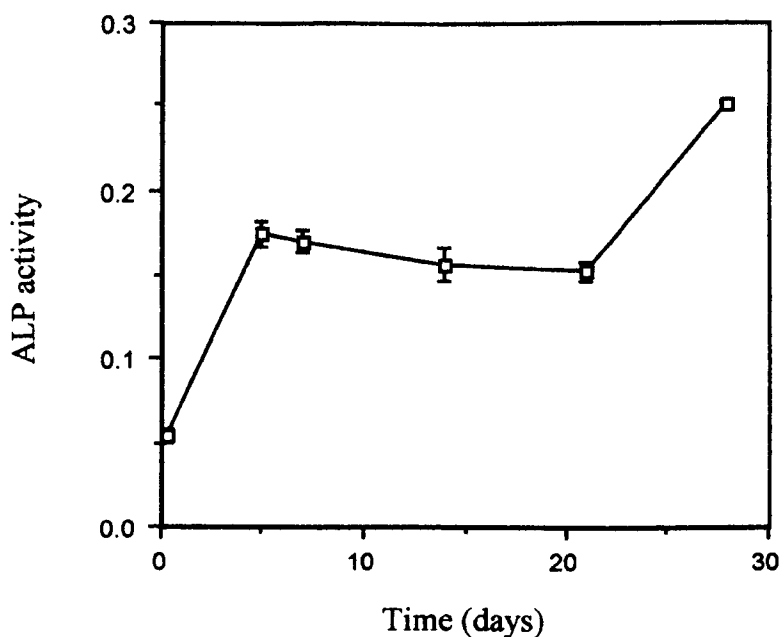


**Figure 2.4** Activity of the alkaline phosphatase enzyme in HOB cultures over a 28 day time period. Error bars represent standard error of the mean, n=4.

#### 2.2.3.2 Immunolocalisation of osteoblast markers.

HOBs stained positively for ALP, OP and ON at 7 days cell culture as seen by CLSM (Figure 2.6). OP and ON staining was cytoplasmic while ALP staining was localised to the cell periphery. Collagen-1 staining was seen in the intercellular spaces at 7 and 21 days cell culture by CLSM (Figure 2.7). Where nodules were present, staining was

confined to the upper few cell layers of the nodule and the surrounding cell multi-layers, but was absent from the centre of the nodule. Cell nuclei in this region appeared small and were stained densely and homogeneously with PI in contrast to the other areas where the nuclear membrane and nucleoli were discernible.

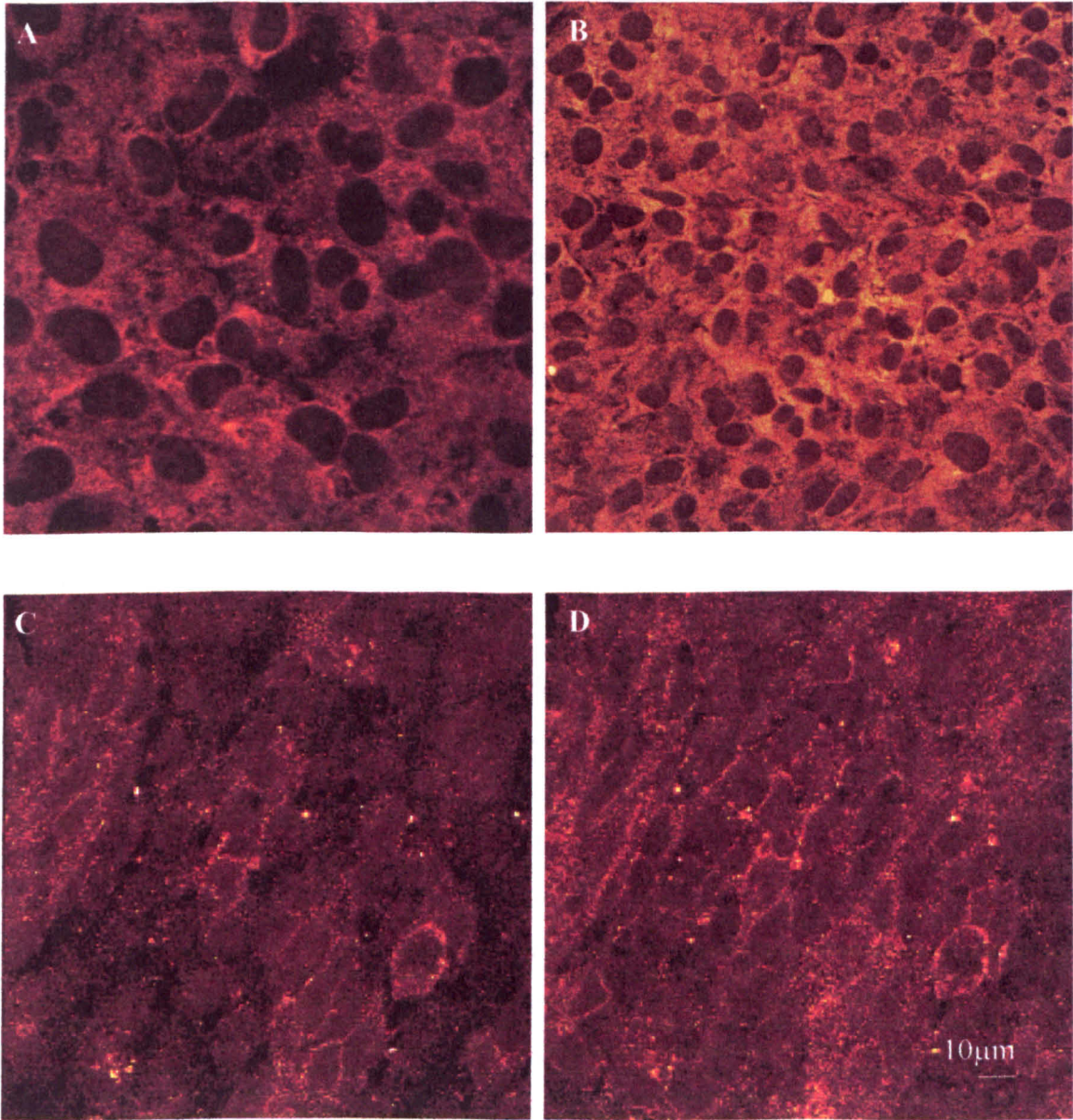


**Figure 2.5** CLSM images of 7 day HOB cultures stained with antibodies to osteonectin (A), osteopontin (B) and ALP (C, D). Osteonectin and osteopontin are localised to the cell cytoplasm. ALP is located at the cell membranes.

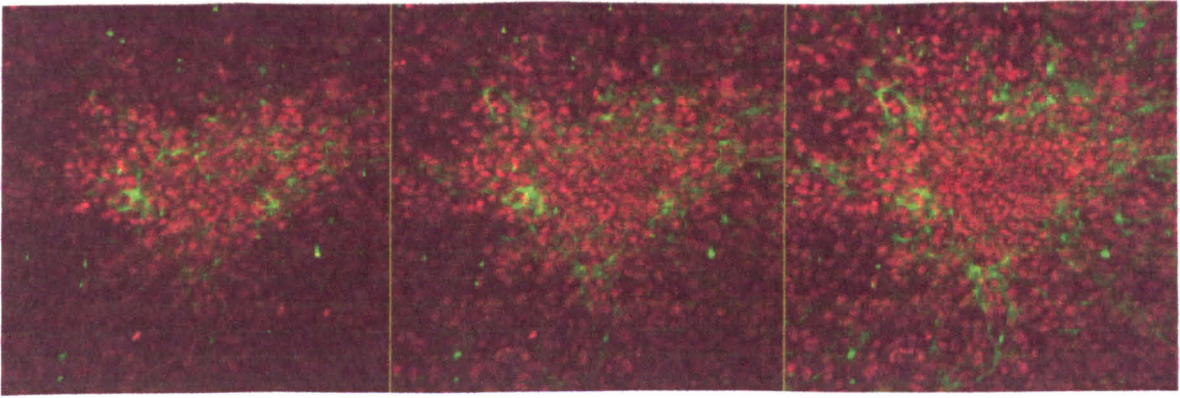


**Figure 2.6** CLSM image showing a gallery of optical slices through a nodule in a day 21 HOB culture. Collagen-1 (green) is localised to the upper cell layers of the nodule and the cell layers around the nodule, but is absent from the interior. Cell nuclei (red) are smaller and tightly packed in the centre of the nodule compared to those of the surrounding cell layers.

### 2.3.4 Ultrastructure.

#### 2.3.4.1 SEM.

Scanning electron microscopy (SEM) was used to demonstrate the topography of the HOB cells in culture (Figure 2.7). Initially cells were polyhedral in shape and were anchored to the surface of the Thermanox disc by numerous cytoplasmic processes. As a multilayer formed, the cells assumed a flattened shape with short processes on their dorsal surface and formed sheets that covered the surface of the disc. Only some cells on the surface of the multilayer or dividing cells retained a rounded / polyhedral profile. The morphology of the cells remained the same when nodules formed. These could be identified clearly at low magnifications. SEM of 28 day samples where the top had been removed from the cultures showed the interior of the nodule. Collagen was not seen. EDX analysis of the nodule interior did not show evidence of calcium phosphate deposits.

#### 2.3.4.2 TEM.

Transmission electron microscopy was used to investigate the cell ultrastructure as shown in figure 2.8. The cells were large with an oval nucleus and several nucleoli. The nuclear morphology suggested the cells were active as little heterochromatin was seen.

---

The cell membrane extended as long fine processes which passed between, and occasionally formed junctional complexes with, neighbouring cells. The secretory nature of the cell was demonstrated by the organelle content. A typical osteoblast exhibited a large, perinuclear golgi complex, rough endoplasmic reticulum, mitochondria and deposits of glycogen. Bundles of type-1 collagen were interspersed between cells from 5 days cell culture.

Sections of cultures at later time-points revealed the structural organisation of the nodules. Figure 2.9a shows a semi-thin (0.5 $\mu$ m) resin section stained with toluidine blue. This demonstrates that the outer layers of the nodule contained cells whose ultrastructure resembled that described above while the inner portion contained many intercellular spaces and dying cells. TEM of the different parts of the nodule are shown in the remainder of the figure. The nuclei of the cells in the interior of the nodule contained clumps of heterochromatin and the cytoplasm was composed of vesicles and unidentified, extensive electron dense deposits. Although collagen bundles were present, evidence of a mineralised matrix was not observed, either in the extracellular spaces or among the collagen fibres and bundles.

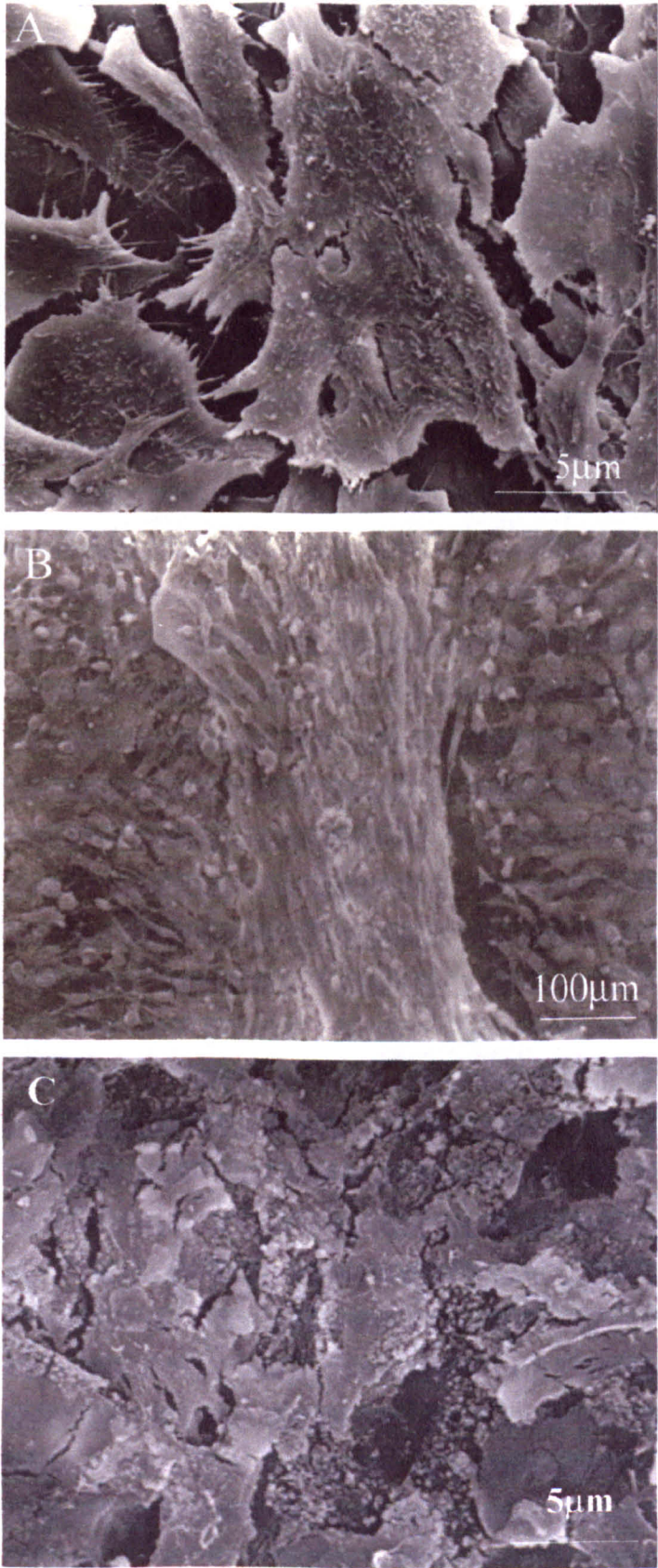


**Figure 2.7** Scanning electron micrographs of HOB cells. (a) A 7day culture showing a cell multilayer (right = top, left = bottom). The cells are flattened and have short dorsal processes. The bottom cell layer is anchored to the surface by long cytoplasmic processes. (b) A low magnification image of a 28 day culture showing a nodule. (c) A 28 day culture with the upper cell layers of the nodule removed

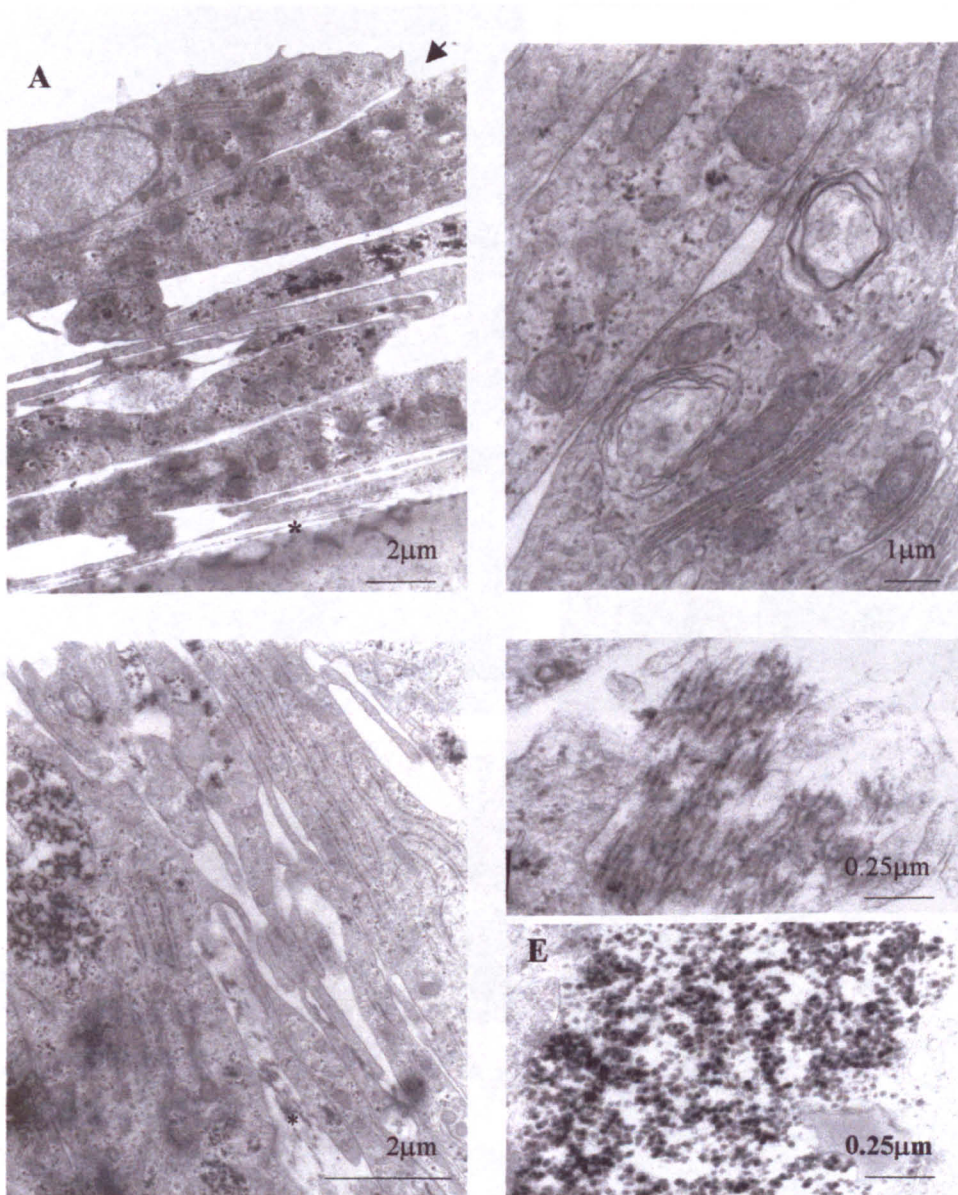


**Figure 2.8** Ultrastructure of HOBs. (a) A 7day HOB culture showing the typical morphology of the cell layers. Cells contain mitochondria and rough ER consistent with their secretory nature. A cell-cell contact is seen (arrow). The base of the culture is marked with (\*). (b) Cell ultrastructure at 14days showing golgi apparatus. (c) Collagenous matrix between cell layers at day14 (\*). (d) and (e) Collagen fibres in a 20 day culture.

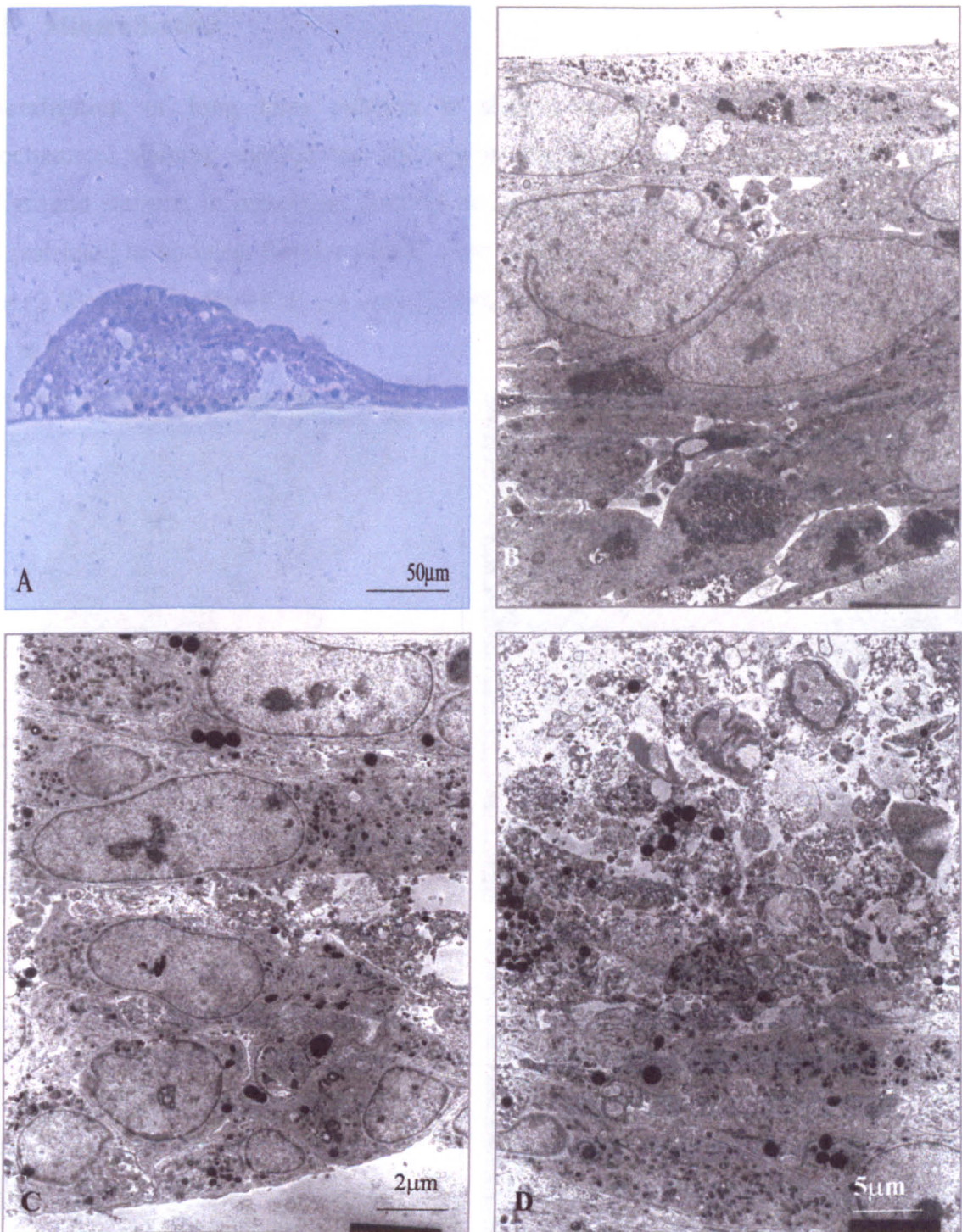


**Figure 2.9** Ultrastructure of nodules. (a) A resin section through a nodule of a 20 day culture stained with toluidine blue. The outer layers of the nodule appear to consist of healthy cells while the interior appears less homogeneous. (b) TEM image of a section through a similar nodule. (c) Ultrastructure of cells in the outer layers of the nodule. (d) Ultrastructure of cells in the nodule interior.

### 2.3.5 Mineralisation

Mineralisation of long term cultures is shown in figure 2.10. Alizarin red S histochemical staining showed red staining in the bone chip (2.10a) but only weak background staining in osteoblast cultures at 28 days (Figure 2.10b). Positive staining was restricted to nodules. Similar results were observed for von kossa staining of bone chips (2.10c) and 28 day HOB cultures (2.10d). For an image of an unstained bone chip refer to figure 2.1a.

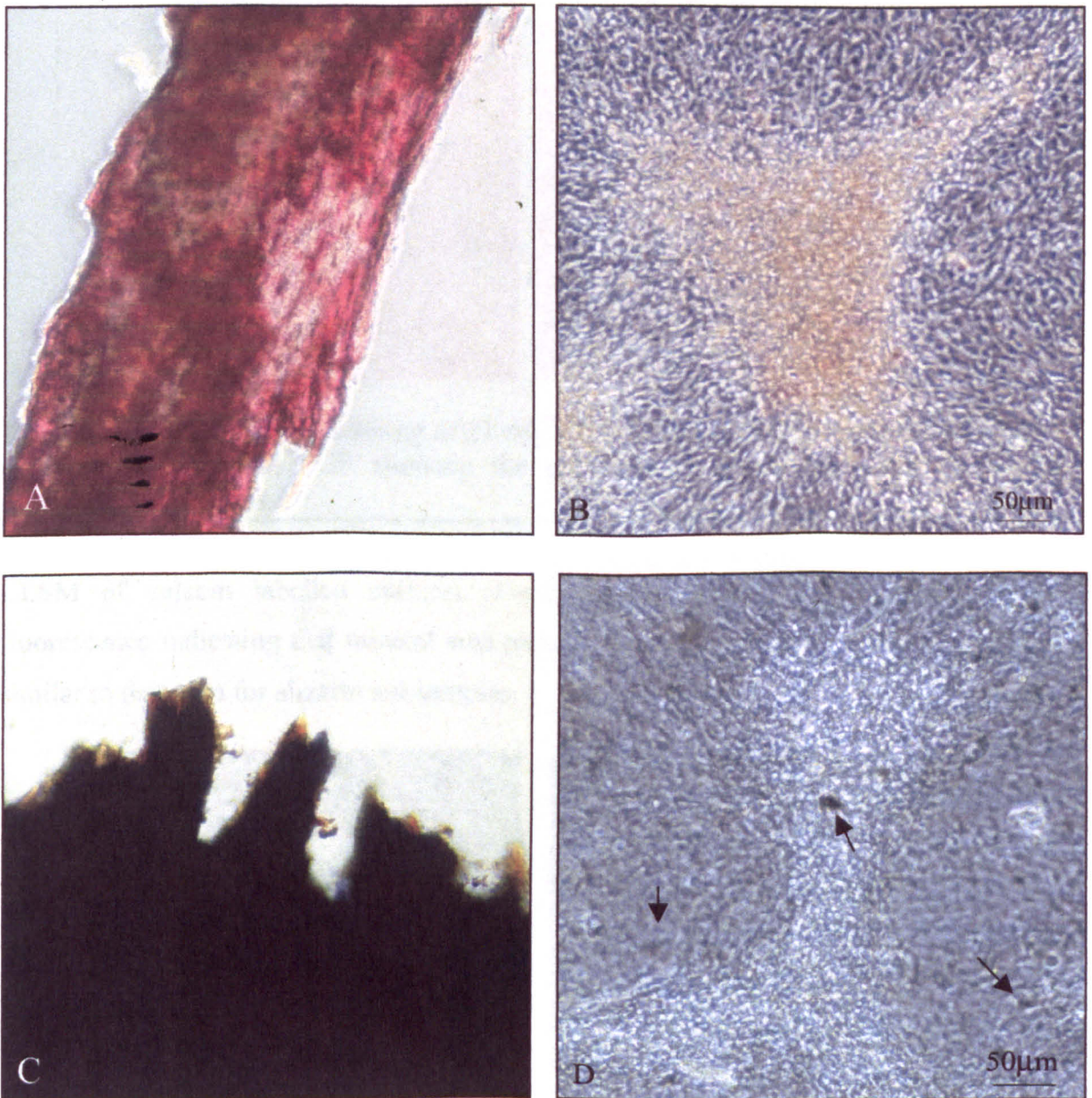


**Figure 2.10** Mineralisation of HOB cultures. (A) Bone chip stained with alizarin red S for calcium deposits (red). (B) Day 28 nodules stained with alizarin red S. The nodule has stained faint red. (C) Bone chip stained with von Kossa for calcium deposits (black). (D) Day 28 nodules stained for calcium deposits. Small areas of positive staining are seen (arrows).

### 2.3.6 The Effect of Mineral Supplements.

The addition of DEX and/or BGP to the growth medium had no apparent effect on osteoblast nodule formation. Alizarin red S was used to identify calcium deposits in 14, 21 and 28 day cultures. Staining was minimal in day 14 cultures and no differences between the supplemented and unsupplemented cultures were noted however, positive staining of supplemented cultures was clearly seen at 21 days (Figure 2.11). Staining was minimal in control cultures.

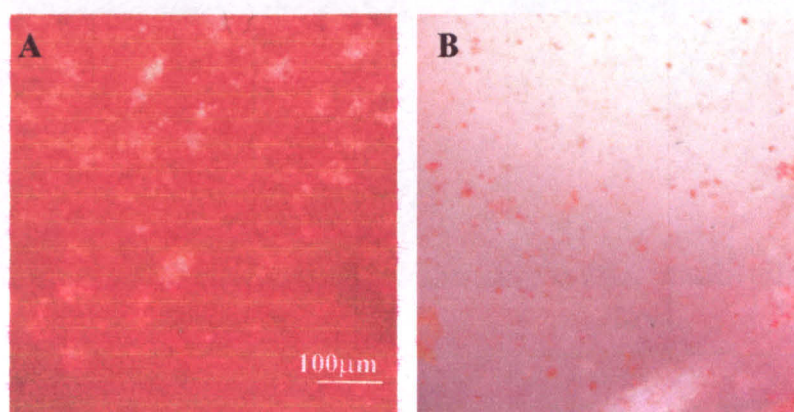


**Figure 2.11** Alizarin red staining of 21 day HOB cultures with (a) and without (b) the addition of DEX and BGP showing the red staining of calcium deposits in the supplemented cultures.

CLSM of calcein labelled cultures (Figure 2.12) showed large areas of green fluorescence indicating that mineral was present. The distribution of staining appeared similar to that seen for alizarin red samples.

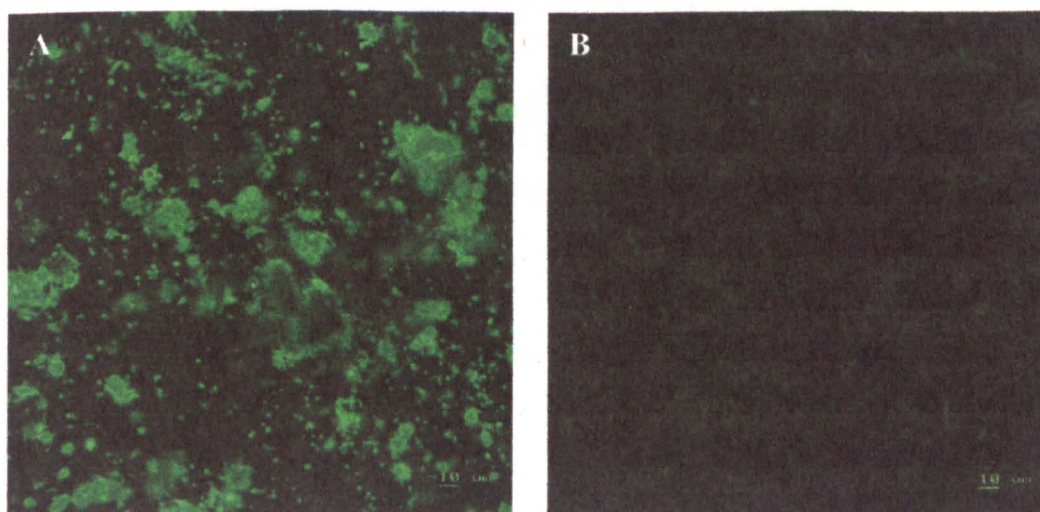


**Figure 2.12** Mineralisation of HOB cultures supplemented with DEX and BGP. Calcein labelling of calcium in 21 day cultures with (a) and without (b) the addition of DEX and BGP.

Quantitative calcein labelling at 21 days showed that mineral was present in the cultures supplemented with DEX and BGP (figure 2.13) and that this was significantly higher ( $p < 0.001$ ) than controls. The control cultures had a slightly higher than background level of calcium so it is possible that these cultures have a limited capacity to form mineral.

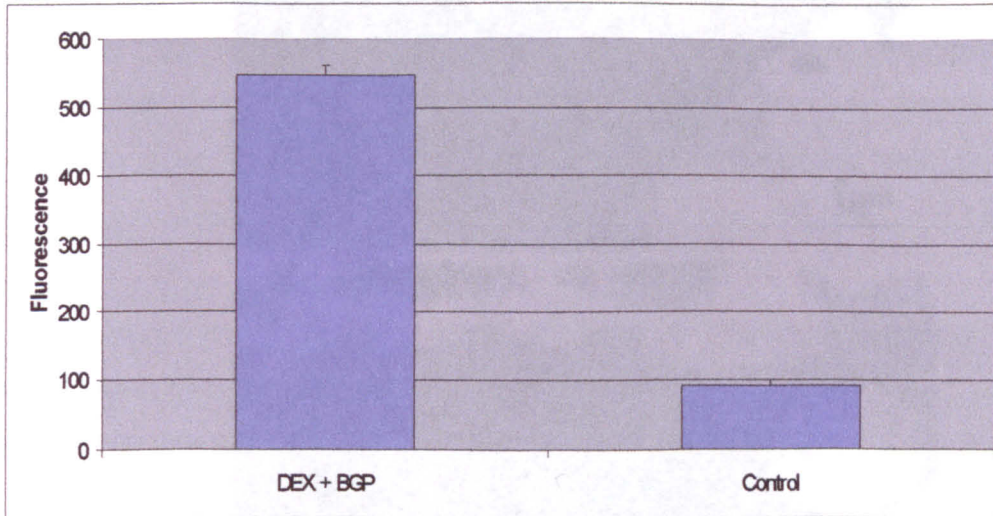


**Figure 2.13** Calcein labelling of HOB cultures at 21 days and 28 days. Significantly more mineral ( $p < 0.001$ ) was present in the cultures supplemented with DEX and BGP.

TEM of 28 day samples treated with DEX and BGP are shown in figure 2.14. Dense aggregates of needle-like crystals were located above, below and between cell layers. These were often associated with collagen bundles although unmineralised areas of collagen were also seen. Mineralised deposits were not observed in control cultures which appeared similar to the cultures shown in figure 2.9.

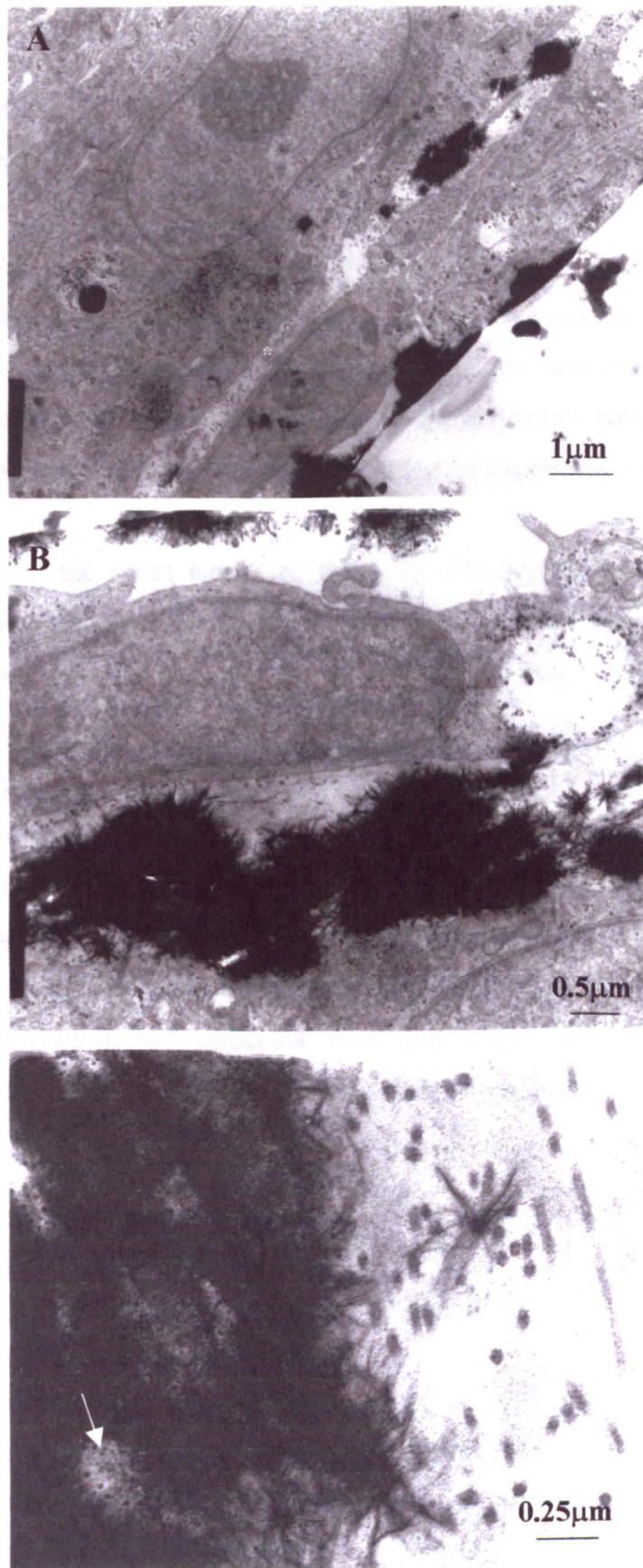


**Figure 2.14** TEM of 28 day samples supplemented with DEX and BGP. Mineralised areas are seen between cell layers (a). Note the areas of un-mineralised collagen (\*). These are composed of needle-like crystals (b). (c) Collagen fibrils can be seen interspersed within the dense mineralised aggregates (arrow).

## 2.4 Discussion.

Primary human osteoblasts (HOBs) were successfully isolated and cultured and could be maintained for numerous passages (at least 50) without loss of expression of the osteoblast phenotype. This system has the advantage over primary bone marrow cell cultures in that the cells isolated are less heterogeneous than marrow cultures and are committed to the osteoblast lineage. HOB isolation yields a large number of cells which can be subcultured and stored in liquid nitrogen. This allows wide ranging experimentation on cells from the same primary culture at similar passages, reducing variation in results and allowing direct comparisons between experiments to be made.

A question arises as to the exact nature of the cells obtained using this method of isolation. The cells are of the osteoblastic lineage and the method employed here leads to the assumption that the cells isolated are osteocytes. Gheron-Robey (1995) isolated cells from human trabecular bone fragments and hypothesised that these originated from osteocytes which became preosteoblasts in culture as they started to proliferate. It is unknown whether these cells will mature in the same way as preosteoblasts isolated directly from bone. Similarly Ecarot-Charrier (1983) suggested that the ability of the isolated cells to divide implied dedifferentiation into precursors. Conversely, Gundle and Beresford (1995) suggested that marrow clonogenic cells (or a population of) may be the source of osteoblastic cells in both trabecular bone and marrow cultures. Turksen and Aubin (1991) have identified 2 kinds of osteoprogenitor (OPC) cells in bone tissue, an early OPC cell which exists mainly in bone marrow and is ALP negative and DEX dependant. The second is a mature OP which exists in the periosteum and is ALP positive. This type forms bone nodules in the presence and absence of DEX. In light of the results obtained in this work the cells could fall into the mature OPC category.

HOB cells have been previously characterised (Di Silvio, 1995) and were shown to produce ALP, osteocalcin and cAMP in response to parathyroid hormone. This work has further characterised the osteoblastic nature of the cells by using longer periods of cell culture to examine the mineralisation process. HOBs were shown to form large, numerous nodules in culture. Such heterogeneity has previously been reported in osteoblast cultures due to various stages of differentiation in the cultures (Marie, 1995). The reason for nodule formation in culture has been attributed to a requirement for high

---

levels of organic phosphate for mineralisation to occur and that this only occurs in the microenvironment created by multilayered nodular areas (Ecarot-Charrier, 1983).

Analysis of HOB ultrastructure was carried out using TEM. HOBs contained abundant rER and mitochondria. Cells were linked by junctional complexes. These were probably gap junctions as they have been demonstrated in bone tissue and osteoblasts *in vitro* where they are related to cell differentiation (Donahue, 2000) and mediate PTH stimulation of mineralisation (Schiller, 2001).

HOBs exhibited a typical secretory cell ultrastructure and were surrounded by a collagenous matrix which is consistent with the appearance of osteoblasts *in vivo*. Collagen-1 staining was present from 5 days cell culture. At later stages (from 21 days) collagen-1 was absent from the centres of the nodule. This was alluded to in TEM observations but was clearly proven using confocal.

Another feature of the nodular structures seen in the osteoblast cultures was the cell viability within the nodules. Cell layers at the nodule surface appeared similar to cells from the internodular regions, however, cells from the nodule interior had dense, shrunken nuclei seen using confocal microscopy. TEM revealed chromatin clumping in the cell nuclei and the cytoplasm contained numerous vacuoles and vesicles. Some papers have reported the occurrence of apoptosis in nodules prior to mineralisation (Boyce, 1996) It is not clear whether this process was a natural part of osteoblast mineralisation or a state induced by prolonged cell culture. It is possible that these structures do not get adequate diffusion of nutrients due to their large size. Considering that each nodule only covered a small area and that other culture systems (eg. Skin) are successfully grown as multilayers (Gray oral communication) would seem to support the hypotheses that the cell death seen is either the result of the natural mineralisation process or the death of cells resulting from a missing component from the medium which is required for mineralisation *in vitro*.

Although osteoclast and osteocyte cultures have been established (Roodman, 1995; van der Plas and Nijwerde, 1992), it is the osteoblast, or bone forming cell, which has received most attention from *in vitro* studies. Many types of culture system exist and

extensive studies have shown that most of these produce many proteins common to the osteoblast phenotype. One feature of osteoblast cells has proved more elusive *in vitro* however and that is the production of a mineralised ECM.

Convincing evidence for mineralisation was not observed in HOB cultures in normal medium over 4 weeks, despite the extensive methods employed to identify mineralised areas (SEM, TEM, Von Kossa, Alizarin red S and calcein labelling). Weak staining of nodules with alizarin red S was seen after 4 weeks in culture and mineralised areas were not observed using TEM. This is not an unusual finding for osteoblast cultures however as many cell lines do not form collagen or mineral *in vitro* and even in primary cultures where mineralisation sometimes occurs this is only a fraction of the cells (Marks and Hermey, 1996). Gehron-Robey (1995) reported that cultures from trabecular bone form nodules that start to mineralise, using collagen-1 and matrix vesicles but never become heavily mineralised in the same way that cells from heterogeneous cultures suggesting that the last stages may require other cell types or cells at a different maturation stage.

There is some evidence to suggest that 'fine tuning' of the growth conditions may increase the osteogenic potential of the cells. The level of ALP activity increased over time in culture which is in agreement with the Di Silvio osteoblast model (1995). Di Silvio (1995) reported increasing collagen-1 and osteocalcin synthesis over a 4 week culture period. Recently the same HOB cells grown on HA surfaces showed small areas of mineral deposits related to collagen fibrils (Scotchford et al, in preparation). A prerequisite for mineralisation in any bone culture system is the formation of an extracellular matrix to support it (Gerstenfeld *et al.*, 1988). It is possible that stimulation of increased collagen production in HOBs may lead to a more substantially mineralised matrix and this area warrants further study.

Mineralisation was inducible using the supplements DEX and BGP and mineral was first detectable after 2 weeks supplementation. Mineralised deposits covered the entire culture well and were not restricted to nodules. Significantly, mineral was seen in association with the collagenous ECM. Bellows *et al.* (1990) found that DEX caused increased proliferation in a certain population of osteoprogenitor cells with a low proliferative capacity. DEX is associated with bone marrow cell culture (Bellows *et al.* 1990; Rickard

*et al.*, 1994) and calvaria derived cultures (Abe *et al.*, 2000). BGP is almost universally added to all osteoblast-like cultures and is a requirement for mineralisation with 2 exceptions: KS 4, a calvarial osteoblastic cell line, and Pro IRPC cells obtained from foetal rat mandible with neutral protease (Abe *et al.*, 2000). The question arises as to the specificity of these supplements to osteoblasts. Ecarot-Charrier (1983) treated fibroblasts and osteoblasts with BGP but the collagenous matrix of the fibroblast cultures did not mineralise.

Many systems rely on the addition of supplements to the medium whose methods of action are not well understood. The addition of DEX and BGP has become routine in *in vitro* bone biology (Boyan *et al.*, 2000) and in the field of biomaterials where the majority of papers cited use supplemented cells to evaluate biocompatibility. It is unlikely that these substances are involved in the development of bone *in vivo*. It is preferable to either use cultures which do not require their addition for the formation of mineral, or to find alternative, better understood mechanisms to induce the formation of mineral rather than relying on additives whose underlying mechanisms remains unclear.

The main disadvantage of the system is that the source of bone is restricted to older patients undergoing total hip replacement and this may have an effect on the metabolism of the isolated cells in comparison to those isolated from younger patients. Craniofacial osteoblasts (CFCs) have been successfully isolated using similar methods and these are from much younger patients. They have much lower ALP activity but increased collagen-1 production (unpublished observations). Whether these differences are a result of donor age or anatomic site or other has not been investigated. Donor age and site of HOBs have shown differences in the response of many osteoblastic markers, including collagen-1, in response to vitamin  $1,25(\text{OH})_2\text{D}_3$  (Martinez *et al.*, 1999). Katzburg *et al.* (1999) also demonstrated differences in expression of osteoblastic markers in pre and post menopausal women and the responsiveness of these to vitamin  $\text{D}_3$ . Such differences were not noted in men of the same age groups. HOBs used in the present work were from donors corresponding to the older groups in both studies.

In summary, the culture system investigated here exhibited many osteoblastic markers such as ALP, OC and collagen-1 and shows a progression towards mineralisation (Di

---

Silvio, 1995). This work has further added to the knowledge surrounding this model. The localisation of other osteoblastic markers such as OP and ON and collagen-1 have been demonstrated. The ultrastructure of osteoblasts and the formation of nodules during extended periods of culture have been examined.

Finally the osteogenic potential, of the system has been investigated. Mineralisation was minimal in the normal culture system and localised to nodules using alizarin red S staining. TEM studies did not show mineral in unsupplemented cultures grown on tissue culture plastic. Further work may develop the osteogenic potential of HOBs. A mineralised matrix was inducible using DEX and BGP supplementation of the growth medium as seen using TEM.

Currently a host of substances are being investigated for their ability to promote or inhibit osteoblast growth, differentiation and mineralisation *in vitro*. Further studies would allow the components of growth medium to be tailored so as to control the growth and differentiation characteristics of osteoblasts at a molecular level. Clarification of the control of the mineralisation process *in vitro* is an important future goal. This would be invaluable in the design of biomaterials and tissue engineered constructs and would aid identification of subtle differences between cell responses to surfaces.

## **Chapter 3**

### **The Effect of Silica Supplementation on Osteoblast Growth and Mineralisation *in vitro*.**

### 3.1 Introduction.

Silicon is the second most abundant element on the biosphere after oxygen and it is found in many different forms in food, drink and the environment as summarised in the general introduction. It is perhaps not surprising that silicon has been accepted as an essential trace element in animal nutrition. The essentiality of silicon in the chick was proposed by Carlisle (1972) who administered silica in the form of sodium metasilicate ( $\text{Na}_2\text{SiO}_3 \cdot 9\text{H}_2\text{O}$ ) at 100 parts per million (ppm) and found enhanced bone growth. In the same year a study by Schwartz and Milne (1972) evaluated the effect of sodium metasilicate supplementation in rats and found similar results. A series of experiments followed which led to silica being accepted as an essential trace element in animal nutrition (Carlisle, 1972; 1974; 1976a,b; 1980a; 1980b; 1982; 1986; Carlisle and Alpenfels, 1980; Carlisle and Alpenfels, 1986). These centred on the two criteria for establishing essentiality which are 1) repeated and significant responses in growth or health to dietary supplements of the element and that element alone, and 2) development of a deficiency state on a diet which is otherwise adequate (Carlisle, 1974). A silicon deficient diet caused abnormal bone and cartilage formation resulting in stunted bone growth, thinner cortex, altered epiphyseal cartilage morphology and reduced collagen content in chicks (Carlisle, 1980b).

The main action of silica has been on bone and cartilage in experimental animal studies. Increased dietary silica in chicks resulted in increased growth, increased rate of mineralisation and amount of bone formed and increased matrix production in bone and cartilage (Carlisle, 1986). Dietary silica supplementation causes increased growth rate, increased amounts of articular cartilage, increased bone water content and biochemical changes in the mineral, hexosamine and collagen content of bone (Carlisle, 1974; 1980a). Other studies suggest silica supplementation has no effect on growth rate or skeletal development in chickens (Elliot and Edwards, 1991).

There has been some suggestion in the literature that silica increases the proliferation and differentiation of osteoblasts. A study by Keeting *et al* (1992) showed that HOBs cultured in the presence of Zeolite A, a compound containing silica and alumina, demonstrated increased proliferation and differentiation as shown by increased AP,

osteocalcin, and TGF- $\beta$  release. Collagen-1 was not affected. Increased proliferation appeared to be accounted for by the silica content of the compound.

The proliferative response seen was dependent on cell number indicating that an autocrine mechanism may be involved in the interaction between ZA and bone cells. The supposition is that ZA may mediate the synthesis and release of factors including TGF- $\beta$ . This probably occurs at a post-transcriptional level as the mRNA values increased much later than the secretion of TGF- $\beta$ . The implication is that silica-containing compounds may affect cells at the molecular level but whether this is due to the silica component has not been investigated.

Silica has been localised in the active growth areas of bone by electron microprobe analysis. Its concentration increases at the same rate as calcium in the early stages of calcification and then falls off as the CaPi ratio approaches that of hydroxyapatite (Carlisle, 1969; 1970a; 1980a).

Silica is a major anion in osteoblasts and is present in similar amounts to magnesium and phosphorous. It has been localised to the mitochondria of osteoblasts (Carlisle, 1976a) and rat liver, kidney and spleen cells (Johnson and Volcani, 1978). Some organelles contain silicon and calcium before ossification begins (Carlisle, 1975).

It would seem that the relationship of silica and calcium is important in mineralisation (Carlisle, 1970b). Silica supplemented organ cultures showed an increase in weight, collagen production, calcium content and faster matrix polysaccharide synthesis in bone (Carlisle and Alpenfels, 1978) and cartilage (Carlisle and Alpenfels, 1986). The increased growth has been attributed to increased collagen production (Carlisle and Alpenfels, 1980).

Silica is required for collagen and glycosaminoglycan (GAG) formation and it appears to be located in the GAG-protein complexes of the ground substance (Carlisle, 1976b). Schwartz (1973) examined the structure of silicon in GAGs and polyuronides and concluded that silicon is present as a derivative of silicic acid and that it probably acts as a cross-linking agent imparting resilience to connective tissue. Silica appears to be

important for collagen synthesis by cartilage (Carlisle and Alpenfels, 1984; Carlisle and Garvey, 1982) and bone (Carlisle, Berger and Alpenfels, 1981) and increases the action of prolyl hydroxylase, an enzyme necessary for hydroxylating proline in collagen synthesis (Carlisle, Berger and Alpenfels, 1981; Carlisle and Alpenfels, 1984). Cartilage growth has been increased in organ cultures when silica and ascorbate are added and this is demonstrated by increased hexosamine and proline synthesis (Carlisle and Suchil, 1983).

In summary, the main effect of silica appears to be on the matrix of cartilage and bone with a possible secondary role in the early stages of mineralisation (Carlisle, 1986).

The ability of silica to promote mineral precipitation is not confined to bone and cartilage. Urinary stone formation has been observed in dogs and humans treated with magnesium trisilicate, an antacid, over long periods (Newberne and Wilson, 1970; Dobbie, 1986). Silicic acid affects the action of inhibitors of urinary stone formation (Dobbie, 1986). High doses of sodium saccharin lead to the formation of silicate-containing precipitate in urine of rats and these appear to be cytotoxic to the superficial bladder epithelium (Cohen *et al.*, 1991). The same group found similar results a year later using tetraethyl orthosilicate (Okamura *et al.*, 1992).

Silica is present in trace amounts in human saliva and it may cause the mineralisation of dental plaque to form calculus especially in areas of hard water or where the diet contains large quantities of silica-containing foods such as wheat and rice (Damen and Cate, 1989). *In vitro* studies have shown that the presence of silica stimulated mineral formation in simulated plaque fluid even in the presence of inhibitors of CaP precipitation such as phosphoproteins from saliva and products of bacterial metabolism. It is possible that silica, used in thickening agents in dentrifices, could cause calculus formation (Damen and Cate, 1992).

The aims of the work presented here were to investigate the effect of silica on the osteoblast *in vitro*. Specifically, the effect of silica on the rate of osteoblast mineralisation and the amount of mineral formed. Osteoblasts were grown in medium supplemented with a range of silica concentrations and the growth, differentiation and mineralisation examined. The HOB cells were used for the majority of the studies.

Primary human craniofacial osteoblasts (CFC) were used in parallel with osteoblasts for some of the mineralisation studies. The bone chips were obtained from craniofacial surgery and the cells are released and cultured in the same way as HOBs. The main differences between these cells and HOBs are the fibroblastic cell shape, low ALP production, abundant collagen-1 production and capacity for rapid mineralisation when DEX and BGP are added to the growth medium. The range of silica concentrations were be 1-450ppm, corresponding, at the lower end, to the amount found in the circulating fluids of the body. The higher concentrations used, although unlikely to be found in the body naturally, were still trace amounts and therefore could theoretically be leached from a biomaterial in the body. Any direct effect of silica, adverse or beneficial, on the osteoblast would add significantly to the knowledge available which is scant owing to the difficulty of measuring silica accurately in the past.

## **3.2 Materials and Methods.**

### **3.2.1 Preparation of Silica Containing Medium.**

Double strength complete Dulbeccos Modified Eagles Medium (DMEM) was prepared from a 10x concentrate (Gibco) to which was added 20% Foetal calf serum (FCS, Gibco), 0.04M L-glutamine, 5% sodium bicarbonate, 0.02M HEPES, 200 units/ml penicillin/streptomycin, 4% sodium pyruvate (all Gibco) and 300µg/ml ascorbic acid (BDH). Silica solutions were prepared at double the concentration required from a 1000ppm stock solution of sodium metasilicate (BDH). HEPES (1M) was added to silica solutions to ensure physiological pH (up to 15% for the higher concentrations). The stock solutions were stored at 4°C. Equal volumes of medium and silica solution were added together to make the working solution. In this way the correct concentration and pH of the media was preserved. Cell activity (Alamar Blue) and cell number (DNA assay) were measured for cells with a range of pH values (7.0-7.6) and HEPES concentrations (5-10%) to ensure that the ranges used in the experiments (pH 7.2-7.4) did not have any measurable effect on cell metabolism.

### **3.2.2 Effect of Silicate Supplementation on Initial Cell Attachment and Growth.**

#### **3.2.2.1 Protein adsorption.**

The amount of protein adsorbed to tissue culture plastic from medium containing a range of silica concentrations (0-450ppm) was measured at 90 min and 24 hr using the Lowry assay (Lowry *et al.*, 1951). Serum free medium containing silica was used as controls. Medium (1ml) was added to 24 well tissue culture plates for 90 min or 24 hr. The medium was removed at the appropriate time and the wells were rinsed in normal saline (0.9% NaCl in sterile water). 250µl of 1M NaOH was added to each well and the samples were stored in the fridge until further analysis. A standard curve (0- 500mg/ml) was prepared from bovine serum albumin (BSA, Sigma) in reagent A (2% NaCO<sub>3</sub> in 0.1M NaOH). 1ml of solution D (0.5% CuSO<sub>4</sub> in 1% Na tartarate diluted 1 in 50 in 2% NaCO<sub>3</sub>) was added to the standards and test solutions for 10 min. 100µl of Folin phenol

reagent (50% in distilled water, Sigma) was then added. The solution was mixed and left for 1hr and the absorbance read at 750nm on a UNICAM UV/VIS spectrometer.

### 3.2.2.2 Cytoskeletal organisation and vinculin receptor staining.

For cell attachment studies cells were seeded onto 13mm diameter Thermanox coverslips in a 24 well tissue culture plate at a density of  $8 \times 10^4$  cells/ml. They were cultured in medium containing a range of silica concentrations (0-350ppm) for 90 min and 24 hr. Immunofluorescence labelling of the filamentous actin cytoskeleton with phalloidin was carried out at 90 min and 24 hr. The vinculin receptor was labelled with with a human monoclonal antibody to vinculin at 24 hr.

At the appropriate time the samples were rinsed in PBS and fixed in 4% paraformaldehyde for 5 min. They were rinsed in 1% PBS/BSA and permeabilised using a Triton X-100 (0.5% Triton X-100 (pH 7.6) in 20mM Hepes, 300mM sucrose, 40mM NaCl and 3mM  $MgCl_2$ .) solution for 5min at 0°C. A further 2 rinses in 1% PBS/BSA at 37°C were carried out as a blocking step.

FITC-conjugated phalloidin (Sigma, 250 $\mu$ g/ml in 1% BSA in PBS) was added to the samples for 20 min at 4°C. For vinculin receptor labelling samples were incubated in human monoclonal antibodies to vinculin (Sigma, 1 in 400 dilution in 1% BSA in PBS) for 1 hr at 37°C. The samples were washed in 1% BSA in PBS and rabbit anti-mouse FITC-conjugated secondary antibodies (DAKO, 1 in 20 dilution in 1% BSA in PBS) were added to the samples for a further hour at 37°C.

After removal of the phalloidin/vinculin the samples were rinsed 3 times in 1% BSA in PBS before adding propidium iodide (Sigma, 0.01mg/ml) for 30 seconds. The samples were rinsed again, mounted in glycerol/PBS containing 1-4 diazabicyclo-2-2-2-octane (DABCO, Sigma) and viewed using a Leica TCS 4D confocal microscope with an ArKr laser. The 488nm laser line was used to excite the green fluorescence of FITC-conjugated phalloidin or FITC-labelled vinculin. The red fluorescence of propidium iodide was scanned simultaneously using the 568nm laser line. Optical sections (1 $\mu$ m thick) were collected as a z series. A maximum intensity projection was created (a

composite image from the brightest pixels per scan) using the associated Scanware software.

### 3.2.2.3 Cell activity and cell number.

Cells were trypsinised from confluent flasks and seeded in 24 well plates at a density of  $8 \times 10^4$  cells/ml and incubated with medium containing various concentrations of silica ranging from 0 - 150ppm at 37°C, 5%CO<sub>2</sub> for 90min and 24hr. Cell activity (Alamar Blue assay) and cell number (DNA assay) were measured as described below.

The Alamar Blue assay (Serotec) was used to measure cell activity. The medium was removed from the cultures and they were gently rinsed in Earle's balanced salt solution (EBSS, Gibco). A 1 in 20 dilution of Alamar Blue dye in Hanks' balanced salt solution (HBSS, Gibco) was prepared and 1ml of this solution was added to each well. The plate was incubated under normal conditions for 20 min. Aliquots (100µl) from each well were placed in a 96 well plate and the fluorescence measured at 560nm excitation wavelength and 590nm emission wavelength on a cytofluor. The cultures were rinsed in sterile PBS and 1ml of sterile double distilled water was added to each well. Cultures were then freeze thawed for subsequent assays.

Cell number was determined using the fluorochrome bisbenzimidazole (Hoechst 33258, Sigma) as described by Rago *et al.* (1990). DNA standards were prepared from 20µg/ml stock solutions of purified calf thymus DNA (Sigma) to give a DNA content of 10, 6, 5, 4, 3, 2, 1, 0.5 and 0.25 µg/ml per well. Aliquots from cell lysates were placed in 96 well tissue culture plates. A 1 in 50 dilution of the dye in TNE buffer (10mM Tris, 2M NaCl and 1mM EDTA; pH 7.4) was prepared from a 1mg/ml stock solution and an equal volume of this was added to the test solutions and standards in the plate. Fluorescence was measured immediately at 350nm excitation wavelength and 460nm emission wavelength on a cytofluor. A standard curve was prepared and DNA values were calculated.

### **3.2.3 The Effect of Silicate Supplementation on Osteoblast Growth and Differentiation in Long Term Cell Culture.**

The assays listed above were also carried out on cultures supplemented with 0 - 450ppm sodium silicate for 2 and 4 days.

The effect of silicate supplementation (0-100ppm) was measured in the same way for cells cultured for longer (7-28 days) periods of time. Alkaline phosphatase activity was measured for cultures at 4, 7, 14, 21, 25 and 28 days as a measure of cell differentiation. The method is described fully in the previous chapter. Briefly, the Granutest kit for detection of alkaline phosphatase (ALP) activity (Merck) was used. Equal amounts of 4-nitrophenylphosphate and cell lysate were added to a 96 well tissue culture plate and the amount of 4-nitrophenol was measured at 485nm using an Anthos plate reader using 620nm as the reference wavelength.

### **3.2.4 The Effect of Silicate Supplementation on Osteoblast Mineralisation *in vitro*.**

Long term mineralisation studies were carried out using low concentrations (1, 5, 10 and 50ppm) of sodium metasilicate for 4 weeks. HOBs were seeded at  $8 \times 10^4$  cells/ml and cultured in control medium and medium containing DEX ( $10^{-8}$ M) and BGP (10mM). Primary human craniofacial cells (CFC) were seeded in parallel experiments in growth medium containing DEX and BGP. The cells were seeded at the same density as HOBs and were cultured in medium supplemented the range of silicate for 4 weeks.

Alizarin red S histochemical staining for calcium was carried out on HOB and CFC at 14, 21 and 28 days. The cells were rinsed in TBS, stained with 1% Alizarin red S in 0.028%  $\text{NH}_4\text{OH}$  for 2 min, rinsed and mounted in glycerol/DABCO. They were photographed using a Nikon EM camera mounted on a Nikon Diaphot inverted phase contrast microscope.

At 28 days the HOB and CFC cultures were incubated with medium containing  $1 \mu\text{g/ml}$  calcein (Sigma) for 4 hrs and read on a cytofluor at 485nm excitation, 530nm emission.

This is a semi-quantitative method for the detection of calcium in bone cultures (Hale and Santerre, 2000). Immunofluorescence labelling of calcium with calcein was carried out at 28 days (Hale and Santerre, 2000). Cells were treated with culture medium containing 5µg/ml calcein overnight, rinsed with PBS and viewed using a Leica TCS 4D CLSM. The 488nm laser line was used to view the green fluorescence of the calcein labelling. The samples were counterstained with PI so the cell nuclei could be visualised using the 568nm laser line.

Statistical analysis of all assays in this section was carried out using a one way analysis of variance (ANOVA) with a Tukey-Kramer post test for multiple comparisons.

### 3.3 Results.

#### 3.3.1 Effect of Silicate Supplementation on Initial Cell Attachment and Growth.

##### 3.3.1.1 Protein adsorption.

Protein adsorption to tissue culture plastic was measured using the Lowry assay after 90 min and 24 hr incubations of silica containing medium. Protein adsorption was higher on the surface of wells treated with higher concentrations of silica. The trend was the same at 24 hr incubations. Although protein adsorption appeared to be enhanced in wells containing silica containing medium the data was not statistically significant. Measurement of protein adsorption to control wells showed that silica did not interfere with the assay. Figure 3.1 shows protein adsorption to tissue culture plastic from control medium and medium containing up to 450ppm silicate. There was no statistically significant difference between samples at 90 min or 24 hr.

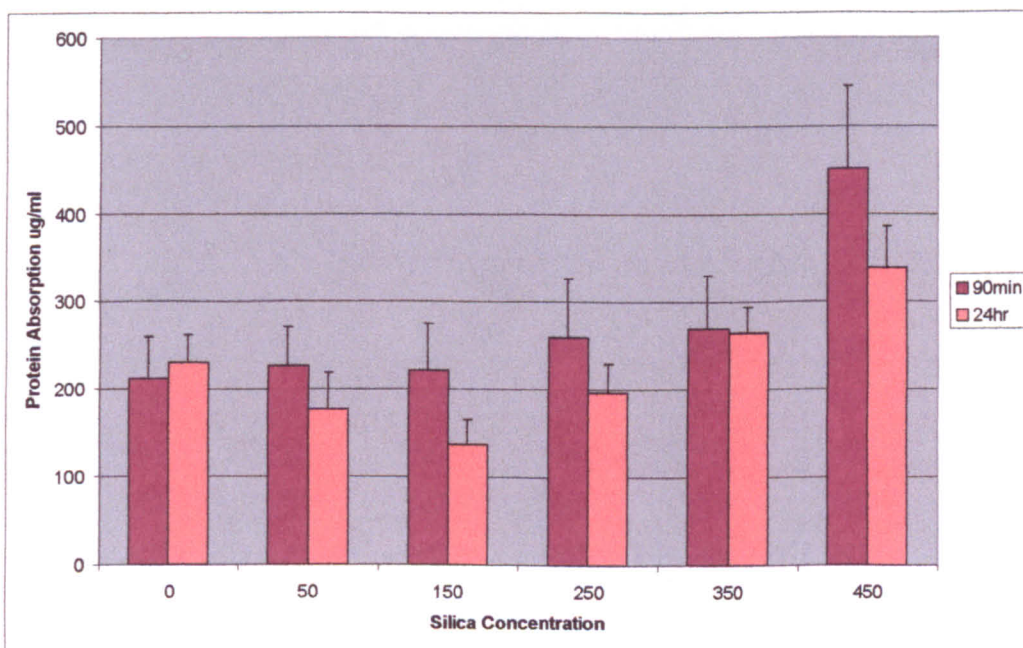


**Figure 3.1** Protein adsorption to tissue culture plastic from serum containing medium (serum free controls have been subtracted) supplemented with a range of silica concentrations. Error bars represent standard error of the mean, n=4.

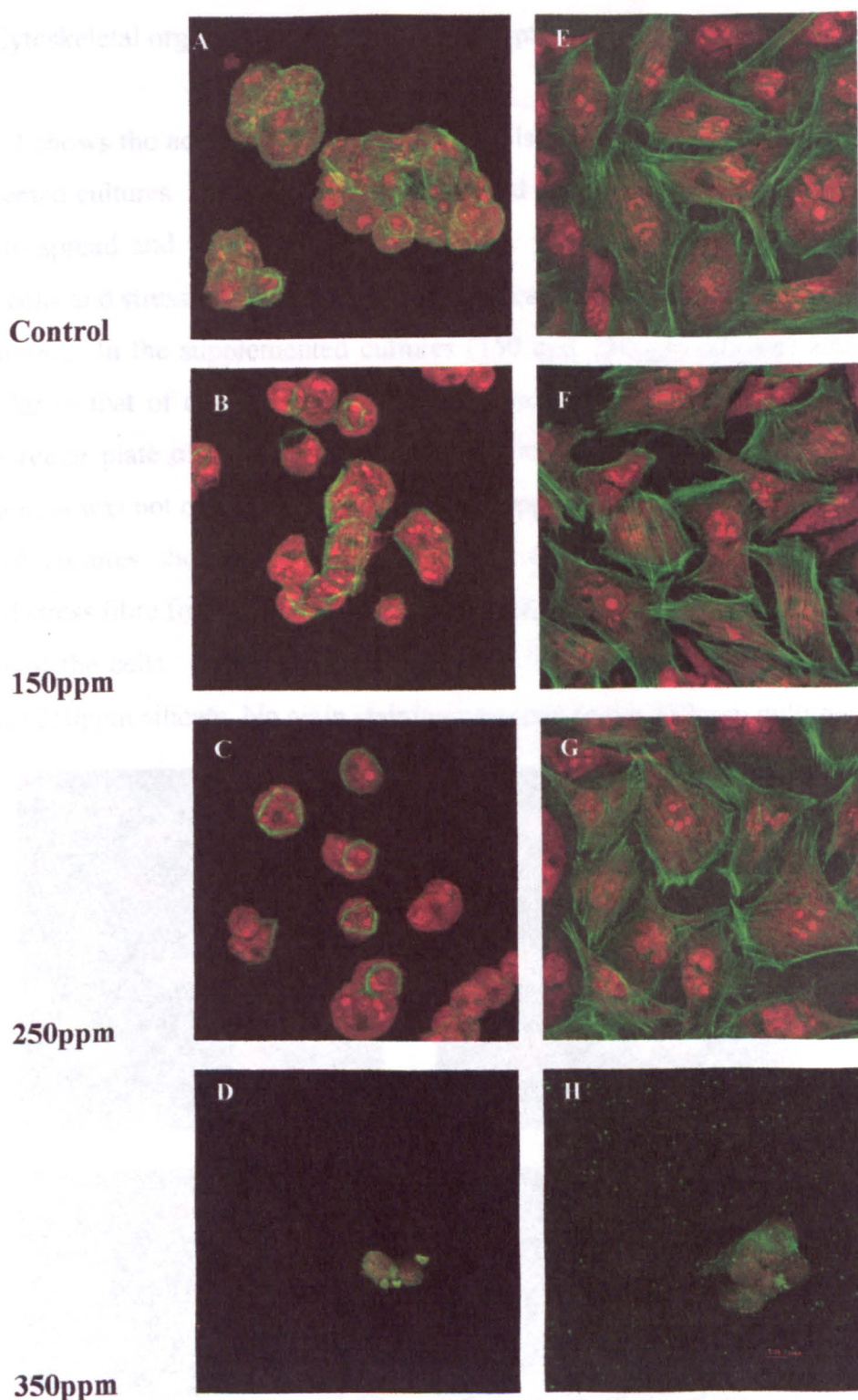


**Figure 3.2** CLSM images showing the filamentous actin cytoskeleton (green) and cell nuclei (red) of HOBs at 90 min (a-d) and 24 hr (e-h) in medium containing 0 (a, e), 150 (b, f), 250 (c, g) and 350ppm silica (d, h). Cultures supplemented with up to 150ppm are similar to controls at 90min and 24hr. 250ppm supplemented cultures show rings of actin between the cells and the substrate at 90 min. Cells are similar to controls at 24 hr. Cells supplemented with 350ppm silica show little actin organisation at 90 min or 24 hr.

### 3.3.1.2 Cytoskeletal organisation and vinculin receptor staining.

Figure 3.2 shows the actin cytoskeleton of the cells at 90 min and 24 hr for a range of supplemented cultures. At 90 min unsupplemented osteoblast cultures showed the cells starting to spread and were arranged in clusters. Actin fibres arranged cortically in rounded cells and stress fibres were seen in the spread cells. Rounded cells did not show actin staining. In the supplemented cultures (150 and 250ppm silicate) actin staining was similar to that of control cells. Some cells were attached to the thermanox via a narrow circular plate of actin arranged cortically at the base of the cell (Figure 3.2c). Actin staining was not observed on the 350ppm supplemented cultures at 90 min. By 24 hr control cultures showed well spread cells with an established cytoskeleton and organised stress fibre formation. Thick actin filaments were seen arranged parallel to the long axis of the cells. Similar staining was seen in supplemented cultures up to (and including) 250ppm silicate. No actin staining was seen in the 350ppm cultures.

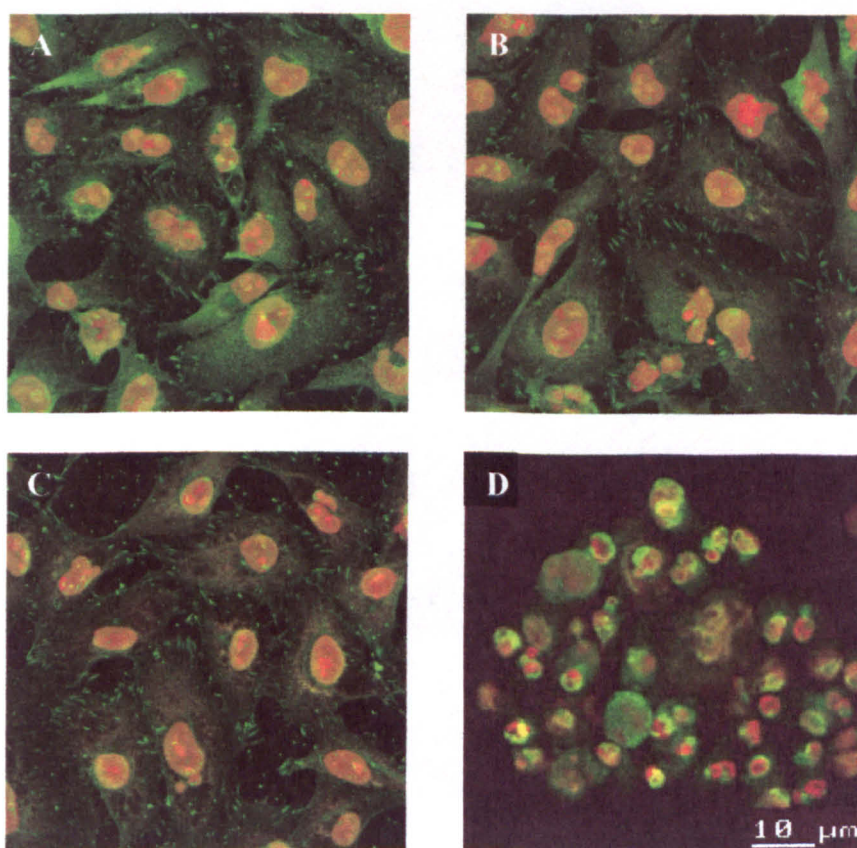


**Figure 3.3** CLSM images of HOBs labelled with antibodies to vinculin after 24hr cell culture in a range of silica concentrations. Control cells (a) show punctate receptor labelling (green) at the edges of cells. Cells treated with 150 (b) and 250ppm (c) were similar to controls. Cells treated with 350ppm silica show no vinculin receptor staining (d). Cell nuclei are labelled with propidium iodide (red).

Figure 3.3 shows labelling of the vinculin receptor. Punctate receptors were visualised on the bottom surface of the control cells at 24 hr. Similar staining was seen for cells supplemented with 150 and 250ppm silicate. Receptor staining was absent for 350ppm supplemented cultures.

### 3.3.1.3 Cell activity and cell number.

Figure 3.4 shows the cell activity and DNA content of cells supplemented with up to 150ppm silica. Silicate supplementation did not significantly affect cell activity or cell number at 90 min or 24 hr.

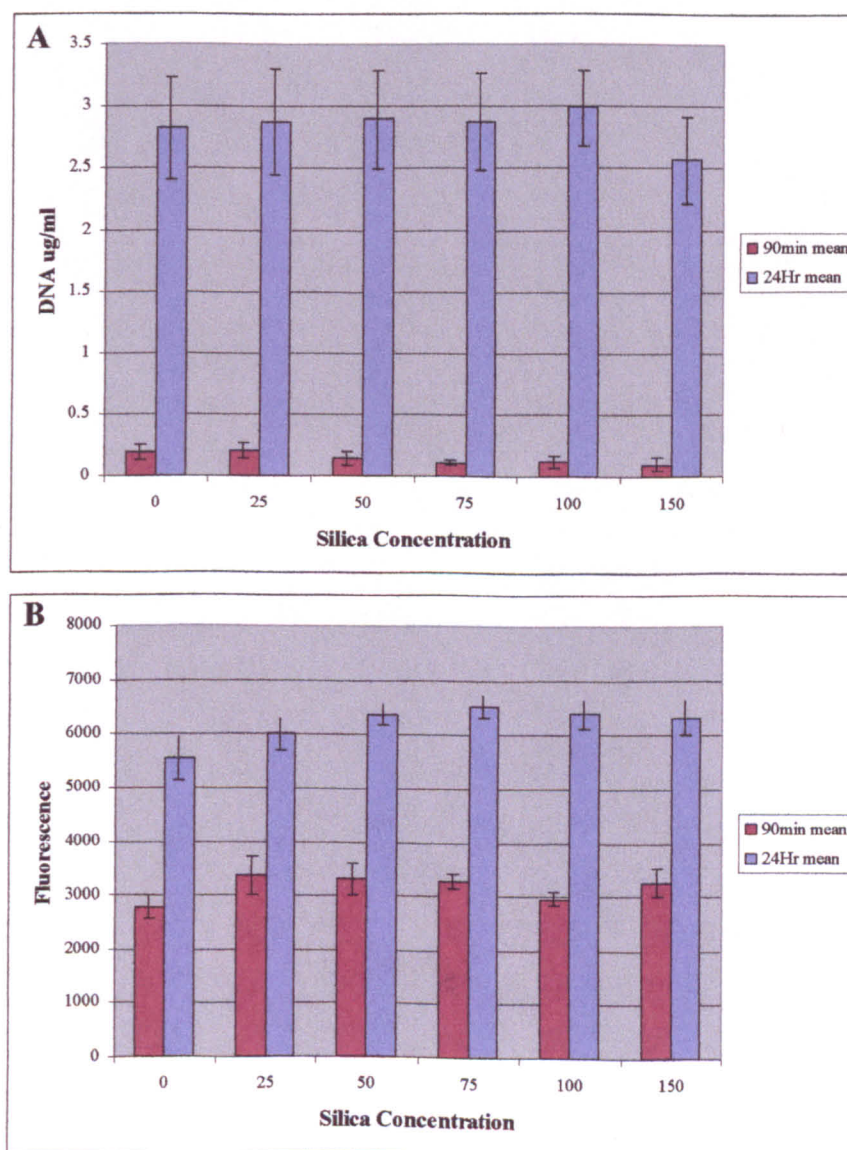
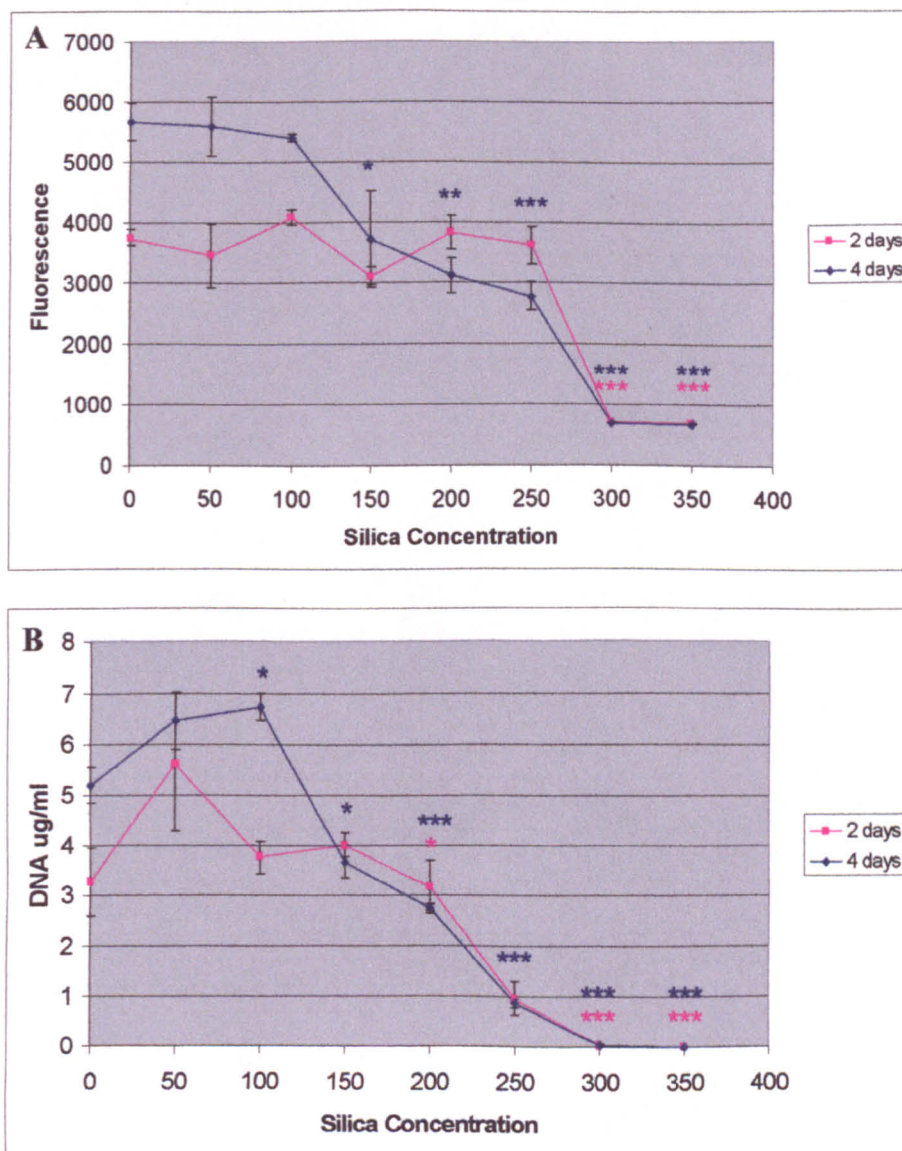


**Figure 3.4** DNA content (a) and cell activity (b) of HOBs grown in medium containing 25-150ppm silicate for 90 min and 24 hr. There was no significant difference between silicate-containing and control cultures. Error bars represent standard error of the mean, n=4.

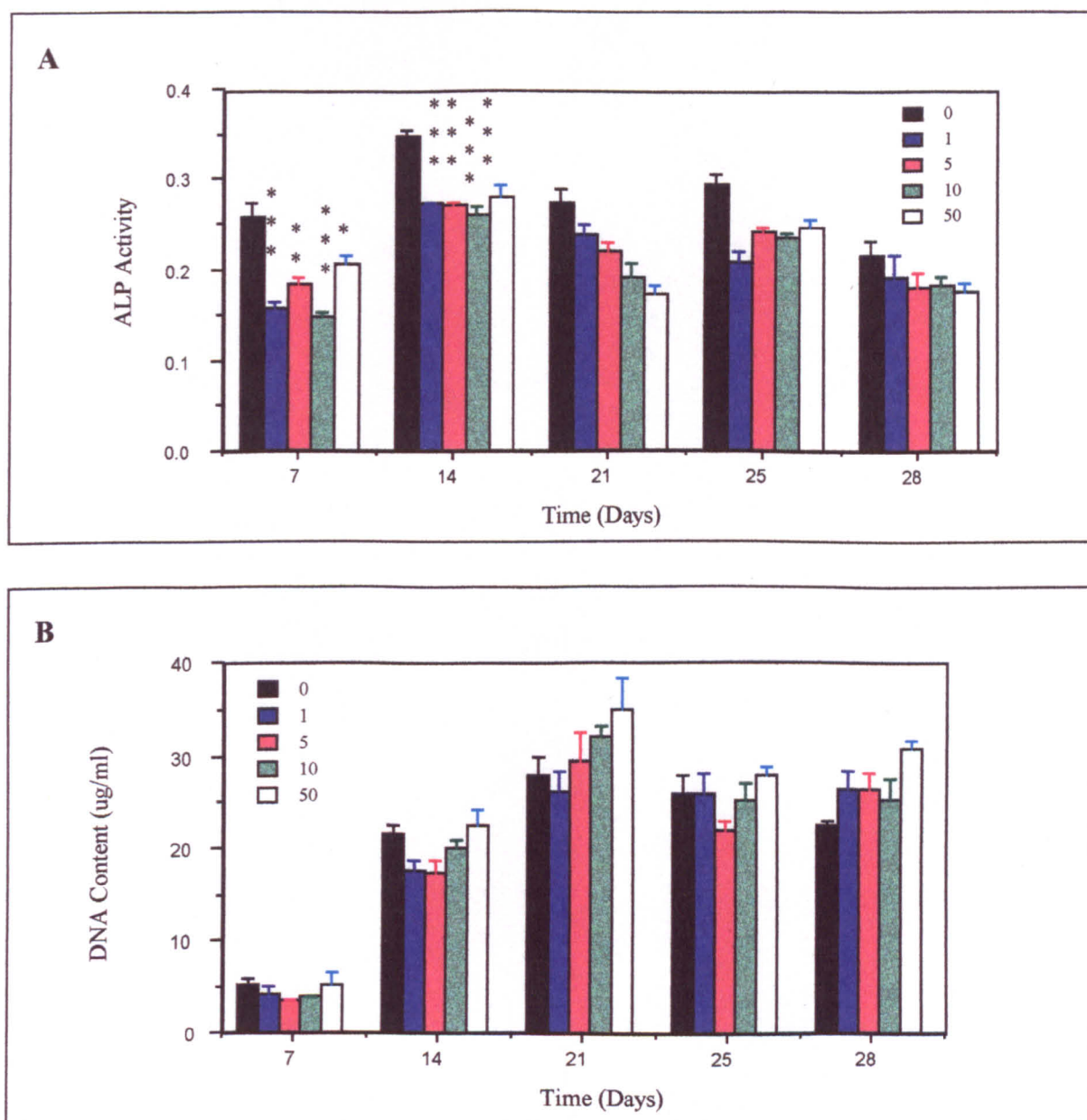
### **3.3.2 Effect of Silicate Supplementation on Osteoblast Growth and Differentiation in Long Term Culture.**

Figure 3.5 shows the effect of sodium silicate supplementation (0-450ppm) on HOB cells for 2 and 4 days cell culture. At 48hr cell activity remained at similar levels to controls for silicate concentrations of up to 100ppm and then began to fall off at amounts greater than 150ppm. Cell activity fell sharply and remained at background levels for concentrations of 300 - 450ppm of sodium silicate indicating cell death. DNA content analysis showed the same trends as cell activity. HOB cell activity and DNA content had increased by 4 days in comparison to 2 day cultures for silicate concentrations up to 150ppm. Concentrations above this showed less cell growth than at 48hr.

Figure 3.6 shows the long term effects of silicate supplementation (0-50ppm) for timepoints ranging from 4 to 28 days. Alkaline phosphatase activity was significantly greater in control cultures than for cultures supplemented with 1-100ppm silicate at 7, 14, 21 and 25 days in some experiments although this was not always the case. When ALP activity per cell was calculated for these experiments the data appeared non significant. At 28 days differences in ALP activity for supplemented cultures were not significantly different to controls. DNA content of control cultures was not significantly different to supplemented cultures (1-100ppm silicate) for 7, 14, 21, 25 and 28 days.



**Figure 3.5** Cell activity (a) and DNA content (b) of HOB cultures supplemented with 0-350ppm for 2 and 4 days. Cell death is seen in cultures supplemented with more than 300ppm silica. There is no significant reduction in activity or DNA content between controls and cells supplemented with less than 100ppm. Cell growth is reduced in cultures over 150ppm. (\* =  $p < 0.05$ , \*\* =  $p < 0.01$ , \*\*\* =  $p < 0.001$  with respect to control cultures) At 4 days cells supplemented with less than 150ppm show an increase in cell growth and activity in comparison with data for 2 days. Silica supplementation with amounts above 150ppm show less growth at 4 days than at 2 days. Error bars represent standard error of the mean,  $n=4$ .



**Figure 3.6** ALP activity (a) and DNA content (b) of HOBs grown in 0-50ppm silicate-supplemented medium for up to 28days. Error bars represent standard error of the mean, n=4. (\* =  $p < 0.05$ , \*\* =  $p < 0.01$ , \*\*\* =  $p < 0.001$ )

### 3.3.3 The Effect of Silicate Supplementation on Osteoblast Mineralisation *in vitro*.

The effect of silica supplementation on HOB mineralisation is shown in figure 3.7. Alizarin red staining was not observed in any of the cells where DEX and BGP were not included in the growth media. This was true for controls and samples supplemented with silica.

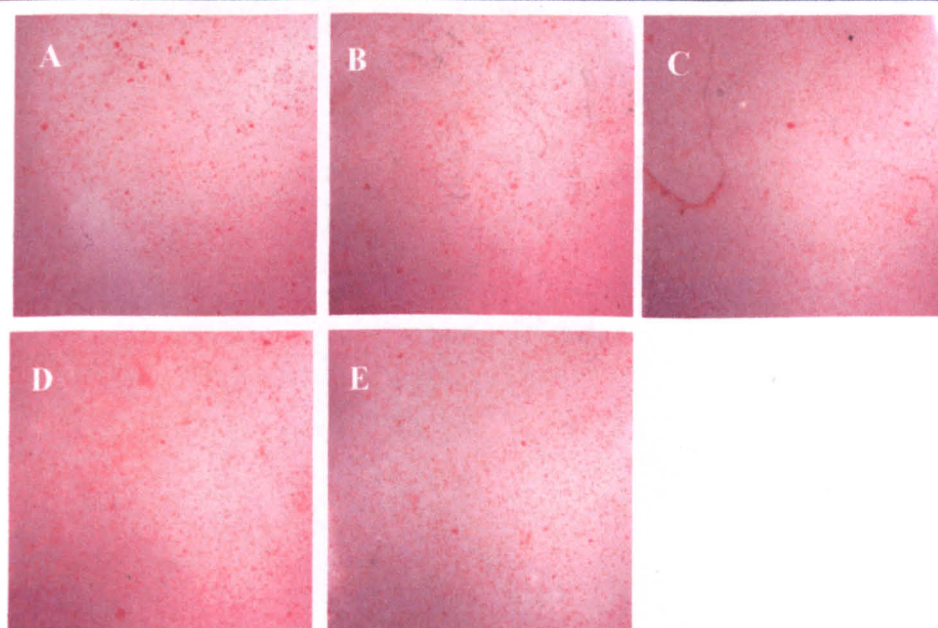


**Figure 3.7** Alizarin red S staining of calcium deposits in 28 day HOB cultures in medium (without DEX and BGP) supplemented with 0 (a), 1 (b), 5(c), 10(d) and 50 (e) ppm silicate.

The percentage of wells containing nodules was increased when the growth medium was supplemented with silica in some experiments. At 17 days cell culture 8% of control wells contained nodules compared with 12.5% for cultures supplemented with 1ppm silica. By 21 days control cultures contained the same number of nodules as at 17 days and 47.6% of wells supplemented with 1ppm silica contained nodules (Table 3.1).

	Control	1 ppm Si	5 ppm Si	50 ppm Si	100ppm Si
<b>17 days</b>	8%	12.5%	16.6%	12.5%	16.6%
<b>21 days</b>	8%	47.6%	28.6%	19%	19%
<b>23 days</b>	58%	75%	71.4%	35.7%	64.3%

**Table 3.1.** Percentage of silicate treated wells containing nodules.

Alizarin red staining of CFCs (with DEX and BGP) is shown in figure 3.8. By 21 days the control cultures were stained with alizarin red and the staining in the silica containing cultures was more intense than in the controls. Staining intensity was increased in all cultures at 28 days and the supplemented cultures were more densely stained than controls. Quantitative measurement of the calcium content of the CFC cultures using the calcein assay showed that there was no statistically significant difference between the calcium content of controls and silica supplemented cultures at 4 weeks.

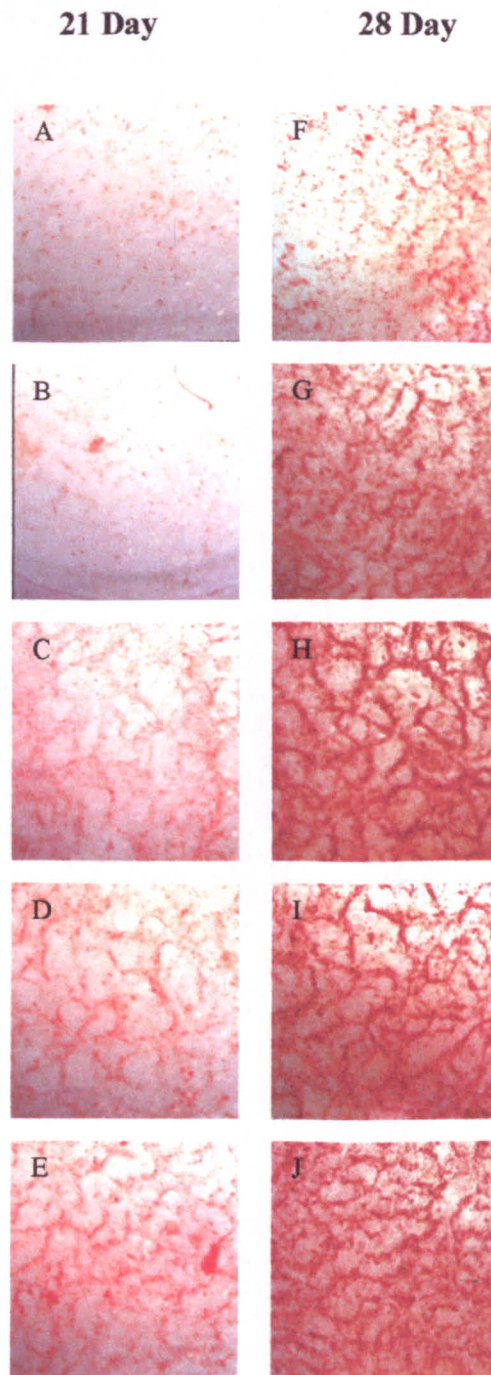


**Figure 3.8** Alizarin red S staining of craniofacial osteoblasts (CFC) supplemented with 1-50ppm silica. CFCs grown in control medium for 21 (a) and 28 days (b). (b-e) CFCs supplemented with 1 (b), 5 (c), 10 (d), and 50ppm silica (e) at 21 days. Minimal staining is seen in controls and 1ppm. 5, 10 and 50ppm show some staining. Figures 3.8 (f-j) show the same results after 28 days cell culture. Overall staining is more intense than at day 21. Increased staining intensity is seen from controls to 50ppm silica.

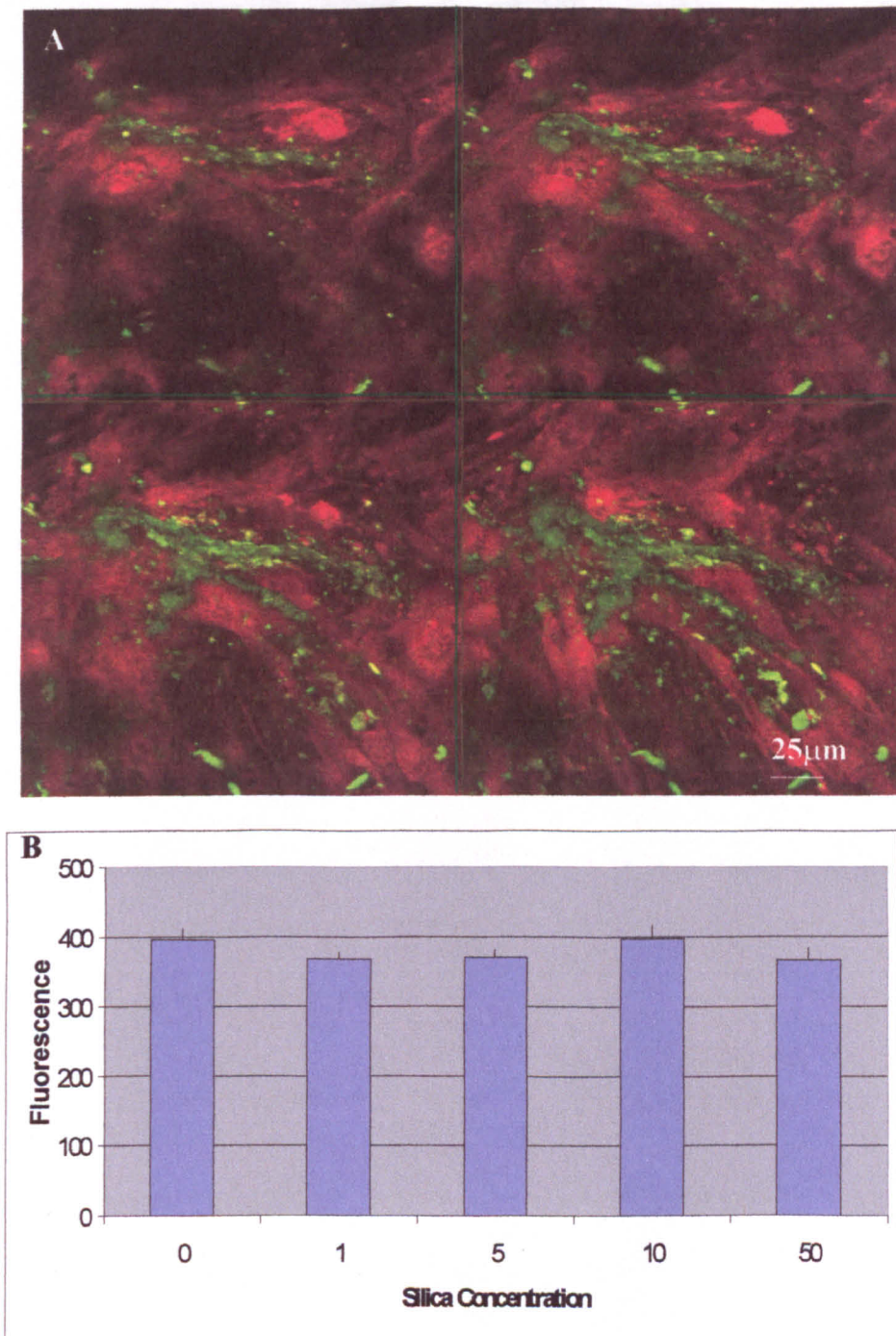


**Figure 3.9** (a) Gallery of CLSM images of calcein labelled mineral in a 28 day CFC culture, showing cell nuclei (red) and mineral (green). The mineral is located in the same plane as the cells in the extracellular spaces between them. (b) Calcein labelling of mineral content of cultures supplemented with 0-50ppm silica for 28 days. Error bars represent standard error of the mean, n=4.

### 3.4 Discussion.

The aim of this work was to investigate the role of silica on osteoblast growth and mineralisation *in vitro*. Previous work has shown that silica is present in the mitochondria of the osteoblast and is localised in areas of active calcification *in vivo*. It has also been revealed as a structural component in glycosaminoglycans (GAG) and increases the amount of GAG and collagen formed in bone (Carlisle 1986). HOB cultures were supplemented with up to 450ppm sodium metasilicate ( $\text{Na}_2\text{SiO}_3$ ) in order to determine any beneficial/adverse effects of silica on the osteoblast. This compound was the same as that used in the initial experiments that established the essentiality of silicon for normal mineralisation of rat and chick bones (Schwartz and Milne, 1972; Carlisle, 1972).

Protein adsorption to tissue culture plastic from silica-containing medium showed that silica had no significant effect on the amount of protein adsorbed. There was a trend for increased adsorption with higher silica concentrations but this was not significant. Similarly, there was no obvious effect of silica supplementation on cell spreading on tissue culture plastic in osteoblast cultures supplemented with less than 300ppm silicate for 90min and 24hr. DNA synthesis and cell activity were also similar with no statistically significant difference between cells supplemented with up to 150ppm compared to control cultures at 90min and 4hr.

In contrast, cells supplemented with more than 300ppm silica showed a lack of cytoskeleton formation at 90min which was not improved after 24hr in culture. The vinculin receptor was absent at 24hr in these cultures also. This posed a question as to the viability of the cells in this concentration. Viability was assessed using the DNA and alamar blue assays for cultures supplemented with up to 350ppm silicate for 48hr and 4 days. DNA and AB assays confirmed cell death within 48hr for cells supplemented with 300ppm silicate. A cytotoxic effect of silicate solutions on bone cells has not been reported previously. The response of the dying HOBs to the silicate solution followed a distinct pattern of events and this will be further investigated in the next chapter.

It is interesting to note that while silica was seen to cause a statistically significant reduction in cell activity and number, the cytoskeletal profile of the cells and receptor

---

staining was similar for amounts up to 300ppm. Similarly cell morphology in culture was not noticeably affected by amounts smaller than 300ppm. Supplementation with concentrations above 150ppm caused cell activity to be markedly reduced at 2 days. Cell activity and number was reduced by 4 days in comparison to 2 days. This result suggests that prolonged contact with these concentrations in the long-term may be harmful without necessarily causing cell death. Silicate supplementation had little effect on HOBs at lower concentrations over short-term culture periods and concentrations up to 150ppm had no discernible adverse or beneficial effect on cell activity or DNA synthesis in the first 4 days. The fact that silica forms polysilicic acid oligomers at neutral pH in concentrations above ~100ppm may contribute to the cell death seen (Birchall, 1995).

Attention was then switched to lower concentrations over longer time periods to ascertain whether these had any beneficial effects on HOBs. Some long-term experiments showed that silicate, although not cytotoxic, caused a significantly reduced level of ALP in osteoblast cultures in the range 1-100ppm silicate over a 4 week culture period. DNA synthesis was not affected. This finding seems to suggest that even minuscule amounts of silica may affect osteoblast differentiation. The reason for this, or the mechanism by which it occurred is unclear. The DNA and ALP assays may not be sensitive enough to reliably detect subtle influences of silica on osteoblast differentiation and mineralisation. It is difficult to get reproducible results over long time periods as cell multilayers and nodules are difficult to disperse evenly. A potential area for further study would be to isolate the effect of silica on the osteoblast at a molecular level.

In some experiments very low amounts of silicate (1-5ppm) appeared to increase the rate and number of nodules formed in osteoblast cultures without the addition of DEX and BGP. The amount of mineral formed by HOB cultures was not affected by silicate supplementation however. Alizarin red S staining was negative up to 28 days cell culture. Semi-quantitative analysis of calcein labelling demonstrated background levels of mineral in the cultures. Considering that increased ALP was not the cause of the increased numbers of nodules, and that silica has been shown to increase the collagen content of bones *in vitro*, a possible explanation for this result could be a stimulatory effect of silica on collagen formation. Carlisle and Suchill (1993) demonstrated a

relationship between silica and ascorbate in cartilage. Silica supplementation caused an increase in the amount of hexosamine, proline and total protein only in the presence of ascorbate. Ascorbate is essential for collagen formation *in vitro* and this further supports the hypothesis that silica affects collagen formation. Collagen was not measured in this work and this was in part due to the fact that the assay employed was not successful due to interference from the constituents of the medium. The assay was not sensitive enough to detect the small amount of collagen produced by HOBs. A highly sensitive means of detecting changes in collagen production by bone cells in response to silica would be invaluable in elucidating the effect of silica on the osteoblast.

When DEX and BGP were added to the growth medium as promoters of mineralisation silica appeared to have a positive effect on mineralisation. Alizarin red S staining of 21 day craniofacial osteoblast (CFC) cultures supplemented with DEX and BGP showed that staining was more intense in cultures supplemented with 1-50ppm silicate than in controls. A similar picture was seen at 28 days. The findings from these experiments suggest that silica caused an increase in the amount of mineral formed in osteoblast cultures when the mineral promoters DEX and BGP are used. The fact that silica appeared to increase the amount of mineral in CFCs may be significant as they produce abundant collagen (unpublished observations) so more sites for the nucleation of mineral may be present. Quantification of the mineral using the calcein assay showed no significant difference in the quantity of mineral however. This may be attributable to the lack of sensitivity of the assay or the fact that the differences were not as striking at 28 days when control cultures had caught up.

The present study isolates the effect of silica on the osteoblast. The main findings were a potential increase in nodule formation with a concomitant decrease in AP activity. Osteocalcin was not measured. This was in agreement with the findings of Hench (Hench, 2001; Hench *et al.*, 2001; Xynos *et al.* 2000; Hench *et al.*, 2000) using Bioglass-a material comprising Si, Na and P. The findings presented in this chapter suggest that silica alone may be the main factor responsible for this response. The findings reported by Keeting *et al.* (1992) suggesting the potential of silica-containing compounds to mediate autocrine activity in HOBs secretion of TGF- $\beta$  demonstrates that investigations into the molecular mechanisms potentially affected by silica are warranted.

Additionally, the findings by Keeting *et al*, (1992) that the increased proliferation in the presence of Zeolite A could mainly be accounted for by the silicic acid content of the material, together with the results of this chapter, demonstrate that silicic acid has the potential to affect osteoblast cell behaviour.

In summary, the findings presented here show that silica is not capable of inducing mineral formation in cultures without DEX and BGP but may affect the formation of nodules. Craniofacial osteoblast cultures supplemented with DEX and BGP appeared to form more mineral with increasing amounts of silica supplementation. There is some evidence that silica may enhance osteoblast mineralisation *in vitro*, but the results were variable. This was disappointing but the fact that such trace amounts of silica appeared to have demonstrable effects on ALP, rate and number of nodules formed and osteoblast mineralisation is encouraging and should provoke further research. The use of specialised techniques to assess the interaction of silica with collagen and non-collagenous proteins would aid this research significantly. These should include fluorescence techniques to determine the interaction of silicates with osteoblasts and proteins (Cladera *et al*, 2000) and molecular and genetic techniques capable of identifying subtle effects of trace amounts of silica on the osteoblast (Xynos *et al*, 2001).

## **Chapter 4**

### **Silicate Toxicity.**

## 4.1 Introduction.

One of the principle goals of the project is to incorporate silica into biomaterials. It is necessary to address potential problems of toxicity. Cell death in relation to biomaterials is underrepresented in the literature (Gough, 1999). Surfaces which are seen as cytotoxic are not generally used as biomaterials for obvious reasons, however products of materials may contribute to the failure of an implant, such as degradation products including wear particles (Stea *et al.*, 2000a) and ions leached into the tissue surrounding an implant (Shettlemore and Bundy, 1999). For these reasons it is important to follow up any sign of toxicity to osteoblasts from the potential products of materials which are implanted in the body in addition to any beneficial effects. In the previous chapter cell death was seen in cultures supplemented with more than 300ppm silica as sodium metasilicate

Silica toxicity is not a new phenomenon and industrial exposure to dust containing respirable (0.5-5 $\mu$ m) silica particles is known to cause silicosis. This is a type of progressive, irreversible pneumoconiosis which has cytotoxic and fibrogenic effects. Inhaled silica particles are engulfed by alveolar macrophages and subsequently adsorbed onto cell membrane systems causing their rupture and cell death (Allison *et al.*, 1977). Macrophages damaged by this process release factors (such as collagenase) which stimulate fibroblasts to produce collagen (Burrell and Anderson, 1973), and fibronectin (Driscoll *et al.*, 1991; Driscoll, 1990). The amount of fibrogenesis is dose dependent, with more collagen formation resulting from lower doses of silica. Higher doses of silica cause macrophage death and consequently, less fibrogenesis (Allison, 1977). The toxicity of the silica particles has been related to their positive charge (Bagchi, 1992). Oxidative stress has been implicated as the mediator of silica induced toxicity to alveolar macrophages (Zhang *et al.*, 2000).

Silicic acid reacts with biological membranes and can alter permeability (Dobbie, 1982). Inhalation of silica particles causes silicic acid release in lung tissue, as a result of the partial solubilisation of the particles, causing denaturation of protein (Dobbie, 1982). The fact that adherence of the particulate silica to biological membranes in Allison's studies was effected by a layer of solubilised silica lends some weight to the

theory that silicic acid may be cytotoxic. Silicic acid has been shown to be the main pathogenic factor in the toxicity of silicate dusts (Singh *et al.*, 1985).

Industrial exposure to silica appears to affect other systems in the body. Intravenous administration of particulate silica exacerbates herpetic hepatitis in mice (Irie *et al.*, 1998). Patients with silicosis were noted to have renal problems implicating silica in renal nephropathy (Bolton *et al.*, 1981; Saldhana *et al.*, 1975). A survey of workers exposed to silica for less than 2 years showed subclinical signs of kidney dysfunction in the absence of silicosis (Hotz *et al.*, 1995). A recent study of the medical records of ceramic workers showed a threefold increase in end stage renal disease compared to the expected amount and that this was increased over in subjects who worked in the industry in the long term (Rapiti *et al.*, 1999).

Renal damage has also been seen after ingestion of certain silica containing compounds in experimental animals. Renal damage and urinary stone formation has been observed in dogs and humans treated with magnesium trisilicate, an antacid, over long periods (Newberne and Wilson, 1970; Dobbie, 1986). Kidney damage may also result from treatment with sodium silicate (Newberne *et al.*, 1970) which is used to treat tuberculosis and atherosclerosis (Dobbie *et al.*, 1982a). In a study by Newberne and Wilson (1970) a variety of silica containing compounds were fed to dogs and rats over a period of 4 weeks. Renal lesions were observed in the dogs which had been fed sodium silicate or magnesium trisilicate but not in those fed silicon dioxide or aluminum silicate. No lesions were observed in the rats. The study concluded that, in view of the large number of pharmaceutical and food products containing these silica compounds, their toxicity warranted further investigation. Dobbie and Smith (1982a) found renal lesions in guinea pigs treated with magnesium trisilicate for 4 months. This study also investigated the link between the silica content of drinking water and a condition known as Balkan nephropathy where the diffusion of silicates from the granite in the area into drinking water is associated with a distinct nephrotoxic effect.

Crystalline silica has been accepted as a carcinogen (Lim *et al.*, 1999; Borm and Driscoll, 1996) but this is drawn into question by Hessel *et al.* (2000) who state that current research does not demonstrate a causal effect between lung cancer and exposure

to crystalline silica in humans. Although silicosis and other diseases relating to exposure to particulate silica is well documented, there is scant information in the literature concerning toxicity of cells to silica in solution. The eye irritation potential of a range of soluble sodium silicates has been assessed using an *in vitro* rabbit enucleated eye test (York *et al.*, 1994). The nature of the route and form in which silica is absorbed in the intestine is also unclear. The effect of silica, in any form, on the osteoblast has not been reported.

Dietary silica supplementation in experimental animals has always been considered beneficial to bone in terms of the amount and rate of bone formed (Carlisle, 1972; Schwartz and Milne, 1972). These studies used the same silica compound, sodium metasilicate, as was used in the previous chapter. The fact that supplementation of bone cell cultures with concentrations of more than 300ppm silica caused cell death is the first evidence that silica may be toxic to bone cells and warrants further investigation.

The aim of this chapter is to establish the method of cell death that occurs in osteoblasts supplemented with toxic levels of silica. The extent of cell death will be investigated, along with the ability of osteoblasts to recover from toxic levels of supplementation. This chapter also aims to ascertain whether silica toxicity is a phenomenon exclusive to osteoblasts or whether other cell types are affected *in vitro*. Finally, an attempt will be made to elucidate the cellular mechanism underlying silica toxicity.

---

## **4.2 Materials and Methods.**

### **4.2.1 Preparation of Silica Containing Medium.**

Silica medium was prepared as in the previous chapter. Briefly, double strength complete Dulbeccos Modified Eagles Medium (DMEM) was prepared from a 10x concentrate (Gibco). A 900ppm, buffered, silica solution was prepared from a 1000ppm stock solution of sodium metasilicate (BDH). The final 450ppm solution was made by combining equal volumes of media and silica solution.

### **4.2.2 Morphology of Cell Death.**

Human osteoblasts (HOBs) were seeded onto Thermanox discs (Nunc) at a density of  $8 \times 10^5$  cells/ml in complete medium or medium supplemented with 450ppm sodium metasilicate. The process of cell death was recorded over 48hr using a Nikon Diaphot inverted phase contrast microscope with a Nikon EM camera. The presence of apoptotic cells was determined at 90min, 3, 6, 12, 24 and 48hr. Cells were rinsed in sterile PBS and fixed using a 50% ethanol solution with 1% acetic acid and stained with either propidium iodide (0.01mg/ml, Sigma) or Hoechst 33258 (0.2 mg/ml, Sigma). Propidium iodide stained samples were viewed with a Leica TCS CLSM using the 568nm laser line. Hoechst 33258 stained samples were viewed under UV light using a Nikon UFX-DXII fluorescence microscope.

### **4.2.3 Cell death of Attached Cells in Monolayer Culture.**

The effect of treating cells in monolayer culture with silicate was investigated to ascertain whether established cells, which have attached and spread are susceptible to silicate toxicity in the same way as cells, which have been seeded directly into silicate containing medium. HOBs were seeded at a density of  $8 \times 10^4$  cells/ml in 24 well tissue culture plates in control medium for 48 hr. The medium was then replaced with medium supplemented with a range of silica concentrations (0-450ppm) for a further 48 hr. Cell activity was measured at 48 hr (before addition of the silicate-containing medium) and at 4 days using the alamar blue assay. Cell number was assessed at 4 days using the

DNA assay as previously described. Cells were photographed during these experiments using a Nikon EM camera mounted on a Nikon TMS phase contrast microscope.

Propidium iodide staining was used to visualise the nuclear morphology of the cells. For these experiments, HOBs were seeded on thermanox discs at a density of  $8 \times 10^4$  cells/ml in control medium. for 24 hr after which time the medium was replaced with silicate containing (450ppm) medium. Cells were fixed and stained as described previously at 24 hr (control), 30hr (6 hr post supplementation), 38hr (8 hr post supplementation)c and 4 8 hr (24 hr post supplementation).

#### **4.2.4 Analysis of Membrane Integrity.**

Cells treated with 450ppm sodium metasilicate for 90 min and 4 hrs were stained with the trypan blue exclusion dye (Gibco) which is only taken up by dead cells with damaged membranes. Duplicate wells were fixed in 3% glutaraldehyde and stained with the dye as a positive control.

#### **4.2.5 Recovery of HOBs from Toxic Levels of Silicate Supplementation.**

The ability of osteoblasts to recover from toxic levels of silicate was measured at 48 hr. HOBs were incubated in 450ppm silicate for various times (90 min, 3 hr, and 6 hr) after which they were re-fed with control medium for the remainder of the 48 hr period. HOBs seeded in non-supplemented medium for 48 hr were used as a control. Cell activity was measured at 48 hr using the alamar Blue assay. Total DNA was measured using the Hoechst 33258 dye. All cultures were examined by phase contrast microscopy and photographed at 48 hr total culture time.

#### **4.2.6 Effect of Silicate Supplementation on Different Cell Types.**

The succceptibility of other cell types to silicate toxicity was tested using a murine fibroblast cell line (3T3-L1, *Journal of Immunology*, (1975) 114, 898) and a murine macrophage cell line (J774, *Cell*, (1974) 1, 113). The cells were maintained in culture in DMEM supplemented with 0.02M L glutamine, 1% non essential amino acids and 100

units/ml Penicillin/streptomycin. The serum used was 10% FBS for 3T3 cells and 10% new born calf serum for J774 cells. These were seeded at a density of  $8 \times 10^4$  cells/ml in 24 well tissue culture plates and incubated in control medium or medium supplemented with 450ppm sodium metasilicate for 48 hours. The cell morphology was recorded after 48 hr using phase contrast microscopy.

Cell activity was measured over a range of silica concentrations (0-450ppm) using the alamar Blue assay for 3T3s. Macrophage J774 cells were not assayed as macrophages may interfere with the alamar Blue assay by producing oxidising agents. The proliferation of J774 and 3T3 cells was determined by DNA content analysis using the Hoechst 33258 assay.

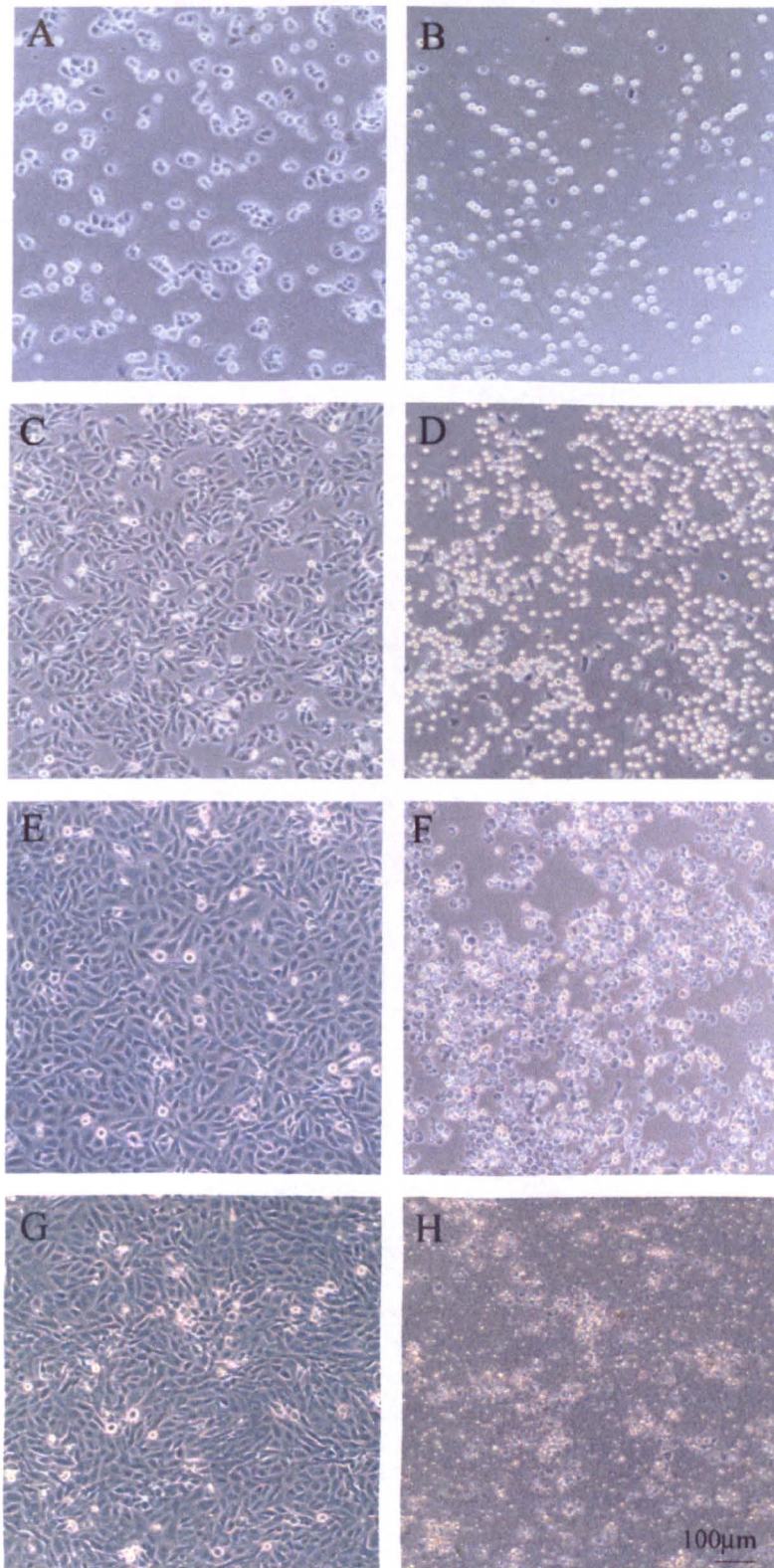
Statistical analysis of all assays in this section was carried out using a one way analysis of variance (ANOVA) with a Tukey-Kramer post test for multiple comparisons.

## 4.3 Results.

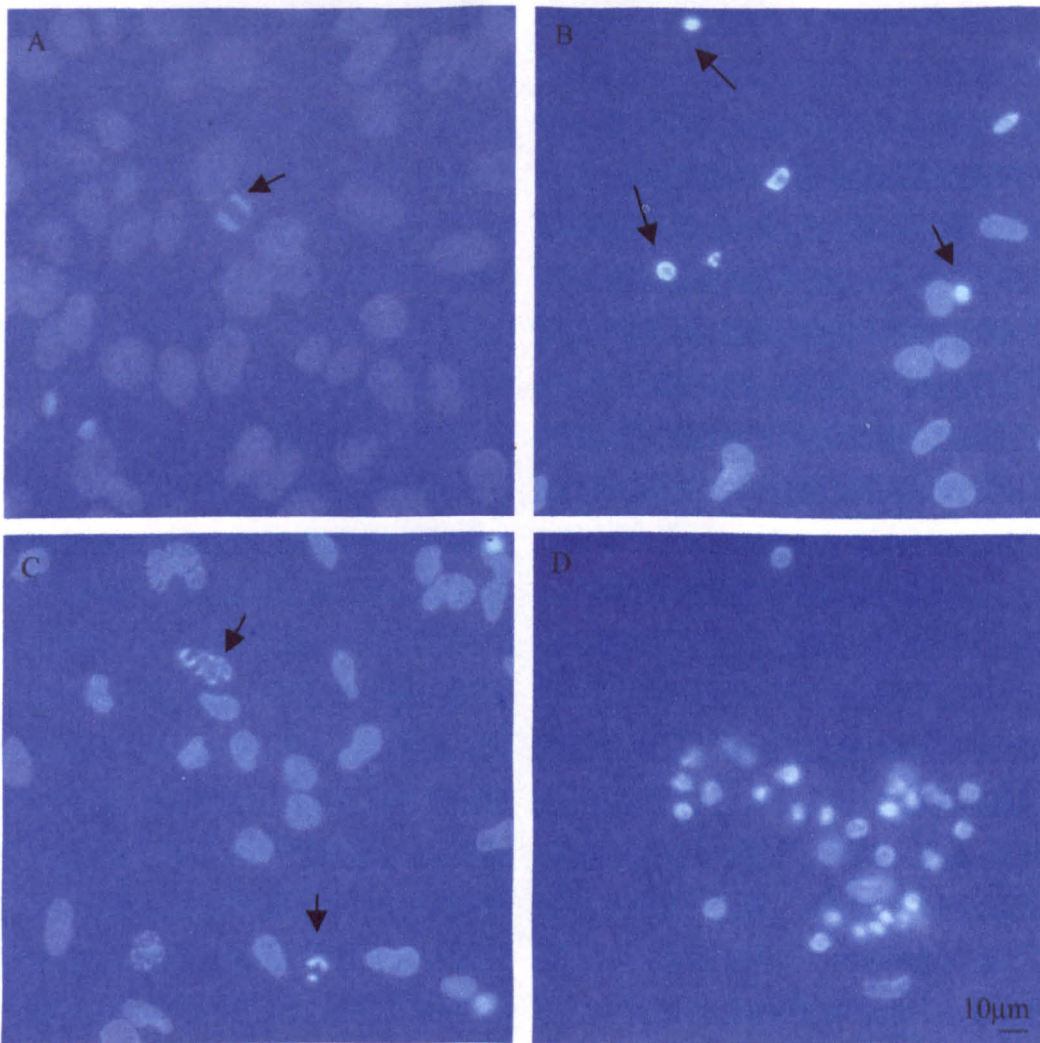
### 4.3.1 Morphology of Cell Death.

Figure 4.1 records the process of cell death of HOBs supplemented with 450ppm silicate using phase contrast microscopy. Osteoblasts in control medium had attached to tissue culture plastic by 90 min after seeding and had started to spread. In contrast, supplemented HOBs attached but remained rounded. This effect was more marked at 4 hr. By 24 hr after seeding supplemented cells had begun to detach from the surface, were smaller than control cells and were disc shaped. Over the next 24hr most of the cells fragmented into small particles with only few adherent, spread cells remaining.

HOBs supplemented with 450ppm silicate solution were stained with PI or Hoechst to ascertain the mechanism of cell death. This was confirmed as apoptosis using fluorescence microscopy and confocal laser scanning microscopy. The morphological features used to identify apoptotic cells were condensed nuclear chromatin forming characteristic caps around the nuclear membrane, nuclear blebbing and the formation of apoptotic bodies (fragmented packets of nuclear material). Apoptotic cells were seen using fluorescence microscopy of Hoechst stained cells after just 90 min in culture and by 4 hr the majority of supplemented cells were shown to be apoptotic (Figure 4.2). CLSM of PI stained cells showed similar, more convincing results (figure 4.3). CLSM was identified as a useful technique for confirming apoptosis as the ability to optically section the cells resulted in at least one definitive apoptotic image of each cell where conventional microscopy yielded a less certain result (figure 4.4).



**Figure 4.1** Phase contrast micrographs of cell death of HOBs supplemented with 450ppm sodium silicate for 90 min (b) 4 hr (d), 24 hr (f) and 48 hr (h) with corresponding control cultures (a, c, e, g). Control cultures have attached and started to spread by 90 min and form a confluent layer by 48 hr. Silicate supplemented HOBs have attached but not spread at 90 min (b). They remain rounded at 4 hr (d). The cells appear disc shaped and detach by 24 hr (f) Only cell fragments remain by 48 hr (h).



**Figure 4.2** Fluorescence images of HOBs stained with Hoechst 33258 (a) Control 24 hr culture showing normal nuclei and a mitotic spindle (arrow). (b) Cells seeded in 450ppm HOBs after 90 min in culture. Some apoptotic cells are seen (arrows). (c) After 4 hrs some cells are apoptotic (arrows). (d) At 24 hr most cells are apoptotic.

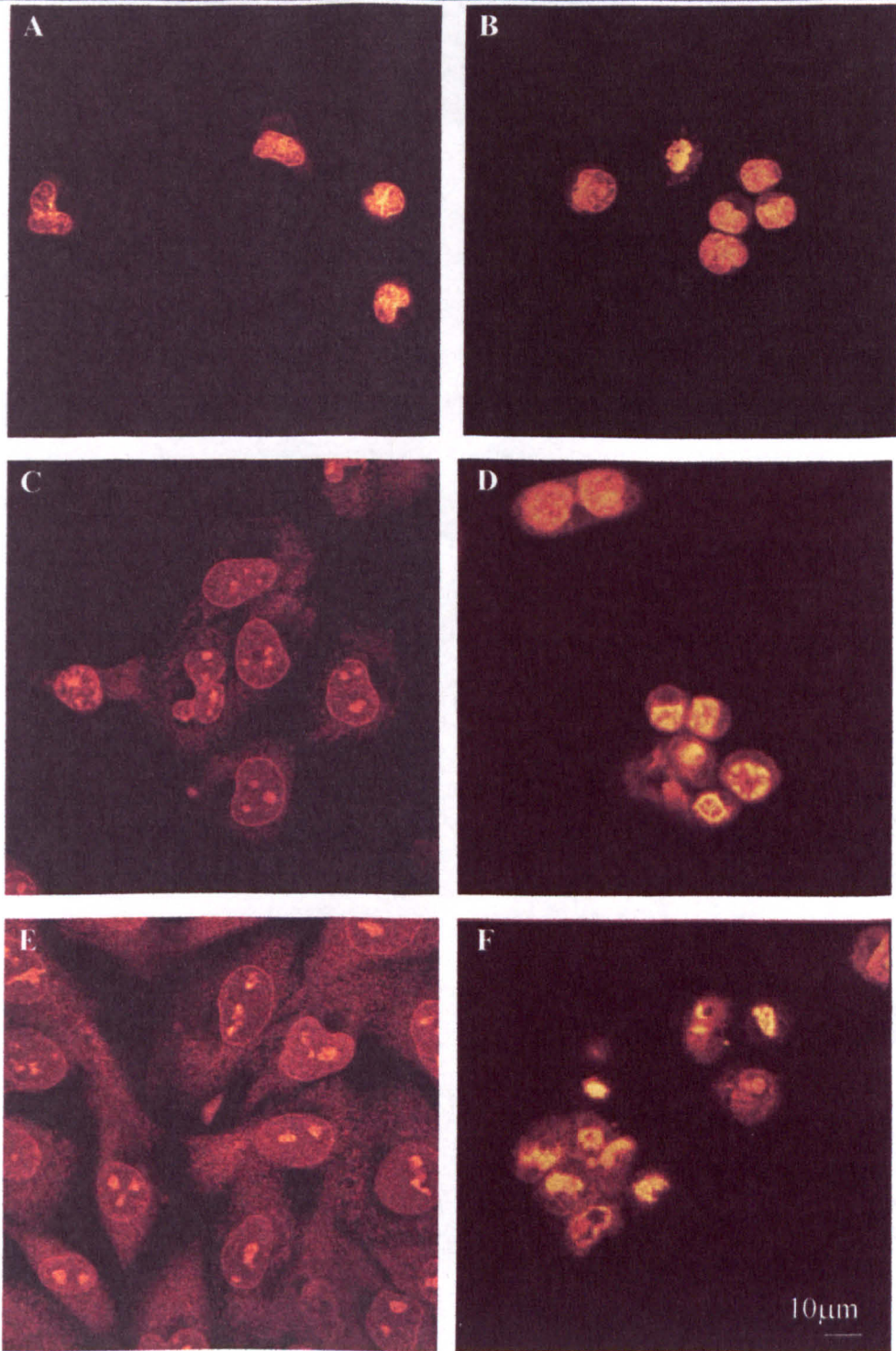


**Figure 4.3** CLSM images of HOBS seeded in control medium (a-c) and medium supplemented with 450ppm silicate (d-f). Nuclei of control and treated cells appear similar at 90 min (a, b). At 4 hr many treated cells are apoptotic (d). By 24 hr almost all cells are in the later stages of apoptosis (f).

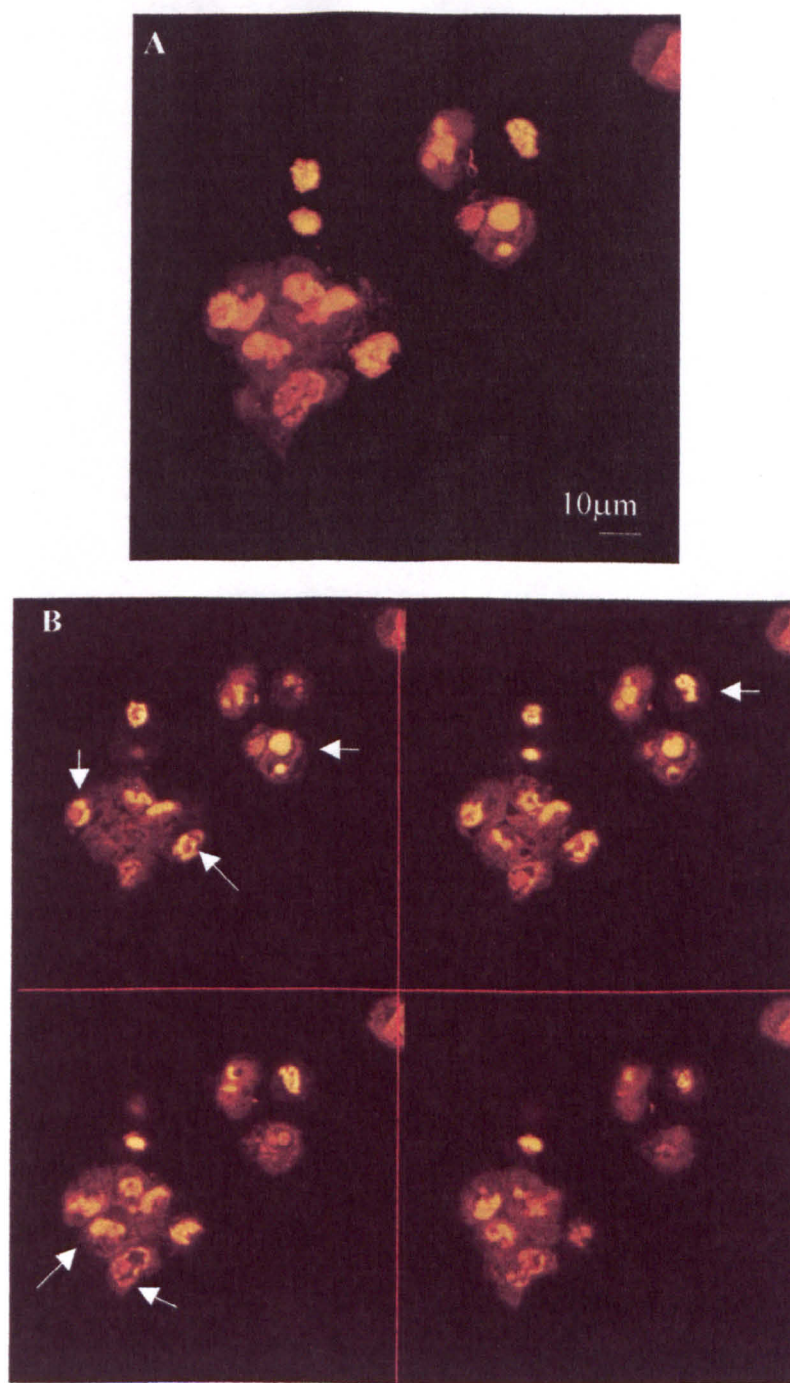


**Figure 4.4** CLSM images of cells treated with 450ppm for 24hr and stained with PI. (a) Maximum intensity projection of all optical slices through the cells comparable to images obtained using conventional epifluorescence microscopy. Some cells cannot be definitively identified as apoptotic. (b) Gallery of optical slices through apoptotic cells (1  $\mu\text{m}$  apart). Each cell can be identified as apoptotic in at least 1 slice (arrows).

### 4.3.2 Cells in Monolayer Culture.

The profile for cell activity as measured by alamar blue reduction was similar whether cells were seeded in silicate or established in monolayer culture first. Cell activity for cultures at 48hrs (before the addition of silicate) and at 4 days (48hr post silicate treatment) show that the profile of cell activity is similar to cells seeded directly in silicate for 48hr. (Figure 4.5a). DNA content analysis was also similar for samples 48hr after the addition of silicate whether the cells were seeded directly in medium containing silicate or allowed to become confluent first (figure 4.5b).

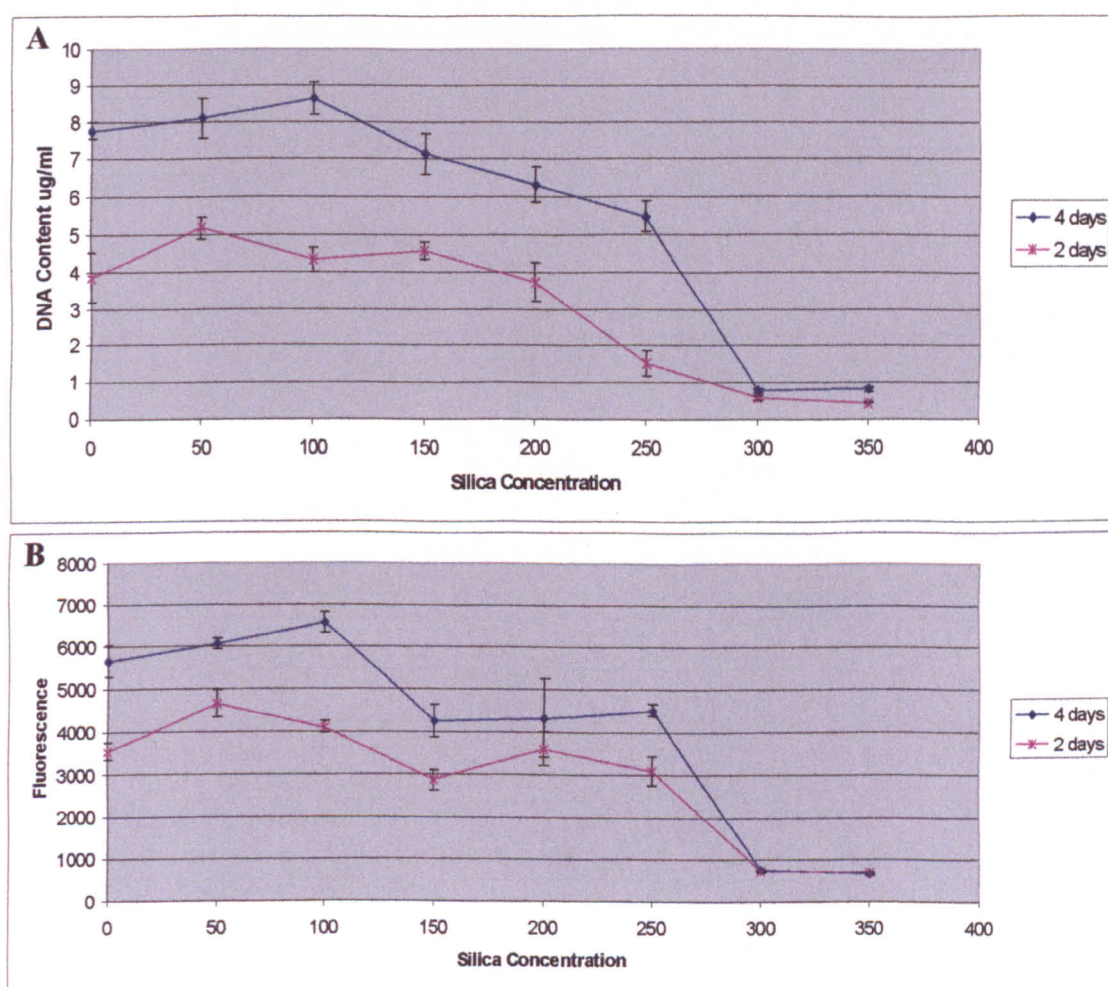


**Figure 4.5** (a) Cell activity of HOBS seeded in silicate for 48 hr or seeded in control medium for 48 hr and silicate-containing medium for a further 48 hr. (b) DNA content of cultures at 4 days. The cells were grown in standard medium for 48 hrs followed by silicate supplemented medium for 48 hrs. Error bars represent standard error of the mean,  $n=4$ .

The appearance of the cells during the period after silica supplementation is shown in figure 4.6. Phase contrast microscopy shows that the cells were confluent at 34hr. Six hours after the addition of silicate containing medium the cells remained attached and spread but the medium contained particulate matter. The cells appeared to have fragmented after a total of 48hrs in silicate containing medium.

Figure 4.7 shows the nuclear morphology of cells seeded in control medium for 24 hr prior to silicate supplementation for a further 6, 8 and 24 hr. A confluent layer of HOBs had formed by 24 hr culture in normal medium (figure 4.7a). At this point the medium was replaced with silicate containing medium. Figures 4b-d show the propidium iodide staining of the resulting cell death 6, 8 and 24 hr later. Some apoptotic cells were seen in the 6 and 8hr supplemented cultures. By 24hr post silicate supplementation most of the cells were apoptotic and the majority were in the advanced stages of apoptosis with apoptotic bodies clearly identified.

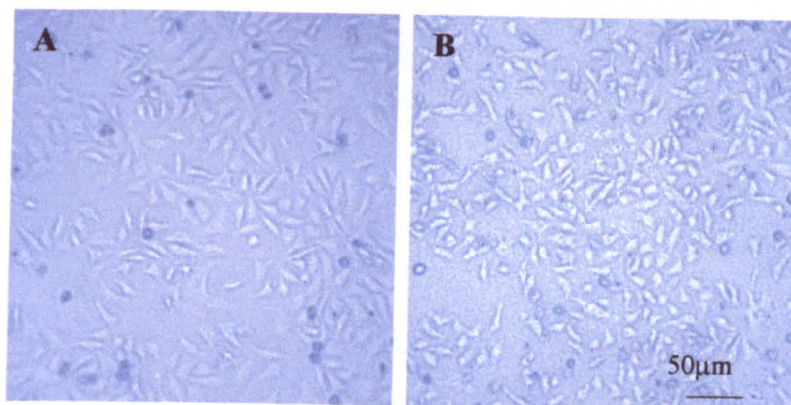


**Figure 4.6** (a) HOBs seeded in control medium for 34hr. (b) HOBs seeded in control medium for 24hr followed by 450ppm silicate for 6hr. Note the particulate matter in the background.

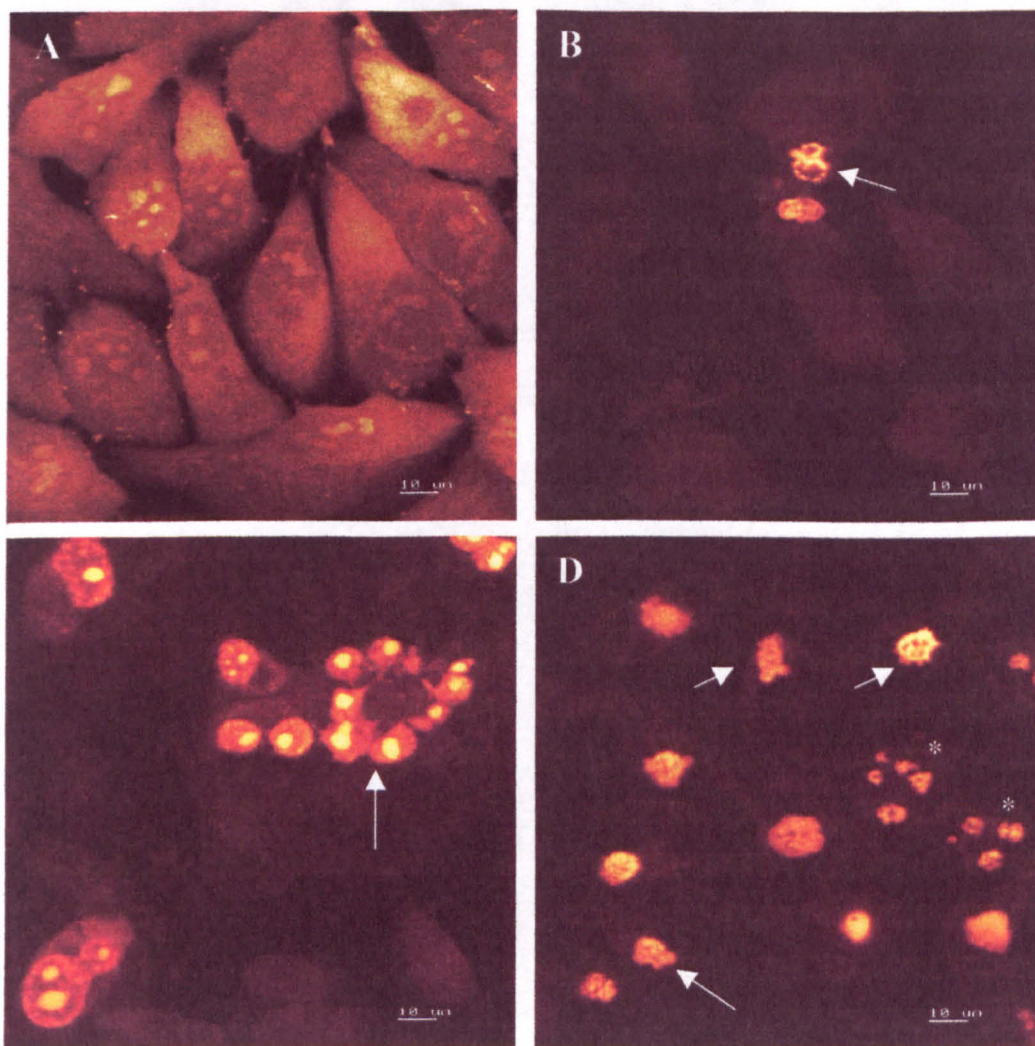


**Figure 4.7** CLSM of HOBs stained with propidium iodide. Cells were grown in control medium for 24 hr (a) after which the medium was replaced with medium containing 450ppm silicate for a further 6 (b), 8 (c) and 24 hr (d). Apoptotic nuclei were seen in all supplemented cultures (arrows). Almost all of the cells grown in supplemented medium for 24 hr were apoptotic and many had fragmented into apoptotic bodies (\*).

### 4.3.3 Analysis of Membrane Damage.

Figure 4.8 shows phase contrast images of HOBs seeded in control and silicate-containing medium for 90min and 4hr. No membrane damage was seen in cells which remained attached to the tissue culture plastic according to the trypan blue method. Cells which were floating in the medium were stained blue.

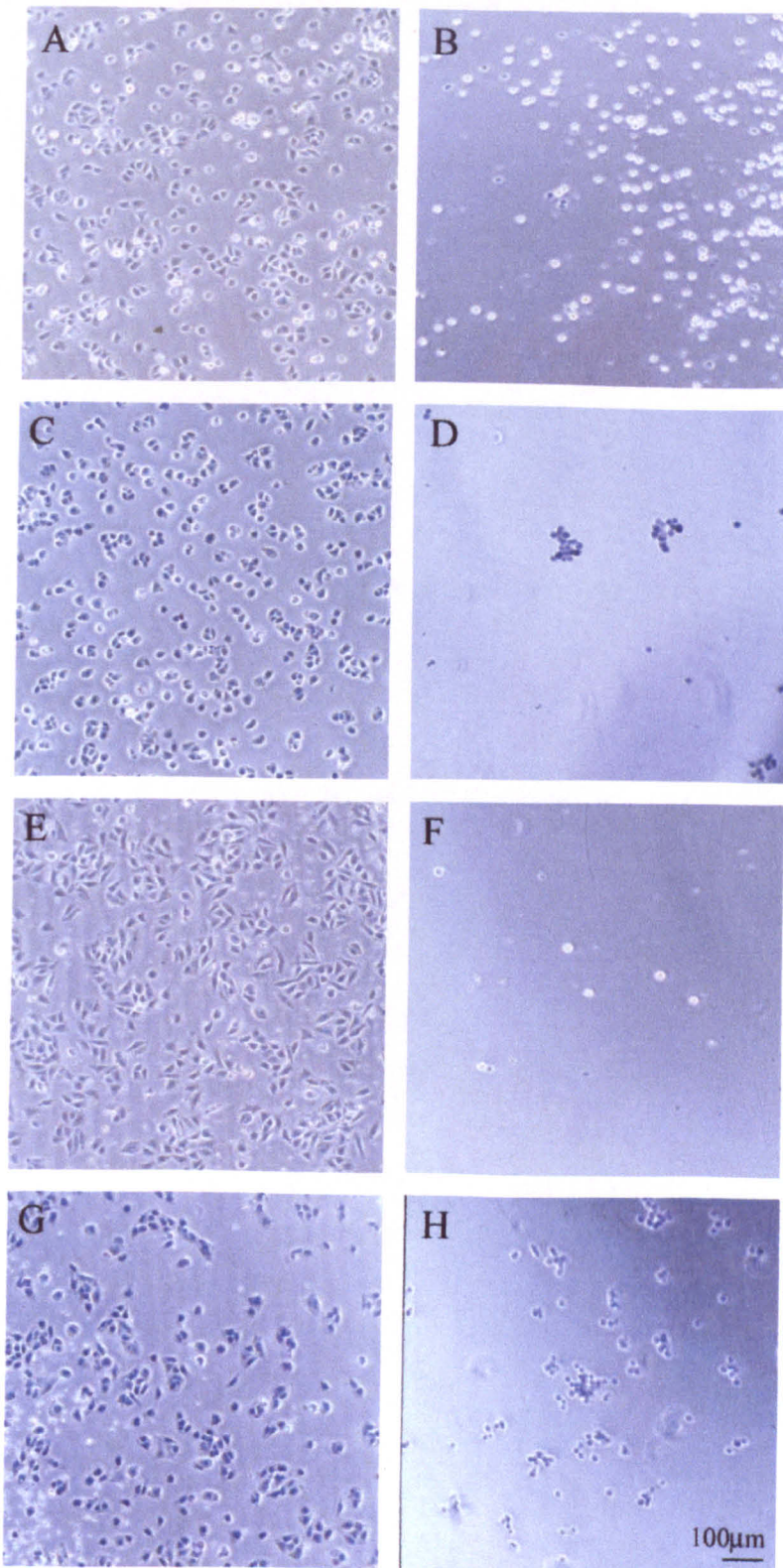


**Figure 4.8** Phase contrast micrographs of HOBs stained with trypan blue with and without silicate treatment for 90 min (a-d) and 4 hr (e-h). Figure (a) shows HOBs at 90min culture stained with trypan blue. The dye is not taken up by the cells. (b) HOBs stained with trypan blue after 90 min treatment with 450ppm silicate. Cells are unstained. Figures (c) and (d) show the blue cell staining of the corresponding positive controls which have been fixed prior to trypan blue staining. Figures (e) to (h) show the same set of cells at 4 hr.

#### 4.3.4 Cell Recovery.

In order to test whether the toxic effect of silicate was reversible, a series of cultures were set up in which all cells, except controls, were seeded in medium containing 450ppm of silicate. HOBs were then re-fed with control medium either at 90 min, 3 hr or 6hr and cell tests were performed at 48 hr. Although many cells were washed off the thermanox discs during re-feeding, the morphology at 48hr of those that had remained was similar to those of control 48 hr cultures for 90min, 3hr and 6hr (figure 4.9). Re-fed cultures exhibited higher cell activity than those incubated for 48 hr in 450ppm silicate (figure 4.10a), indicating that these cells have some capacity to recover. However, activity was significantly lower ( $p < 0.001$ ) than control cultures as measured by alamar Blue reduction. DNA content was much lower than controls for re-fed cultures also (figure 4.10b  $p < 0.001$ ). When the amount of activity per cell was calculated (by dividing alamar blue reduction by total DNA) it was observed that for 90 min and 3hr re-feeds activity per cell was similar to control values even though fewer cells were present (figure 4.10c). Cells re-fed at 6 hr had a reduced capacity for recovery but this was not statistically significant.

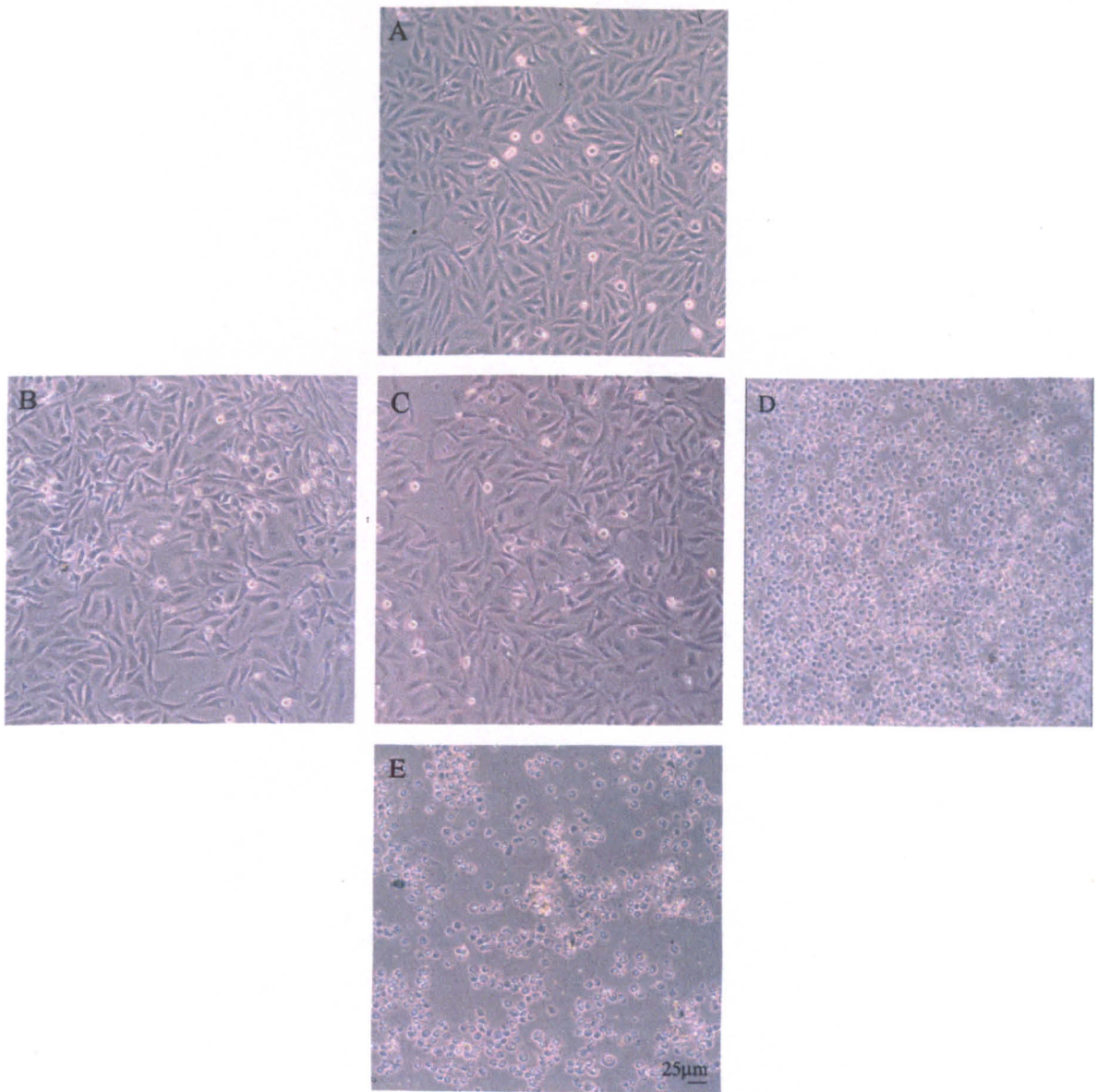


**Figure 4.9** Phase contrast images of HOB cells at 48 hr cell culture. (a) HOBs grown in control medium for 48 hr. (b) HOBs seeded in medium supplemented with 450ppm sodium silicate for 90min which was then replaced with control medium for the remainder of the 48 hr culture period. (c) HOBs seeded in 450ppm silicate for 4 hr and re-fed with control medium. (d) HOBs seeded in 450ppm silicate and re-fed with control medium after 24 hr. (e) HOBs seeded in 450ppm silicate for 48 hr.

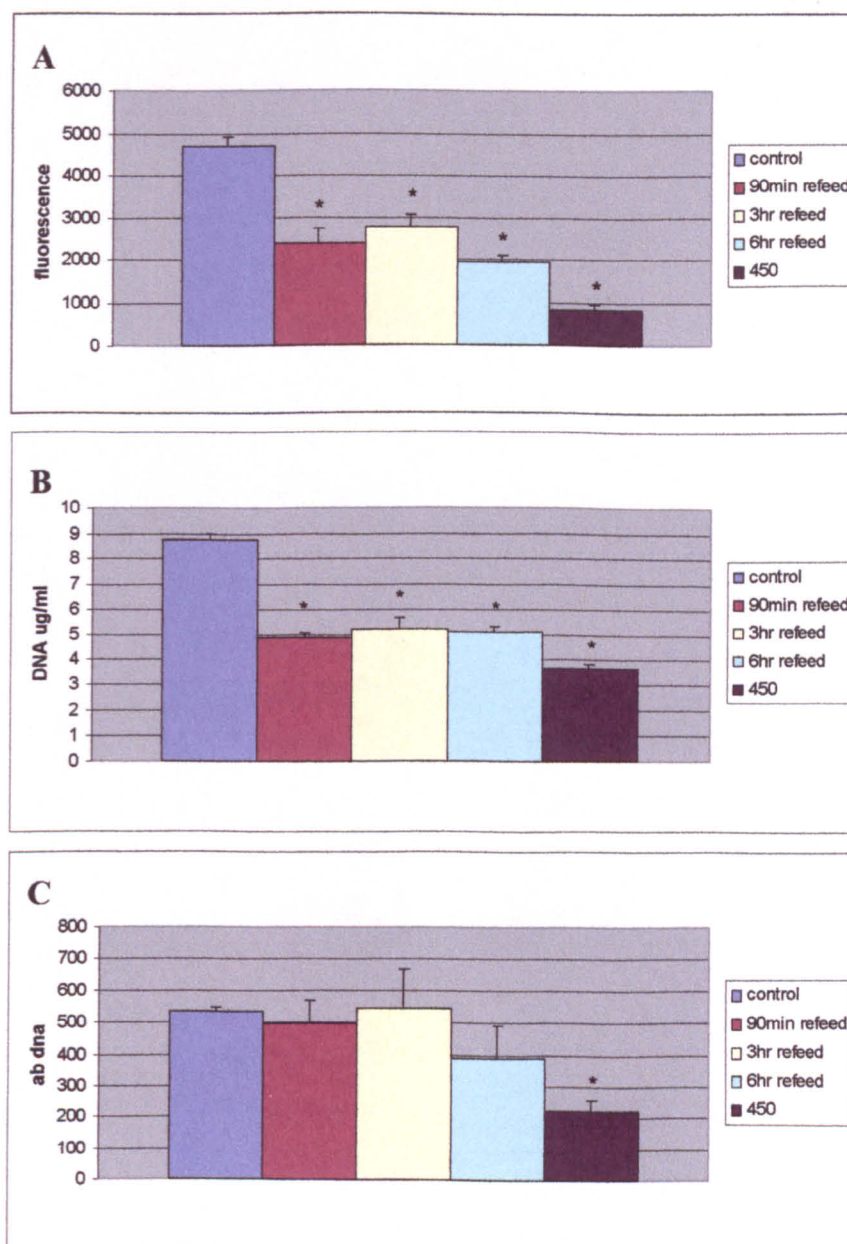


**Figure 4.10** Cell activity (a) and DNA content (b) of HOBs seeded in 450ppm silica which was replaced with control medium at 90 min, 3 hr and 6 hr. Cell activity and cell number are markedly reduced for 90 min, 3 hr and 6 hr ( $p < 0.001$ ). (c) Cell activity expressed per cell (AB/DNA) of HOBs. Although fewer cells are present the activity per cell is similar and there was no statistically significant difference between samples for all the treated samples. Cells treated with 450ppm silicate for 48 hr were significantly lower than controls ( $p < 0.001$ ). Error bars represent standard error of the mean,  $n=4$ .

### 4.3.7 Effect of Silicate Supplementation Different Cell Types.

Other cell types were grown in medium supplemented with a range of sodium silicate concentrations ranging from 0 -450ppm to ascertain whether the toxic effect of high concentrations of silica were specific to osteoblasts. These were murine fibroblasts (3T3) and murine macrophages (J774). Both cell types cells exhibited the same pattern of reduced cell growth and eventual cell death with increasing silicate concentrations. This could be seen by observation of the cultures using phase contrast microscopy (figure 4.11). Alamar Blue reduction was minimal in cultures supplemented with 450ppm silicate for 3T3 cells (figure 4.12c). The alamar blue assay was not carried out on J774 cultures because macrophages produce oxidising agents which interfere with the assay. Total DNA for both cell lines was similar after 48 hr (figure 4.12a, b).

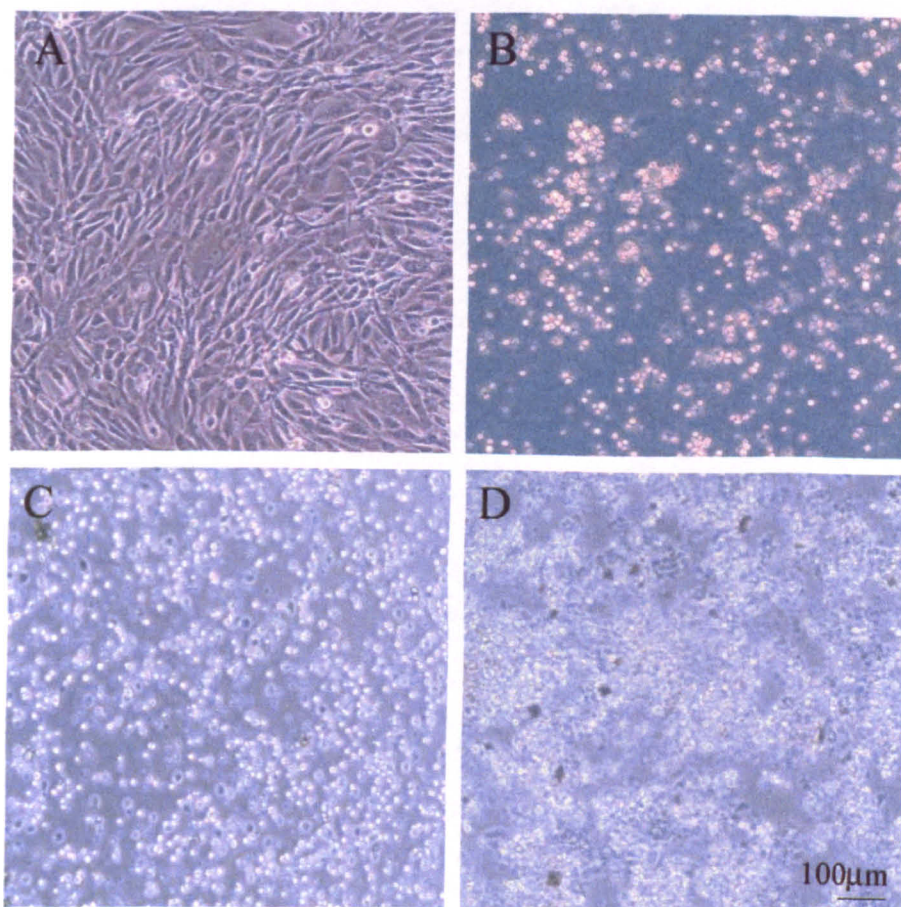


**Figure 4.11** Phase contrast micrographs of 3T3 fibroblasts (a, b) and J774 macrophage cell lines in control medium (a, c) and medium supplemented with 450ppm silicate (b, d) after 24 hr.

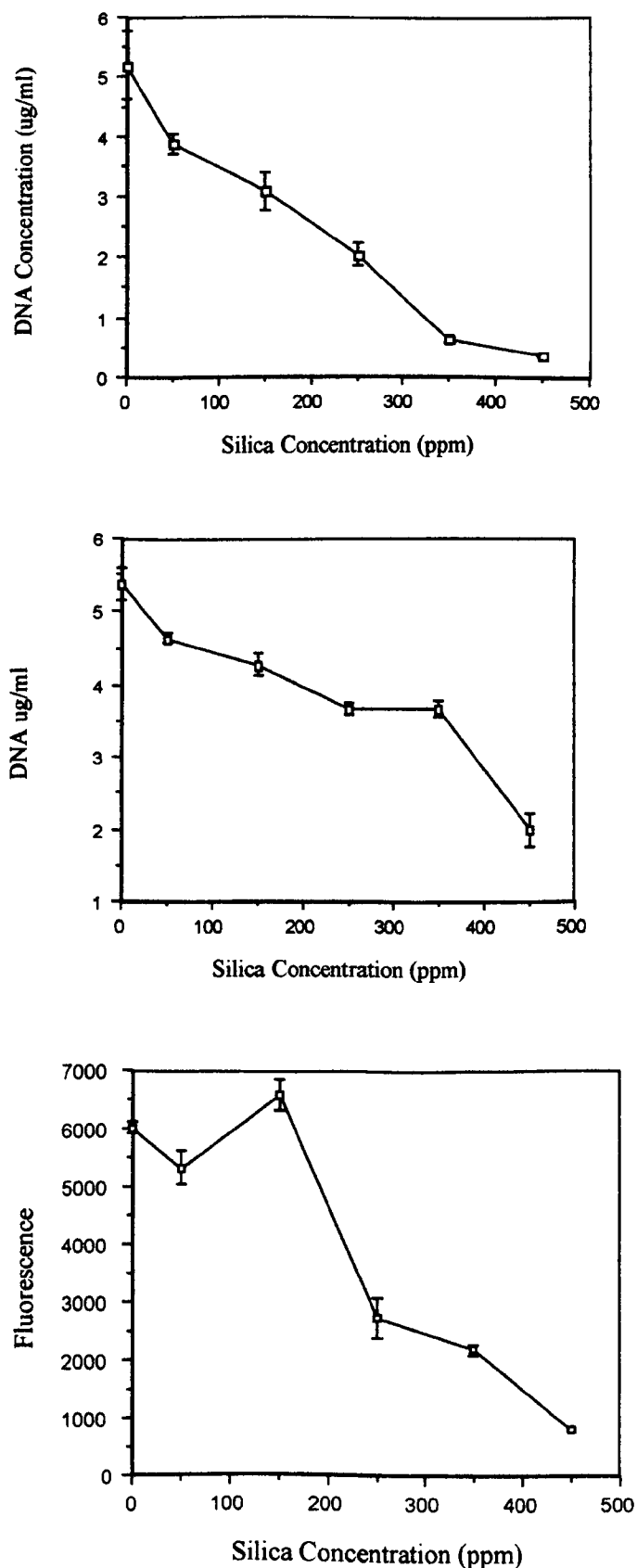


**Figure 4.12** Total DNA content for J774 (a) and 3T3-L1 (b) cell lines supplemented with up to 450ppm silicate for 48 hr. (c) Activity of 3T3-L1 cells measured by Alamar Blue reduction after 48 hr supplementation with up to 450ppm silicate. Error bars represent standard error of the mean, n=4.

#### 4.4 Discussion.

HOB cultures were supplemented with up to 450ppm in order to investigate the nature of the cell death seen in the previous chapter when osteoblast cultures were exposed to concentrations >300ppm. Sodium metasilicate was used in the initial experiments which established the essentiality of silicon for normal mineralisation of rat and chick bones (Schwartz and Milne, 1972; Carlisle, 1972).

The response of HOBs to the silicate solution followed a distinct pattern of events. Cells attached to the tissue culture plastic but remained rounded, then detached and fragmented. The use of fluorescent dyes to stain nuclei confirmed that the mechanism of cell death was apoptosis. A cytotoxic effect of silicates inducing apoptosis in cultured cells has never previously been demonstrated.

Apoptosis can be defined as a series of biochemical processes which achieve the non-inflammatory destruction of the cell (Gottlieb, 2000). It is a tightly controlled process which happens in response to both cell insult and as a normal part of tissue development where cells decide whether to undergo division or cell death (Wang and Wang 1999a; Hetts, 1998). In this way organisms control developmental plasticity and homeostasis (Wang and Wang, 1999a). Dysregulation of apoptosis is associated with the development of disease states such as cancer, autoimmunity, neurodegeneration and heart disease (Hetts, 1998). Understanding the apoptotic process is important as manipulation of apoptosis, whether by enhancing or suppression may allow treatment in disease (Wang and Wang, 1999b). The entire energy dependent process happens within the confines of the cell membrane so that the cell contents are not released into the environment (Hetts, 1998). The other common form of cell death is necrosis which generally occurs after tissue injury. In this case cell organelles and energy levels are compromised (Nicotera *et al.*, 1999). Apoptotic cells are characterised morphologically by clumping of cellular DNA into cap-like aggregates and membrane blebbing leading to the formation of apoptotic bodies. These are cleared by phagocytic cells. The body of literature that exists on apoptosis is vast, and beyond the scope of this thesis but there are many recent reviews in the literature (Gottlieb, 2000; Nicotera *et al.*, 1999; Wang and Wang, 1999a, b; Hetts 1998).

Although the level of silicate ingested may be high, the level of silica absorbed in the small intestine is likely to be small as the amount of silica in serum is consistently the range 1-5ppm (Dobbie and Smith, 1982b; Carlisle, 1974). It is unlikely therefore, that the levels of silicate used in these studies would be found in the body under normal circumstances. The use of silicate based antacids and artificial silica based implants may however be cause for concern.

Because cell attachment and spreading are clearly affected by toxic levels of silica supplementation there may be implications for the recruitment of osteoblasts to an implanted, silica containing, biomaterial surface. Considering the concentration of silica required to induce apoptosis is small, it is not unreasonable to suppose that silica-containing biomaterials could conceivably release these amounts into the tissues immediately surrounding an implant. The silicic acid release characteristics of existing silica-containing biomaterials *in vitro* or *in vivo* have not been reported but the possibility of medical implants and devices leaching small quantities cannot be overlooked. Silicic acid release is associated with the formation of a calcium phosphate layer on implant surfaces in a simulated body fluid *in vitro* which encourages the formation of a strong attachment between silica-containing implants and bone *in vivo* (Hench *et al.*, 1971). A relationship between silicic acid and the osteoblast, beneficial or otherwise, has never been previously been demonstrated.

The mechanism of apoptosis induced by silica seems to involve direct interaction between the silica particles and cell and lysosomal membranes (Kane *et al.*, 1985, Kane *et al.*, 1980). The trypan blue exclusion dye was used in our studies to assess whether the cell membrane integrity was compromised during apoptosis. There was no evidence to suggest that membrane damage was involved in apoptotic process.

Few studies have examined the induction of apoptosis by silica. Those that have, used particulate silica and none to date have used bone cells. Particulate silica can induce apoptosis and this has been shown *in vitro* (using A459 bronchial epithelial cancer cell line) and *in vivo* using leucocytes from bronchiolar lavage (Lim *et al.* 1999). Murine resident peritoneal macrophages have been studied by Sarih *et al.*, (1993). In this study silica particles caused apoptosis in adherent peritoneal murine macrophages at doses of

>50 $\mu$ g/ml using gel electrophoresis and fluorescence labelling with DAPI. Apoptotic cells were seen at 4hr and apoptotic bodies were seen at 20hr indicating that the process was rapid. The apoptosis seen in the present study followed a similar timescale to the A459 cells. A connection between the toxicity of siliceous dust and silicic acid has been theorised (Dobbie, 1982). Whether the apoptosis by cells exposed to silicic acid and particulate silica is not known but if so, it may provide an insight into the relevance of silicic acid in the development of silicosis.

While it is useful to use the cell culture model to investigate the effects of single ions and molecules on cells, this is not always directly relevant to the *in vivo* situation. For this reason the response of established osteoblasts in monolayer culture may be more in keeping with events at an established interface between host bone tissue and an implanted device containing silica. In this case attached, spread cells underwent apoptosis and what appeared to be cell fragmentation shortly after coming into contact with toxic levels of silica. Alterations to established cellular cytoskeletal integrity and cell permeability were not investigated here but would be useful in determining the mechanisms underlying cell death. When considering the potential cytotoxic effects of silica containing biomaterials, it must be remembered that these systems are continually bathed in body fluids and that the levels of silica in the region may be in fact very low. Silica containing biomaterials have been used successfully as implants for many years with few reported cytotoxic effects. A study by Nagase *et al.* (1992) implicated silica-containing CaP glasses as highly cytotoxic by injecting pulverised samples into the peritoneal cavity in mice. It was suggested that the effects seen were a result of dissolved silica ions. This study was subsequently highly criticised by Andersson (1993) who argued that increased phosphate release from the silica containing materials was responsible.

Sarih *et al.* (1993) showed that although, apoptosis can generally be reversed by LPS this was not the case for silica induced apoptosis. The toxic effects were reversible when the silicate medium was replaced with control medium within a certain time. Around half of the cells recovered when the medium was replaced with control medium within 6hr. These cells were as active as the control cells. Whether silica induced

apoptosis could be protected against was not investigated but this would be of interest in future studies.

It is interesting to note that osteoblasts are susceptible to apoptosis after exposure to relatively low concentrations of silica and that the effect is not confined to primary cultures but also osteoblast cell lines. Indeed the same characteristics of cell death were seen in other connective tissue cell types including murine fibroblast (3T3) and macrophage (J774) cells. This implies that silicate induced toxicity is wide ranging for human and animal cell cultures. In the event of an inflammatory response following implantation of a biomedical device it is likely that macrophages would be recruited to the area so it would be interesting to investigate whether silica release at an implant site was cytotoxic or beneficial. Certainly cell death which confined the degradation products to within the cell membrane may be more desirable.

Particulate silica as an inducer of apoptosis is now being used to further investigate the molecular biology of apoptosis. For example Hamilton *et al.* (2000) used silica induced apoptosis of macrophages to show that macrophage apoptosis is mediated by a scavenger receptor SR-A II. The same group showed that amorphous silica had no significant apoptotic potential. (Iyer *et al.*, 1996). Other work uses particulate silica to deplete macrophages so that the underlying conditions of disease can be simulated and the effect of drugs on these can be compared with activated macrophages (Henry *et al.*, 1999; Irie *et al.*, 1998). Other work has shown that for macrophages *in vitro*, particle (ceramic and polyethylene) induced apoptosis is size and concentration dependent rather than the composition (Catelas *et al.*, 1999). There is certainly potential to use sodium metasilicate as an apoptosis inducer for similar experiments. Use of a silica solution instead of particulates would be a cleaner system to use and would further the understanding of the apoptotic process in macrophages and other cell types.

There is little in the literature on osteoblasts and apoptosis in general. Meleti *et al.* 2000, showed that inorganic phosphate activates osteoblast apoptosis which may be important in bone turnover and in understanding disease of bone turnover. Osteoblast apoptosis can be prevented by treatment with PTH (Jilka *et al.*, 1999). Glucocorticoid

---

has been reported to increase (Weinstein *et al.*, 1998; 1997) and inhibit (Nakashima *et al.*, 1998) osteoblast apoptosis.

Information about osteoblast apoptosis is scant specifically in relation to biomaterials (Gough, 1999). Recent studies examining osteoblast apoptosis in relation to biomaterials include the study of metal alloy particles (Massari *et al.*, 2000) and HA wear particles (Liu *et al.*, 1999), Stea *et al.* (2000b) studied retrieved implants and found increased apoptosis in areas near wear debris from metal. Phagocytosis of titanium particles by osteoblasts *in vitro* led to apoptosis (Pioletti *et al.*, 1999). Gough and Downes have investigated osteoblast apoptosis on a range of polymeric biomaterials (in press). As the field of biomaterials moves toward tissue engineering of devices control of cell function becomes increasingly important (van Kooten *et al.*, 2000).

Recent studies have shown an increase in the number of osteoblasts undergoing apoptosis when cultured on Bioglass 45S5 (Hench, 2001; Hench *et al.*, 2000; Xynos *et al.*, 2000). This was related to increased numbers of cells undergoing mitosis from other osteoblasts in the same cultures. Osteoblast grown on tissue culture plastic had a low incidence of apoptosis and the cells rapidly divided to form a monolayer. The implication was that class-A bioactive materials stimulate the reproduction of cells that have a more mature osteoblast phenotype and that more immature precursor cells are lost via apoptosis. This is further supported by the finding that genes and transcription factors relating to both the regulation of the cell cycle and apoptosis were up-regulated when osteoblasts were cultured in medium containing ionic dissolution products of bioglass (Xynos *et al.*, 2001). The findings presented in this chapter show that silica, in isolation, can cause apoptosis in osteoblasts and further supports the theory that the silica component of bioactive materials directly affects cell behaviour.

## **Chapter 5**

**The Osteoblast Response to a Silica gel *in vitro*.**

## 5.1 Introduction.

A range of silica containing glasses and glass ceramics in the system  $\text{SiO}_2\text{-Na}_2\text{O-CaO-P}_2\text{O}_5$  are bioactive and are used as biomaterials (Hench, 1991; Kokubo, 1992). Silica is the main component of these materials. Bone bonding ability is lost when the silica content exceeds 60 mol% (Kokubo, 1991). It has been proposed that a prerequisite to bone bonding is the formation of a biologically active carbonate containing hydroxyapatite (HCA) layer on a material surface under physiological conditions (Hench, 1991; Kokubo, 1992). This intermediate apatite layer has compositional and structural characteristics common to those of bone apatite and facilitates the binding of the implant to bone (Pereira and Hench, 1996). The strength of this bond is as strong as bone itself within 3-6months (Hench, 1998). Hydrated silica, which is formed on the implant surface in the body, causes the nucleation of the apatite layer (Kitsugi *et al.*, 1995). The thickness of the hydrated silica gel layer is reported to be in the range 0.2-0.5 $\mu\text{m}$  when apatite deposition begins (Andersson and Karlsson, 1992). It is difficult to study the role of silica in this process because apatite inducers (such as CaO,  $\text{Na}_2\text{O}$  and  $\text{P}_2\text{O}_5$ ) dissolve from bioactive glasses and glass ceramics. To isolate the role of silica in bone bonding, a pure silica gel prepared by hydrolysis and polycondensation of tetraethoxysilane (TEOS) in aqueous solution containing poly(ethylene glycol) has been used (Li *et al.*, 1992; 1994a).

Silica gels have the ability to produce a layer of apatite on their surfaces when they are immersed in a simulated body fluid (SBF) for an extended period of time (usually weeks). The thickness of this layer is reported to be 0.5 $\mu\text{m}$  (Neo *et al.*, 1994). SBF is a calcium phosphate solution whose ionic concentration is almost identical to that of blood plasma (Cho *et al.*, 1996a). HCA cannot form *de novo* from the ions in solution because biological fluid is metastable i.e. with respect to apatite. This means that there are insufficient calcium and phosphate ions in body fluids to allow a spontaneous precipitation of  $\text{CaPi}$  but enough to contribute to the process once it has begun (Anderson, 1980). Much of the work on gels to date has used an *in vitro* approach, using SBF to ascertain the conditions under which a silica gel will form a surface apatite layer (Cho *et al.*, 1996a,b; Pereira and Hench, 1996; Li *et al.*, 1994b).

It has been suggested that the silanol (SiOH) groups on the surface of the gel act as nucleation sites for the apatite (Cho *et al.*, 1996a) although this view is not universally accepted (Pereira and Hench, 1996). Titania gels have the ability to form apatite on their surfaces as they have many hydroxyl groups. Aluminium surfaces, which are described as bioinert, are encapsulated with fibrous tissue and do not form an apatite layer on their surfaces when implanted even though they have many hydroxyl groups. The surface of titania and silica gels is negatively charged, whereas alumina gels have a positively charged surface. It is proposed that materials that have a negative charge and numerous hydroxyl groups will induce apatite formation in physiological fluid (Li *et al.*, 1994b).

A study by Cho *et al.* (1996a) suggests that a certain structural unit of the silanol group is responsible for apatite nucleation. Porous silica gels prepared in different media had the same number of silanol groups but apatite formation was only seen on the gel prepared in polyethylene glycol (PEG). There were structural differences between the gels however, as only gels prepared in PEG had nanopores smaller than 1.7nm. In two more recent studies by the same group all the gels prepared in different media were shown to be capable of producing apatite. This was achieved by either a) using SBF with 1.5 times the concentration of calcium ion (Cho *et al.*, 1996b), or b) using a biomimetic process whereby ions were leached from the gels in SBF and adsorbed on a second substrate (polyether sulfone - PESF). Apatite was then formed on the PESF when it was immersed in a solution with ion concentrations 1.5 times that of SBF. This was not observed using silica glass. It was concluded that silicate ions in aqueous solution could induce apatite nucleation (Cho *et al.*, 1996c).

Other factors determine the ability of silica gels to form apatite on their surfaces in a simulated body fluid. The texture of the gel is important as the apatite nucleation rate increases with increasing pore size and volume (Pereira and Hench, 1996; Pereira, *et al.*, 1995). The temperature at which the gels are sintered has an effect on apatite formation when they are rehydrated in SBF. Gels sintered at 900-1100°C formed apatite on their surfaces in SBF. This ability was lost as sintering temperature increased to 1200°C (Li *et al.*, 1994a). This was explained by the structural relaxation of the gels as they became rehydrated so that they became more like silica glass and the rate of

hydrolysis (i.e. the number of silanol groups) on the surface was reduced. Silica gels sintered at 1200°C were almost insoluble and comparable to silica glass.

Some studies have used animal models to further elucidate the interaction of silica gels with bone (Kitsugi *et al.*, 1995; Li *et al.*, 1995). The apatite forming ability of implanted silica gels is also affected by sintering temperature. It has been shown that the gels that perform well *in vitro* do not necessarily exhibit bone bonding *in vivo*. In a study by Klein *et al.* (1995), gels which were sintered at low temperatures (400-600°C) were easily degraded and evoked an inflammatory response when implanted in the femora of goats for 12 weeks. Sintering (900-1000°C) increased the stability of the gel so that it became more crystalline, less porous and similar to silica glass. This caused a decrease in the amount of dissolution of the gel with a concomitant increase in bone bonding after implantation and a decrease in inflammatory cell response. This is in agreement with the findings of Li *et al.* (1995) who demonstrated bone bonding via a calcium phosphate rich layer in an implanted silica gel sintered at 900°C. Kitsugi *et al.* (1995) found that bone bonding, via an intermediate apatite layer, was rarely observed when silica gels were implanted in rabbit tibiae for 4-8 weeks. An inflammatory reaction at the implantation site was not observed. The limited apatite formation (on 400-800°C sintered materials) was reduced as sintering temperature increased which may result from a reduction in the number of silanol groups available at the gel surface. A calcium phosphate rich layer was never observed on the surface of gels heat treated above 1000°C (Kitsugi *et al.*, 1995).

Few studies have been carried out on the osteoblast response to silica containing materials *in vitro*. (Ozawa and Kasugai, 1996; El Gannham *et al.*, 1997; Vrouenvelder *et al.*, 1993). Much of the work has concentrated on the capacity of these materials to form a surface apatite layer when immersed in physiological fluid. Other studies have examined the interface between implanted materials and bone. It has been shown that foetal rat calvarial osteoblasts grown on 45S5 bioactive glass produced significantly more alkaline phosphatase than those cultured on stainless steel, titanium or hydroxyapatite (Vrouenvelder *et al.*, 1993). Alkaline phosphatase activity is reduced if the bioactive glass surface is altered by either an apatite layer or serum protein adsorption. If both layers are present alkaline phosphatase activity was elevated and a

mineralised matrix was formed (El-Ghannam *et al.*, 1997). Glass ceramics containing 43.6wt% silica have been shown to increase alkaline phosphatase activity and calcium production in primary cultured human osteoblasts as compared to tissue culture plastic controls but levels were not as high as those on hydroxyapatite. Silica containing glass ceramics had no effect on osteoblast expression of differentiation markers such as osteopontin and bone sialoprotein (Ozawa and Kasugai, 1996).

The aim of this work was to assess the osteoblast response to a silica surface without the interference of the other ions present in glasses and glass ceramics. The properties of a silica gel deposited onto Thermanox coverslips were investigated in terms of silica release and bioactivity. The behaviour of human osteoblasts on the surface was evaluated using markers of osteoblast differentiation and mineralisation.

## 5.2 Materials and Methods.

### 5.2.1 Preparation of Biomaterials.

A silica sol - gel was prepared using 10ml tetraethyl orthosilicate (TEOS, Sigma) mixed for 1hr with 10.23ml dried ethanol and 3.165ml 0.2M HCl giving a final molar ratio of 4: 4: 1 TEOS: ethanol: water. This was spin cast onto 12mm diameter Thermanox discs (Nunc) and allowed to dry so that a thin, even film was formed. The surface topography of the discs was viewed using a Philips XL30 FEG field emission environmental SEM (ESEM) in auxiliary mode at 10kV using nitrogen as the chamber gas. Energy dispersive x-ray (EDX) microanalysis was carried out and the thickness of the coating was measured. Uncoated Thermanox discs were used as the controls for the cell culture experiments.

### 5.2.2 Characterisation of Silica Gel.

#### 5.2.2.1 Bioactivity.

The bioactivity of the silica discs was assessed using a simulated body fluid (SBF). SBF was prepared as described previously (Cho *et al.*, 1996 a,b) using the reagents NaCl, NaHCO<sub>3</sub>, KCl, K<sub>2</sub>HPO<sub>4</sub>, MgCl<sub>2</sub>.6H<sub>2</sub>O, CaCl<sub>2</sub> and Na<sub>2</sub>SO<sub>4</sub> added in that order to give an ionic concentration almost equal to that of human plasma (see table 5.2.1). The pH of the solution was brought to 7.4 using 1M HCl and Tris buffer. Silica coated discs were incubated in SBF or tissue culture medium at 37°C for 11 days. The surfaces were air-dried and viewed using a Philips XL30 FEG ESEM with EDX microanalysis. Thermanox discs incubated under the same conditions were used as a control.

	Na <sup>+</sup>	K <sup>+</sup>	Ca <sup>2+</sup>	Mg <sup>2+</sup>	Cl <sup>-</sup>	HCO <sup>3-</sup>	HPO <sub>4</sub> <sup>2-</sup>	SO <sub>4</sub> <sup>2-</sup>
Plasma	142.0	5.0	2.5	1.5	103.0	27.0	1.0	0.5
SBF	142.0	5.0	2.5	1.5	148.8	4.2	1.0	0.5

**Table 5.2.1** Ion concentration (mM) of SBF and human blood plasma (Oliveira, *et al.*, 1995).

### 5.2.2.2 Release of silicic acid from biomaterials.

Silica coated discs and Thermanox discs were immersed in SBF for 2, 4 and 11 days. The amount of silicic acid released from the gels was determined using a molybdenum blue assay. This method is used for detection of monomeric and dimeric silicic acid in solution however interference of phosphate ions has been reported (Iler, 1955). For this reason SBF and tissue culture medium samples were used as controls. The method was based on that of Mullen and O'Reilly (1955) and modified according to Perry and Keeling-Tucker (2000). Briefly, silica standards were prepared from 1000ppm solution of SiO<sub>2</sub> (as sodium metasilicate; BDH) in a solution containing 6% acidified ammonium molybdate solution. Test samples were prepared in the same way. After 10 min, 30% of a reducing solution containing 4(methylamino) phenol sulfate (metol) was added and the absorbance at 810nm was read on a UNICAM UV/VIS spectrometer after 2-48hr.

### 5.2.3 Osteoblast Response to the Silica Gel.

#### 5.2.3.1 Cell morphology and ultrastructure.

Silica gels were placed in 24 well tissue culture plates (Falcon) with the silica surface uppermost. Primary human osteoblasts (HOBs) were seeded on the silica surfaces at a density of  $8 \times 10^4$  cells/ml and maintained in culture 37°C; 5% CO<sub>2</sub> for up to 31 days. Uncoated Thermanox discs were used as controls. The culture medium was changed every 2-3 days. Some silica discs were placed in an inverted position to rule out topographical effects. At various timepoints discs were removed for analysis by SEM (2 days) and TEM (7, 14, 21 and 28 days). The samples were processed according to the methods described in Chapter 2.

#### 5.2.3.2 Cell activity and differentiation.

Cell activity up to 31 days was recorded using the alamar Blue assay as previously described. Briefly, the medium was removed from the cultures and a 5% solution of alamar Blue in Hanks' balanced salt solution (HBSS) was added to each well. These

were incubated at 37°C; 5% CO<sub>2</sub> for 20 min. The fluorescence was measured at an excitation wavelength of 560nm and an emission wavelength of 590nm on a cytofluor. The cultures were then rinsed in sterile PBS and 1ml of sterile double distilled water was added to each well. Cultures were then repeatedly freeze thawed for subsequent assays.

Cell number was quantified from cell lysates at 2, 4 and 7 days using the DNA assay described in Chapter 2. Alkaline phosphatase (ALP) activity was measured using the Granutest kit (Merck) as described in Chapter 2.

#### 5.2.3.3 Uptake of silicic acid by osteoblasts.

The molybdenum blue assay was used to determine the release of silicic acid from the silica discs in the presence and absence of cells. Silica and Thermanox discs were incubated in DMEM for 4 days with and without cells, For the cell studies, primary human osteoblasts were seeded at a density of  $8 \times 10^4$  cells/ml on silica and Thermanox discs. Blank silica and Thermanox discs, without cells, were incubated as controls. The medium was changed at 2 days. The silica content of the medium (0-2 day and 2-4 day) was determined using the molybdenum blue assay as previously described.

#### 5.2.3.4 Mineralisation.

The ability of the cultures to mineralise was determined by alizarin red S staining and tetracycline labelling.

Alizarin red S staining was carried out according to the method of Ohgushi *et al.* (1996) to identify calcium containing deposits. The medium was removed from 14 day cultures and they were rinsed in Tris buffered saline. Alizarin red S (1% Alizarin red S (Sigma) in 0.028 NH<sub>4</sub>OH) was added to the wells for 4 min after which the discs were rinsed in buffer, mounted and photographed using an Olympus SC-35 camera mounted on an Olympus SZ-PT dissecting microscope.

Mature cultures (14 days) were labelled with tetracycline and counterstained with propidium iodide (PI). Tetracycline is incorporated into calcium containing deposits as they form and can therefore be used as a marker of mineralisation (Ott, 1996). Tetracycline (9 $\mu$ g/ml) supplemented growth medium was added to each well and incubated for 24hr (JE Davies, oral communication). Discs were then fixed in a 50% ethanol solution containing 1% acetic acid and stained with 0.01mg/ml propidium iodide for 30 seconds. They were then rinsed in phosphate buffered saline, mounted and viewed using a Leica TCS 4D confocal laser scanning microscope (CLSM).

## 5.3 Results.

### 5.3.1 Characterisation of Silica Gel.

#### 5.3.1.1 Surface analysis.

SEM of the silica disc surface revealed that it was flat and featureless even at high magnifications. However upon immersion in aqueous media, the gel surface of the disc became hydrated and swollen. ESEM showed the presence of silicon and oxygen peaks in the surface with a ratio of 1:2. The Thermanox disc alone showed carbon and oxygen peaks (Figure 5.1). The thickness of the  $\text{SiO}_2$  layer was measured as 0.5-2 $\mu\text{m}$ .

#### 5.3.1.2 Bioactivity.

Bioactivity was determined using ESEM with EDX to detect the presence of an apatite layer on the surface of the silica gel after a 2 week immersion in SBF at 37°C. Figure 5.2 shows characteristic calcium phosphate deposition over much of the surface of the silica gel. In some areas calcium phosphate was deposited as discrete units, whereas in other areas the appearance was of clusters of crystals resembling apatite. The silicon peaks in the EDX spectra were reduced or absent suggesting that the layer was quite thick. The calcium: phosphorous (Ca:Pi) ratio varied from 1.2 to 1.9 showing that apatite (1.67) had formed over at least some of the gel surface. The presence of a carbon peak suggested the apatite was carbonated.

#### 5.3.1.3 Silicic acid release.

The amount of silicic acid (in the monomeric and dimeric forms, see table 1.1) released into SBF and tissue culture medium from the silica gels was measured using the molybdenum blue assay. Figure 5.3 shows the release of silicic acid from the gels into the SBF. Figure 5.3a shows the standard calibration obtained. The gels had leached ~3ppm/ml silicic acid into SBF in 3 days. The amount of silicic acid released into the medium over the same period was less but the control value was high indicating interference by proteins in the medium with the assay (Figure 5.3b). The release of

silicic acid from the gels over time was measured in SBF. The rate of silicic acid release was equivalent to  $\sim 1$  ppm/ml per day (Figure 5.3c).

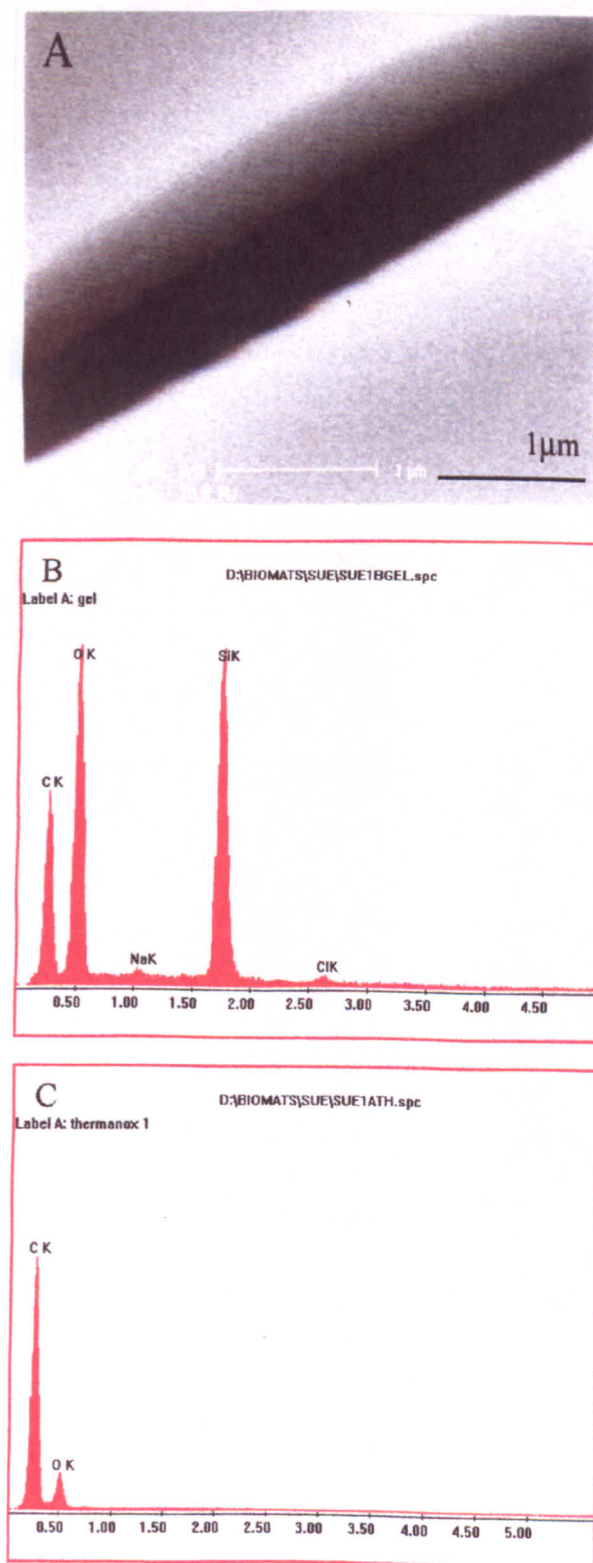


**Figure 5.1** ESEM secondary electron image of the surface of the silica gel (a) showing a featureless layer around  $0.5\ \mu\text{m}$  thick. (b) EDX analysis of the silica disc showing silicon and oxygen peaks. (c) EDX analysis of Thermanox discs. Only carbon and oxygen are present. (axes:  $x=\text{keV}$ ,  $y=\text{counts/sec}$ ).

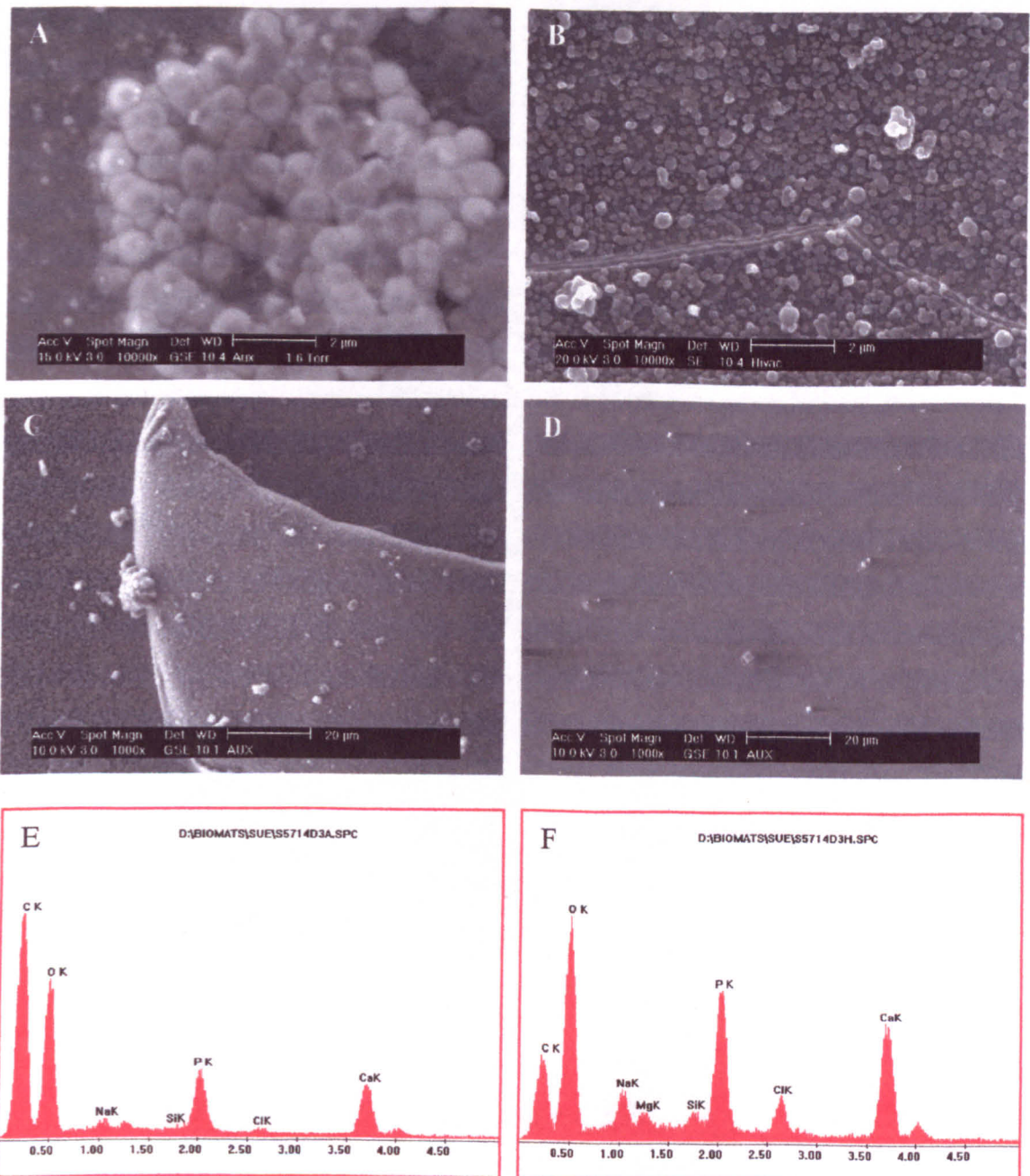
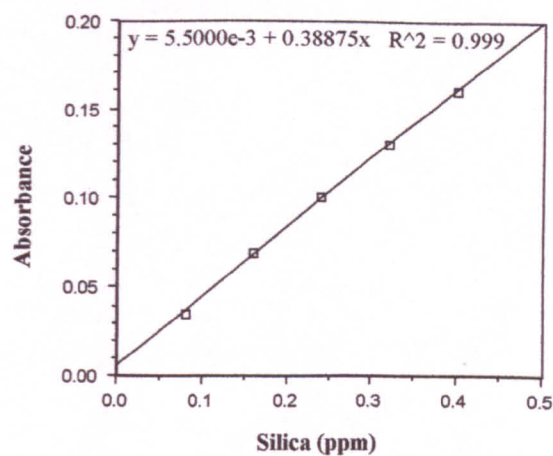
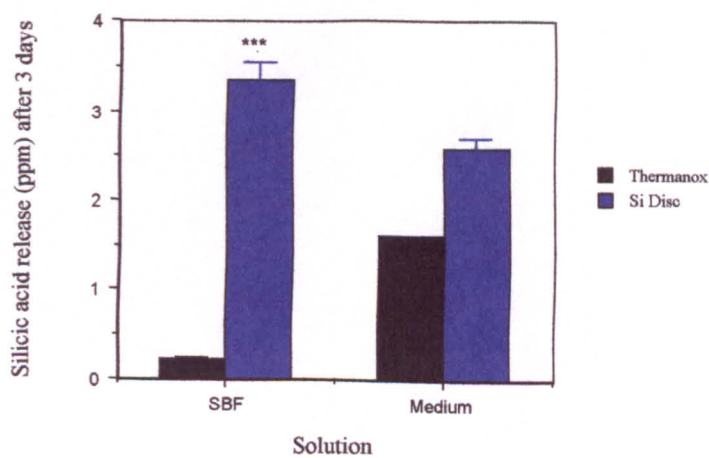


**Figure 5.2** (a-c) ESEM secondary electron images of silica discs after 14 days in SBF. Calcium phosphate deposits are seen as discrete clumps or over the entire surface. A CaPi layer was not seen on the thermnox control (d). EDX analysis of 2 areas (e,f) shows the calcium and phosphorous peaks. The CaPi ratio was 1.90 (e) and 1.41 (f) atomic percent. (axes: x=keV, y=counts/sec).

A



B



C

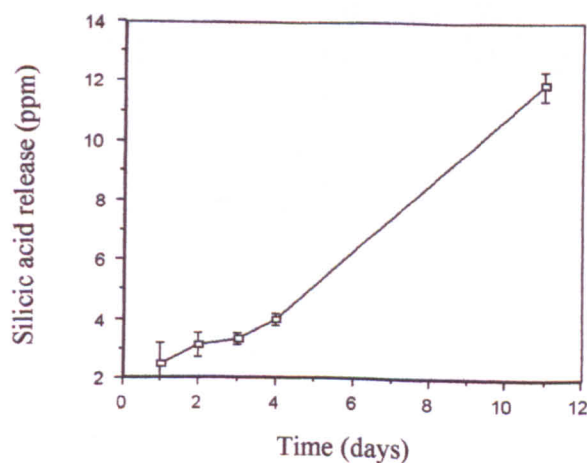


**Figure 5.3** (a) Standard curve for known quantities of sodium silicate using the molybdenum blue assay. (b) Release of silicic acid into SBF and complete medium from silica gels over 3 days. (c) Release of silicic acid into SBF over time.

### 5.3.2 Osteoblast Response to Silica Gel Coatings.

#### 5.3.2.1 Morphology and ultrastructure.

Cell growth on the silica gels was observed by phase contrast microscopy, TEM and SEM. HOB cells were confluent by 48 hr. In some areas the cells were clearly oriented along discontinuities in the silica coating. Cells continued to grow and proliferate on those parts of the gel that had lifted off the Thermanox disc and were floating in the medium. Cultures had formed multilayers on silica gels and Thermanox controls by 7 days. Nodules were formed earlier on the silica-coated discs than on the controls (Fig. 5.4). This was independent of the timescale of nodule formation on the controls. Cell

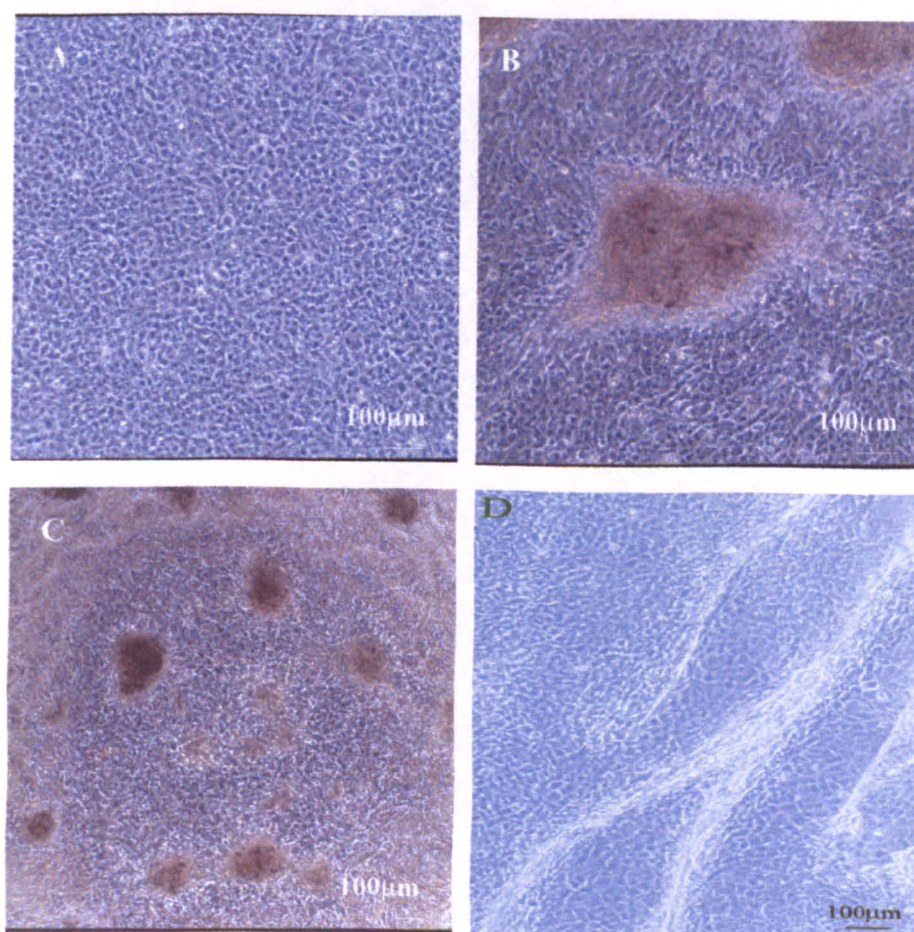


**Figure 5.4** Nodule formation by HOBs on silica discs. Phase contrast images of: (a) HOBs cultured on Thermanox discs for 10 days. Cells have formed multilayers. (b) HOBs cultured on silica discs for 10 days show a large, mature nodule. (c) Distribution of nodules on silica coated discs after 10 days in culture. (d) HOBs cultured on a silica disc for 4 days. Cells were aligned along defects in the silica gel and had started to form nodules.

clustering was seen in control cultures at 14 days and nodules began to form between 18 and 24 days. Osteoblasts grown on silica coated surfaces produced mature nodules between 4 and 10 days when control samples were at the multilayer stage. Nodules were larger and more numerous on the silica coated surfaces at later timepoints up to 31 days. The shape of the nodules formed on the silica-coated surface was sometimes elongated in comparison to the controls. This was attributed to the earlier alignment of cells along defects in the gel caused by contact with aqueous medium.

HOBs were also grown on inverted silica coated discs. These cells had access to the silica released from the gels but were not influenced by the surface topography or surface chemistry. Nodule formation was earlier than control cultures on these discs (8-14 days) but was not as advanced as on the upright discs (Figure 5.5)

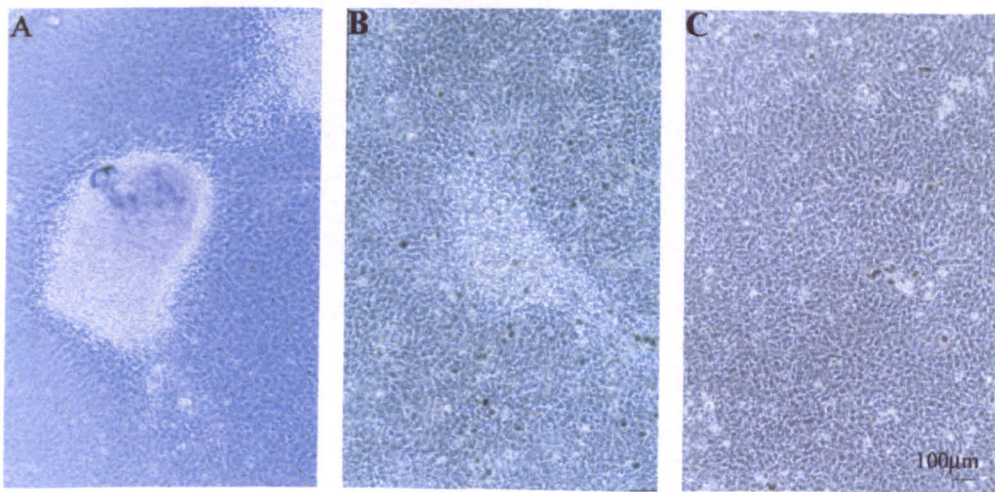


**Figure 5.5** HOBs cultured on upright (a) and inverted (b) silica discs for 10 days. Nodule formation is less advanced on the inverted disc, but is more advanced than the cells on Thermanox (c).

The morphology of the cells as seen by SEM was comparable for silica gel and control surfaces (Figure 5.6). TEM showed that the ultrastructural features of the cells grown on silica surfaces were indistinguishable from those of the controls (Figure 5.7). Collagen was seen between the cell layers but evidence of mineralisation was not seen. An electron dense line was often seen between the cell layers. This was unlikely to have

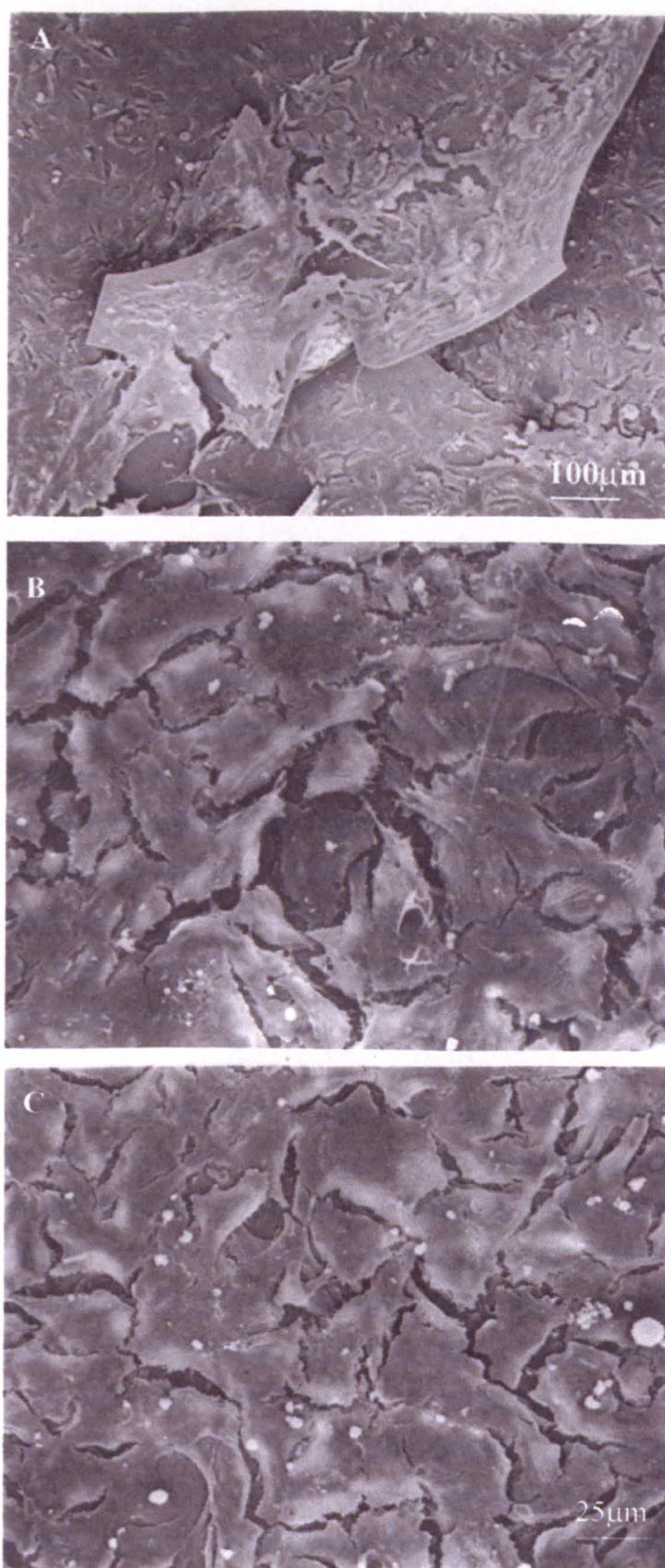


**Figure 5.6** Scanning electron micrographs of HOBs on a silica gel after 48hr cell culture. (a) Low magnification image showing cell coverage and topography of the silica gel surface. Higher magnifications revealed that cell morphology was similar on Thermanox (b) and silica surfaces (c).

been the gel itself but may have been indicative of the formation of a CaPi layer *in vitro*.

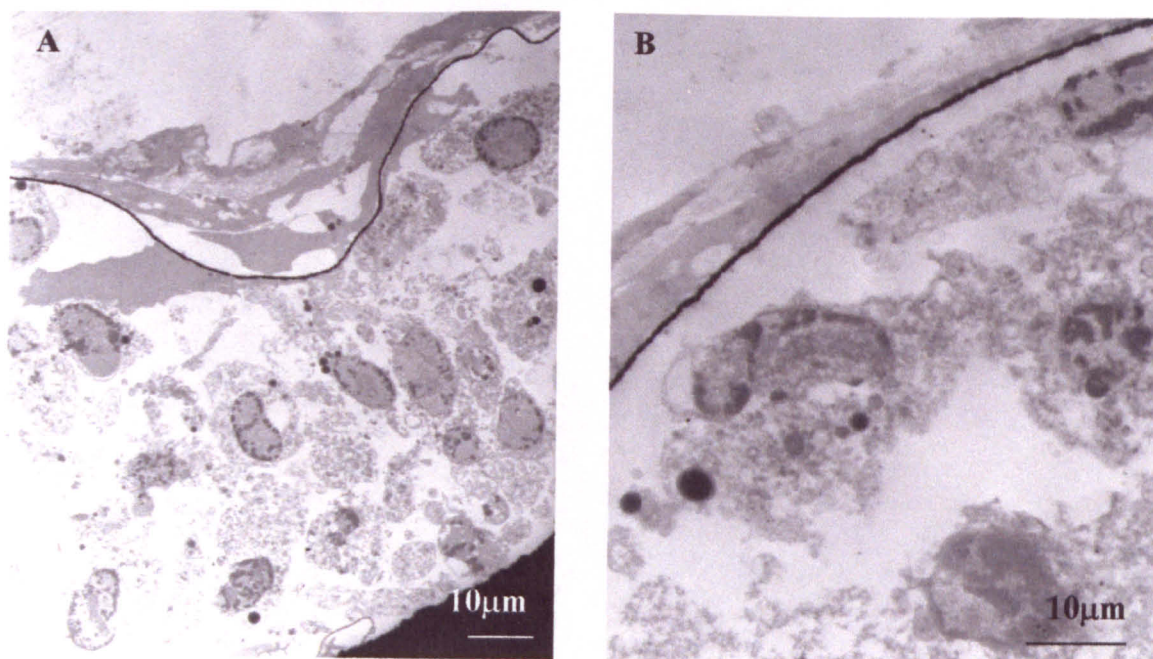


**Figure 5.7** TEM of cells on silica discs. The morphology of the cells and nodules is similar to control cultures. Note the electron dense line between cell layers in the nodule.

### 5.3.2.2 Cell activity and differentiation.

The response of HOBs to growth on a silica gel surface was determined biochemically using parameters such as cell activity (alamar Blue assay), cell number (DNA content) and differentiation (ALP activity). Cell activity was comparable on both surfaces with no significant difference between Thermanox and silica coated discs over a period of 31 days. DNA content and ALP activity were also similar for experimental and control samples for 2, 4 and 7 days (Figure 5.8).

### 5.3.2.3 Silicic acid uptake by HOBs.

The release of silicic acid from silica gels into the medium was measured in the presence or absence of HOB cells after 2 and 4 days. For both timepoints (0-2 and 2-4 days) the silica released from the gels was significantly reduced ( $p < 0.01$ ) when osteoblasts were grown on the gel surface and approximated the control (Thermanox) levels (Fig 5.9).

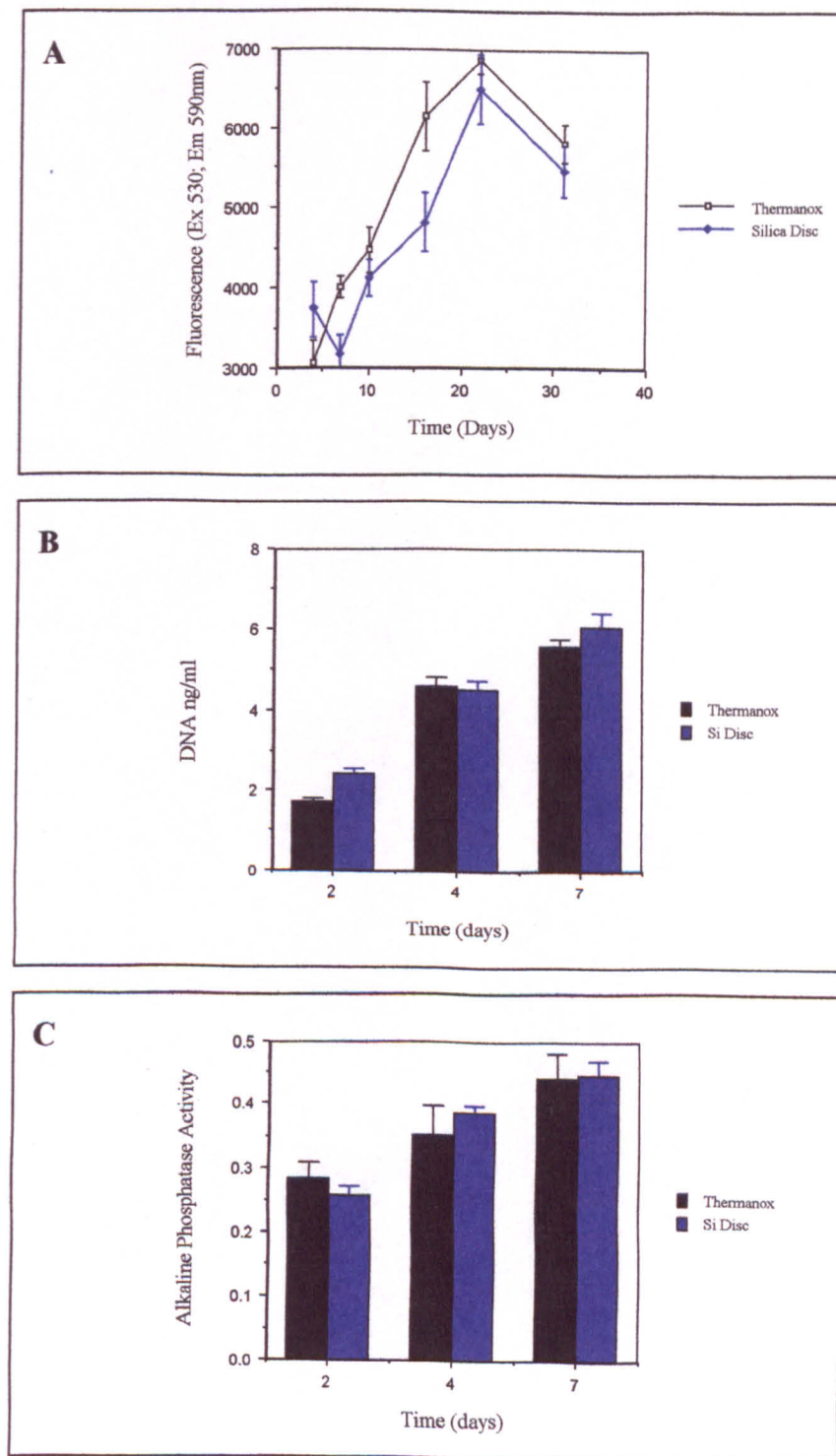


**Figure 5.8** Cell activity of HOB cultures grown on Thermanox discs or silica gels for 31 days (a). DNA content (b) and ALP activity (c) of HOBs grown on Thermanox discs and silica gels for up to 7 days. There was no statistically significant difference between the silica discs and controls. Error bar represents standard error of the mean,  $n=4$ .

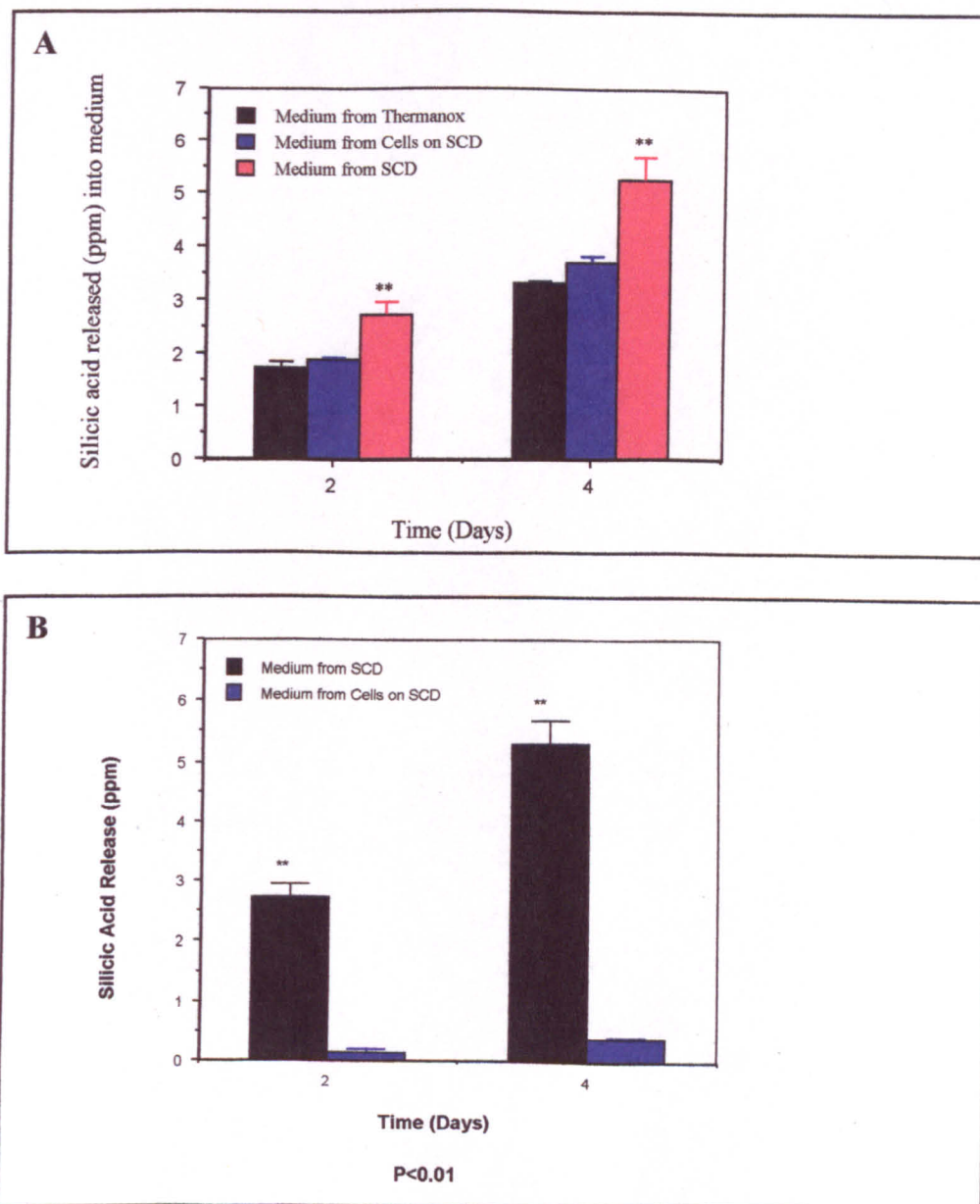


**Figure 5.9** (a) Silicic acid content of medium from wells containing Thermanox coverslips and silica coated discs (SCD) with and without cells for 0-2 and 2-4 days, as determined by the molybdenum blue assay. The amount of silicic acid released from the silica coated discs is significantly reduced ( $P < 0.01$ ) when cells are cultured on the surface. (b) Representation of (a) with control (Thermanox) values subtracted. Error bar represents standard error of the mean,  $n=4$ .

## 5.3.2.4 Mineralisation.

Nodules on silica surfaces stained positively with alizarin red S at 14 days (Fig 5.10). Cultures were labelled with tetracycline at 14 days when cells on silica gels had formed mature nodules and control cultures were beginning to form cell clusters. Figure 5.11 shows minimal tetracycline incorporation by control cultures compared with striking positively labelled nodules formed on silica surfaces. Closer examination of the pattern of tetracycline incorporation revealed that mineralisation most likely began at the centre of the nodule and proceeded towards the periphery.

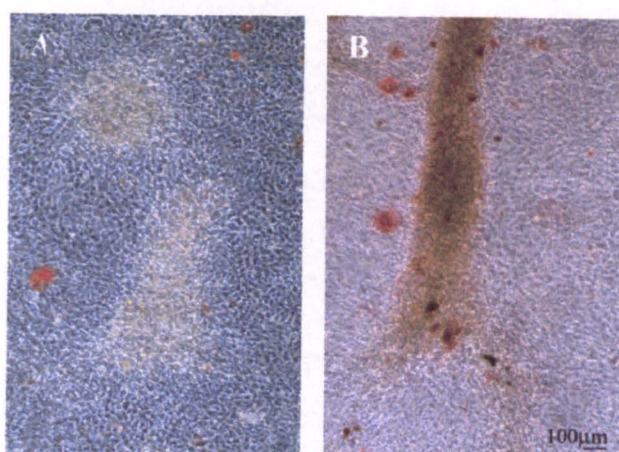


**Figure 5.10** Mineralisation of nodules on Thermanox (a) and silica (b) discs at 21 days. The nodule in (b) is stained red.

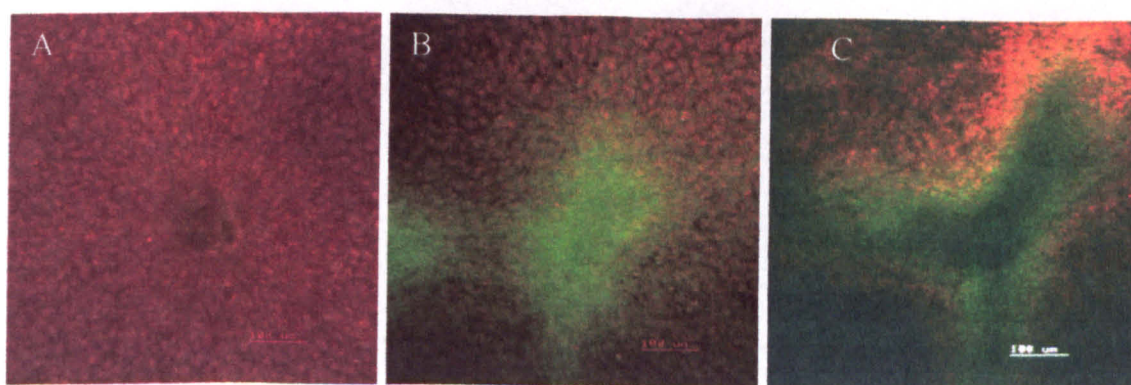


**Figure 5.11** Mineralisation of nodules on silica gel surface at 14 days. (a) HOB cells on Thermanox disc showing PI stained nuclei of a cell multilayer of cells (red) with minimal tetracycline labelling (green). (b) HOB cells on silica discs showing a nodule (red) with tetracycline incorporation in calcium-containing deposits representing mineralised areas (green). (c) Mineralisation of the nodules appears to proceed from the centre of the nodule towards the edges indicating that the nodule shown in (c) may be more mature than the nodule in (b). (Bar = 100µm).

## 5.4 Discussion.

In this Chapter HOBs were grown on a thin film of silica gel in order to establish the effect of silica on osteoblast growth and differentiation. Silica gels have been used in the past to eliminate the effects of the other ions present in glasses and glass ceramics but these have concentrated on the ability of the gels to form an apatite layer on their surface when soaked in SBF for an extended period of time. Few studies have investigated the cell response to growth on a silica surface.

The gel used in this work was prepared using TEOS and spin cast onto Thermanox coverslips. The surface was composed of silicon and oxygen only as seen by EDX analysis. The gel was shown to produce a CaPi layer when immersed in SBF for 11 days. EDX analysis of this layer showed the Ca: Pi ratio to be in the range 1.2-1.6 which approaches that of hydroxyapatite. Carbon was present in the EDX spectra in addition to calcium and phosphorous so it is likely that the calcium phosphate was carbonated. The Ca:Pi ratio of the mineral portion of bone is ~1.5. It was concluded that the gel was bioactive.

In addition to the formation of a CaPi layer, gels leached a measurable amount of silicic acid into the SBF. This is in keeping with the established process of apatite layer formation *in vitro* (Li *et al.* 1994a, Hench, 1991).

The response of osteoblasts to the silica gel surface was striking. HOBs formed nodules on silica surfaces as early as 4 days. Nodule formation was always earlier on silica coated surfaces than on controls and nodules were larger and more numerous. In some cases osteoblasts aligned along defects in the silica gel and nodules later formed in these areas. It is clear that in these cases early nodule formation may have been due to the physical topography of the surface rather than the silica present on the surface. However this was not always the case and cells grown on discs which remained more stable in solution also produced nodules reproducibly earlier than on controls. Alizarin red S staining and tetracycline labelling of the nodules formed showed positive labelling in relation to control cultures and suggested that the nodules had mineralised.

HOBs were also grown on inverted silica discs to address the problem of topography. In this way cells had access to silica that was released from the discs but the surface available to the cells was the same as that exposed to the controls (Thermanox). In these cultures nodules formed earlier than on controls but not as early as the upright silica discs. This demonstrates that topography alone was not responsible for the early mineralisation of HOBs on silica surfaces. It is still unclear whether the surface chemistry of the gel affects the osteoblast response but it is thought that the surface of the gel is composed of silanol (OH) groups (Perry, oral communication) which are reported to be favourable sites for apatite nucleation (Carlisle, 1986).

The gel used in the present work was shown to release silicic acid into SBF and tissue culture medium in the monomeric and dimeric forms. Silica is thought to be metabolised in the body as monomeric silicic acid (Carlisle, 1986). When cells were cultured on the silica gel coated surfaces, the amount of silicic acid in the medium was comparable to the control level. This implies that osteoblasts either prevent the release of silicic acid from the gels or that they absorb the silicic acid released. Such a relationship between osteoblasts and silicic acid has never been previously demonstrated. The apparent ability of osteoblasts to absorb silicic acid coupled with the early nodule formation on both upright and inverted silica discs shows that osteoblast mineralization is enhanced on a silica surface *in vitro*.

It is interesting to note that despite reliable early nodule formation on silica coated discs, cell activity, number and ALP activity were not affected. *In vitro* studies of the osteoblast response to bioactive glasses and glass ceramics have shown increased ALP activity on the silica containing surfaces (Ozawa and Kasugai, 1996; Vrouenvelder *et al.*, 1993). To our knowledge the osteoblast response to silica gels has not been documented. Silica has been linked with collagen formation (Carlisle *et al.*, 1981) and may affect the expression of osteocalcin and it is possible that silica affects these and/or other proteins involved in the mineralization process.

In summary, a simple silica sol-gel can be used to investigate the osteoblast response to a silica surface *in vitro*. Surface analysis of the silica gel coated disc after immersion in SBF showed that a CaPi layer was formed on the disc and that this was accompanied by silicic acid release from the disc. From these observations it was concluded that the gel

was bioactive. These findings support the theory that silica release from the implant surface is required for class A bioactivity and that this provides nucleation sites for apatite deposition. Furthermore, silicic acid was not detected in the medium collected from discs on which osteoblasts were grown suggesting that osteoblasts stabilise the surface or utilise the silica in some way. Nodule formation was reproducibly enhanced on the silica surface and it would appear that silica surfaces enhance the mineralisation of osteoblasts *in vitro*. Nodule formation was less markedly enhanced on inverted discs where the cells were exposed to the silicic acid released from the discs, but not the surface chemistry. It is likely that both the surface characteristics of the silica gel and silicic acid released from the disc affect osteoblast behaviour.

## **Chapter 6**

### **Comparison of the Growth of Human Osteoblasts (HOBs) on Silicon (Si), Etched Silicon (ESi) and Patterned Si/ESi Surfaces**

## 6.1 Introduction.

In the previous Chapter human osteoblasts were seen to respond favourably *in vitro* to a silica sol-gel. The reasons for this were hypothesised as a combination of the effects of surface chemistry and silicic acid release from the sample with subsequent uptake by osteoblasts. The surface used was unstable in aqueous solution however, leading to difficulties in analysing the hydrated surface and in ruling out the effect of surface topography. Silica has long been known to be bioactive but, although the mechanism of CaPi layer formation has been explained (Lobel and Hench, 1996), the specific reasons for the favourable osteoblast response warrant further investigation.

In this section the effect of silicon surface chemistry are investigated using stable, model silicon wafer surfaces prepared as a result of a collaboration with Dr Martin Winkelmann at the Laboratory for Surface Science and Technology, ETH, Zurich and Department of Applied Physics, Chalmers University of Technology, Gothenburg, Sweden. The wafers were used as received (Si) or with the oxide layer removed by wet etching (ESi). The response of osteoblasts to the two surfaces was compared. Patterned surfaces were also prepared using nano-etching techniques and these were subjected to broadly the same analyses.

Silicon surfaces have been used in previous studies where the effects of topography on cells and cellular responses to topographical guidance cues were investigated (Meyle *et al.*, 1995; Meyle *et al.*, 1991). Fromherz and co-workers have cultured neuronal cells on silicon surfaces to record the flow of ionic currents in the region of cell adhesion (Schatzthauer and Fromherz, 1998). The cells seeded on to the silicon chips which were rendered hydrophobic and coated with concanavalin A. These were not related to research into the mechanism of the bioactivity of silica. Healy *et al* (1996) have used quartz surfaces with different terminal surface molecules, arranged as a pattern by photolithographic techniques, to examine osteoblast attachment and mineralisation but these required the pre-adsorption of serum proteins for the attachment of cells. Patterning of surfaces with different growth factors, cell adhesion factors, physicochemical properties and surface topographies have been used to manipulate cell function and these are reviewed by Ito (1999).

Silicon, the semiconductor, has recently shown bioactive properties when it is porosified by anodisation (Canham, 1995). These surfaces support the formation of a CaPi layer in SBF, whereas bulk silicon wafers did not even after extended (6wk) incubations in SBF (Canham and Reeves, 1996). Subsequent work by the same group showed that the porosity of the silicon produced affected both the bioactive and biodegradation properties of the material. Highly porous mesoporous Si was rapidly dissolved, whereas non porous and macroporous Si was bioinert. Low porosity Si which was meso or microporous exhibited bioactive properties (Canham and Reeves, 1996; Canham *et al.*, 1999). Extensive CaPi layer formation could be achieved within hours if a cathodic bias was introduced to the surface. This was retarded by anodisation (Canham *et al.*, 1997a).

The biocompatibility of these surfaces has been evaluated *in vitro* (Bayliss *et al.*, 1999) and *in vivo* (Bowditch *et al.*, 1999). Bayliss *et al.* (1999) cultured hinese hamster ovary (CHO) and (B50) cells on porous Si surfaces for up to 4 days and showed no signs of cytotoxicity. Porous Si implanted subcutaneously in guinea pigs showed good tissue compatibility and *in vivo* calcification at the surface of the implant which was not seen with either bulk Si or titanium (Bowditch *et al.*, 1999).

The potential applications of the different types of porous Si are reviewed in Canham *et al.* (1997b). Bayliss *et al.* (1999) have suggested potential applications as biological interfaces, neural networks and biosensors. They have reported that the optoelectronic properties of the semiconductor (preventing the risk of the influence of electromagnetic fields (EMFs) on cellular responses) combined with its low cytotoxicity (relative to other semiconducting materials) make it suitable for use in devices for replacing tissues in the ear, eye skin and nasal cavity. Despite the increasing body of evidence supporting the potential use of silicon as a biomaterial, no research concerning silicon and bone exists in the literature.

The aims of the work were threefold. Firstly the bioactivity of the Si and ESi surfaces was compared in terms of calcium phosphate layer formation in SBF and silicic acid release from the samples (reliable indicators of future bone formation from the last Chapter). The silica sol-gel from the previous Chapter was used as a positive control for CaPi layer formation in SBF. Thermanox cover-slips were used as negative controls as

---

they do not form a CaPi layer in SBF. Secondly, the osteoblast response to Si and ESi surfaces in the short and longer term was measured by studying initial cell attachment to the surfaces and nodule formation in long term cultures. Initial cell attachment is a good indicator of future differentiation of bone cells *in vitro* (Scotchford *et al.*, 1998). Thirdly, patterned Si/ESi surfaces were made with regions of different geometry (spots and stripes) and different dimensions (one set 50-150 $\mu$ m- spots and stripes; one set 5-15 $\mu$ m stripes). These were used to allow direct comparison between the two surfaces.

---

## 6.2 Materials and Methods.

### 6.2.1 Preparation of Si and ESi surfaces.

Si and ESi samples were prepared by Martin Winkelmann at the Swedish Nanometer Laboratory in a class-100 clean room. Silitronix (100)-surface polished silicon 2" wafers with 8000 Å thermo-oxide layer were used as the Si surfaces. The oxide layer was removed by wet etching to form the ESi surfaces. (for a more detailed description of the procedure refer to section 6.2.6 'Use of patterned surfaces'). Before use the samples were cleaned in an ultrasonic bath (18 mOhm) in acetone, isopropanol and deionized water and dried in nitrogen.

### 6.2.2 Surface Analysis

Cleaned samples were examined using a Phillips FEG-ESEM with EDX microanalysis to assess the elemental content of the surfaces. The microscope was operated at 10kV in auxiliary mode using nitrogen as the chamber gas so that the samples could be viewed without coating. XPS was carried out on Si and ESi surfaces.

#### 6.2.2.1 Calcium phosphate layer formation in SBF and silicic acid release.

Si and ESi (n=3) surfaces were placed individually in the wells of a 6 well tissue culture plate (Falcon). Samples were sterilised using UV light and immersed in 10ml of SBF for 14 days at 37°C to investigate the formation of a CaPi layer on the surface. Silica sol-gel samples (as used in Chapter 5) and Thermanox discs (Nunc) were used as positive and negative controls respectively. After 14 days the samples were removed from the SBF, rinsed gently in sterile distilled water and air-dried. They were mounted on aluminium stubs with adhesive carbon tabs (Agar) and viewed in a Phillips FEG-ESEM operated in auxiliary mode using nitrogen as the chamber gas. This was done to alleviate the need to coat the samples with gold before viewing which would interfere with the analysis of phosphorous in the samples. Secondary imaging and EDX microanalysis was carried out on each sample at 10kV.

The SBF was collected from the plates and the samples were analysed using the molybdenum blue assay, as previously described, to quantify the amount of silica released over 14 days as mono- and dimeric silicic acid.

### **6.2.3 Cell Response to Si and ESi Surfaces.**

#### **6.2.3.1 Cell attachment and spreading.**

Cell attachment and spreading was assessed on the Si and ESi surfaces. Thermanox discs and silica sol-gels were used as controls. Samples were placed individually in the wells of a 24 well tissue culture plate (Falcon) and sterilised using UV light. HOBs were added to the wells at a concentration of  $8 \times 10^4$  cells per ml of DMEM supplemented in the usual manner. The plates were incubated at 37°C in a humidified atmosphere (5% CO<sub>2</sub>) for 90 min, 2.5 hr and 24 hr. The medium was then removed from the wells and the samples were rinsed in PBS and fixed in 4% paraformaldehyde for 5 min. The samples were rinsed in 1% PBS/BSA and permeabilised using a Triton X-100 (0.5% Triton X-100 (pH 7.6) in 20mM Hepes, 300mM sucrose, 40mM NaCl and 3mM MgCl<sub>2</sub>.) solution for 5min at 0°C. After a further 2 rinses in 1% PBS/BSA at 37°C FITC-conjugated phalloidin (Sigma, 250µg/ml) was added for 20min at 4°C. This was removed and the samples rinsed 3 times in PBS/BSA before adding propidium iodide (Sigma, 0.02mg/ml) for 30 seconds. The samples were rinsed again, mounted in glycerol/DABCO, cover-slipped and viewed using a Leica TCS 4D confocal microscope with an ArKr laser. The 488nm laser line was used to excite the green fluorescence of FITC-conjugated phalloidin. The red fluorescence of propidium iodide was scanned simultaneously using the 568nm laser line. Optical sections (1µm thick) were collected as a z series. A maximum intensity projection was created (a composite image from the brightest pixels per scan) using the associated Scanware software.

#### **6.2.3.2 Nodule formation.**

Nodule formation was assessed by confocal microscopy at 21, 29 and 35 days cell culture. Cells grown on each of the surfaces (Si, ESi, Thermanox and silicon sol-gel) were maintained in long-term culture and re-fed every 2-3 days with fresh tissue culture

medium The samples were fixed in 4% paraformaldehyde for 5min and stained with 0.02mg/ml propidium iodide for 30sec to visualise the nuclei. Propidium iodide also stains the RNA in ribosomes so the cell outline could also be partially distinguished. The samples were mounted in glycerol/DABCO and viewed using the Leica TCS-4D confocal microscope using the 568nm laser line.

## 6.2.4 Use of Patterned Surfaces.

### 6.2.4.1 Chemical patterning of surfaces.

The patterned samples were prepared by Martin Winkelmann in the Swedish Nanometer Laboratory in a class-100 clean room. Silitronix (100)-surface polished silicon 2" wafers with 8000 Å thermo-oxide layer were spin-coated with 1.5µm thick (3500 rpm, 90 s) Shipley S-1813 Microposit positive photoresist. They were then baked on a hot-plate for 1 min. at 90C. Then the samples were exposed for 4 seconds to UV light (360 nm mercury; standard UV; 20 mWatt/cm<sup>2</sup>) with a Karl Süss MJB-II Contact Printer through a chromium mask. Exposed portions of the photoresist were removed from the wafer surface by developing it 65 seconds in a 1:5 diluted Shipley MF-351 or in an undiluted Shipley MF322 Microposit developer for 30sec. Both developers were equal. The development was stopped by dipping the wafer in deionised water and the samples were dried in N<sub>2</sub>.

The oxide layer from photoresist uncovered areas was etched by wet etching. A buffered oxide etch (BOE) was used rather than plain diluted HF because the buffer keeps the strength and thus the etch rate closer to constant. After rinsing in distilled water, a 1:6 mixture of 49% HF and 40% NH<sub>4</sub>F at RT was used. In this way the etching of the oxide layer was uniform on the whole wafer. The control of the etching was also easier. From time to time the wafer was removed from the BOE solution and the back of the wafer was examined. If the silicon dioxide had not been completely etched away, there was still a film of the solution adhering to the whole surface of the wafer and it appeared wet. If all of the SiO<sub>2</sub> had been removed the wafer appeared dry and dull grey. Normally it took about 5-7 min to etch through the oxide layer. The quality and completion of the etching was inspected under a microscope.

The lift-off of the remaining resist was in acetone. The samples were then cleaned in an ultrasonic bath in acetone, isopropanol and deionized water (18 mOhm) and dried with nitrogen. The pattern from the chromium mask had now been transferred onto the surface.

As a protection against Si dust, the wafers were coated again with 1.5 $\mu\text{m}$  thick Shipley S-1813 Microposit positive photoresist and cut with a Loadpoint Microace 3+ diamond saw into samples of 9x11 mm. The resist on the samples was removed by 2 minutes of sonication in acetone, isopropanol, and deionized water and the samples were dried with nitrogen. Before using the surfaces for cell culture tests, they were given in a radiofrequent glow discharge (RFGD) treatment for 5 minutes at 0.42 mbar, 2.7sccm and a RF power of 100 W to improve the surface wettability of the substrates.

The geometry of the pattern consisted of 6 spatially patterned regions (9x11 mm) of dots and stripes. The dimensions of the patterns ranged between 50, 100 and 150  $\mu\text{m}$  (Figure 6.2.1).

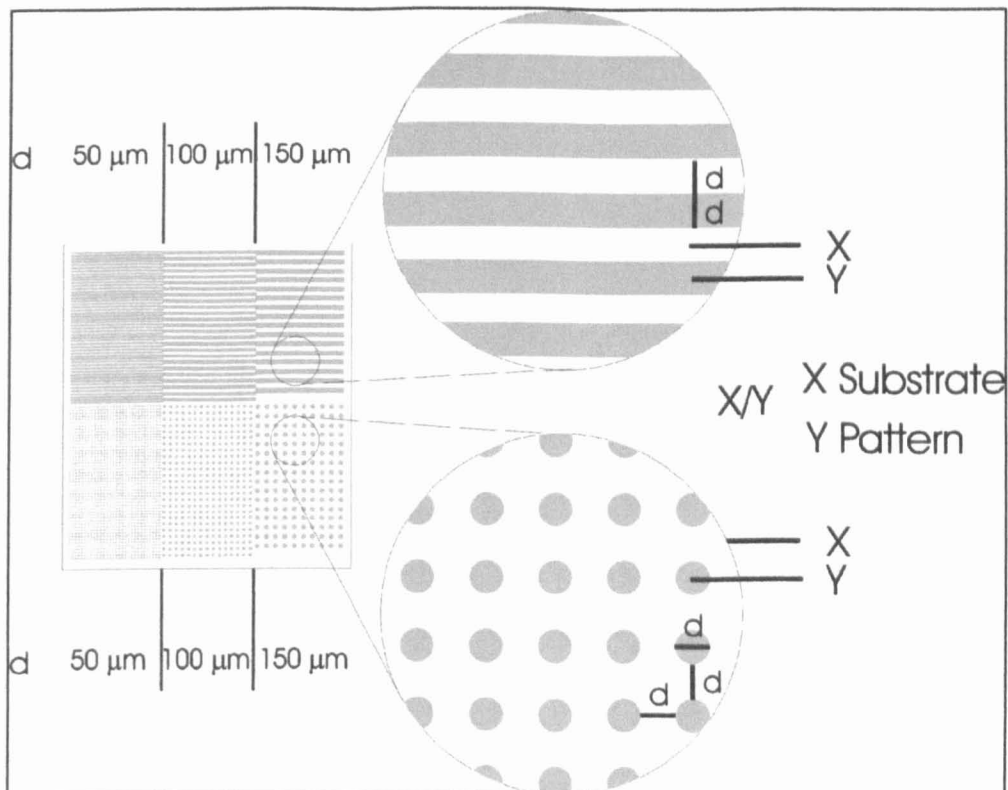


**Figure 6.2.1** Diagram showing the detail of the patterned surface.

---

Patterned surfaces were also used to examine the response of cells to patterns of different dimensions. These were prepared as previously described but in this case the pattern consisted of 5, 10 and 15 $\mu$ m stripes of ESi separated by 15 $\mu$ m thick gaps of Si. These are described as 15/5, 15/10 and 15/15 patterns, where the first number represents the Si areas and the second refer to the ESi areas.

#### 6.2.4.2 Characterisation of the patterned surface.

The geometry of the pattern was checked and the thickness of the oxide layer measured using a Jeol JSM-6301F field emission scanning electron microscope. Calcium phosphate layer formation in SBF was analysed after 14 days as described previously.

#### 6.2.4.3 Cell attachment and Nodule formation.

Cell attachment and spreading was viewed using the confocal microscope using FITC-conjugated phalloidin and propidium iodide as previously described. Patterned samples were fixed and stained at 2.5 hr, 24 hr, 7 days and 21 days. Si and ESi surfaces were used as controls. Patterned striped surfaces were viewed at 2.5 hr, 24 hr and 7 days. Reflectance confocal microscopy was used to visualise the areas of the pattern.

### 6.3 Results.

#### 6.3.1 Surface Analysis of Si and ESi Surfaces.

Si and ESi surfaces were examined using ESEM with EDX microanalysis. The surfaces were flat and featureless (data not shown). Figure 6.2 shows that the Si surface was composed of silicon and oxygen. The ESi surface was composed only of silicon.

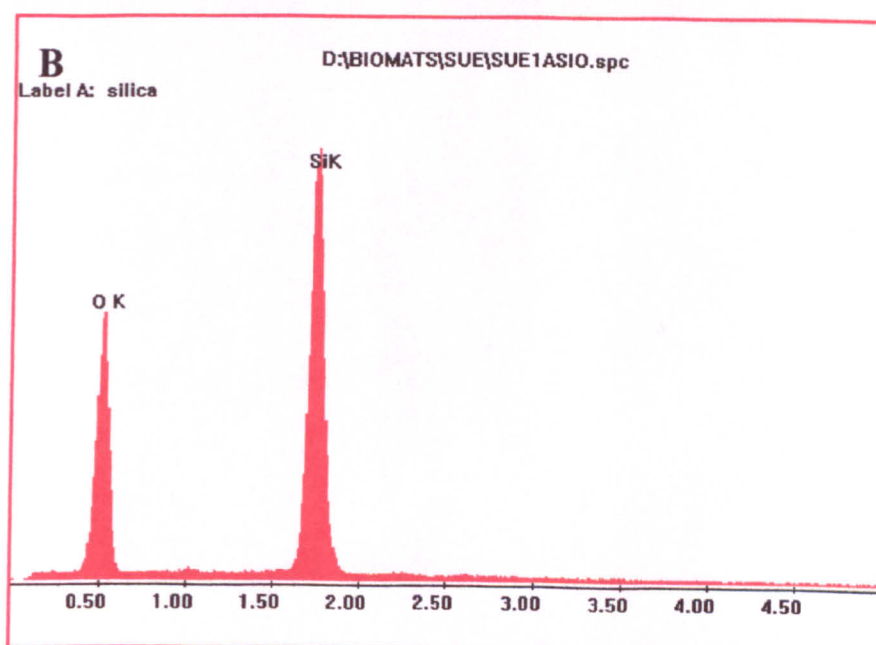
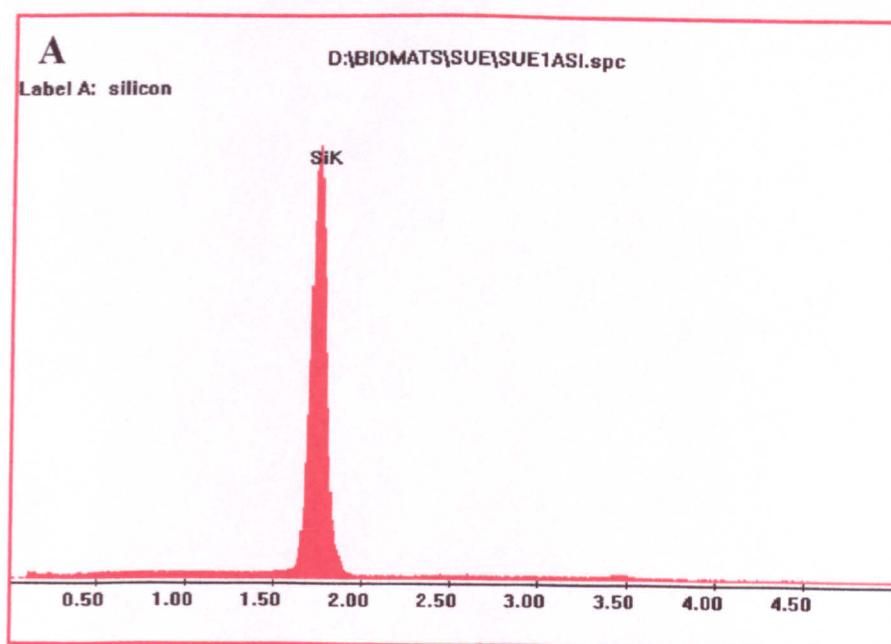
In contrast, XPS data showed that oxygen was present on the ESi surface (Table 6.1). For the Si samples (n=3) the atomic percent of silicon was 34.5 and for oxygen was 63.9% (carbon contamination made up the rest). For the ESi samples (n=3) the percentage silicon was 60% with 37.7% oxygen present. This may be due to the formation of an oxide layer on the surface of the metal, which is too thin to be picked up by EDX or contamination at the surface. As the samples were plasma cleaned the latter explanation seems unlikely.

	<b>ESi Surface</b>	<b>Si Surface</b>
<b>Silicon (At %)</b>	60%	35%
<b>Oxygen (At%)</b>	40%	65%

**Table 6.1** XPS analysis of ESi (a) and Si surfaces (b) taken at a 15° angle showing the atomic percentage of silicon and oxygen present.

##### 6.3.1.1 CaPi layer formation in SBF and silicic acid release.

The samples were viewed using ESEM with EDX microanalysis (Figure 6.2). At lower magnifications (x1000) large (4 $\mu$ m) and smaller (0.5 $\mu$ m) spherical deposits could be seen on the ESi surface. At higher magnifications (x8000) the entire surface of the sample was covered with a carpet of needle-like crystals. EDX microanalysis revealed the nature of these crystals to be calcium phosphate deposits with an average (n = 7) Ca:Pi ratio of 1.36. The calcium phosphate layer also contained a substantial amount of



C

	ESi Surface	Si Surface
<b>Silicon (Atomic Percent)</b>	>99%	48%
<b>Oxygen (Atomic Percent)</b>	<1%	52%

**Figure 6.1** EDX microanalysis of ESi (a) and Si surfaces (b). The silicon surface (a) shows only a silicon peak. The silica surface (b) shows silicon and oxygen peaks. The atomic percentage for silicon was 54% and for oxygen was 46% for this sample. (axes: x=keV, y=counts/sec). (c) Table showing mean Si and O content (At%) for Si and ESi samples (n=3)

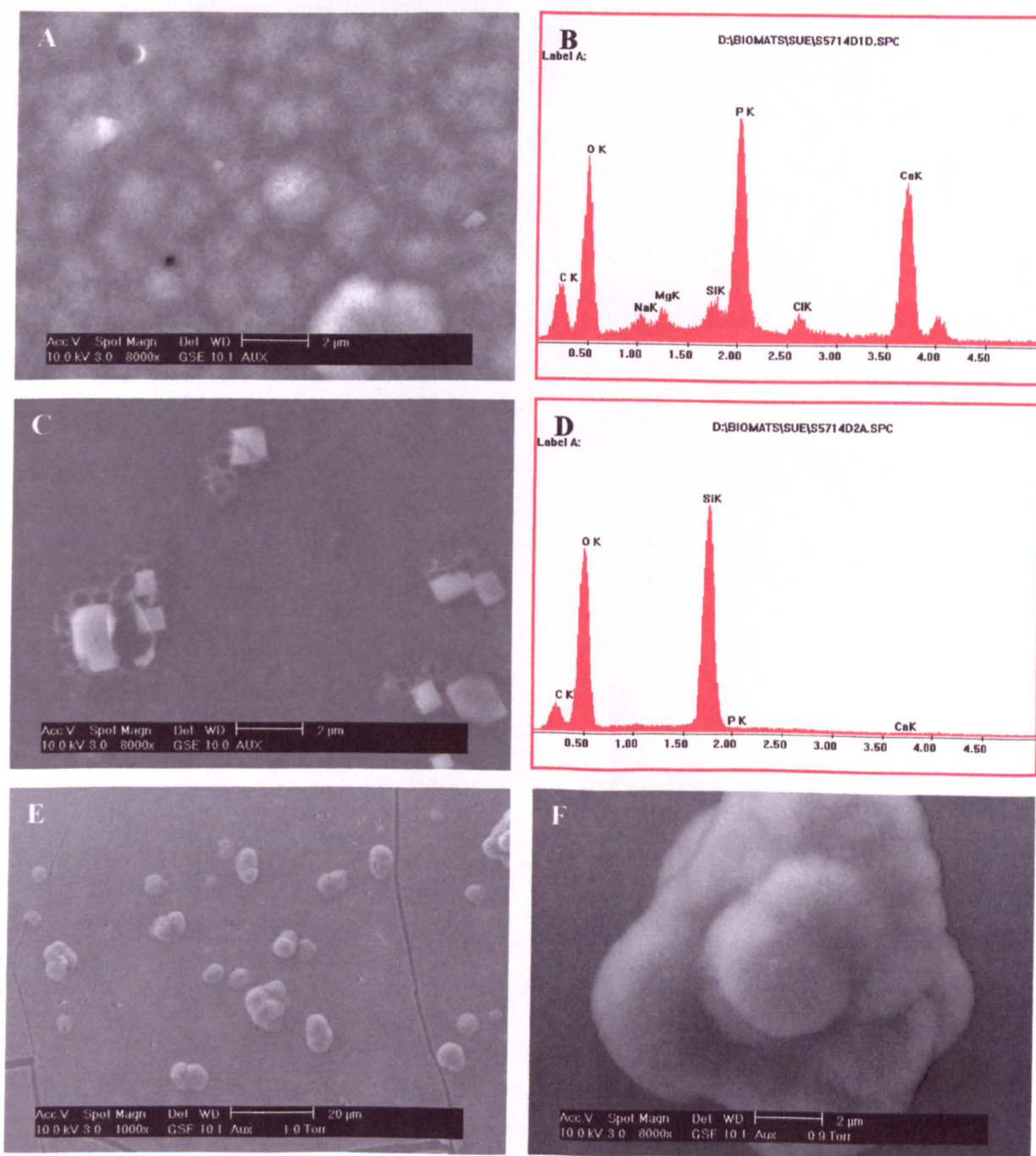


**Figure 6.2** ESEM micrographs of Si and ESi surfaces after 14 days in SBF. The ESi surface (a) is covered with a carpet of needle-like crystals interspersed with a variety of larger deposits (e, f). This is confirmed as a calcium phosphate layer by EDX analysis (b). The ratio of Ca:P was 1.34.. In contrast, no deposits are seen on the Si surface (c). EDX analysis confirms the presence of silicon, oxygen and carbon on the surface (d). (axes: x=keV, y=counts/sec). (e, f) Low and high magnification views of the ESi surface. Large, spherical deposits are seen on a carpet of crystals (shown at higher mag in (a)).

oxygen (average atomic percent 50.5%;  $n=6$ ). Numerous cuboidal salt (NaCl) crystals were also seen on the surface and some magnesium was also detected. The silicon peak was small which could indicate that the CaPi layer was quite thick, as at 10kV there is some penetration into the surface. The Si surface showed no CaPi deposition. The positive (silica sol-gel) controls were covered with a CaPi layer. The average ( $n=6$ ) Ca:Pi ratio of the layer was 1.43. A large quantity of oxygen was also seen in the CaPi layer (average atomic percent 63.6%;  $n=4$ ). The negative (Thermanox) controls had no CaPi deposits on the surface. A few salt (NaCl) crystals were seen (Figure 6.3).

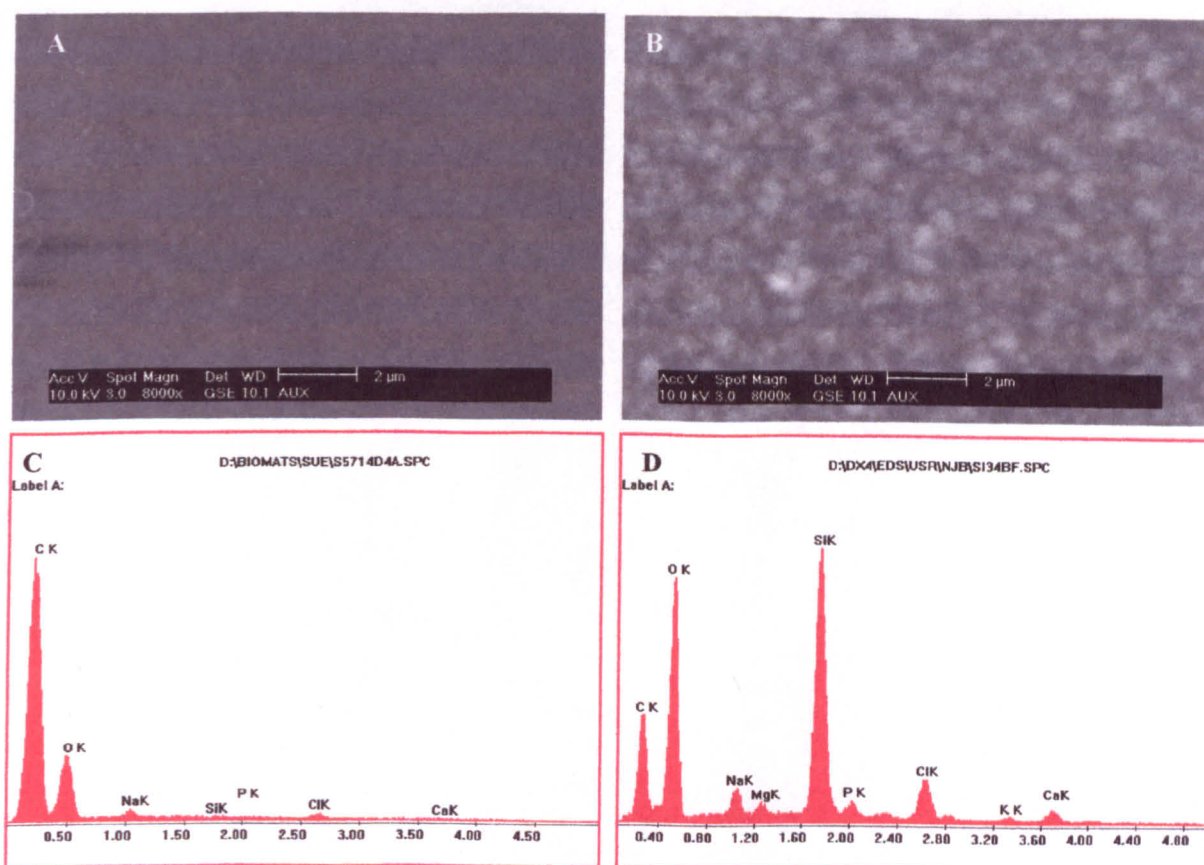


**Figure 6.3** EDX spectra for positive and negative controls for the above experiments. Thermanox was used as the negative control (a). A silica sol-gel was as a positive control (b). The presence of a calcium phosphate layer was confirmed with a Ca:P ratio of 1.47. (axes:  $x=keV$ ,  $y=counts/sec$ ).

Figure 6.4 shows a graph of silicic acid released in the monomeric and dimeric forms during 14 days in SBF. Silicic acid release was seen from the silicon and silica sol-gel samples (positive control). No silicic acid was released into SBF from the silica and Thermanox samples (negative control).

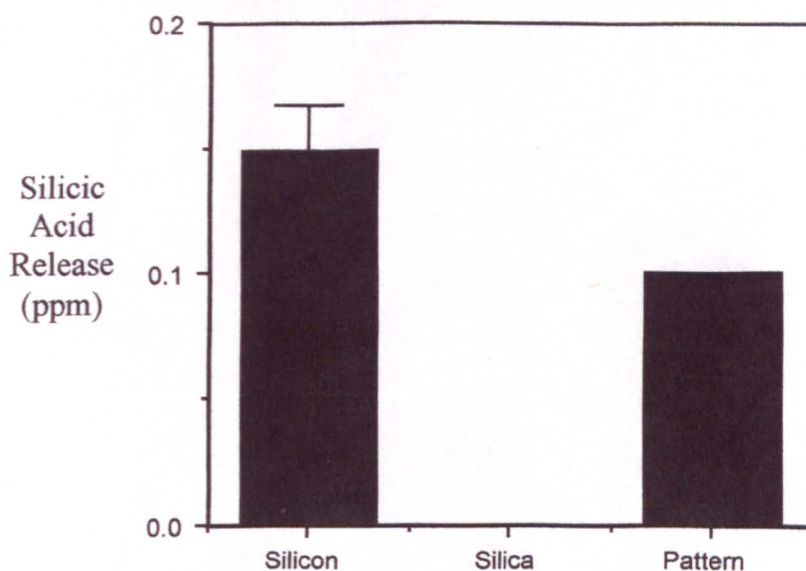


**Figure 6.4** Silicic acid release into SBF from silicon (ESi), silica (Si) and patterned surfaces, measured at 14 days using the molybdenum blue assay. Silicic acid is released from the ESi surface only. Bar represents standard error of the mean,  $n=3$

### 6.3.2 Cell Responses to Si and ESi Surfaces.

#### 6.3.2.1 Cell attachment and spreading.

Cell attachment and spreading was assessed at 90 min and 24 hr cell culture. The filamentous actin cytoskeleton was visualised using confocal microscopy of ESi, Si, Thermanox and silica sol-gel samples. These were stained with phalloidin for filamentous actin and the nuclei were counter-stained with propidium iodide. After 90 min cell culture, slight differences in cell shape were noted. The cells grown on Thermanox were typically stellate and exhibited actin staining along the long axis of the cell. In contrast, cells grown on the silica sol-gel were more rounded in shape with thick bands of actin running around the periphery of the base of the cell where it was attached to the substrate. The cells on the ESi surface were similar in appearance to the sol gel samples. Cells grown on the Si surface were rounded and often displayed no actin staining. Any actin staining seen was cortical in nature (Figure 6.5). The morphology and actin profile of cells grown on all four surfaces were indistinguishable after 24 hr. All cells appeared typically spread and formed a confluent layer over the surfaces (Figure 6.6).

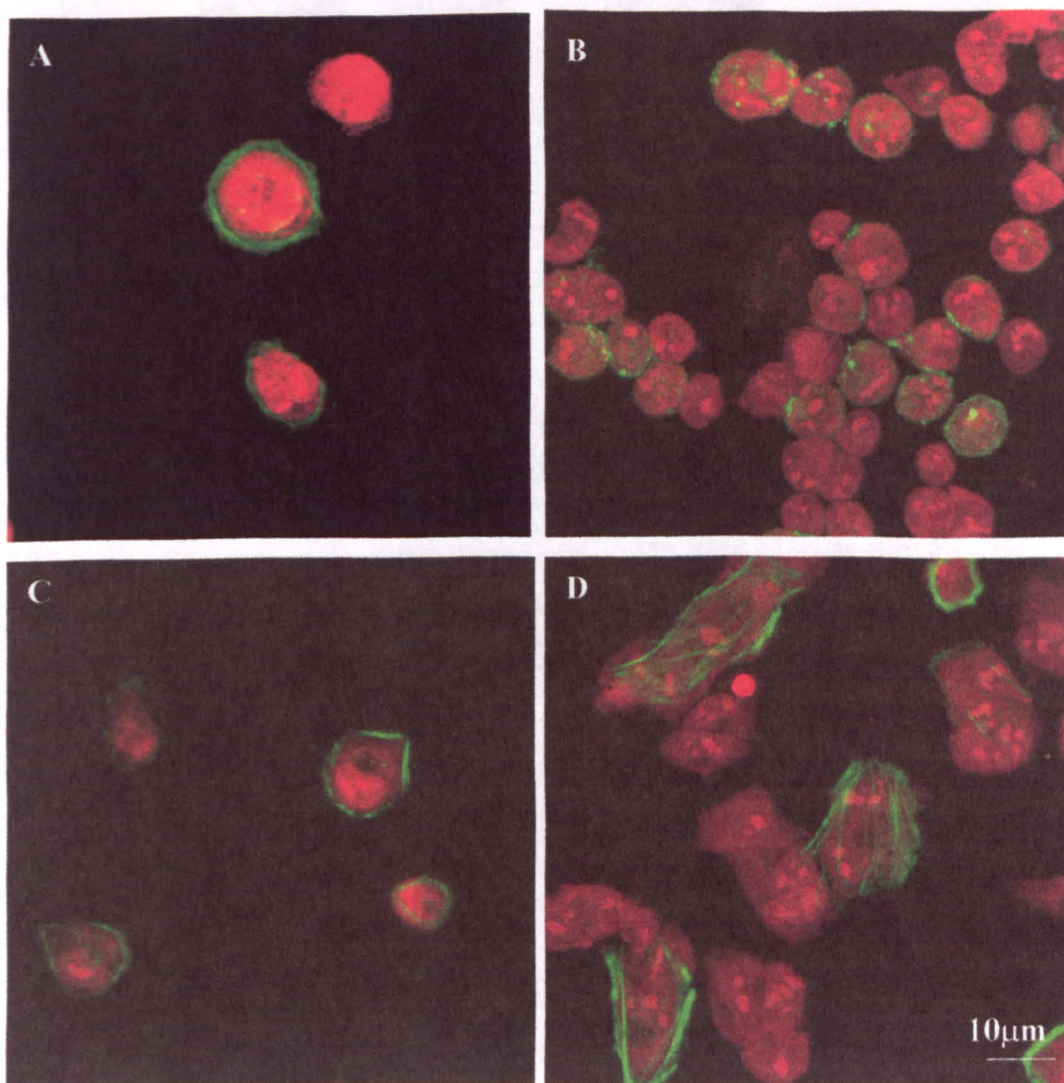


**Figure 6.5** Confocal image (maximum intensity) of HOB attachment on Si and ESi surfaces at 90min. The cells are stained with FITC conjugated phalloidin for filamentous actin (green). The nuclei are stained with propidium iodide (red). Cells on the ESi surface (a) are rounded with small amounts of actin around the base of the cell. Cells on the Si surface (b) are rounded with little actin staining. Cells on the silica sol-gel (c) are rounded with thick bands of actin at the base of the cells. Cells on Thermanox (d) are starting to spread.

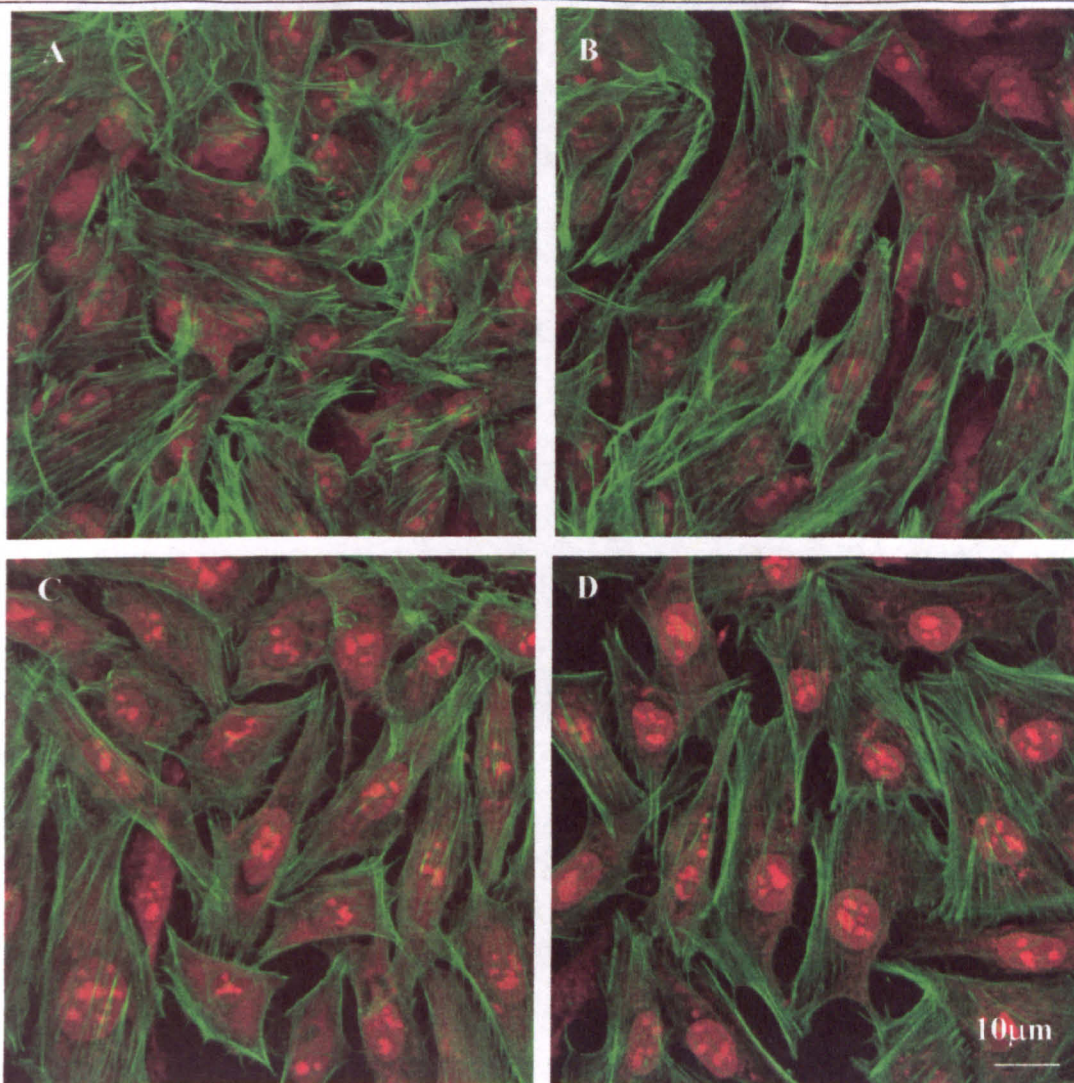


**Figure 6.6** Confocal image (maximum intensity) of cells after 24 hrs on ESi (a), Si (b), Thermanox (c), and silica sol-gel (d) surfaces. The cells are stained with FITC conjugated phalloidin for filamentous actin (green). The nuclei are stained with propidium iodide (red). Cells on all surfaces are spread.

### 6.3.2.2 Nodule formation.

Nodule formation in the cultures was examined for all four surfaces. HOBs were stained with propidium iodide. By 29 days in culture HOBs grown on all 4 surfaces had formed nodules (Figure 6.7).

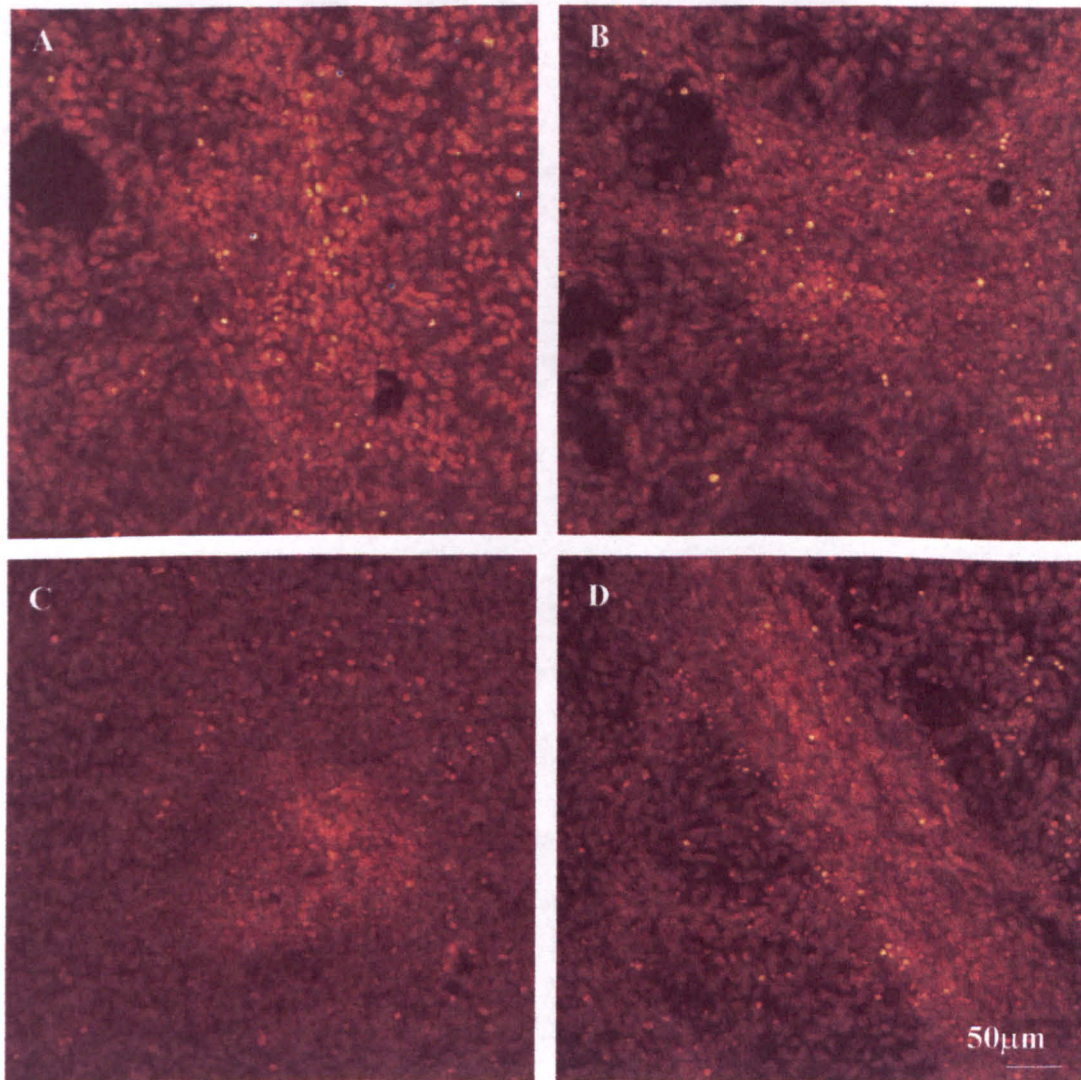


**Figure 6.7** Confocal image (maximum intensity) of HOB cells grown on ESi (a), Si (b), Thermanox (c) and silica sol-gel (d) surfaces for 29 days stained with propidium iodide. Nodular structures are seen on all surfaces.

### 6.3.3 Use of Patterned Surfaces.

#### 6.3.3.1 Characterisation of the surface.

Figure 6.8 shows a selection of SEM micrographs from the patterned surface. These show that the pattern dimensions and measurements are accurate. The thickness of the layer was measured as  $0.33\mu\text{m}$  (Figure 6.9). A calcium phosphate layer was present over the entire patterned surface and could be seen both within and without the pattern as a continuous layer (Figure 6.10). The average Ca:Pi ratio was measured as 1.34 ( $n=3$ ). Silicic acid release from the patterned surfaces was measured and shown in figure 6.4.

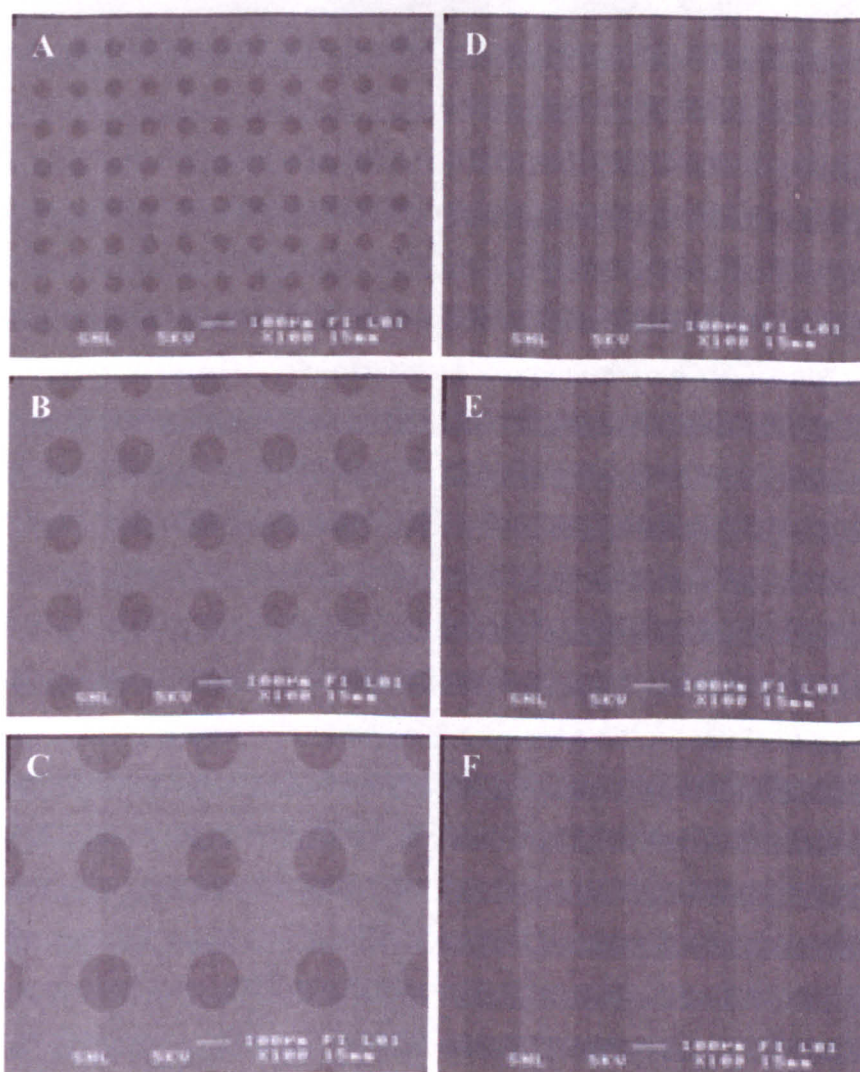


**Figure 6.8** SEM of the six distinct regions on the patterned surface (a-f) showing the detail and dimensions of the pattern. The pattern consisted of spots and stripes at intervals of  $50\mu\text{m}$  (a, b),  $100\mu\text{m}$  (c, d) and  $150\mu\text{m}$  (e, f). Bar =  $100\mu\text{m}$ .

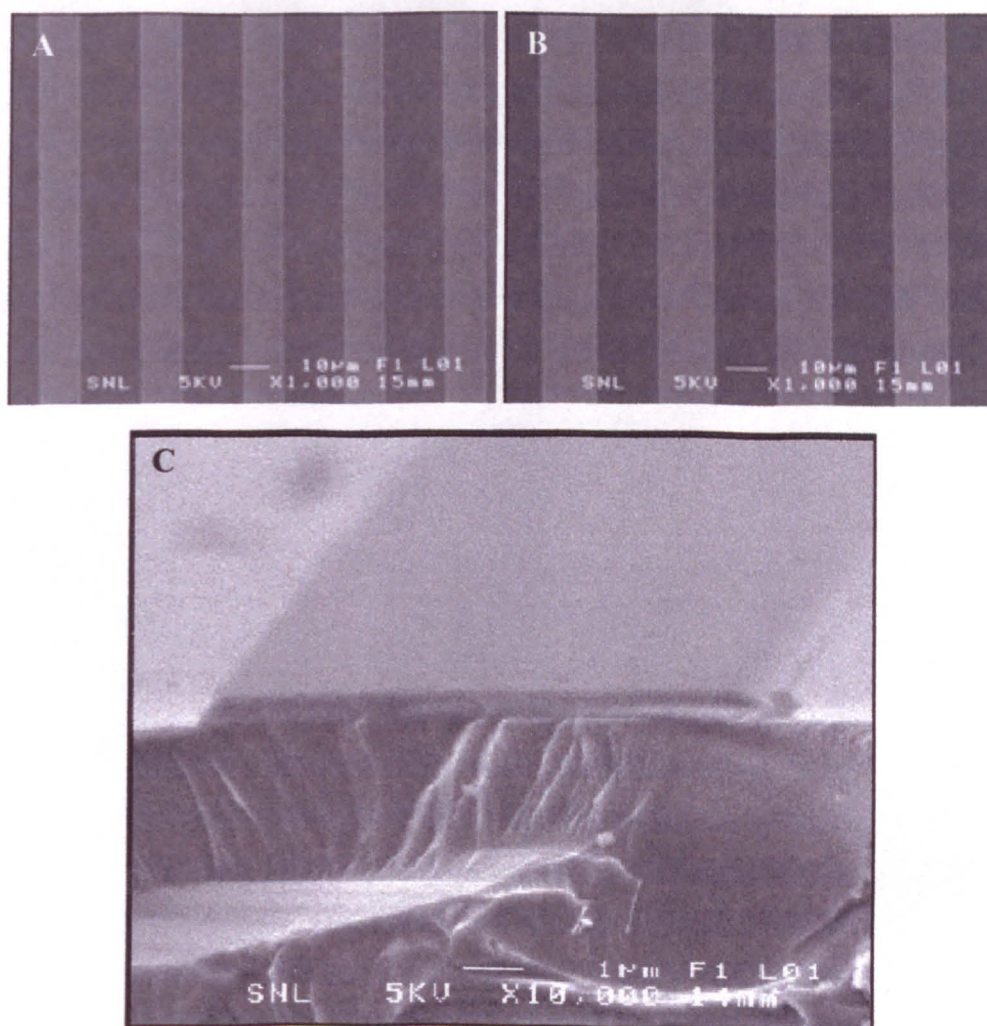


**Figure 6.9** SEM showing the detail of the small scale, striped pattern ( $a = 15/10$ ,  $b=15/15$ ). (c) shows the topography of patterned regions which are  $0.33\mu\text{m}$  thick.

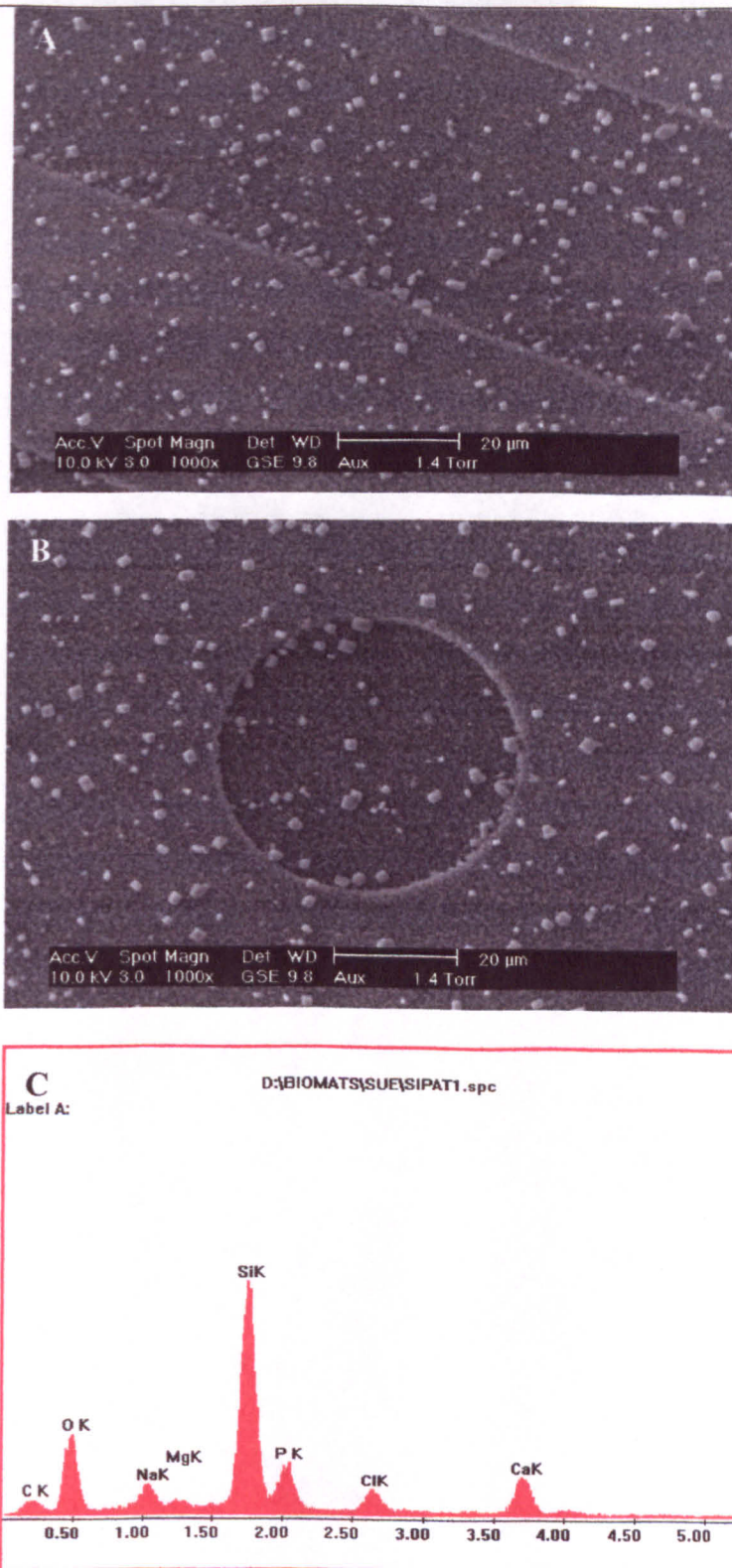


**Figure 6.10** ESEM images of the CaPi layer deposited on regions of the patterned surface (a) and (b). The EDX spectrum (c) shows a Ca:Pi ratio of 1.81. (axes: x=keV, y=counts/sec).

## 6.3.3.2 Cell response

Initial cell attachment (90 min and 4 hr) studies showed that there was little discernible difference between cells on the different regions of the pattern. The typical morphology was of rounded cells with cortical actin fibres (Figure 6.11). By 24 hr many more cells had adhered to the ESi regions of the pattern and the different regions were clearly distinguished (Figure 6.12). The edges of cells bordering along the edge of each pattern were aligned along the features with actin fibres running along the cell membranes. This was more markedly observed on the striped areas and the circular features were less clearly delineated. Few cells remained on the Si regions. It is unclear whether cells had migrated to the ESi areas of the pattern or had died on the Si areas but there were no signs of cell death and cells on the Si regions were similar in morphology to those on the pattern.

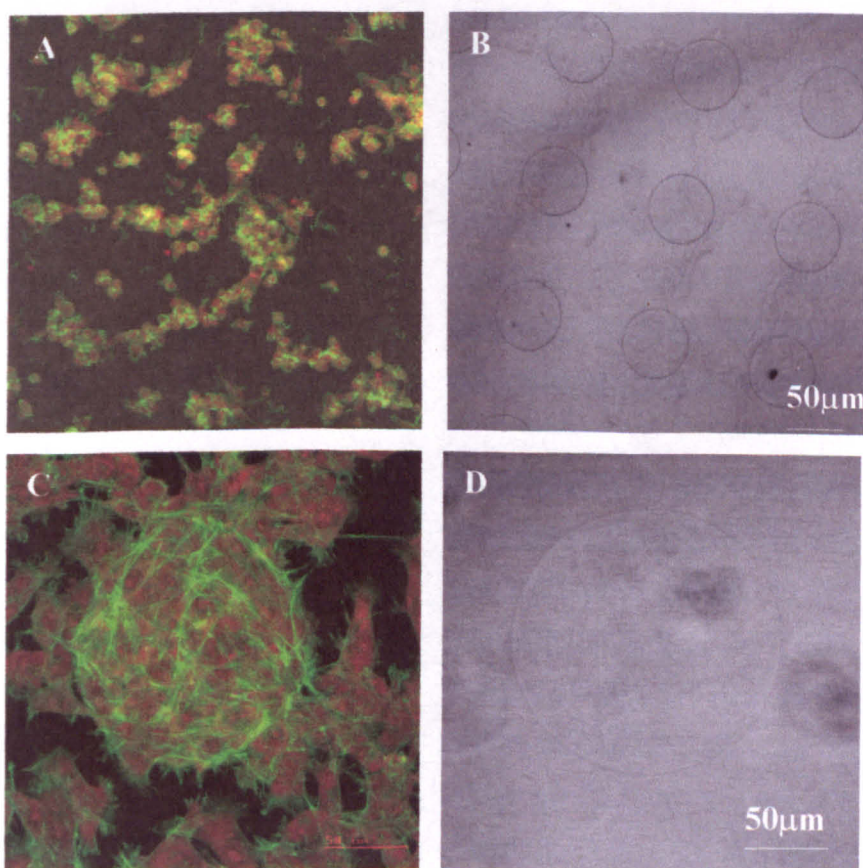


**Figure 6.11** CLSM images of HOBs grown on patterned Si/ESi surfaces. At 90 min no obvious alignment is seen and cells are randomly distributed on the surface (a), which can be confirmed by reflectance imaging of the underlying patterned surface (b). At 24 hr the cells follow the pattern (c) and (d).

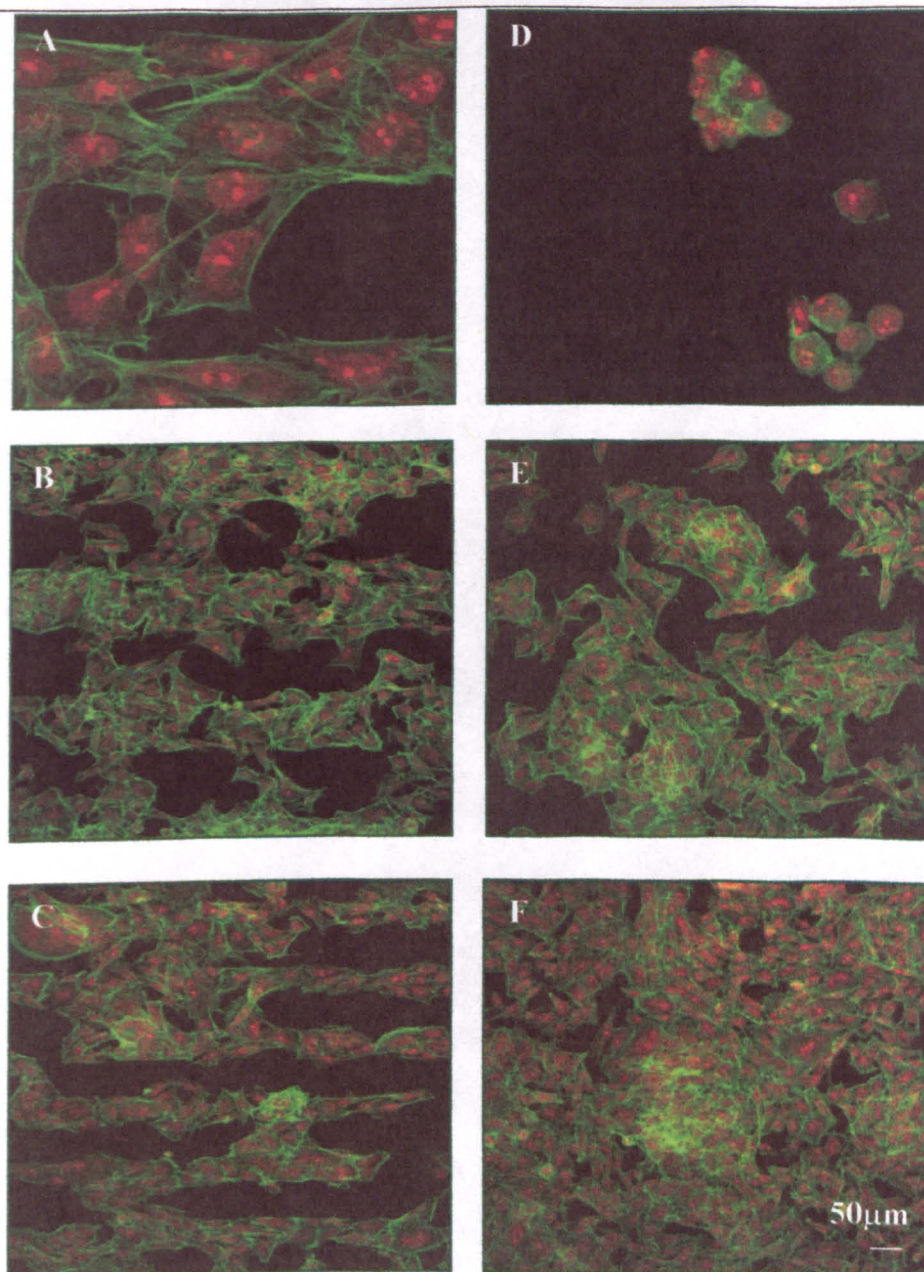


**Figure 6.12** CLSM images of HOBS grown on patterned Si/ESi surfaces for 24hr. The pattern consisted of stripes and spots at intervals of 150 $\mu$ m (a, b), 100 $\mu$ m (c, d) and 50 $\mu$ m. Cells are predominantly growing on the ESi regions.

---

At 7 days cell growth still followed the geometry of the pattern, especially on the 150 $\mu\text{m}$  regions (spots and stripes) where very few cells were seen to bridge the gap between one pattern feature and another. Some cells were seen growing on the silica regions on the 100 $\mu\text{m}$  features and these were often arranged perpendicularly to the pattern on the striped areas and bridging the gap between spots (Figure 6.13). The pattern was less clear on the 50 $\mu\text{m}$  areas but was still discernible with the cells forming multi-layers on the patterned regions and only partially covering the silica regions (Figure 6.13). At 21 days the cells covered most of the surface but the nodules were aligned along the patterns (Figure 6.14).

The results for the surfaces with smaller patterns (5-15 $\mu\text{m}$  stripes) were similar to those for the patterned surfaces. At 90 min cell morphology was similar on all regions of the pattern (Figure 6.15). Use of reflectance confocal microscopy showed that cell contacts were aligned over the ESi regions of the pattern. By 24hr cells were aligned on the ESi areas and the pattern appeared very defined (Figure 6.16). Only cells on the 15/5 $\mu\text{m}$  stripes were regularly seen bridging the 15 $\mu\text{m}$  gap. Actin fibres were aligned along the long axis of the cell. After 7 days cell alignment could still be seen on these surfaces using confocal microscopy. This was used to separate the upper and lower cell layers in the multi-layer by optical sectioning. The upper cells did not appear to be aligned but the lower levels remained aligned along the pattern (Figure 6.17).

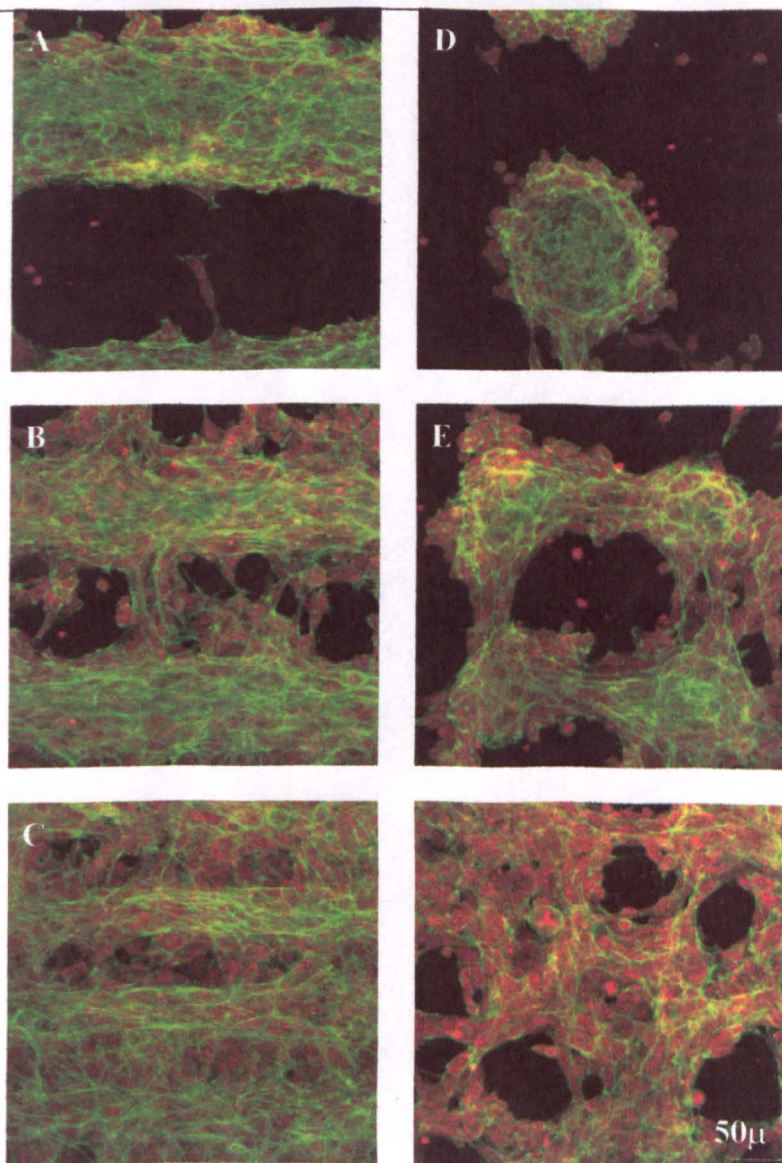


**Figure 6.13** CLSM images of HOBS grown on patterned Si/ESi surfaces for 7 days. Cells are predominantly growing on the ESi regions. The pattern consisted of stripes and spots at intervals of  $150\mu\text{m}$  (a, b),  $100\mu\text{m}$  (c, d) and  $50\mu\text{m}$ .

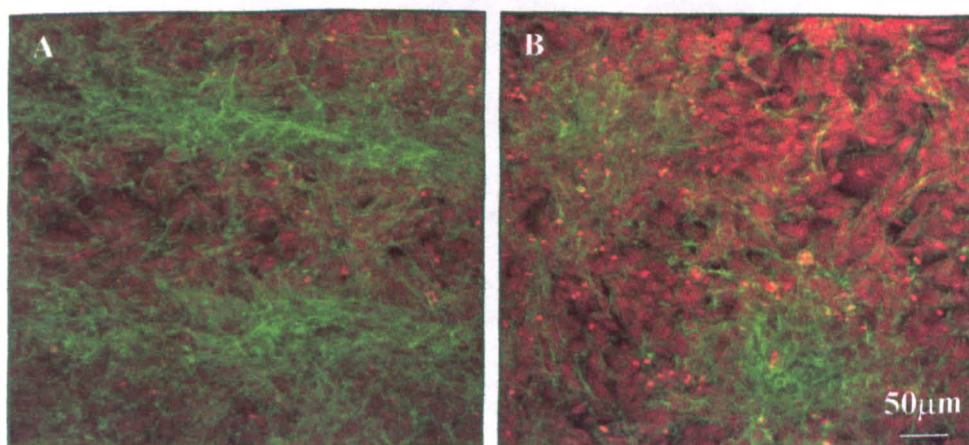


**Figure 6.14** CLSM images (maximum intensity) of HOBS grown on patterned Si/ESi surfaces for 21 days. (a)  $150\mu\text{m}$  stripe. (b)  $150\mu\text{m}$  spot.

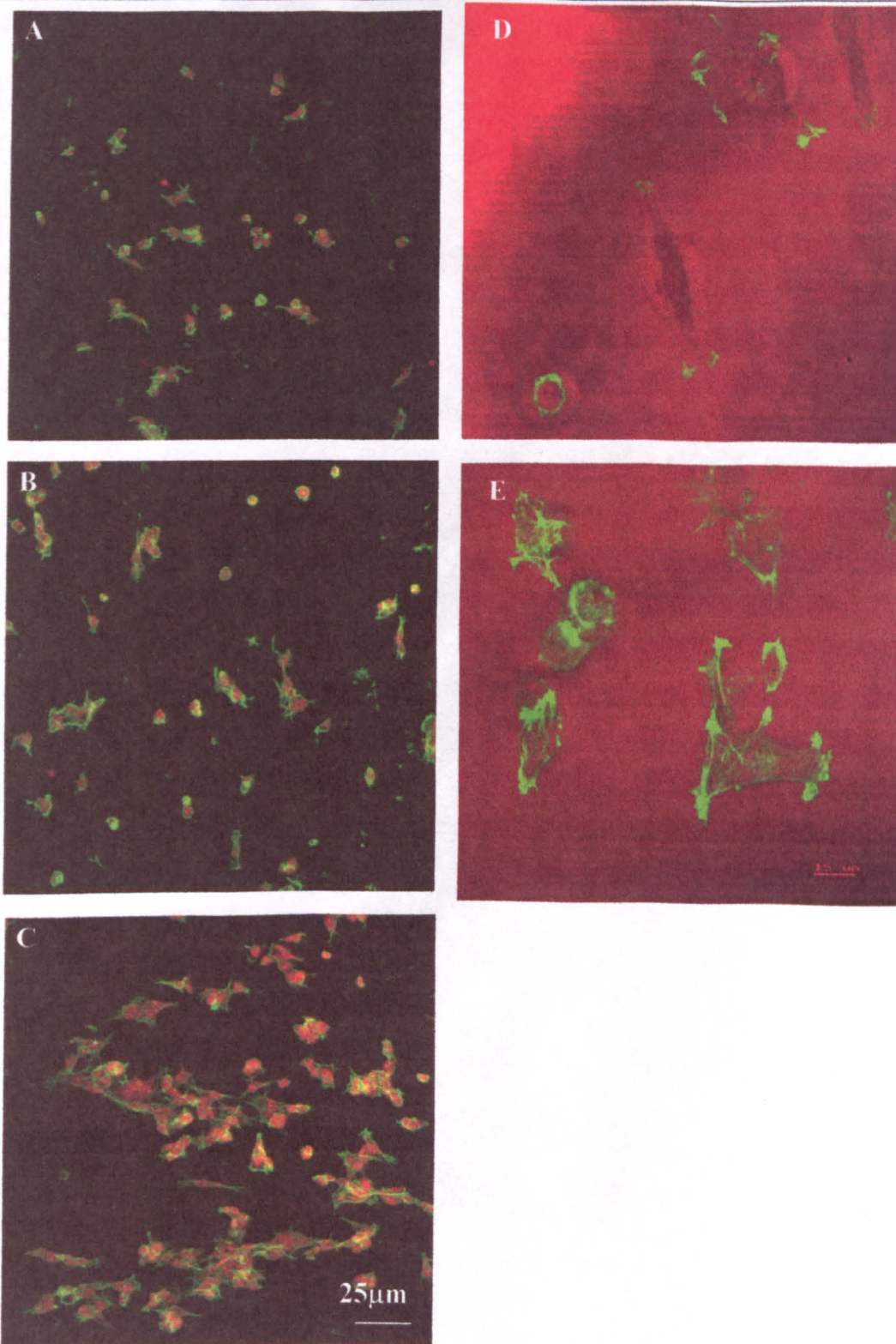


**Figure 6.15** CLSM images of HOBs grown on patterned surfaces for 90min. (a) 15/5 striped pattern, (b) 15/10 striped pattern, (c) 15/15 striped pattern. Some alignment of the cells is confirmed by overlaying reflectance images with images of HOBs as seen in (d) 15/15 surface and (e) 15/5 surface.

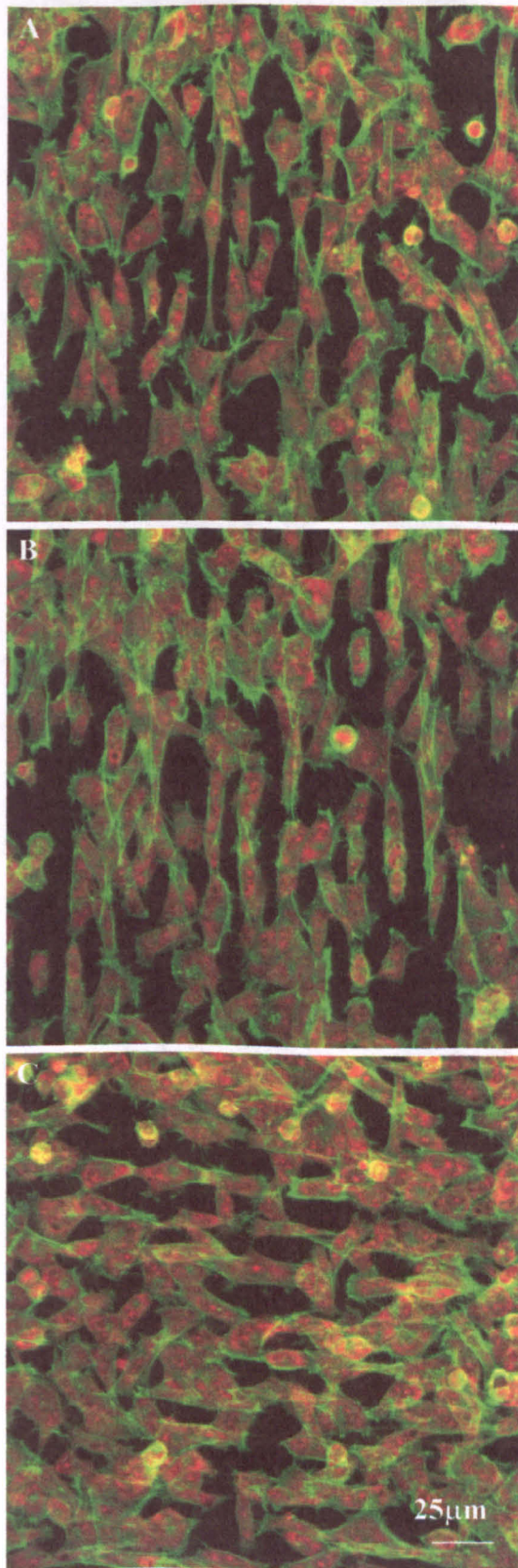


**Figure 6.16** CLSM images of HOBs grown on patterned surfaces for 24 hr. (a) 15/5 striped pattern, (b) 15/10 striped pattern, (c) 15/15 striped pattern.

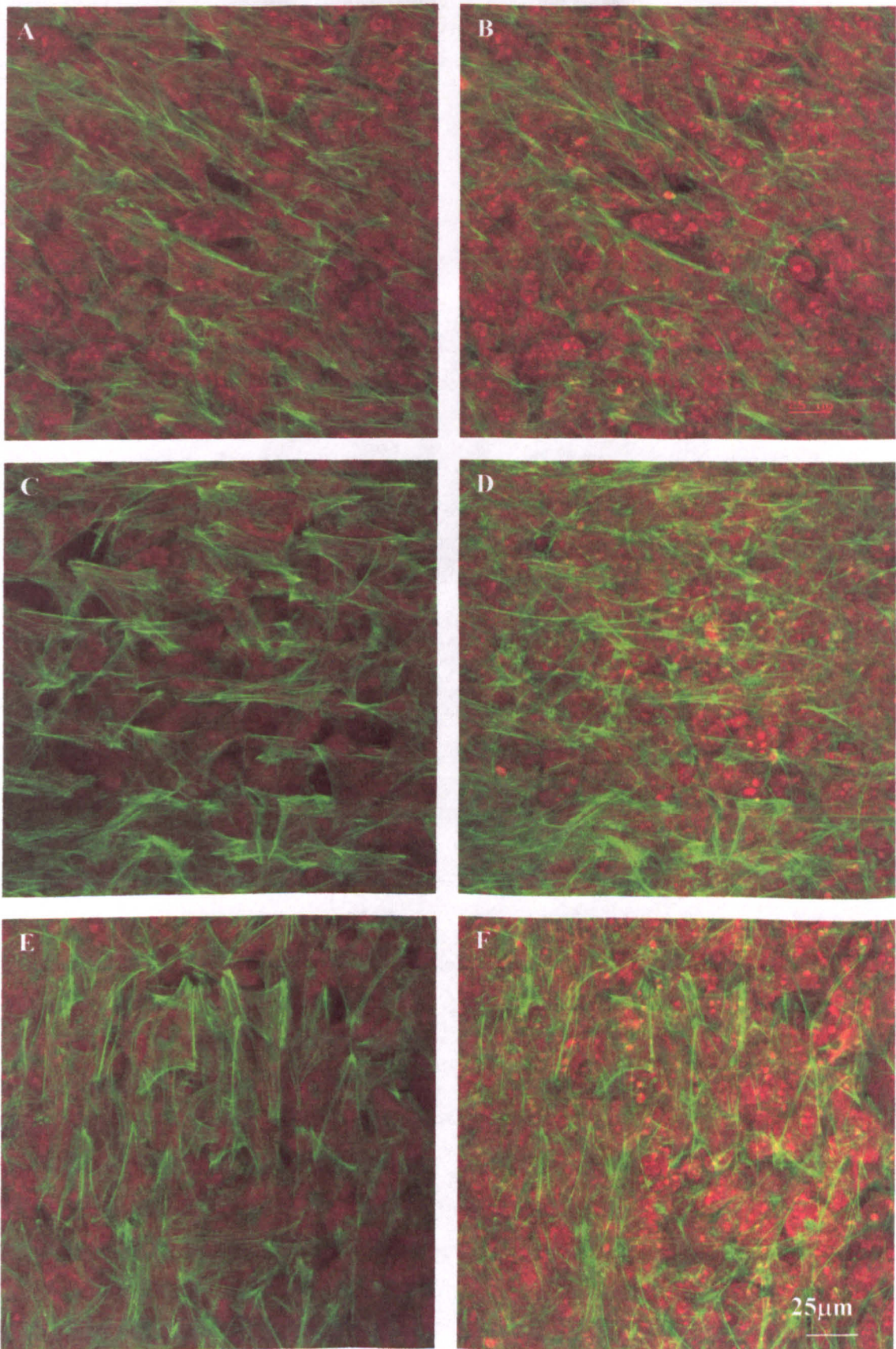


**Figure 6.17** CLSM images of HOBs grown on patterned surfaces for 7 days. Optical sections through the basal layer of cells (a, c, e) are shown with maximum intensity projections of the entire multilayer (b, d, f) for 15/5 (a, b), 15/10 (c, d) and 15/15 (e, f) striped surfaces.

## 6.4 Discussion

In this Chapter the effect of silicon surfaces on osteoblast growth was investigated. Silicon wafers (Si) were used along with wafers that had the oxide layer removed (ESi). It was thought that the silicon dioxide wafer could act as a more stable substrate for the evaluation of the osteoblast response as the gels used in the previous Chapter were unstable in aqueous medium. The initial hypothesis was that silicon dioxide would be a better surface than elemental silicon alone in terms of bioactivity and cell response because its elemental composition was more similar to the gel from the previous Chapter. A patterned surface of the two surfaces used was prepared by photolithography and used to make a direct comparison between the surfaces.

The surface analysis using EDX confirmed that the Si surface contained silicon and oxygen and that silicon only was present on the ESi surface. Analysis of the XPS data showed that oxygen was present in the ESi surface. This may be explained by the differences between the techniques used. EDX analysis, carried out at 10kV, would penetrate the sample surface to a certain degree whereas XPS, carried out at an angle of 75 degrees, would take measurements from the surface layers. Considering the travelling time involved between sample manufacture in Sweden and testing in the UK, it seems likely that oxygen was present, in different amounts, on both surfaces.

The use of silicon wafers as biomaterials has never been considered previously except by the Canham group (1995, 1996, 1997a, b, 1999). They have demonstrated the bioactive potential of silicon by a novel means of porosification leading to biodegradable properties as well as enhanced bone bonding properties. This work has shown for the first time that a bulk silicon surface can be rendered bioactive by the etching of the native oxide layer. This allowed silicic acid release from the surface and subsequent CaPi layer formation in SBF. Neither of these occurred on the non-etched Si surface. This was an unexpected result, as bulk silicon has never before been shown to have bioactive potential. It is not clear why the differences in bioactivity were present in such similar surfaces. The nature of the surface chemistry and the surface wettability are likely to be important.

---

All the surfaces used in this work were immersed in either SBF or tissue culture medium in order to perform the experiments. It is probable that surfaces changed upon hydration. Hydration in SBF could allow silicic acid release and the formation of OH groups on the material surface. In tissue culture medium, surface changes due to hydration could cause differences in the adsorption or conformation of proteins. These are important considerations in clarifying the exact cause of the enhanced bioactivity seen in the etched surfaces.

This work lends weight to the assumption that bulk silicon, in its unaltered form, is not bioactive. The present work also strengthens the observation from the previous Chapter that silicic acid release and CaPi layer formation are correlated, a theory which is widely accepted in the mechanism of CaPi layer formation on bioglass (Lobel and Hench, 1996).

The cell response to the surfaces was then evaluated using cell attachment and spreading observations and nodule formation. There was no apparent difference between the cell response to the surfaces using these parameters. No attempt was made to look in detail at the effect of the surfaces on protein adsorption or expression of markers such as ALP and Collagen-1 although these would be advantageous in the future.

When the patterned surfaces were viewed, surface analysis allowed the different regions of the pattern to be distinguished, using EDX analysis for SBF work and reflectance microscopy for cell response work. Silicic acid was released from patterned surfaces and a CaPi layer formed over the entire surface of the material. The Ca:Pi ratio on the patterned surface was similar to that seen on the ESi surface, although the amount of silicic acid released, the amount of carbon present and the thickness of the layer formed appeared to be reduced. The formation of a CaPi layer on the patterned surface was not surprising as the silicic acid released from the ESi part of the pattern would stimulate the formation of the calcium phosphate layer which would then be deposited at random. Other studies have shown how CaPi layer formation can be induced on a non-bioactive surface in a biomimetic way (Cho *et al.*, 1996c).

The way in which the cells behaved was interesting. Although the cells appeared to be randomly distributed at 90 min, by 24 hr it was clear that the cells were aligning on the areas of the pattern where the oxide layer had been removed. Cells responded to patterned surface from a number of sizes and dimensions. Stripes were used varying in width from 5-150 $\mu\text{m}$ . There was an obvious response on all surfaces by 24 hr. This was maintained for 7 days and even at 21 days the geometry of the pattern was still apparent, showing that the head start gained by the cells on the ESi regions was never lost. Although patterned surfaces have been used to analyse cellular responses to terminal chemistry (Scotchford *et al.*, 1998), these methods have never been previously applied to bioactive versus non-bioactive surfaces. The results presented here demonstrate a clear preference of cells for the bioactive surface over the non bioactive one. This was not apparent when either surface was used alone.

The question arises as to whether the cells respond to topographical guidance cues rather than the nature of the surface and it is true that the cells adhere preferentially to the etched, and therefore lower, regions of the pattern. Grooved surfaces are known to enhance bone formation *in vitro* (Gray *et al.*, 1996). Surface geometry has been shown to elicit a significant cellular response *in vivo* and *in vitro* (Cheroudi *et al.*, 1992). The thickness of the step between the different regions of the pattern was 0.33 $\mu\text{m}$ . Work done by others in our group using different metal surfaces prepared in the same way has shown that cells do not respond to the pattern alone. This was demonstrated by the use of patterned titanium surfaces where cells were exposed to the topographical effects of the pattern while the surfaces used were the same in each region. The cells did not respond to the pattern in this case (unpublished observations).

In summary, the work presented in this Chapter has shown that a silicon surface can be rendered bioactive (in terms of CaPi layer formation) by removal of the surface oxide layer. Comparison of cell response to Si and ESi surfaces showed minor differences in cell attachment and similar patterns of nodule formation. HOBs displayed a clear preference for the bioactive regions when presented with a patterned surface. This presents opportunities to manipulate cell responses to surfaces in a controlled manner and has potential implications in the fields of tissue engineering and biosensing.

## **Chapter 7**

# **The Incorporation of Silica into a PCL Polymer System.**

## 7.1 Introduction.

The results demonstrated in Chapters 5 and 6 shows that osteoblasts respond favourably to bioactive silicon and silica surfaces. The surfaces used in the 2 preceding Chapters were purely experimental in nature. The original aims of the project stated the desire to incorporate silica into a suitable biomaterial vehicle, should it promote bioactivity, as a long-term goal. In this Chapter the incorporation of silica into a potential working implant is explored.

Aseptic loosening is the most common cause of implant failure. This is due to factors such as stress shielding of an implant, leading to bone resorption, movement of the implant, causing the development of a soft tissue interface and the presence of wear particles causing osteolysis (Vander Sloten *et al.*, 2001). Stress shielding and micromotion could both be reduced if stability of fixation of implants such as hip stems, could be achieved (Vander Sloten *et al.*, 2001). For these reasons cemented hip stems have been used and the cemented Charnley prosthesis introduced in 1967 remains the gold standard for total hip replacement (Vander Sloten *et al.*, 2001). Polymers are currently used in many biomaterial applications such as wound dressings (Corden *et al.*, 1998), sutures, capsules for controlled drug delivery, tissue adhesives and bone cements (Donkerwolcke *et al.*, 1998) and as the smooth covering of joint surfaces on metal implants (eg. acetabular components), among many others. The current state of research on polymeric scaffolds for tissue engineered constructs is reviewed in a recent paper by Hutmacher (2000). Despite the many uses and types of polymer available, they do not possess bioactive properties like their glass and glass-ceramic counterparts such as bioglass and hydroxyapatite (Donkerwolcke *et al.*, 1998).

Poly- $\epsilon$ -caprolactone (PCL) is a bioabsorbable polymer. It is currently used in biomaterial applications such as wound dressings and the encapsulation of drugs for controlled release and shows good biocompatibility with osteoblasts (Corden *et al.*, 1998). In this work the potential benefits of incorporating silica particles into a PCL system were tested in terms of bioactivity and initial cell response. PCL (formula,  $C_{26}H_{48}O_2$ ) was chosen as the vehicle for the silica particles because of its low melting (60-62°C) temperature and because it hardens at room temperature, reducing the chance of

the alteration of the properties of the silica particles due to heating effects. The viscosity of the molten polymer (443 Pascal seconds at 150°C) would enable the particles to be easily dispersed throughout the polymer matrix (Corden *et al.*, 1998).

There is some work in the literature about the use of bone cements and silica. Calcium metasilicate particles have been implanted into polymethyl methacrylate (PMMA) substrates (Tsuru *et al.*, 1998) and this has imparted bioactive properties to the polymer as measured by the formation of a CaPi layer in SBF. Fujita *et al.* (2000) have cemented a hip implant with a bioactive bone cement, composed of apatite and wollastonite-containing (AW) glass ceramic powder, silica glass powder and bisphenol-A-glycidyl dimethacrylate (bis-GMA) based resin in dogs. They found the material to have better mechanical and bone bonding properties than PMMA fixed implants, however implant failure occurred after 24 months at the acetabular component. A previous study by the same group showed that the bioactive cement penetrated deeper into acetabular anchor holes than PMMA (Fujita *et al.*, 1999).

In contrast to PMMA, there is little in the literature concerning the formation of PCL/silica composites. One study examined the drug release characteristics from poly(epsilon-caprolactone/DL-lactide) copolymer/silica gel composite and found that the release rate of the drug was enhanced when it was incorporated in the silica xerogel (Rich *et al.*, 2001). Lowry *et al.* (1997) used a PCL/glass fibre composite as fracture fixators in a rabbit humeral model and found that the tissue inflammatory response was minimal, active bone formation around the implant and no evidence of osteolysis. The implant was not strong enough for load bearing applications however, and potential uses for carpal fixation, patellar fixation and paediatric applications were suggested. A PCL/biodegradable glass fibre composite is being developed for potential use in maxillofacial reconstruction due to trauma, tumour removal and congenital malformations (Corden *et al.*, 1998). It is unclear whether the glass fibres used in the latter two papers are silica based.

The aims of this Chapter were to prepare a polymer containing silica and to analyse whether bioactive properties were conferred on the polymer as a result of the addition of silica. The silica particles used were made from 2 sources. The first method employed TEOS, which was used to prepare the silica gels used in Chapter 5. The second used

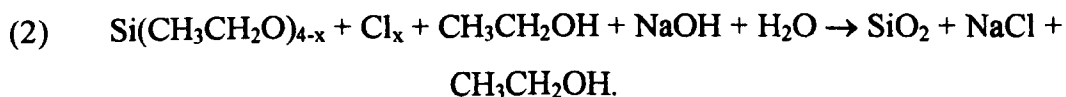
tetrachlorosilane (TCS) which involved a less complex chemical reaction. The resultant particles were analysed and then incorporated into PCL. The PCL/silica composite was evaluated to assess whether the addition of silica increased the bioactivity of the polymer. Preliminary experiments were undertaken to evaluate the early response of the osteoblast to the silica containing polymers.

## 7.2 Materials and Methods.

### 7.2.1 Formation of Silica -Particles from TEOS.

One part concentrated HCl was added to 2 parts tetraethoxy silane (TEOS, Sigma). The solution was stirred slowly and 3 parts 10M NaOH was added. The mixture was again stirred slowly and filtered. The resulting particles were thoroughly washed to remove the NaCl, which occurred as a result of the reaction. The powder was filtered and dried in a 37°C oven.

The reaction for the production of silica particles using TEOS was:



### 7.2.2 Formation of Silica Particles from TCS.

Tetrachlorosilane (TCS, 2ml) was slowly added to 612µl DH<sub>2</sub>O (2:1 moles TCS:H<sub>2</sub>O, Sigma) in an air tight vessel and stirred. The resulting silica powder was washed thoroughly to remove the HCl and the powder was filtered and dried in a 37°C oven.

The reaction for the production of silica particles using TCS was:



### 7.2.3 Incorporation of Silica into PCL.

The PCL (CAPA 650, Solvay Interlox, Warrington, UK) was supplied in sheet form and was melted down at 80°C (melting point of PCL is 60°C) so that the particles could be added. 56mg silica was added to 7g polymer and mixed in a 10ml syringe (Becton Dickinson) and allowed to harden at room temperature. The PCL-silica composite was then removed from the mould and 2mm thick discs were cut from the cylinder using a Reichert Jung 2050 supercut microtome (Leica Microsystems Ltd, Milton Keynes, UK) with a metal blade. PCL discs without silica, prepared in the same were used as controls

throughout the experiments. As the even distribution of particles in the PCL could not be guaranteed, a method was also used in which the entire surface of the polymer was encrusted with silica particles. This was formed by putting a layer of silica particles, prepared from either TEOS or TCS, in the base of a teflon mould, placing a sheet of PCL on top and heating to 80°C. When cooled 13mm samples were punched from the sheet with a cork borer.

#### **7.2.4 EDX Analysis and Elemental Mapping.**

Polymer samples containing silica were examined using a Phillips FEG-ESEM with EDX microanalysis to assess the elemental content. Elemental mapping was carried out to identify the occurrence of silica in the discs. The microscope was operated in auxiliary mode using nitrogen as the chamber gas so that the samples could be viewed without coating.

#### **7.2.5 CaPi Layer Formation and Silicic Acid Release.**

Samples of PCL and silica containing PCL, prepared using TEOS or TCS, were placed individually in the wells of a 6 well tissue culture plate (Falcon). Samples were sterilised using UV light and incubated in 10ml of SBF for 14 days at 37°C. After 14 days the samples were removed from the SBF, rinsed gently in sterile distilled water and air-dried. They were then mounted on aluminium stubs with adhesive carbon tabs (Agar) and viewed in a Phillips FEG-ESEM in auxiliary mode using nitrogen as the chamber gas. This was done to alleviate the need to coat the samples with gold before viewing which would interfere with the analysis of phosphorous in the samples. Secondary imaging and EDX microanalysis was carried out on each sample at 10kV.

Silicic acid release from PCL samples encrusted with silica prepared from TEOS was measured, after 2 weeks in SBF, using the molybdenum blue assay described in Chapter 5. This was compared with silicic acid release from PCL discs.

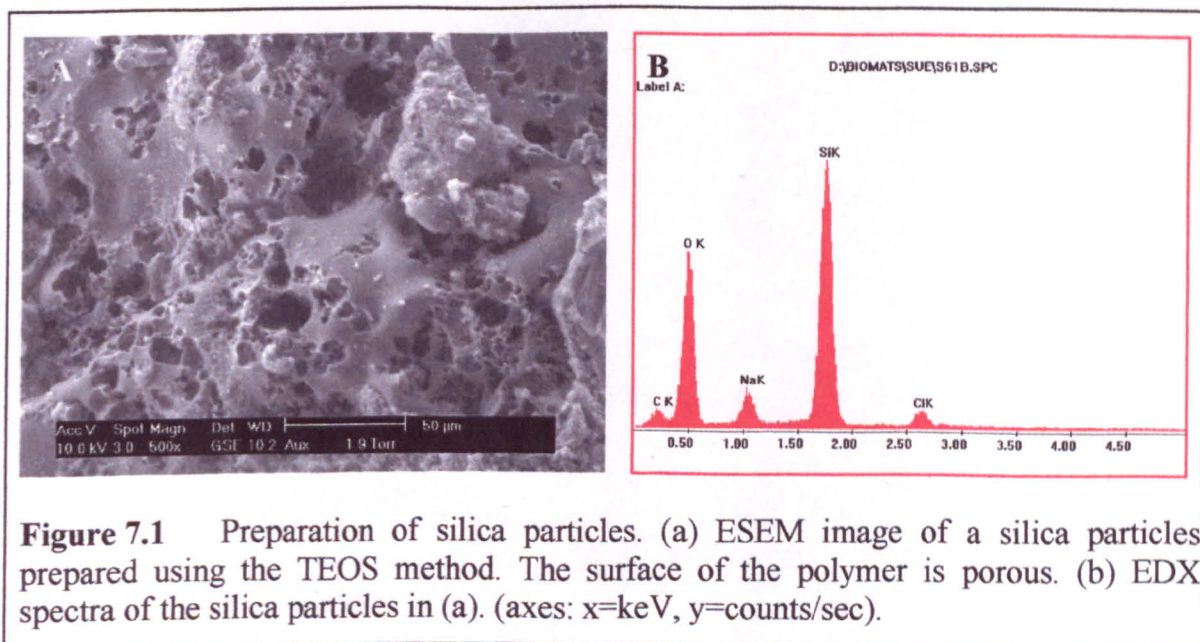
### 7.2.6 Cell Response to Silica Containing Polymers.

The biocompatibility of the silica containing polymer samples was evaluated using SEM and an assay for cell activity (alamar blue). Samples were placed in triplicate in a 24 well tissue culture plate and sterilised using UV light for 30 min. HOBs were added to the wells at a concentration of  $8 \times 10^4$  cells per ml in complete DMEM as described in Chapter 2 and incubated at 37°C 5% CO<sub>2</sub>. Plain PCL discs and Thermanox coverslips were used as controls. The alamar blue assay was carried out, at 24 hr cell culture, using the method described in Chapter 2. To ensure that the activity of cells growing on the tissue culture plastic was not measured, samples were removed to a fresh plate before the assay was carried out. Blank polymers, without cells, were used as controls to ensure polymer samples did not interfere with the assay. For SEM studies, the medium was removed from the wells after 90 min or 24 hr cell culture. The discs were rinsed in PBS and the samples were fixed in 1.5% glutaraldehyde in 0.1M phosphate buffer for 30 min. After rinsing in 0.1M phosphate buffer the cells were post-fixed in 1% osmium tetroxide in Millonigs buffer for 30 min. The samples were then rinsed in DH<sub>2</sub>O and dehydrated in a graded ethanol series (2x5min in each of 50, 70, 90% and 3x10min in 100%). The samples were then immersed in hexamethyldisilazane (HMDS) for 2 periods of 5 min, the HMDS was removed and the samples were allowed to air-dry in a fume hood. Once dry, the samples were mounted on aluminium stubs with sticky carbon tabs, coated with gold using an Emscope sputter coater (5mA for 3min) and viewed using a Philips XL30 SEM with LaB<sub>6</sub> filament operated at 10kV.

## 7.3 Results.

### 7.3.1 Analysis of Silica Particle Formation.

The use of both TEOS and TCS resulted in the successful preparation of silica particles. The yield was high (94-99%) for both methods. Generally the particles produced by the TEOS method were larger than those produced by TCS, which produced a fine powder, but this was not quantified. ESEM evaluation of the TEOS particles revealed cuboidal pores over the surface of the polymer and this was probably due to the crystals of NaCl, a by product of the reaction, which were removed from the sample by washing (Figure 7.1a). EDX microanalysis revealed the presence of silicon and oxygen in the samples in addition to carbon, sodium and chlorine (Figure 7.1b). The average atomic ratio of O:Si was 1.55.



### 7.3.2 Surface Analysis of Silica Containing Polymers.

Elemental mapping was carried out on polymer discs containing silica prepared from TEOS. Figure 7.2 shows images of polymer discs containing silica and polymer discs encrusted with silica.

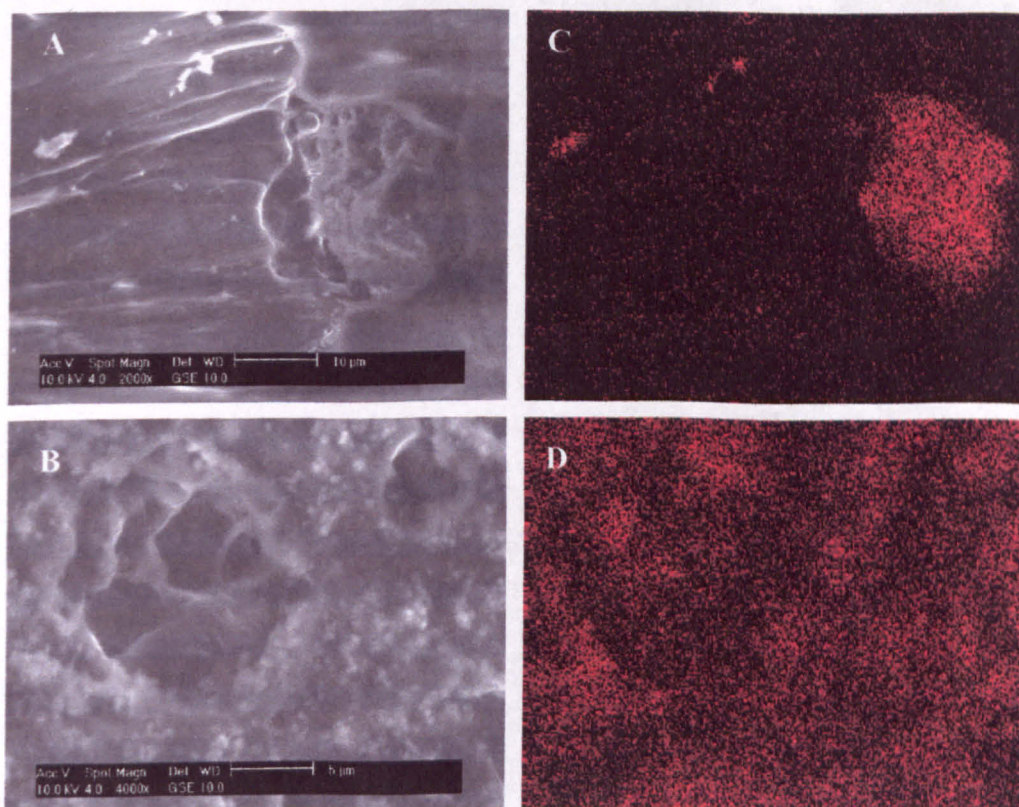


**Figure 7.2** ESEM images of PCL containing silica by impregnation (a) or encrustation (b). The areas of the images containing silica are shown in the corresponding elemental maps (c, d).

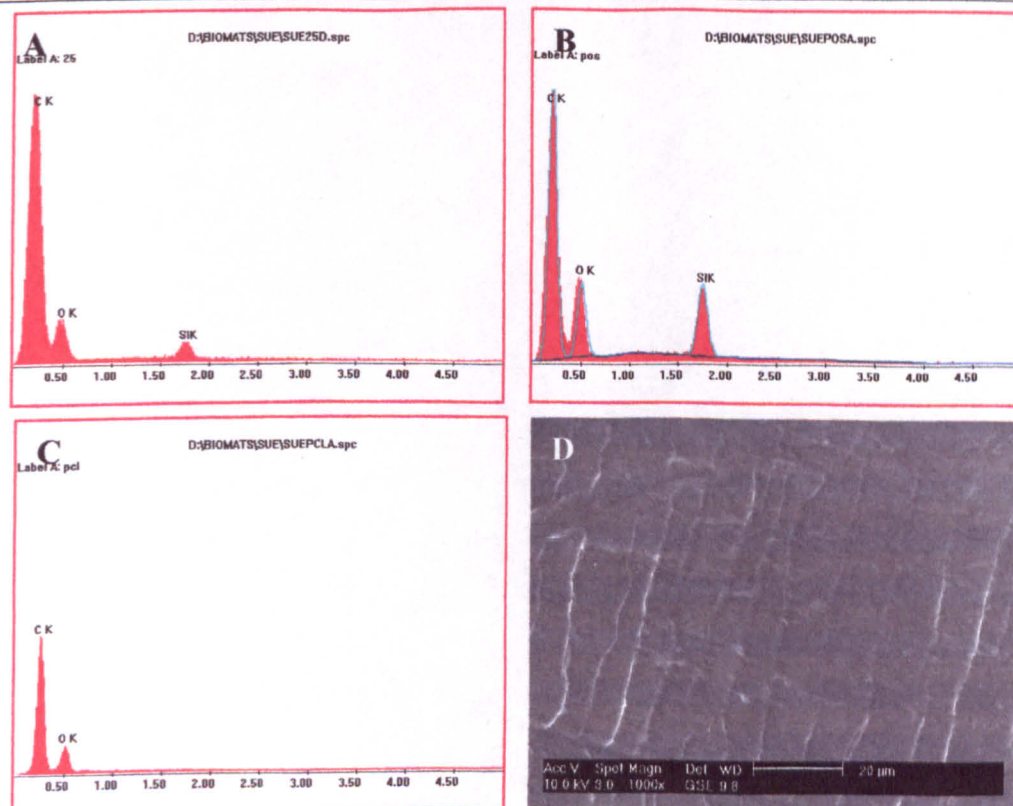


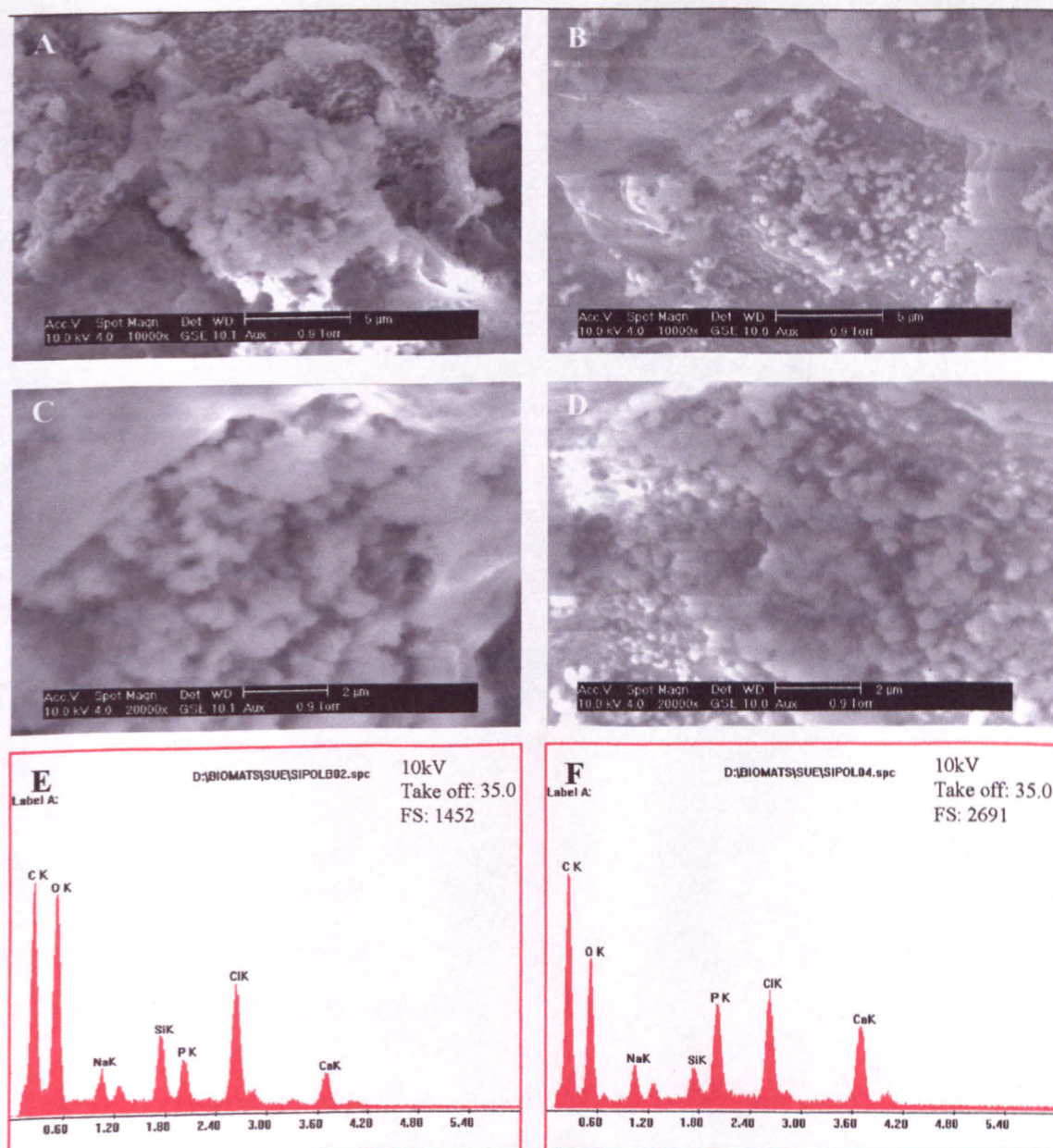
**Figure 7.3** EDX spectra for the areas shown in figure 7.2 (a) and (b) and for PCL without silica (c). (axes:  $x = \text{keV}$ ,  $y = \text{counts/sec}$ ). (d) ESEM image of PCL without silica, corresponding to the EDX spectrum in (c).

EDX analysis allowed the amount of silica in the samples to be calculated (Figure 7.3). Polymer discs containing silica showed the atomic percentage of silicon to be 2.83 At% (SEM = 1.71). Polymer samples prepared by encrusting the surface with silica particles showed a higher silica percentage of 4.46 At% (SEM = 0.50). The distribution of particles was more even in the encrusted samples and this was reflected in the standard errors.

### **7.3.3 CaPi Layer Formation and Silicic Acid Release in SBF.**

The formation of a CaPi layer after 2 weeks in SBF was detected using ESEM. An almost continuous CaPi layer was present on encrusted PCL samples prepared with both TEOS and TCS and is shown in figure 7.4a, b. No deposition was observed on the PCL controls. EDX analysis of 25x15 $\mu$ m areas (n=3) showed the silica content of the polymers. The content for polymers prepared with TEOS was 3.30 At% (SEM=1.26) and for TCS was 2.74 At% (SEM=0.20). EDX analysis of the same regions showed the presence of calcium phosphate (Figure 7.4c, d) and allowed the Ca:Pi ratio to be calculated using the elements atomic percent. The average CaPi ratio for TEOS samples was 1.96 and for TCS samples was 1.50.

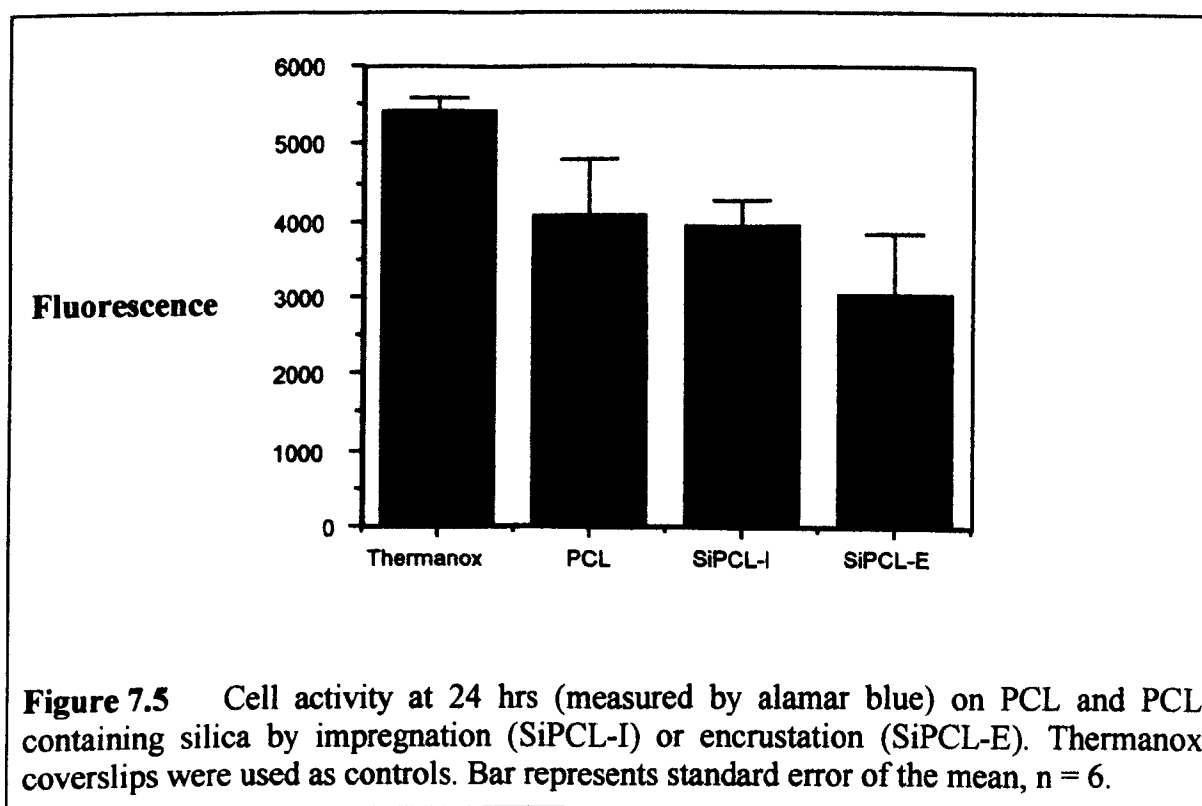
Silicic acid release into SBF from PCL containing silica prepared from TEOS, was measured after 2 weeks. Small amounts of silicic acid (0.10-0.15ppm) were released from the silica containing polymers. Silicic acid was not released from PCL controls.



**Figure 7.4** ESEM images of polymers encrusted with silica particles prepared using TEOS (a, c, e) or TCS (b, d, f) after 2 weeks in SBF. CaPi deposition was seen on both surfaces. EDX spectra confirm the presence of Ca and Pi in the samples. (axes: x=keV, y=counts/sec).

### 7.3.4 Initial Cell Response.

None of the materials used were toxic to HOBs as measured by the alamar blue assay (Figure 7.5) which showed no statistically significant difference between Thermanox, PCL and silica containing PCL prepared by either impregnation or encrustation. The results of the SEM studies are shown in figures 7.6 and 7.7. The cells appeared viable at both timepoints and were well spread on all samples by 24 hr. Cells were aligned along the knife marks resulting from slicing the PCL and silica containing PCL discs. Samples prepared by encrusting the silica particles into the PCL surface were randomly oriented in a similar fashion to the Thermanox controls. It was not possible to determine whether cell processes were attached to silica particles.



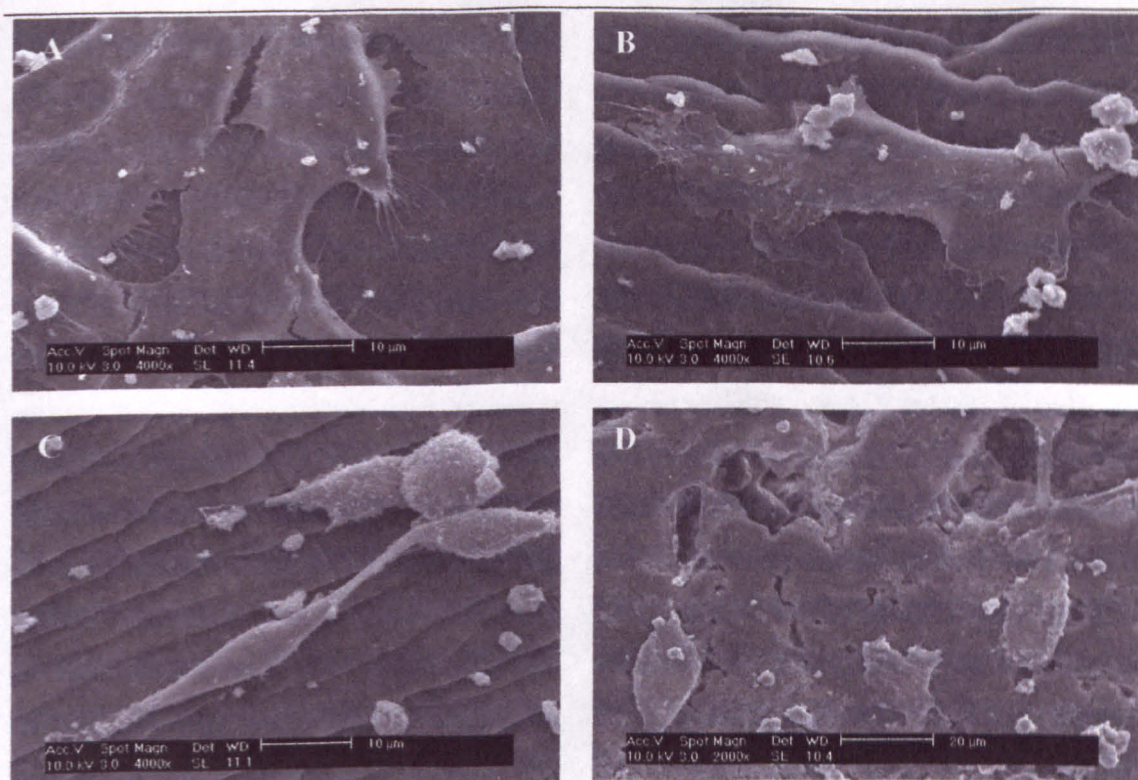


**Figure 7.6** SEM images of HOBs after 90min culture on Thermanox (a), PCL (b), PCL impregnated with silica (c) and PCL encrusted with silica (d).

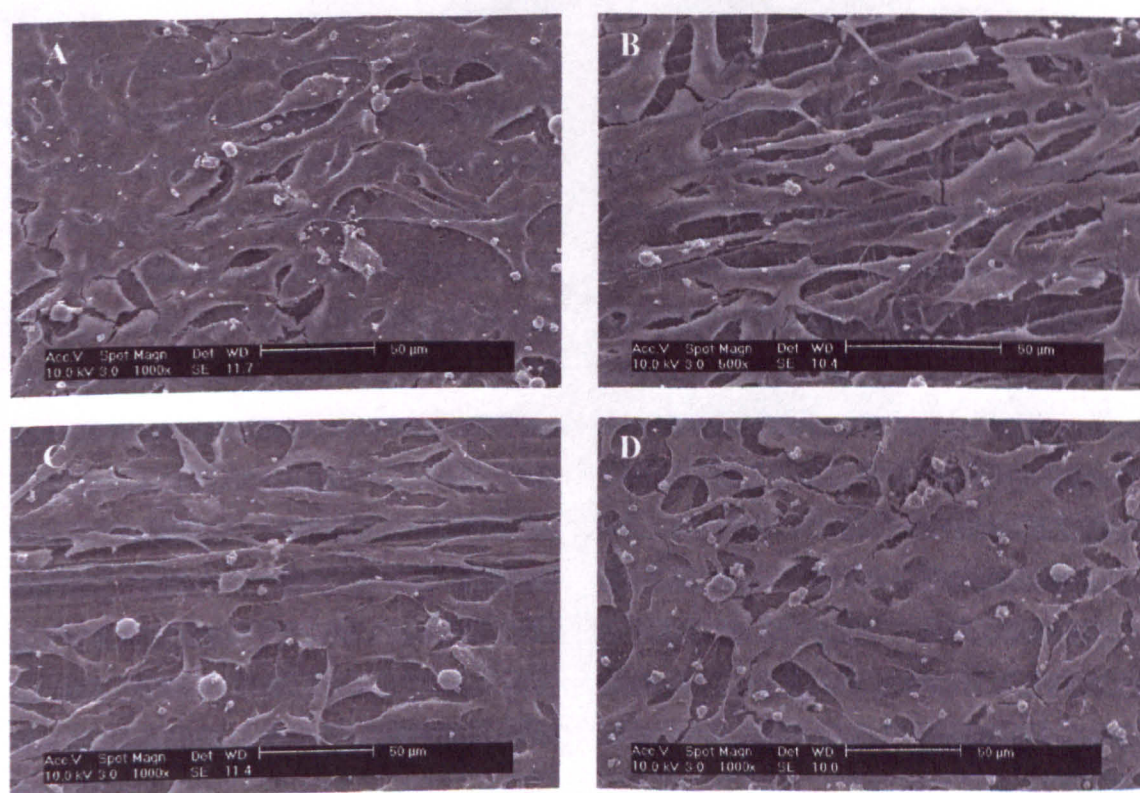


**Figure 7.7** SEM images of HOBs after 24hr culture on Thermanox (a), PCL (b), PCL impregnated with silica (c) and PCL encrusted with silica (d).

## 7.4 Discussion.

The aim of the work presented in this Chapter was to incorporate silica into a polymer system that is currently used in the field of biomaterials and to make preliminary investigations into the properties of the silica-polymer composite. This was achieved using methods for assessing bioactivity and by testing the ability of the composite to support cell growth.

Silica particles were successfully prepared using TEOS and the composition of the particles was checked using ESEM with EDX microanalysis. The porous nature of the particles was confirmed and porosity is reported to be favourable for osteoblast ingrowth *in vitro* and *in vivo* (Lu *et al.*, 1999). This resulted from the formation of NaCl crystals as a by product of the reaction which were subsequently washed from the system. This led to the formation of cuboidal pores that were probably not interconnected. It is possible that NaCl could be leached from an implant containing these particles and the potential effect of this on cells has not been investigated. Particles were also prepared using TCS. This system had the advantage of involving less chemical reactions and particles were easier to prepare. The resulting particles were not porous in nature. It may be possible to prepare porous silica particles by either using saline in place of water or, by incorporation PMMA spheres with the silica during the reaction. These could then be dissolved from the particles using chloroform. Both systems used gave a high yield of particles.

PCL was chosen as a vehicle to test the properties of the silica particles because it is currently used in the field of biomaterials, but has no bioactive properties. Other properties of the polymer made it a practical choice for the testing of the bioactive potential of the particles. The melting point of PCL is low, making the incorporation of silica particles simple to perform. Also, the effect of heat on the bioactivity of the particles is unknown. It was thought that the viscosity of the molten polymer would prevent the uneven dispersion of the particles in the polymer matrix.

The addition of silica to the PCL polymer was via 2 routes. Initially molten PCL was impregnated with particles in a cylindrical mould and discs were cut from this for use in experiments. The problems with this system were twofold. Firstly, the even dispersion

of the particles was difficult using this method and many discs cut from the cylinder would have contained no particles. The amount of silica that could be incorporated into the polymer in this was small, as otherwise the polymer became brittle and difficult to cut. Secondly, the cutting process resulted in knife marks on the PCL discs. This could clearly be seen using SEM and caused the cells to align along the grooves. This would result in the difficulty of isolating the effect of the inclusion of silica from the effects of the topography of the surface.

The second method of incorporating the silica particles into the polymer matrix involved encrusting the surface layer of the molten polymer with silica particles. While this made the amount of silica difficult to measure, it allowed the surface of the polymer to be roughened only by the silica itself, thus negating the differential effects of surface topography. It is clear however, that a suitable method of ensuring the particles even distribution would be desirable.

The addition of silica to the polymer system caused silicic acid release and CaPi layer formation on PCL surface encrusted with silica prepared from TEOS and TCS. CaPi deposition was seen on silica particles and on areas of polymer where silica was not seen. The formation of a CaPi layer on non-bioactive surfaces by biomimesis has been shown previously (Cho *et al.*, 1996c) but these studies are based on techniques using 1.5x SBF. Recent studies have shown that the induction time for apatite nucleation and the adhesive strength of the layer for a range of substances was improved if the surfaces were pretreated with UV irradiation (Liu *et al.*, 1998) or HCl (Tanahashi *et al.*, 1995). Induction of apatite formation on a non bioactive surface was demonstrated using patterned Si/Esi surfaces in Chapter 6. The amount of silica required to impart bioactivity to the polymer surface is unknown and would benefit from further study.

Initial studies of cell responses to the silica-PCL composite are encouraging. Cell activity was not significantly different on any of the surfaces examined. SEM studies showed the cells were well spread on all surfaces by 24 hrs.

The fact that PCL can be moulded opens up exciting possibilities for designing biodegradable, bioactive implants for craniofacial applications and other areas where intricately moulded, non load bearing implants are required (Corden *et al.*, 1998).

Despite the choice of PCL for this work, there is no reason why the particles prepared here could not be incorporated into a number of other systems. Calcium metasilicate glass particles have been implanted into PMMA and these composites have formed a CaPi layer in SBF (Tsuru *et al.*, 1998). Two recent papers have incorporated silica into hydroxyapatite (Tancred *et al.*, 2001) and PMMA (Arcos *et al.*, 2001). In the first paper, bioglass was added to HA in order to test the effect of silica inclusion on the mechanical strength of an implant. Fracture toughness was increased in the HA with bioglass addition but other mechanical properties were not improved. The effect of silica addition on the bioactive properties was not investigated but has been previously reported to reduce the amount of time required to form a CaPi layer *in vitro* (Santos *et al.*, 1996). The cell response to HA-bioglass composites is unclear. The second paper describes a glass ( $\text{SiO}_2\text{-CaO-P}_2\text{O}_5$ )/PMMA composite with bioactive properties which was used successfully as a drug delivery system *in vitro*. The cell responses to the composite *in vitro* and *in vivo* have yet to be studied.

The results presented in this Chapter demonstrate that the inclusion of suitable silica particles in a non-bioactive polymer matrix can confer bioactive properties on the polymer. These initial findings are encouraging but further work to identify the amount of silica required for bioactivity would be beneficial. Important considerations for future research include the effect of the inclusion of particles on the mechanical strength of an implant and other handling properties such as pliability for bone cements. As PCL is a degradable polymer system, the fate of released particles from the matrix must be addressed as well as any potential toxic effects. For these reasons future work should test the potential toxicity of the particles by growing macrophages in culture with the particles or with growth medium that had been conditioned with the particles.

## **Chapter 8**

### **General Discussion.**

---

The original aims of this thesis were to further understand the effect of silica on the osteoblast *in vitro*. Two distinct approaches were employed to investigate the role of silica in bone biology. Firstly, the interaction of soluble silicates with osteoblasts by supplementation of the growth medium was used to determine beneficial or adverse effects of the treatments over a range of concentrations (Chapters 3 and 4). Secondly, the interaction of osteoblasts with silica surfaces *in vitro* was examined using silica gels (Chapter 5), silicon surfaces (Chapter 6) and a bioabsorbable polymer impregnated with silica particles (Chapter 7).

The emphasis at the beginning of the work was to examine an osteoblast cell culture system (Chapter 2). The HOB cell culture system had previously been used to investigate novel polymeric biomaterials for controlled drug delivery (Di Silvio, 1995). The cells were shown to produce markers of the osteoblast phenotype such as ALP, collagen-1, osteocalcin and cAMP production in response to parathyroid hormone. Few mineralisation studies had been performed. These suggested that the cells isolated were capable of producing a mineralised ECM without the addition of mineral supplements such as DEX and BGP whose function remains unclear (Di Silvio, 1995). In this work several established methods were used to determine the presence of mineral, including ultrastructural and elemental techniques such as TEM, anhydrous TEM and SEM with EDX microanalysis, and histochemical methods such as alizarin red S, von kossa, tetracycline and calcein staining (see figures 2.7-2.10). Mineral was not seen at any stage. The reasons for the inability of unsupplemented cells to produce large amounts of mineral are unclear but the same is true for many other culture systems (Gehron Robey, 1995, Marks and Hermey, 1996).

Cultures were supplemented with dexamethasone (DEX) and sodium  $\beta$ -glycerophosphate (BGP) to investigate the capability of the cells to produce mineral. These revealed the presence of mineral using several techniques (TEM, calcein and Alizarin red S staining, Figures 2.11-2.14) and the mineral produced was associated with collagen-1 as shown by TEM. Although the inclusion of these supplements is essential for bone marrow derived osteoblast cultures (Ohgushi *et al.*, 1996) and is routine in the culture of calvaria-derived osteoblast cultures (Bellows *et al.*, 1987), the exact nature of their function remains unclear. It is generally accepted that DEX is

required for the expression of the osteoblast phenotype in bone marrow cultures (Ohgushi *et al.*, 1996) and that BGP increases the available phosphate in the system (Gronowicz and Raisz, 1996). Recently concern has been expressed regarding the use of mineral supplements in bone cultures suggesting that the levels used may lead to dystrophic (non-biological mineral that is not associated with collagen-1 or any biological process) mineralisation (Boyan, 2000). The use of such supplements may obscure the true nature of the interaction of osteoblasts with materials and for this reason DEX and BGP were not used in the experiments evaluating the osteoblast response to biomaterial surfaces. The early onset of nodule formation in osteoblasts cultured on silica gel surfaces occurred without the addition of DEX and BGP to the growth medium and this may be a more reliable indicator of a favourable osteoblast response than the visualisation of mineral for this culture system. The osteogenic potential of the HOB culture system warrants further study, however there is some evidence to suggest that mineralisation could be induced in this osteoblast model. Faint staining was seen in alizarin red S labelled 35 day cultures (Figure 2.10) and the results presented in Chapter 5 suggest that mineralisation of osteoblast cultures occurred on the silica gel (Figures 5.10 and 5.11). An investigation into the cellular responses to a range of calcium phosphate ceramics, using the same cell culture system, revealed deposits of apatite-like crystals in osteoblast cultures by TEM (Scotchford *et al.*, in preparation).

The use of immunofluorescence techniques demonstrated the osteoblast phenotype by the ability of the cells to produce ALP, OP, ON and collagen-1 (Figures 2.4-2.6). TEM and confocal studies showed that while collagen-1 was noted after day 5 in culture this was never in abundant amounts. It is possible that the lack of mineral produced by HOBs was in part due to the fact that an adequate extracellular matrix was not laid down to support the nucleation of apatite. This is a potential area for further study and the formation of collagen-1 could be stimulated using growth factors such as IGF-1 (Chevalley *et al.*, 1998). Another cell system was used in this work, the craniofacial osteoblast (CFC). These cells are isolated from a different anatomical site and the age of the donors is lower than HOBs (McDougall, in preparation). These cells produce abundant collagen 1 but produces less ALP than HOBs (McDougall, in preparation). It is unclear whether the differences between HOBs and CFCs are due to the donor age and site but irrespective of this there is potential to use both systems together to give additional information about the osteoblast response to systems under investigation.

Ultrastructural investigations demonstrated the presence of junctions between the cells (Figure 2.8a) and these were likely to be gap junctions, as these are the usual means of intercellular communication in bone (Donahue, 2000). Confirmation of this could be obtained by immunolocalisation with connexin 43. Cell death was noted in the centre of the nodules in long-term cultures. (Figure 2.9a, d) This may have been due to necrosis related to the difficulty in diffusion of nutrients due to the large size of the structures or apoptosis which has been reported as the fate of the 80% of osteoblasts that do not become osteocytes (Boyce, 1996).

The effect of silicate supplementation of HOB growth medium was investigated in Chapter 3. Sodium silicate was used and this was the same compound as that used by Carlisle in the series of experiments leading to the establishment of silicon as an essential trace element (Carlisle, 1986). Parameters such as ALP production, nodule formation and mineralisation were investigated. While a reduction in ALP activity with a concomitant increase in the number of nodules formed was seen in some experiments supplemented with 1-50ppm silicate, a clear, reproducible effect of silica on the osteoblast or the mineralisation process was not demonstrated. Quantitative analysis of collagen-1 formation was not undertaken in this work due to financial and practical considerations, but it is clear from the work undertaken, as well as the reported inclusion of silica in collagen as a structural component (Carlisle, 1986), that analysis of this important protein may yield information on the role of silica in the osteoblast mineralisation process in the future. For example, use of CFCs instead of HOBs, with their abundant formation of collagen may have revealed an association of silica supplementation and increased collagen formation.

The biologically active range of silica was within the range of concentrations used in this work and any beneficial effects are likely to be seen in the range 1-50ppm. Increased rates of nodule formation, with decreased ALP activity and increased mineral staining was noted in some of the long term studies using low levels of silicate supplementation in Chapter 3 (Figures 3.6-3.9). The amount of silicic acid released from the silica gels used in Chapter 5 was in the lower end of the range seen to have an effect on the osteoblast (Figure 5.9). The apparent effects of concentrations as low as 1ppm silica are supported by the fact that the amount of silica measured in the

circulating body fluids has been measured as 1-5ppm (Dobbie and Smith, 1982a). Although not conclusive, the findings in this work suggest that concentrations as low as 1-5ppm affect the osteoblast *in vitro* and highlights the need for further research in this area. It is likely that the techniques used in this work were not sensitive enough to detect potential subtle effects of low levels of silica. The results presented here show that silica is unlikely to be an essential supplement for osteoblast mineralisation *in vitro* and that the beneficial effects seen may be specific to certain differentiation states or the expression of specific proteins or growth factors, making the role of silica difficult to isolate. The interaction of molecules with the cell membrane and proteins has been investigated extensively using fluorescence techniques (Cladera *et al.*, 2000) and the application of these to the problem as well as the use of genetic techniques such as gene arrays (Xynos *et al.*, 2001) may give important information concerning the precise interaction of silica with osteoblasts *in vitro*. These techniques may reveal a requirement of silica for mineralisation in bone.

Recent work has shown increased proliferation of osteoblasts, as shown by an increase in the number of cells in stages S and G2/M phases of the cell cycle, on bioactive glass surfaces (Xynos *et al.*, 2000; Hench *et al.*, 2000). Their findings also show that osteoblasts *in vitro* exhibit lower AP levels and increased nodule formation when cultured on Bioglass 45S5 for 12 days and that this is linked to an increase in osteocalcin production (Hench, 2001; Hench *et al.*, 2001; Xynos *et al.*, 2000; Hench *et al.*, 2000). Osteocalcin production was not measured in the current studies. The results presented in chapter 3 show that silica, in isolation, can affect nodule formation and AP activity in a similar manner to that of bioglass suggesting that the silica component of these glasses may be responsible for the enhanced cell response reported.

Additionally, the same group have used genetic array studies and shown that cell cycle related genes and transcription factors are up-regulated when osteoblasts are cultured in the presence of dissolution products of bioglass (Xynos *et al.*, 2001). Cell cycle studies were not carried out in this thesis but future studies should attempt to isolate the role of silica alone on osteoblast proliferation, differentiation and mineralisation.

Keeting *et al.* (1992) showed that increased proliferation seen in HOBs cultured in the presence of Zeolite A (a compound containing silica and alumina) could mainly be

accounted for by the silicic acid content of the material. This demonstrates that silicic acid has the potential to affect osteoblast cell behaviour. The results presented in chapter 3 showed that silicic acid affected osteoblast performance during long term administration in terms of AP activity, nodule formation and mineralisation. The proliferative response seen by Keeting et al (1992) was dependent on cell number, indicating that an autocrine mechanism may be involved in the interaction between ZA and bone cells. Furthermore, ZA appeared to increase the secretion of TGF- $\beta$  at a post transcriptional level. In light of these findings it is perhaps surprising that there is scant reference in the literature since to the role of silica containing compounds in stimulating osteoblasts. The present work was carried using the same cell concentration throughout and no attempt was made to examine the molecular interaction of silica with osteoblasts at the but these finding show that the potential interactions of silica-containing compounds with osteoblasts may be quite specific at a molecular level. Further research examining the potentially complex role of silica, in isolation, on cell signalling at the molecular and genetic levels in bone cells is warranted.

Supplementation of cultures with more than 300ppm silicate caused cell death within 48 hr (Figure 3.5). There was a marked decrease in cell activity between 24 and 48 hr for cultures supplemented with 150ppm silicate (Figure 3.5). These levels of silica are unlikely to be found in the body under normal circumstances, but could conceivably leach from implanted biomaterials, or arise locally from drug treatments. The local levels of silicic acid surrounding silica-containing implants *in vivo* has not been measured but would be important in ensuring that material toxicity did not override beneficial effects of low levels of silicic acid release.

The cell death seen in cultures supplemented with more than 300ppm silicate was further investigated in Chapter 4. The process by which cell death occurred was identified as apoptosis (Figures 4.2-4.4). Apoptosis was demonstrable in cultures after 3hr and appeared to result form the failure of cells to spread normally in culture (Figure 4.1). Nuclear profiles of cells appeared similar at 90 min but cell morphology as shown by phase contrast microscopy was different. Typical actin cytoskeleton and focal adhesion contact formation was absent. It is interesting to note that cell attachment and

spreading was indistinguishable in cultures supplemented with up to 250ppm silicate (Figures 3.2 and 3.3).

Cell death occurred whether the cells were allowed to attach and become established in culture or seeded directly into the silicate supplemented medium (Figures 4.5 and 4.6). The phenomenon was not restricted to bone cells but was seen in fibroblasts and macrophages (Figures 4.11 and 4.12). The HOBs recovered from the toxic insult if the medium was replaced with complete medium within a few hours (Figures 4.9 and 4.10). It is not clear what caused the cell death. Silica particles are known to cause membrane rupture and cell death in macrophages (Allison *et al.*, 1977, Dobbie, 1982), but membranes were shown to remain intact in these studies (Figure 4.8). Oligomers form at neutral pH in silicate solutions above 100ppm (Birchall, 1995) and it is more likely that these may contribute to the toxic effect by interaction with serum proteins. The results of the protein adsorption assay in Chapter 3 showed that the trend for adsorption of BSA increased with increasing silica concentration although the data were not statistically significant (Figure 3.1). It is known that osteoblasts do not attach in the usual way to surfaces coated with albumin (Curtis and Forrester, 1984). The fact that the induction of the apoptotic pathway appeared to be initiated by the failure of cells to attach and spread in a normal fashion lends weight to the hypothesis that silica interacts with proteins. Silica particles bind to serum proteins (Barrett *et al.*, 1999) and proteins have been investigated as a potential control molecules in biosilification (Perry and Keeling-Tucker, 2000). The adsorption of proteins to silica surfaces has been demonstrated and these retain their function so there is potential to affect osteoblast function (Lobel and Hench, 1996).

The finding that silicate causes osteoblast apoptosis is a new one and has implications in the field of biomaterials as the amount of silica required to induce apoptosis was small and therefore theoretically possible to leach from an implant although these figures have not been studied. Osteoblast apoptosis, especially in relation to biomaterials is the subject of much current research (Massari *et al.*, 2000, Liu *et al.*, 1999, Stea *et al.*, 2000b, Pioletti *et al.*, 1999) and the work presented in Chapter 4 represents a reliable means of inducing rapid apoptosis in large numbers of osteoblast cells.

Recent findings (Hench, 2000; Hench *et al.*, 2001; Xynos *et al.* 2000; Hench *et al.*, 2000), demonstrate that bioglass surfaces can exert control over the osteoblast cell cycle and apoptosis. The results presented in chapter 4 demonstrate that silica alone can cause apoptosis in osteoblasts and show that the silica component of bioactive materials may directly affect cell behavior. Further work is necessary to elucidate the full extent of the involvement of silica, in isolation, in bone cell turnover, interactions and metabolism.

A model silica gel surface was prepared as outlined in Chapter 5 and the osteoblast response to it was evaluated. The gel served as a model surface to reflect the osteoblast/biomaterial surface *in vivo*. The biomaterials aspect of the work was split into two distinct categories, (a) surface bioactivity and silicic acid release *in vitro* and (b) cell response. In this way, the formation of a CaPi layer, sustained silicic acid release and a favourable osteoblast response could be correlated. The silica gel maintained a sustained release of silicic acid into SBF for 11 days (Figure 5.3) and formed a CaPi layer in SBF (Figure 5.2). The osteoblast response was enhanced reproducibly on the silica surface in comparison to controls in terms of onset of nodule formation ((Figure 5.4). In addition, the release of silicic acid was absent when osteoblasts were grown on the surface (Figure 5.9). Although not conclusive evidence, this gives rise to the possibility that small quantities of silicic acid may be utilised by osteoblasts to enhance the mineralisation process. Further circumstantial evidence in this work further supports this hypothesis such as the finding that nodule formation was increased in some cultures supplemented with 1 and 5ppm silicate (see section 3.3.3) and that increased mineral staining was seen in cultures supplemented with 1-50ppm silicate (Figure 3.8). The nature of the silica gel coated disc surface allowed use of both upright and inverted surfaces to hypothesise that both the nature of the surface and the release of silicic acid contributed to the bioactivity and the subsequent cell response.

The results presented in chapter 5 lend weight to the role of the silica component of materials in the bioactive phenomenon of class A bioactive materials. Recent work suggests that both bioactive material surfaces and ionic dissolution products of materials containing silica select for more mature osteoblasts, demonstrated by cell shape, enhanced nodule formation, increased decreased AP and increased osteocalcin (Xynos *et al.*, 2001; Xynos *et al.*, 2000; Hench *et al.*, 2000).. The results of the silica gel studies presented in chapter 5 show that a surface composed of silica alone can mimic the

results found with bioglass surfaces in terms of cell shape and enhanced nodule formation. This supports the theory that the silica component of bioactive materials can directly affect osteoblast behaviour.

The response of human osteoblasts to different silicon surfaces was compared in Chapter 6. This work gave the first indication of the bioactivity of bulk silicon in the semiconductor form as a result of the removal of the surface oxide layer. This has far reaching consequences in the design of implanted biosensors, etc. Both silicic acid release and the ability to form a CaPi layer were central to the concept of bioactivity in terms of enhanced cell response and also were related to each other. Surfaces that did not release silicic acid did not form a CaPi layer and *vice versa* (Figures 6.3-6.5). This was also observed in the silica gel studies from Chapter 5 (Figure 5.2), and in the polymer studies reported in Chapter 7 (Figure 7.3). The interesting finding here came with the use of patterned surfaces. The cells clearly expressed a preference for the bioactive surface over the non-bioactive surface and this effect was long lasting. This was surprising as on their own neither surface appeared better than the other in terms of osteoblast growth. Patterned surfaces have proved useful in determining cellular preferences to specific surface chemistries (Scotchford *et al.*, 1998) and cellular responses to topography (Meyle *et al.*, 1991, 1995). Patterned surfaces have not previously been used to evaluate the cellular responses to bioactive surfaces.

The findings presented in this thesis have implications for the *in vitro* screening of new biomaterials. In some cases cell proliferation and viability assays (such as alamar blue, MTT and DNA content assays) are used, along with other cell tests, to screen a range of surfaces for biocompatibility (Green *et al.*, 2000, Rizzi *et al.*, 2001). While these assays were used to good effect in this thesis to indicate cytotoxicity in Chapter 3 (Figure 3.5), they did not predict the bone enhancing effects of the silica gel used in Chapter 5 (Figure 5.8) and would probably have shown similar results with the Si and ESi surfaces used in Chapter 6. This suggests that they are useful to screen a broad range of materials for cytotoxic effects but may not easily facilitate differentiation between good surfaces. The use of patterned surfaces in this work allowed the cellular preferences for bioactive surfaces to be visualised (Figures 6.12-6.18). Cell spreading is also used as a marker of the potential of a material to do well in the body. This is not supported by the work presented here. While the bioactive surfaces used in this thesis showed good cell

attachment and spreading they were not as advanced as thermanox at 90 min and were indistinguishable at 24 hrs (Figure 6.6). This criterion alone would not have singled out the better surfaces. The analysis of cellular responses to biomaterials poses practical problems if the surface used is autofluorescent or opaque. The use of confocal microscopy techniques and fluorescent staining of mineral using calcein proved beneficial in measuring the osteoblast response (Figures 2.12, 2.13 and 3.9). Calcein also provides semi-quantitative data allowing the relative amounts of mineral formed on different surfaces to be evaluated simultaneously (Hale *et al.*, 2000).

As soon as a material is placed in solution solutes are adsorbed onto the surface in an ordered way and these in turn will effect the subsequent adsorption of molecules. When a cell comes into contact with a surface the sequence of events (eg conformation of cell binding proteins) will determine the success of an implant. Cell recruitment, attachment, proliferation and differentiation are all affected by the nature of the surface (Boyan *et al.*, 1995). Surface characteristics such as topography, physical characteristics, surface roughness, surface chemistry, energy and crystallinity have all been shown to have an effect on the cellular response to materials. The manipulation of these properties of a material to promote new tissue growth is known as tissue engineering. Biomaterials design to date has mainly been based on trial and error (Lobel *et al.*, 2000). Tissue engineering however, introduces an element of rational design in the biomaterials field. Current work using molecular biological and genetic approaches aimed specifically at assessing the bone response to materials will encourage the design of materials which effectively manipulate the cellular behaviour to promote a desirable response.

Encouraging results were obtained in terms of *in vitro* bioactivity and cell responses using the silica gel in Chapter 5 and the bioactive potential and biocompatibility of silicon wafers was observed in Chapter 6. The next logical step was to investigate the potential of silica to improve the biocompatibility of existing biomaterials which would benefit from improved bone bonding properties. The incorporation of silica into a PCL polymer was investigated in Chapter 7. Silica powders were prepared from TEOS and TCS and these were incorporated into a PCL matrix. Preliminary cell compatibility results indicate that the surface supported cell growth and no adverse effects on bone cells were noted (Figures 7.5-7.7). Investigations into the bioactive properties of the composite showed that a CaPi layer was formed on the surface in SBF and that this

occurred on silica particles and adjacent areas of PCL (Figure 7.4). The deposition of a HCA layer on a non-bioactive surface was also observed in Chapter 6 (Figure 6.11). These findings clearly demonstrate that the preparation of biomaterials composed of bioactive and non-bioactive components lead to bioactivity and may lead to enhanced bone bonding *in vivo* and this warrants further investigation. The use of PCL in this work was primarily based on practical considerations but there is no reason why other substances, with suitable properties for biomaterial applications, such as bone cement or HA, could not benefit from this treatment. Recent studies suggest that the incorporation of silica into other materials to enhance performance is an area of active interest (Arcos *et al.*, 2001, Tancred *et al.*, 2001, Tsuru *et al.*, 1998, Yang *et al.*, 1997, Kobayashi *et al.*, 1997). This also opens up exciting possibilities for improved bone bonding biomaterials with superior mechanical and handling properties.

In summary, the work presented here has further explored the use of *in vitro* models of osteoblast mineralisation to evaluate the role of silica in the mineralisation process and in cytotoxicity. Sodium silicate has been found to be a reliable indicator of osteoblast apoptosis by an as yet unidentified mechanism. The demonstration of the bioactivity of etched silicon wafers leads to their potential use in silicon based biomaterials and biosensors. The incorporation of silica into materials, which have otherwise desirable properties, to enhance bone bonding was shown to be successful in preliminary studies. This work also furthers the tissue engineering goal to manipulate the osteoblast response to biomaterials by means of patterning and also by the incorporation of silica into biomaterials.

---

**REFERENCES.**

- Abe Y, Aida Y, Abe T, Hirofuji T, Anan H, Maeda K. (2000) Development of mineralised nodules in fetal rat mandibular osteogenic precursor cells: requirement for dexamethasone but not for  $\beta$ -glycerophosphate. *Calcified Tissue International* **66** 66-69.
- Alberts B, Bray D, Lewis J, Raff M, Roberts K and Watson JD. (1989). In: *Molecular biology of the cell*. Garland Publishing, New York,
- Allison AC (1977) Mechanism of macrophage damage in relation to pathogenesis of some lung diseases. In *Respiratory defense mechanisms*. Brain JD et al Eds, Basel.
- Anderson HC (1980): Calcification processes. *Pathology annual*; **15** 45-75.
- Andersson OH. (1993) Toxicity of silica-containing calcium phosphate glasses. *Biomaterials* **14** 317
- Andersson OH and Karlsson KH, (1992). Silica gel thickness and calcium phosphate formation at the surface of bioactive glass. Ducheyne, K., van Blitterswijk Eds. Reed healthcare Communications, 79-84.
- Anselme K, Noel B, Flautre B, Blary MC, Delecourt C, Descamps M, Hardouin P. (1999) Association of porous hydroxyapatite and bone marrow cells for bone regeneration. *Bone* **25** S51-S54.
- Arcos D, Ragel CV, Vallet-Regi M. (2001) Bioactivity in glass/PMMA composites used as drug delivery system. *Biomaterials* **22** 701-708.
- Aubin JE, Liu F.(1996) The osteoblast lineage. In: *Principles of bone biology*. Bilezikian JP, Raisz LG, Rodan GA Eds. Academic Press, San Diego.
- Bagchi N (1992): What makes silica toxic? *British Journal of Industrial Medicine*; **49** 163-166.
- Barrett EG, Johnston C, Oberdorster G, Finklestein JN. (1999) Silica binds serum proteins resulting in a shift of the dose response for silica induced chemokine

- expression in an alveolar type II cell line. *Toxicology and Applied Pharmacology*. **161** 111-122.
- Bayliss SC, Heald R, Fletcher ID, Buckberry LD. (1999) The culture of mammalian cells on nanostructured silicon. *Advanced Materials* **11** 318-321.
- Bellia JP, Birchall JD and Roberts NB (1994): Beer: a dietary source of silicon. *Lancet*; **343** 235.
- Bellows CG, Heersche JNM, Aubin JE. (1990) Determination of the capacity for proliferation and differentiation of osteoprogenitor cells in the presence and absence of dexamethasone. *Developmental Biology* **140** 132-138.
- Bellows CG, Aubin JE, Heersche JNM (1987) Physiological concentrations of glucocorticoid stimulate formation of bone nodules from isolated calvaria cells *in vitro*. *Endocrinology* **121** 1985-1992.
- Bernard GW (1969): The ultrastructural interface of bone crystals and organic matrix in woven and lamellar endochondral bone. *Journal of dental research*; **48** 781-788.
- Billah. A. M. E.-M. (1996). Markers of bone turnover in health and disease. PhD Thesis, University of Nottingham.
- Birchall JD. (1995) The essentiality of silicon in Biology. *Chemistry Society Reviews* 351-357.
- Bodine PVN, Komm BS. (1999) Evidence that conditionally immortalised human osteoblasts express an osteocalcin receptor. *Bone* **25** 535-543.
- Bolton WK, Suratt PM and Sturgill BC (1981): Rapidly progressive silicon nephropathy. *American Journal of Medicine*; **71** 823-828.
- Borm PJA, Driscoll K. (1996) Particles, Inflammation and respiratory tract carcinogenesis. *Toxicology Letters* **88** 109-113.
- Bosetti M, Verne E, Ferraris M, Ravaglioli A, Cannas M. (2001) *In vitro* characterisation of zirconia coated by bioactive glass. *Biomaterials* **22** 987-994.

- 
- Boskey AL (1981): Current concepts of the physiology and biochemistry of calcification. *Clinical Orthopaedics and Related Research*; **157** 225-257.
- Boskey AL, (1994). Bone and cartilage mineralisation. In: *Bone Formation and Repair*. Brighton, Freidlander and Lane Eds. 23-38.
- Bowditch AP, Waters K, Gale H, Rice P, Scott EAM, Canham LT, Reeves CL, Loni I, Cox TI. (1999) *In vivo* assessment of tissue compatibility and calcification of bulk and porous silicon. *Materials Research Society Symposium Proceedings* **536** 149-154
- Boyan BD. (2000) The importance of mineral in bone and mineral research. *Bone* **27** 341-342.
- Boyan BD, Hummert TW, Keiswetter K, Schraub D, Dean DD. (1995) Effect of titanium surface characteristics on chondrocytes and osteoblasts *in vitro*. *Cells and Materials* **5** 323-335.
- Boyce BF. (1996) Role of apoptosis in local regulation. In: *Principles of bone biology*. Bilezikian JP, Raisz LG, Rodan GA Eds. Academic Press, San Diego.
- Boyde A. (1980). Electron microscopy of the mineralising front. In: *The Third International Workshop on Bone Histomorphometry* Parfitt and Jee Eds. Societe de Nouvelle Publications Medicales et Dentaires, Sun Valley,
- Boyde A, Machonnie E, Muller-Mai C and Gross U (1990): SEM study of surface alterations of bioactive glasses and glass ceramics in a bony implantation bed. *Clinical Materials*; **5** 73-88
- Burrell R, Anderson M. (1973) The induction of fibrogenesis by silica treated alveolar macrophages. *Environmental Research* **6** 389-394.
- Butler WT, Ridall AL, McKee MD. (1996) Osteopontin. In: *Principles of bone biology*. Bilezikian JP, Raisz LG, Rodan GA Eds. Academic Press, San Diego.
- Brighton CT and Hunt RM (1976): Histochemical localisation of calcium in growth plate mitochondria and matrix vesicles. *Federation Proceedings*; **35** 143-147.

- Canalis E, Hott M, Deloffre P, Tsouderos Y, Marie PJ. (1996) The divalent strontium salt S12911 enhances bone cell replication and bone formation *in vitro*. *Bone* **18** 517-523.
- Canham LT. (1995) Bioactive silicon structure fabrication through nano-etching techniques. *Advanced Materials* **7** 1033-1037.
- Canham LT, Reeves CL, Loni A, Houlton MR, Newey JP, Simons AJ, Cox T. (1997a) Calcium phosphate nucleation on porous silicon: factors influencing kinetics in acellular simulated body fluids. *Thin Solid Films* **297** 304-307.
- Canham LT, Reeves CL. (1996) Apatite nucleation on low porosity silicon in acellular simulated body fluids. *Materials Research Society Symposium Proceedings* **414** 189-194.
- Canham LT, Reeves CL, Wallis DJ, Newey JP, Houlton MR Sapsford GJ, Godfrey RE, Loni I, Simons AJ, Cox TI, Ward MCL. (1997b) Silicon as an active biomaterial. *Materials Research Society Symposium Proceedings* **452** 579-589.
- Canham LT, Reeves CL, Newey JP, Houlton MR, Cox TI, Buriak JM, Stewart MP. (1999) Derivatised mesoporous silicon with dramatically improved stability in simulated human blood plasma. *Advanced Materials* **11** 1505-1507.
- Carlisle EM (1969): Silicon localisation and calcification in developing bone. *Federation Proceedings*; **28** 374.
- Carlisle EM (1970a): A relationship between silicon and calcium in bone formation. *Federation Proceedings*; **29** 565.
- Carlisle EM (1970b): Silicon: A possible factor in bone calcification. *Science*; **167** 179-180.
- Carlisle EM (1972): Silicon: An essential element for the chick. *Science*; **178** 619-620.
- Carlisle EM (1974): Silicon as an essential element. *Federation Proceedings*; **33** 1758-1766.
- Carlisle EM (1975): Silicon in the osteoblast. *Federation Proceedings*; **34** 927.

---

Carlisle EM (1976a): Bone cell silicon stores and interrelationships with other elements. *Federation Proceedings*; **35** 256.

Carlisle EM (1976b): *In vivo* requirement for silicon in articular cartilage and connective tissue formation in the chick. *Journal of Nutrition*; **106** 478-484.

Carlisle EM (1979): A silicon-molybdenum interrelationship *in vivo*. *Federation Proceedings*; **38** 553.

Carlisle EM (1980a): Biochemical and morphological changes associated with long bone abnormalities in silicon deficiency. *Journal of Nutrition*; **110** (5): 1046-1056.

Carlisle EM (1980b): A silicon requirement for normal skull formation. *Journal of Nutrition*; **10** 352-359.

Carlisle EM (1982): The nutritional essentiality of silicon. *Nutrition Reviews*; **40** (7): 193-198.

Carlisle EM (1986): Silicon as an essential trace element in animal nutrition. *Ciba Foundation Symposium*; **121** 123-139.

Carlisle EM and Alpenfels WF (1978): A requirement for silicon for bone growth in culture. *Federation Proceedings*; **37** 787.

Carlisle EM and Alpenfels WF (1980): A silicon requirement for normal growth of cartilage in culture. *Federation Proceedings*; **39** 787.

Carlisle EM and Alpenfels WF (1984): The role of silicon in proline synthesis. *Federation Proceedings*; **43** 680.

Carlisle EM and Alpenfels WF (1986): A silicon requirement for normal growth of cartilage in culture. *Federation Proceedings*; **39** 787.

Carlisle EM, Berger JW and Alpenfels WF (1981): A silicon requirement for prolyl hydroxylase activity. *Federation Proceedings*; **40** 866.

- Carlisle EM and Garvey DL (1982): The effect of silicon on the formation of extracellular matrix components by chondrocytes in culture. *Federation Proceedings*; **41** 461.
- Carlisle EM and Suchil C (1983): Silicon and ascorbate interaction in cartilage formation in culture. *Federation Proceedings*; **42** 398.
- Catelas I, Petit A, Zukor DJ, Marchand R, Yahia L, Huk OL. (1999) Induction of macrophage apoptosis by ceramic and polyethylene particles *in vitro*. *Biomaterials* **20** 625-630.
- Cheroudi B, Ratkay J, Brunette DM. (1992) The role of implant surface geometry on mineralisation *in vivo* and *in vitro*; A transmission and scanning electron microscopic study. *Cells and Materials* **2** 89-104.
- Chevalley TH, Rizzoli R, Manen D, Caverzasio J, Bonjour J-P. (1998) Arginine increases insulin-like growth factor-1 production and collagen 1 synthesis in osteoblast-like cells. *Bone* **23** 103-109.
- Cho S, Miyaji F, Kokubo T, Nakanishi K, Soga N and Nakamura T (1996a): Apatite-forming ability of silicate ion dissolved from silica gels,. *Journal of Biomedical Materials Research*; **32** 375-381.
- Cho S, Nakanishi K, Kokubo T, Soga N, Ohtsuki C and Nakamura T (1996b): Apatite formation on silica gel in simulated body fluid: Its dependence on structures of silica gels prepared in different media. *Journal of Biomedical Materials Research*; **33** 145-151.
- Cho S, Miyaji F, Kokubo T, Nakanishi K, Soga N and Nakamura T. (1996c) Apatite formation on various silica gels in a simulated body fluid containing excessive calcium ion. *Journal of the Ceramic Society of Japan* **104** 399-404.
- Cladera J, Martin I, O Shea P. (2000) The fusion domain of HIV gp41 interacts specifically with heparan sulphate on the T-lymphocyte cell surface. *EMBO* **20** 1-8.
- Cohen SM, Cano M, Earl RA, Carson SD, Garland EM. (1991) A proposed role for silicates and protein in the proliferative effects of saccharin on the male rat urothelium. *Carcinogenesis* **12** 1551-1555.

- Corden TJ, Jones IA, Rudd CD, Christian P, Downes S. (1998) Initial development into a novel technique for manufacturing a long fibre thermoplastic bioabsorbable composite: in-situ polymerisation of poly-ε-caprolactone. *Composites: Part A: applied science and manufacturing* **30** 737-746.
- Cormack DH. (1984). In:*Introduction to histology* . JB Lippencott Company, Philadelphia,
- Cross PC and Mercer KL. (1993). In:*Cell and tissue ultrastructure* . WH Freeman and Company, New York,
- Curtis ASG, Forrester JV. (1984) The competitive effects of serum proteins on cell adhesion. *Journal of Cell Science* **71** 17-35.
- Da Silva JJR and Williams RJP. (1991). In:*The biological chemistry of the elements* . Clarendon Press, Oxford,
- Damen JJM and Cate JMT (1989): The effect of silicic acid on calcium phosphate precipitation. *Journal of Dental Research*; **68** (9): 1355-1359.
- Damen JJM and Cate JMT (1992): Silica-induced precipitation of calcium phosphate in the presence of inhibitors of hydroxyapatite formation. *Journal of Dental Research*; **71** (3): 453-457.
- De Bruijn JD (1993) Calcium Phosphate Biomaterials: Bone bonding and biodegradation properties. Leiden University.
- De Giglio E, Motta A, Quagliarella L, Sabbatini L, Solarino G, Zambonin PG. (2001) A combined XPS-SEM/EDX investigation on explanted UHMW polyethylene acetabular cups: Possible role of silicon traces in the wear debris. *Journal of Materials Science: Materials in Medicine* **12** 23-28.
- Di Silvio L. (1995). A novel application of two biomaterials for the delivery of growth hormone and its effect on osteoblasts. PhD Thesis, UCL Medical School.
- Dickson GR. (1984). In:*Methods of calcified tissue preparation* . Elsevier, Amsterdam,

- Dobbie JW (1982): Silicon: its role in medicine and biology. *Scottish Medical Journal*; **27** 1-2.
- Dobbie JW and Smith MJB (1982a): Silicate nephrotoxicity in the experimental animal: the missing factor in analgesic nephropathy. *Scottish Medical Journal*; **27** (1): 10-16.
- Dobbie JW and Smith MJB (1982b): The silicon content of body fluids. *Scottish Medical Journal*; **27** 17-19.
- Dobbie JW (1986): Urinary and serum silicon in normal and uraemic individuals. *Ciba Foundation Symposium*; **121** 194-213.
- Donahue HJ. (2000) Gap junctions and biophysical regulation of bone cell differentiation. *Bone* **26** 417-422.
- Donkerwolcke M, Burny F, Muster D. (1998) Tissues and bone adhesives-historical aspects. *Biomaterials* **19** 1461-1466.
- Driscoll KE, Lindenschmidt RC, Maurer JK, Perkins L, Perkins M, Higgins J. (1991) Pulmonary response to inhaled silica or titanium dioxide *Toxicology and Applied Pharmacology*. **111** 201-210.
- Driscoll KE, Maurer JK, Lindenschmidt RC, Romberger D, Rennard SI, Crosby L. (1990) Respiratory tract responses to dust: Relationships between dust burden, lung injury, alveolar macrophage fibronectin release and the development of pulmonary fibrosis. *Toxicology and Applied Pharmacology*. **106** 88-101.
- Ducy P, Karsenty G. (1996) Skeletal Gla proteins: gene structure, regulation of expression and function. In: *Principles of bone biology*. Bilezikian JP, Raisz LG, Rodan GA Eds. Academic Press, San Diego.
- Ecarot-Charier B, Glorieux FH, van der Rest M, Pereira G. (1983) Osteoblasts isolated from mouse calvaria initiate matrix mineralisation in culture. *Journal of Cell Biology* **96** 693-643.
- Edwardson JA, Moore PB, Lilley JS, Newton GWA, Barker J, Templar J and Day JP (1993): Effect of silicon on gastrointestinal absorption of aluminium. *Lancet*; **342** 211-212.

- El Ghannam A, Ducheyne P and Shapiro, IM (1997): Formation of surface reaction products on bioactive glass and their effects on the expression of the osteoblastic phenotype and the deposition of extracellular matrix. *Biomaterials*; **18** 295-303.
- Elliot MA and Edwards HM (1991): Effect of dietary silicon on growth and skeletal development in chickens. *Journal of Nutrition*; **121** (2): 201-207.
- Evans RA, Dunstan CR and Hills EE. (1980). Extent of resorbing surfaces based on histochemical identification of osteoclasts. In: *The Third International Workshop on Bone Histomorphometry*. Parfitt and Jee Eds. Societe Nouvelle de Publications Medicales et Dentaires, Sun Valley, 29-32.
- Fahal IH, Yaqoob M, Williams PS, Ahmad R, Roberts NB and Bell GM (1994): Does silicon protect against aluminium toxicity in dialysis patients? *Lancet*; **343** 122-123.
- Fernandes MH, Costa MA, Carvalho GS. (1997) Mineralisation in serially passaged human alveolar bone cells. *Journal of Materials Science: Materials in Medicine* **8** 61-65.
- Fratzl-Zelman N, Fratzl P, Horandner H, Grabner B, Varga F, Ellinger A, Klaushofer K. (1998) Matrix mineralisation in MC3T3-E1 cell cultures initiated by B-glycerophosphate pulse. *Bone* **23** 511-520.
- Fresa R, Constantini A, Buri A and Branda F (1996): Effect of the substitution of La<sub>2</sub>O<sub>3</sub> for CaO on the bioactivity of 2.5CaO.2SiO<sub>2</sub> glass. *Journal of Biomedical Materials Research*; **32** 187-192.
- Frondoza C, Gaies MG, Radfar A, Bendall SP, Jinnah RH and Hungerford DS (1996): Bioglass effect on osteoblasts, synoviocytes and macrophages. *Proceedings of the fifth world biomaterials congress*; 419.
- Fujita H, Ido K, Matsuda Y, Iida H, Oka M, Kitamura Y, Nakamura T. (2000) Evaluation of bioactive bone cement in canine total hip arthroplasty. *Journal of Biomedical Materials Research* **49** 273-288.
- Fujita H, Iida H, Kawanabe K, Okada Y, Oka M, Matsuda T, Kitamura Y, Nakamura T. (1999) Pressurization of bioactive bone cement *in vitro*. *Journal of Biomedical Materials Research* **48** 43-51.

---

Gatti AM, Valdre G, and Anderson OH (1994) Analysis of the *in vivo* reactions of a bioactive glass in soft and hard tissue. *Biomaterials* **15** (3) 208-212.

Gehroh-Robey P. (1995) Collagenase treated trabecular bone fragments: A reproducible source of cells in the osteoblast lineage. *Calcified Tissue International* **56** (supplement 1) S11-S12.

Gehron-Robey P. (1996) Bone Matrix proteoglycans and glycoproteins. In: *Principles of Bone Biology*. Bilezikian JP, Raisz LG, Rodan GA Eds. Academic Press, San Diego.

Gerstenfeld LC, Chipman SD, Kelly CM, Hodgens KJ, Lee DD, Landis WJ. (1988) Collagen expression, ultrastructural assembly and mineralisation in the cultures of chicken embryo osteoblasts. *Journal of Cell Biology* **106** 979-989.

Gilbert SF. (194). In: *Developmental biology* . Sinauer Associates, Massachusetts,

Glimcher MJ (1990): The possible role of collagen fibrils and collagen-phosphoprotein complexes in the calcification of bone *in vitro* and *in vivo*. *Biomaterials*; **11** 7-10.

Gottlieb RA. (2000) Programmed cell death. *Drug News and Perspectives* **13** 471-476.

Gough JE. (1999) Apoptosis of human osteoblasts cultured on polymeric biomaterials *in vitro* PhD Thesis, University of Nottingham.

Gough JE, Downes S. (In press) Osteoblast cell death on methacrylate polymers involves apoptosis *Journal of Biomedical Materials Research*.

Gray C, Boyde A, Jones SJ. (1996) Topographically induced bone formation *in vitro*: implications for bone implants and bone grafts. *Bone* **18** 115-123.

Green SM, Grant DM, Wood JV (2000) Cytocompatibility evaluation of surface modified Ni-Ti shape memory alloy using the MTT assay. *Biomedical Engineering Applications Basis Communications* **12** 55-59

Gronowicz G, Raisz JG. (1996) Bone Formation assays. In: *Principles of bone biology*. Bilezikian JP, Raisz LG, Rodan GA Eds. Academic Press, San Diego.

- 
- Gundle R, Beresford JN. (1995). The isolation and culture of cells from explants of human trabecular bone. *Calcified Tissue International* **56** (supplement 1) S8-S10.
- Hale LV, Ma YF, Santerre RF. (2000) Semi-quantitative fluorescence analysis of calcein binding as a measurement of *in vitro* mineralisation. *Calcified tissue international* **67** 80-84.
- Hamilton RF, De Villiers WJS, Holian A. (2000) Class a type II scavenger receptor mediates silica induced apoptosis in chinese hamster ovary cell line. *Toxicology and Applied Pharmacology* **162** 100-106.
- Healy KE, Thomas CH, Rezanian A, Kim JE, McKeown PJ, Lom B, Hockberger PE. (1996) Kinetics of bone cell organisation and mineralisation on materials with patterned surface chemistry. *Biomaterials* **17** 195-208.
- Hench LL. (2001) A genetic theory of bioactive materials. Proceedings of the 13<sup>th</sup> International Symposium on Ceramics in Medicine. *Key Engineering Materials* **192-195**, 575-580.
- Hench LL. (1998) Biomaterials: a forecast for the future. *Biomaterials* **19** 1419-1423.
- Hench LL. (1998) Bioactive materials: the potential for tissue regeneration. *Biomaterials* **19** 511-518.
- Hench LL (1991) Bioceramics: from concept to clinic *Journal of the American Ceramic Society*; **74** 1487.
- Hench LL. (1989) Bioceramics and the origin of life. *Journal of Biomedical Materials Research* **23** 685-703.
- Hench LL, Polak JM, Xynos LD, Buttery LDK. (2000) Bioactive materials to control cell cycle. *Materials Research Innovations*, **3**, 313-323.
- Hench LL, Splinter RJ, Allen WC, and Greenlee TK, (1971) Bonding mechanisms at the interface of ceramic prosthetic materials. *Journal of Biomedical Materials Research Symposium* **2** 117-141.

- Hench LL and Wilson J. (1986). Biocompatibility of silicates for medical use. In: *Silicon Biochemistry*. Wiley, New York,
- Hench LL, Xynos ID, Edgar AJ, Buttery LDK, Polak JM. (2001) Gene activating glasses. *Proceedings of the International Congress on Glass*. **1**, 226-233.
- Henry F, Bretaudeau L, Hequet A, Barbieux I, Lieubeau B, Meflah K. (1999) Role of antigen presenting cells in long term antitumour response based on tumour derived apoptotic body vaccination. *Pathobiology* **67** 306-310.
- Hessel PA, Gamble JF, Gee JBL, Gibbs G, Green FHY, Morgan WKC, Mossman BT. (2000) Silica, silicosis and lung cancer: A response to a recent working group report. *Journal of Occupational and Environmental Medicine*. **42** 704-720.
- Hotz P, Gonzalez-Lorenzo J, Siles E, Trujillano G. (1995) Subclinical signs of kidney dysfunction following short exposure to silica in the absence of silicosis. *Nephron* **70** 438-442.
- Hunter GK, Poitras MS, Underhill M, Grynblas MD, Goldberg HA. (2000) Induction of collagen mineralisation by a bone sialoprotein-decorin chimeric protein. *Journal of biomedical materials research* **55** 496-502.
- Hutmacher DW. (2000) Scaffolds in tissue engineering bone and cartilage. *Biomaterials* **21** 2529-2543.
- Ikeda T, Futaesaku Y, Tsuchida N. (1992) *In vitro* differentiation of the human osteosarcoma cell lines HOS and KHOS. *Virchows Archive B: Cell Pathology* **62** 199-206.
- Iler RK. (1955) In: *The colloid chemistry of silica and silicates*. Cornell University Press, Ithaca, New York.
- Iler RK. (1979) In: *The chemistry of silica*. John Wiley and Sons, New York.
- Irie H, Koyama H, Kubo H, Fukuda A, Aita K, Koike T, Yoshimura A, Yoshida T, Shiga J, Hill T. (1998) Herpes simplex virus hepatitis in macrophage-depleted mice. The role of massive apoptotic cell death in pathogenesis. *Journal of General Virology* **79** 1225-1231.

- Ito Y. (1999) Surface micropatterning to regulate cell functions. *Biomaterials* **20** 2333-2342.
- Iyer R, Hamilton RF, Li L, Holian A. (1996) silica-induced apoptosis mediated via scavenger receptor in human alveolar macrophages. *Toxicology and Applied Pharmacology* **14** 84-92.
- Jallot E, Benhayoune H, Killian L, Irigaray JL, Balossier G, Bonhomme P. (2000) *Journal of Physics: Part D, Applied Physics* **33** 2775-2780.
- Jilka RL, Weinstein RS, Bellido T, Roberson P, Parfitt AM, Manolagas SC. (1999) Increased bone formation by prevention of osteoblast apoptosis with parathyroid hormone. *Journal of Clinical Investigation* **104** 439-446.
- Johnson RN and Volcani BE (1978): The uptake of silicic acid by rat liver mitochondria. *Biochemical Journal*; **172** (3): 605-611.
- Kane AB, Petrovich DR, Stern RO, Farber JL. (1985) ATP depletion and loss of cell integrity in anoxic hepatocytes and silic-treated P388D1 macrophages. *American journal of Physiology-Cell Physiology* **18** C256-C266.
- Kane AB, Stanton RP, Raymond EG. (1980) Dissociation of intercellular lysosomal rupture from the cell death caused by silica. *Journal of Cell Biology* **87** 643-651.
- Karsenty G, Ducy P, Starbuck M, Priemel M, Shen J, Geoffroy V, Amling M. (1999) Cbfa-1 as a regulator of osteoblast differentiation and function. *Bone* **25** 107-108.
- Katzberg S, Lieberherr M, Ornoy A, Klein BY, Hendel D, Somjen D. (1999) Isolation and hormonal responsiveness of primary cultures of human bone-derived cells: Gender and age differences. *Bone* **25** 667-673.
- Keeting PE, Oursler MJ, Wiegand KE, Bonde SK, Spelsberg TC, Riggs BL. (1992) Zeolite A increases proliferation, differentiation and transforming growth factor beta production in normal adult human osteoblast like cells in vitro. *Journal of Bone and Mineral Research* **7**, 1281-1289.
- Kerr JB. (1999) In: *Atlas of functional histology*. Mosby International Publishers, London.

- 
- Kirk MD, Kahn AJ (1995) Extracellular matrix synthesised by clonal osteogenic cells is osteoinductive *in vivo* and *in vitro*: Role of transforming growth factor-beta! In osteoblast cell-matrix interaction. *Journal of Bone and Mineral Research* **10** 1203-1208.
- Kitsugi T, Yamamuro T, Nakamura T and Oka M (1995): Transmission electron microscopy observations at the interface of bone and four types of calcium phosphate ceramics with different calcium/phosphorus molar ratios. *Biomaterials*; **16** (14): 1101-1107.
- Klein CPAT, Li P, de Blicq-Hogervorst JMA and de Groot K (1995): Effect of sintering temperature on silica gels and their bone bonding ability. *Biomaterials*; **16** (9): 715-719.
- Kobayashi M, Nakamura T, Tamura J, Iida H, Fujita H, Kokubo T, Kikutani T. (1997) Mechanical and biological properties of bioactive bone cement containing silica glass powder. *Journal of Biomedical Materials Research* **37**, 68-80.
- Kokubo T (1991): Bioactive glass ceramics: properties and applications. *Biomaterials*; **12** 155-163.
- Kokubo T. (1992). Bioactivity of glasses and glass ceramics In: *Bone Bonding Biomaterials*. Reed healthcare Communications, the Netherlands,
- Laczka-Osyczka A, Turnya B, Dubin A and Laczka M (1997): Comparison of biocompatibility of gel-derived bioactive ceramics in macrophage culture conditions. *Biomaterials*; **18** 1243-1250.
- Landis WJ and Glimcher MJ (1978): Electron diffraction and electron probe microanalysis of the mineral phase of bone tissue prepared by anhydrous techniques. *Journal of Ultrastructure Research*; **63** 188-223.
- Landis WJ, Paine MC and Glimcher MJ (1977): Electron microscopic observation of bone tissue prepared anhydrously in organic solvents. *Journal of Ultrastructure Research*; **59** 1-30.

---

Lechner A, Schutz N, Siggelkow H, Seufert J, Jalob F. (2000) The immediate early gene product hCYR61 localises to the secretory pathway in human osteoblasts. *Bone* **27** 53-60.

Leibau F. (1985) In: Structural chemistry of silicates. Springer-Verlag, Berlin.

Li P, Kangasniemi I, de Groot K, Kokubo T and Yli-Urpo AU (1994a): Apatite crystallisation from metastable calcium phosphate solution on sol gel prepared silica. *Journal of Non Crystalline Solids*; **168** 281-286.

Li P, Ohtsuki C, Kokubo T, Nakanishi K, Soga N and de Groot K (1994b): The role of hydrated silica, titania and alumina in inducing apatite on implants. *Journal of Biomedical Materials Research*; **28** 7-15.

Li P, Ohtsuki C, Kokubo T, Nakanishi K, Soga N, Nakamura T and Yamamuro T (1992) Apatite formation induced by silica gel in simulated body fluid. *Journal of the American Ceramic Society*; **75** 2094.

Li P, Ye X, Kangasniemi I, de Blic-Hogervorst JMA, Klein CPAT and de Groot K (1995): *In vivo* calcium phosphate formation induced by sol-gel-prepared silica. *Journal of Biomedical Materials Research*; **29** 325-328.

Lim Y, Kim J-H, Kim K-A, Chang H-S, Park Y-M, Ahn B-Y, Phee Y-G. (1999) Silica-induced apoptosis *in vivo* and *in vitro*. *Toxicology Letters* **108** 335-339.

Liu GJ, Miyaji F, Kokubo T, Takadama H, Nakamura T, Murakami A. (1998) Apatite-organic polymer composites prepared by a biomimetic process: improvement in adhesion of the apatite layer to the substrate by ultraviolet irradiation. *Journal of Materials Science- Materials in Medicine* **9** 285-290.

Lobel KD, Hench LL, (1996) *In vitro* protein interactions with a bioactive gel glass. *Journal of Sol Gel Science and Technology* **7** 69-76.

Lobel KD, West, JK, Hench LL. (2000) Computer models of molecular structures of biomaterials. In: *Computer technology in biomaterials, science and engineering*. J Vander Sloten Ed. John Wiley and Sons Ltd. New York.

- 
- Lowry KJ, Hamson KR, Bear L, Peng YB, Calaluce R, Evans ML, Anglen JO, Allen WC. (1997) *Journal of Biomedical Materials Research* **36** S36-S41.
- Lowry OH, Rosebrough NJ, Farr AL, Randall RJ. (1951) Protein measurement with the folin phenol reagent. 265-275.
- Lu JX, Flautre B, Anselme K, Hardouin P, Gallur A, Descamps M, Thierry B. (1999) *Journal of Materials Science-Materials in Medicine* **10** 111-120.
- Lyndon Key Jr L, Ries WL. (1996) Osteopetrosis. In: *Principles of bone biology*. Bilezikian JP, Raisz LG, Rodan GA Eds. Academic Press, San Diego.
- Mann S and Perry CC (1986): Structural aspects of biogenic silica. *Ciba Foundation Symposium*; **121** 40-63.
- Majeska RJ. (1996) Culture of osteoblastic cells. In: *Principles of bone biology*. Bilezikian JP, Raisz LG, Rodan GA Eds. Academic Press, San Diego.
- Maniatopolous C, Sodek J, Melcher AH. (1988) Bone formation *in vitro* by stromal cells obtained from bone marrow of young adult rats. *Cell and Tissue Research* **254** 317-330.
- Marie PJ, Connes D, Hott M, Miravet L. (1990) Comparative effects of a novel vitamin D analogue MC-903 and 1,25-dihydroxyvitamin D<sub>3</sub> on alkaline phosphatase activity, osteocalcin and DNA synthesis by human osteoblastic cells in culture. *Bone* **11** 171-179.
- Marie PJ. (1995) Human endosteal osteoblastic cells: relationship with bone formation. *Calcified Tissue International* **56** (supplement 1) S13-S16.
- Marks SC, Hermey DC. (1996) The structure and development of bone. In: *Principles of bone biology*. Bilezikian JP, Raisz LG, Rodan GA Eds. Academic Press, San Diego.
- Martinez ME, Medina S, Sanchez M, Del Campo MT, Esbrit P, Rodrigo A, Martinez P, Sanchez-Cabezudo MJ, Moreno I, Garces MV, Munuera L. (1999) Influence of skeletal site of origin and donor age on 1,25(OH)<sub>2</sub>D<sub>3</sub>-induced response of various osteoblastic markers in human osteoblastic cells. *Bone* **24** 203-209.

- 
- Massari L, Manfredini M, Casto S, Brandolini F. (2000) *In vitro* effects of biocompatible metals on the morphology, proliferation and apoptosis in cultured osteoblast lines. *Minerva Ortopedica e Traumatologica* **51** 79-87.
- Matsuo K, Jochum W, Owens JM, Chambers TJ, Wagner EF. (1999) Function of fos proteins in bone cell differentiation. *Bone* **25** 141.
- Meleti Z, Shapiro IM, Adams CS. (2000) Inorganic phosphate induces apoptosis of osteoblast-like cells in culture. *Bone* **27** 359-366.
- Meyle J, Gultig K, Nisch W. (1995) Variation in contact guidance by human cells on a microstructured surface. *Journal of Biomedical Materials Research* **29** 81-88.
- Meyle J, von Recum AF, Gibbesch B, Huttemann W, Schlagenhaut U, Schulte W. (1991) Fibroblast shape conformation to surface micromorphology. *Journal of applied Biomaterials* **2** 273-276.
- Morais S, Sousa JP, Fernandes AH and Carvalho GS (1998): *In vitro* biomineralisation by osteoblast-like cells. Part 1 - retardation of tissue mineralisation by metal salts. *Biomaterials* **19** 13-21.
- Mullin JB and Riley JP (1955): *Analytical Chim Acta*; **12** 162-176.
- Nagase M, Abe Y, Chigira M, Udagawa E. (1992) Toxicity of silica-containing calcium phosphate glasses demonstrated in mice. *Biomaterials* **13** 172-175.
- Nakashima T, Sasaki H, Tsuboi M, Kawakami A, Fujiyama K, Kiriya T, Eguchi K, Ichikawa M, Nagataki S. (1998) Inhibitory effect of glucocorticoid for osteoblast apoptosis induced by activated peripheral blood mononuclear cells. *Endocrinology* **139** 2032-2040.
- Neo M, Kotani S, Nakamura T, Yamamuro T, Ohtsuki C, Kokubo T and B. Y (1992): A comparative study of ultrastructures of the interfaces between four kinds of surface-active ceramic and bone. *Journal of Biomedical Materials Research*; **26** 1419-1432.
- Neo M, Nakamura T, Ohtsuki C, Kasai R, Kokubo T and Yamamuro T (1994): Ultrastructural study of the A-W GC-bone interface after long-term implantation in rat and human bone. *Journal of Biomedical Materials Research*; **28** 365-372.

- Neo M, Nakamura T, Ohtsuki C, Kokubo T and Yamamuro T (1993): Apatite formation on three kinds of bioactive material at an early stage *in vivo*: A comparative study by transmission electron microscopy. *Journal of Biomedical Materials Research*; **27** 999-1006.
- Newberne PM and Wilson RB (1970): Renal damage associated with silicon compounds in dogs. *Proceedings of the National Academy of Science*; **65** 872-875.
- Nicotera P, Leist M, Ferrando May E. (1999) Apoptosis and Necrosis: different execution of the same death. *Biochemical Society symposium* **66** 69-73.
- Nijweide PJ, Burger EH, Klein Nulend J, Van der Plas A. (1996) The osteocyte. In: *Principles of Bone Biology*. Bilezikian JP, Raisz LG, Rodan GA Eds. Academic Press, San Diego.
- Ohgushi H, Dohi Y, Katuda T, Tamai S, Tabata S and Suwa Y (1996): *In vitro* bone formation by rat marrow cell culture. *Journal of Biomedical Materials Research*; **32** 333-340.
- Okamura T, Garland EM, Johnson LS, Cano M, Johansson SL, Cohen SM. (1992) Acute urinary tract toxicity of tetraethylorthosilicate in rats. *Fundamental and applied toxicology* **18** 425-441.
- Oliveira JM, Correia RN and Fernandes MH (1995): Surface modifications of a glass and a glass ceramic of the MgO- $\beta$ -CaO.P2O5-SiO2 system in a simulated body fluid. *Biomaterials*; **16** 849-854.
- Oreffo ROC, Triffitt JT. (1999) Future potentials for using osteogenic stem cells and biomaterials in orthopaedics. *Bone* **25** S5-S9.
- Ott SM. (1996). Theoretical and methodological approach. In *Principles of Bone Biology*. Bilezikian JP, Raisz LG, Rodan GA Eds. Academic Press, San Diego.
- Ozawa S and Kasugai S (1996): Evaluation of implant materials (hydroxyapatite, glass-ceramics, titanium) in rat bone marrow stromal cell culture. *Biomaterials*; **17** 23-29.

---

Patel N, Bhandari R, Shakesheff KM, Cannizzaro SM, Davies MC, Langer R, Roberts CJ, Tendler SJB, Williams PL. Printing patterns of biospecifically-adsorbed proteins. *Journal of Biomaterials Science, Polymer edition* **11** 319-331.

Peck WA, Birge SJ, Fedak SA (1964) Bone cells: biochemical and biological studies after enzymatic isolation. *Science* **146** 1476-1477.

Pereira MM, Clark AE and Hench LL (1995): Effect of texture on the rate of hydroxyapatite formation on gel-silica surface. *Journal of the American Ceramic Society*; **78** 2463-2468.

Pereira MM and Hench LL (1996): Mechanisms of hydroxyapatite formation on porous gel-silica substrates. *Journal of Sol Gel Science and Technology*; **7** 59-68.

Perry CC, Keeling-Tucker T. (2000) Biosilification: The role of organic matrix in structure control. *Journal of Biological Inorganic Chemistry* **5** 537-550.

Pioletti DP, Takei H, Kwon SY, Wood D, Sung K-LP. (1999) The cytotoxic effect of titanium particles phagocytosed by osteoblasts. *Journal of Biomedical Materials Research* **46** 399-407.

Pri-Chen S, Pitaru S, Lokiec F, Savion N. (1998) Basic fibroblast growth factor enhances the growth and expression of the osteogenic phenotype of dexamethasone-treated human bone marrow-derived bone-like cells in culture. *Bone* **23** 111-117.

Quirk RA, Chan WC, Davies MC, Tendler SJB, Shakesheff KM. Ploy(L-lysine)-GRDS as a biomimetic surface modifier for poly(lactic acid). *Biomaterials* **22** 865-872.

Rago R, Mitchen J and Wilding G (1990): DNA fluorometric assay in 96-well tissue culture plates using Hoechst 33258 after cell lysis by freezing in distilled water. *Analytical biochemistry*; **191** 31-34.

Ralphs JR and Ali SY (1986): induction of calcification in cultures of epiphyseal chondrocytes with calcium beta glycerophosphate. 263-268.

Rapiti E, Sperati A, Miceli M, Forastiere F, Di Lallo D, Cavariani F, Goldsmith DF, Perucci CA. (1999) End stage renal disease among ceramic workers exposed to silica. *Occupational and Environmental Medicine* **56** 559-561.

- Rasmussen ES. (1999) Use of fluorescent redox indicators to evaluate cell proliferation and viability. *In vitro and molecular toxicology*. **12** 47-58.
- Rich J, Kortesu P, Ahola M, Yli-Urpo A, Kiesvaara J, Seppala J. (2001) Effect of the molecular weight of poly(epsilon-caprolactone-co-DL-lactide) on toremifine citrate release from copolymer/silica xerogel composites. *International Journal of Pharmaceutics* **212** 121-130.
- Rickard DJ, Sullivan TA, Schenker BJ, Leboy PS, Kazhdan I. (1994) Induction of rapid osteoblast differentiation in rat bone marrow stromal cell cultures by dexamethasone and BMP-2. *Developmental Biology* **161** 218-228.
- Rizzi SC, Heath DJ, Coombes AGA, Bock N, Textor M, Downes S. (2001) Biodegradable polymer/hydroxyapatite composites: Surface analysis and initial attachment of human osteoblasts. *Journal of Biomedical Biomaterials Research* **55** 475-486.
- Roche P, Goldberg HA, Delmas PD, Malaval L. (1999) Selective attachment of osteoprogenitors to laminin. *Bone* **24** 329-336.
- Rodan GA, Raisz LG, Bilezikian JP. (1996) Pathophysiology of osteoporosis. In: *Principles of bone biology*. Bilezikian JP, Raisz LG, Rodan GA Eds. Academic Press, San Diego.
- Roodman GD. (1995) Application of bone marrow cultures to the study of osteoclast formation and osteoclast precursors in man. *Calcified Tissue International* **56** (supplement) S22-S23.
- Rucker RB, Lonnerdal B, Keen CL. (1994) Intestinal absorption of nutritionally important trace elements. In: *Physiology of the Gastrointestinal Tract*. 3<sup>rd</sup> Ed, LR Johnston Ed. Raven Press, New York.
- Saldanha LF, Rosen VJ and Gonick HC (1975): Silicon Nephropathy. *American Journal of Medicine*; **59** 95-103.
- Salinas AJ, Roman J, Vallet-Regi M, Oliveira JM, Correia RN, Fernandes MH. (2000) *In vitro* bioactivity of glass and glass ceramics of the 3CaO.P<sub>2</sub>O<sub>5</sub>-CaO.SiO<sub>2</sub>-CaO.MgO.2SiO<sub>2</sub> system. *Biomaterials* **21** 251-257.

- 
- Santerre JP, Labow RS, Boynton EL. (2000) The role of the macrophage in periprosthetic bone loss. *Canadian Journal of Surgery* **43** 173-179.
- Santos JD, Jha LJ, Ontiero FJ. (1996) *In vitro* calcium phosphate formation on SiO<sub>2</sub>-Na<sub>2</sub>O-CaO-P<sub>2</sub>O<sub>5</sub> glass reinforced hydroxyapatite composite: A study by XPS analysis. *Journal of materials science-materials in medicine* **7** 181-185.
- Sarih M, Souvannavong V, Brown SC, Adam A. (1993) Silica induces apoptosis in macrophages and the release of interleukin-1 $\alpha$  and Interleukin-1 $\beta$ . *Journal of Leucocyte Biology* **54** 407-413.
- Sautier JM, Kokubo T, Ohtsuki T, Nefussi JR, Boulebach H, Oboeuf M, Loty S, Loty C and Forest N (1994): Bioactive glass containing crystalline apatite and wollastonite induces biomineralisation in bone cell cultures. *Calcified Tissue International*; **55** 458-466.
- Schatzthauer R, Fromherz P. (1998) Neuron-silicon junction with voltage gated ionic currents. *European Journal of Neuroscience* **10** 1956-1962.
- Schiller PC, D'Ippolito G, Balkan W, Roos BA, Howard GA. (2001) Gap junctional communication mediated parathyroid hormone stimulation of mineralisation in osteoblastic cultures. *Bone* **28** 38-44.
- Schwartz K (1973): A bound form of silicon in glycosaminoglycans and polyuranides. *Proceedings of the National Academy of Science*; **70** 1608-1612.
- Schwartz K (1977): Silicon fibre and atherosclerosis. *Lancet*; **1** 454-456.
- Schwartz K and Milne DB (1972): Growth promoting effects of silicon in rats. *Nature*; **239** 333-334.
- Scotchford CA, Cooper E, Leggett GJ, Downes S. (1998) Growth of human osteoblast-like cells on alkanethiol on gold self-assembled monolayer: the effect of surface chemistry. *Journal of biomedical materials research* **41** 431-442.

---

Scotchford CA, Welsh B, Grant DM, Downes S. (in preparation) Osteoblast responses to plasma-sprayed calcium phosphate coatings *in vitro*: effects of varying crystallinity and topography.

Shettlemore MG, Bundy KJ. (1999) Toxicity measurement of orthopaedic implant alloy degradation products using a bioluminescent bacterial assay. *Journal of Biomedical Materials Research* **45** 395-403.

Simkiss K. (1975). In: *Bone and Biomineralisation*. The Institute of Biology; Studies in Biology no53. Edward Arnold Ed.

Singh SV, Khan MF, Rahmann Q. (1985) Interaction of silica with plasma proteins: *in vivo* studies. *Toxicology Letters* **28** 89-92.

Stea S, Visentin M, Granchi D, Ciapetti G, Donatti ME, Sudanese A, Zanotti C, Toni A. (2000a) Cytokines and osteolysis around total hip prostheses. *Cytokine* **12** 1575-1579.

Stea S, Visentin M, Granchi D, Cenni E, Ciapetti G, Sudanese A, Toni A. (2000b) Apoptosis in peri-implant tissue. *Biomaterials* **21** 1393-1398.

Stein GS, Lian JB, Stein JL, van Wijnen AJ, Frenkel B, Montecino M. (1996) Mechanisms regulating osteoblast proliferation and differentiation. In: *Principles of Bone Biology*. Bilezikian JP, Raisz LG, Rodan GA Eds. Academic Press, San Diego.

Strnad Z (1992): Role of the glass phase in bioactive glass ceramics. *Biomaterials*; **13** (5): 317-320.

Sudo H, Kodama H-A, Amagai Y, Yamamoto S, Kasai S. (1983) *In vitro* differentiation and calcification in a new clonal osteogenic cell line derived from newborn mouse calvaria. *Journal of Cell Biology* **96** 191-198.

Suzuki A, Palmer G, Bonjour JP, Caverzasio J. (1998) Catecholamines stimulate the proliferation and alkaline phosphatase activity of MC3T3-E1 osteoblast-like cells. *Bone* **23** 197-203.

Tanahashi M, Yao T, Kokubo T, Minoda M, Miyamoto T, Nakamura I, Yamamuro T. (1995) Apatite coated on organic polymers by biomimetic processes: Improvement in

---

adhesion to substrate by HCl treatment. *Journal of Materials science- materials in medicine* **6** 319-326.

Tancred DC, Carr AJ, McCormack BAO. (2001) The sintering and mechanical behaviour of hydroxyapatite with bioglass additions. *Journal of materials science- materials in medicine* **12** 81-93.

Tortora GJ and Anagnostakos NP. (1987). In: *Principles of anatomy and physiology* . Harper and Row, New York,

Tsuru K, Hayakawa S, Ohtsuki C, Osaka A. (1998) Ultrasonic implantation of calcium metasilicate glass particles into PMMA. *Journal of Materials science- materials in medicine* **9** 479-484.

Turksen K, Aubin JE. (1991) Positive and negative immunoselection for enrichment of two classes of osteoprogenitor cells. *Journal of Cell Biology* **114** 373-384.

Turnya B, Milc J, Laczka A, Cholewa K and Laczka M (1996): Biocompatibility of glass-crystalline materials obtained by the sol gel method: effect on macrophage function. *Biomaterials*; **17** 1379-1386.

van Blitterswijk CA, Bakker D, Hesselting SC and Koerten HK (1991): Reactions of cells at implant surfaces. *Biomaterials*; **12** 187-193.

Van Kooten TG, Klein CL, Kirkpatrick CJ. (2000) Cell-cycle control in cell-biomaterial interactions: Expression of p53 and Ki67 in human umbilical vein endothelial cells in direct contact and extract testing of biomaterials. *Journal of Biomedical Materials Research* **52** 199-209.

Van der Plas A, Nijwerde PJ. (1992) Isolation and purification of osteocytes. *Journal of Bone and mineral Research* **7** 389-396.

Vander Sloten J, Labey L, Van Audekercke R, Van der Perre G. (1998) Materials selection and design for orthopaedic implants with improved long-term performance. *Biomaterials* **19** 1455-1459.

Vansant EF, van der Voort P and V. K, (1995a). Silica preparation and properties. In: *Studies in Surface Science and Catalysis* Eds. 3-30.

- Vansant EF, van der Voort P and V. K, (1995b). The surface chemistry of silica. In: *Studies in Surface Science and Catalysis* Eds. 59-77.
- Vrouwenvelder WC, Groot CG and de Groot K (1993): Histological and biochemical evaluation of osteoblasts cultured on bioactive glass, hydroxyapatite, titanium alloy and stainless steel. *Journal of biomedical materials research*; **27** 465-475.
- Wang TH, Wang HS. (1999a) Apoptosis: (1) Overview and clinical significance. *Journal Formos Medical Association* **98** 381-393.
- Wang TH, Wang HS. (1999b) Apoptosis: (2) characteristics of apoptosis. *Journal Formos Medical Association* **98** 531-542.
- Weinstein RS, Jilka RL, Parfitt AM, , Manolagas SC. (1998) Inhibition of osteoblastogenesis and promotion of apoptosis of osteoblasts by glucocorticoids. *Journal of Clinical Investigations* **102** 274-282.
- Weinstein RS, Jilka RL, Young C, Miller FL, Shelton R, Smith C, Parfitt AM, , Manolagas SC. (1997) Glucocorticoid excess decreases the number of osteoblast progenitors in the marrow and increases mature osteoblast apoptosis in mice. *Journal of Bone and Mineral Research* **12** 256.
- Wergedal JE, Baylink DJ. (1984) Characterisation of cells isolated and cultured from human bone (41843). *Proceedings of the Society for Experimental Biology and Medicine* **176** 60-69.
- Xynos ID, Edgar AJ,, Buttery LD, Hench LL, Polak JM. (2001) Bioglass (TM) Gene-expression profiling of human osteoblasts following treatment with the ionic products of bioglass 45S5 dissolution. *Journal of biomedical materials research*; **55** 151-157.
- Xynos ID, Hukkanen MVJ, Batten JJ, Buttery LD, Hench LL. Polak JM. (2000) Bioglass 45S5 stimulates osteoblast turnover and enhances bone formation in vitro: implications and applications for bone tissue engineering. *Calcified Tissue International*. **67**, 321-329.

---

Yang J-M, Lu C-S, Hsu Y-G, Shish C-H. (1997) Mechanical properties of bone cement containing PMMA-SiO<sub>2</sub> hybrid sol gel material. *Journal of Biomedical Materials Research* **38** 143-154.

York M, Wilson AP, Newsome CS. (1994) The classification of soluble silicates for eye hazard using the rabbit enucleated eye test. *Toxicology in vitro* **8** 1265-1268.

Yuan H, de Bruijn JD, Zhang X, van Blitterswijk CA, de Groot K. (2001) Bone induction by porous ceramic made from Bioglass (45S5). *Journal of biomedical materials research (Applied Biomaterials)* **58** 270-276.

Zhang Z, Shen H-M, Zhang Q-F, Ong C-N. (2000) Involvement of oxidative stress in crystalline silica induced cytotoxicity and genotoxicity in rat alveolar macrophages. *Environmental Research* **82** 245-252.